Cape Peninsula
University of Technology

PHYTOCHEMICAL AND BIOLOGICAL ACTIVITIES OF SOUTH AFRICAN TRADITIONAL MEDICINAL PLANTS

by

Kadidiatou Ndjoubi Ossamy

Thesis submitted in fulfilment of the requirements for the degree

Doctor of Philosophy: Chemistry

in the Faculty of Applied Science

at the Cape Peninsula University of Technology

Supervisor: Prof. Ahmed Mohammed
Co-supervisor: Dr. Sylvester Omoruyi

Bellville (November 2024)

DECLARATION

I, **Kadidiatou Ndjoubi Ossamy**, declare that the contents of this dissertation/thesis represent my own unaided work and that the dissertation/thesis has not previously been submitted for academic examination towards any qualification. Furthermore, it represents my own opinions and not necessarily those of the Cape Peninsula University of Technology.

18/11/24

Signed **Date**

ABSTRACT

Natural remedies have become integral to modern healthcare, with plant-based therapies regaining prominence due to their therapeutic efficacy and cultural significance. Approximately 60-80% of the global population, particularly in developing regions, relies on medicinal plants for primary healthcare, involving over 70,000 species. However, many of these plants remain scientifically unexplored, emphasising the urgent need for research to validate their therapeutic potential and ensure safety.

South Africa's Cape Floristic Region, renowned for its biodiversity, hosts over 30,000 plant species, including *Lessertia frutescens* (cancer bush), *Protea venus*, and *Leucadendron xanthoconus*. While *L. frutescens* is well-documented for its anti-inflammatory, antioxidant, antiviral, anti-HIV and anticancer properties due to its diverse phytochemicals (e.g., amino acids, saponins, phenolics, and flavonoids), the phytochemical and pharmacological properties of *P. venus* and *L. xanthoconus* species remain largely unexplored. These three South African plants were selected for their economic importance, ethnobotanical significance and phytochemical potential.

Phytochemical analysis of *L. frutescens* (syn. *Sutherlandia frutescens*) led to the isolation of 11 compounds (**6.1-6.11**), including two novel metabolites, lessertiosides A (**6.1**) and B (**6.2**), characterised using IR, UV, NMR, and HR-ESIMS techniques. Notably, flavonoids 8-methoxyvestitol (**6.7**) and mucronulatol (**6.8**) were reported for the first time in this plant. The remaining compounds included the amino acid proline (**6.10**), the sugar D-pinitol (**6.11**), cycloartane glycosides [sutherlandiosides B (**6.6**), D (**6.5**), K (**6.3**) and 7*S*,24*S*,25-trihydroxy-9,10*R*-seco-9,19-cyclolanost-2(3),9(11)-diene-25-*O*-*β*-*D*-glucopyranoside (**6.4**)], and the flavonoid sutherlandin C (**6.9**).

Compounds **6.3-6.11** were evaluated for their neuroprotective properties in SH-SY5Y cells under MPP^+-induced PD conditions. At concentrations of 2.5, 5, and 10 µM, the compounds were non-toxic and demonstrated neuroprotective effects by enhancing cell viability, maintaining ATP production, and reducing apoptotic cell death. Compounds **6.6**, **6.8**, **6.9**, and **6.10** significantly restored ATP levels from 51% (under insult) to 73%, 75%, 74%, and 75%, respectively. Furthermore, compound **6.8** exhibited the most potent anti-apoptotic effect, reducing caspase 3/7 activity from 5-fold to 1.5-fold.

Phytochemical analysis of *P. venus*, a hybrid of *P. repens* and *P. aristata*, led to the isolation of 11 distinct compounds (**7.1-7.11)**, including a novel metabolite, *p*-coumaroylcalleryananin (**7.1**). Other compounds included calleryanin (**7.2**), protocatechuoylcalleryanin (**7.3**), *p*-hydroxybenzoylcalleryanin (**7.4**), lacticolorin (**7.5**), kaempferol-3-*O*-rhamnoside (**7.6**), rutin (**7.7**), quercetin-3-*O*-rhamnoside (**7.8**), 3,4-dihydroxybenzoic acid (**7.9**), *p*-hydroxybenzoic

acid (**7.10**) and glucose (**7.11**). The methanolic leaf extract showed a phenolic content of 199.05±1.64 mg GAE/g and exhibited strong antioxidant activity (IC_{50}= 0.042±0.07 µg/mL) compared to the positive control vitamin E (IC_{50}= 0.152±0.67). Among the tested isolated compounds (**7.3**-**7.6** and **7.9**), compounds **7.3**, **7.5**, **7.6** and **7.9** showed significant antioxidant activity with IC_{50} of 0.018±1.11, 0.033±1.27, 0.048±0.53 and 0.018±0.39 mg/mL.

MTT assay results for the tested compounds indicated minimal cytotoxic effects on the H9c2, MCF-7, and C3A cell lines. Moreover, the crude extract and compound **7.6** demonstrated potential cardioprotective activity by significantly enhancing ATP levels in H9c2 cells from 53% (HG+Pal) to 70% and 73%, respectively, in DCM model following treatment.

Phytochemical analysis of *L. xanthoconus* yielded seven compounds (**6.5**, **8.1**-**8.6**), including novel metabolites dichotomain C (**8.1**) and syringetin-3-*O*-(6´´-caffeoyl)-*β*-*D*-glucopyranoside (**8.2**). Compound **8.5** (Syringetin-3-*O*-*β*-*D*-glucopyranoside) displayed good antioxidant activity (IC_{50} = 0.071±0.82) compared to vitamin E and exhibited weak cytotoxicity against H9c2 cells (IC_{50} = 85.79±1.56 µM). Sutherlandioside D (**6.5**), leucodrin (**8.3**), leudrin (**8.4**) and the methanolic extract did not show cytotoxic activities against H9c2 cells. Additionally, none of them exhibited cardioprotective effects.

In silico docking and computational ADME analysis identified compounds **6.7** and **6.8** as potential neuroprotective agents, demonstrating high GI absorption, BBB permeability, drug-likeness, and lead-likeness properties. These two compounds demonstrated favourable binding to MAO-B (-9.3 and -8.9 kcal/mol, respectively) compared to Selegiline (-7.3 kcal/mol) and DJ-1 (-6.3 and -5.3 kcal/mol) compared to levodopa (-5.4 kcal/mol), supporting their neuroprotective potential.

Compound **7.6** from *P. venus* demonstrated strong binding to the KEAP1-NRF2 and weak binding to β_1-AR, suggesting that β_1-AR signalling is unlikely to play a significant role in its activity. These findings indicate that modulation of the KEAP1-NRF2 pathway is its primary mode of action. Like curcumin, its interactions with KEAP1-NRF2 highlight its potential to enhance antioxidant responses and improve cellular stress resistance, thereby supporting its moderate cardioprotective effects.

Overall, this research study highlights underexplored South African plants' phytochemical and therapeutic potential, providing a foundation for further investigations into their phytochemical profiles, pharmacological properties and toxicological safety. It also provides new insights into *L. xanthoconus* secondary metabolites while highlighting their limited bioactivities.

ACKNOWLEDGEMENTS

I wish to thank:

- First and foremost, I am deeply grateful to Allah (SWT) for blessing me with health, strength, and perseverance. Without His grace, completing this research would have been impossible.
- I extend my sincere gratitude to my supervisor, Prof. Ahmed Mohammed. His unwavering support, invaluable guidance, and constant encouragement have been pillars throughout my journey. Prof. Ahmed, your kindness, understanding, and warm-hearted advice have inspired me immensely; I am profoundly thankful.
- I am equally thankful to Prof. Rabia Johnson and Dr. Pritika Ramharack from the Biomedical Research and Innovation Platform at the South African Medical Research Council. Your technical expertise, insightful input, and mentorship have been instrumental in bringing this project to fruition.
- To Dr. Sylvester Omoruyi, I am grateful for your input and support throughout this project.
- My heartfelt thanks go to Dr. Nonhlakanipho Sangweni, Dr. Rajan Sharma, Ms. Nnini Obonye and Mr Fanie Rautenbach; their availability and constant assistance significantly impacted my studies and this research.
- To Ms. Gillian Fennessy-Yon, Mrs. Zandile Thembo, and Ms. Andiswa Valisa, your assistance and enthusiasm helped me through challenging moments, and I am genuinely grateful to each of you.
- I would also like to acknowledge Dr. Massende Yalo, Dr. Makhaba Maxicole, Dr. Zaino Abrahams, Dr. Nireshini Chellan, Ms. Naledi Dorkas Seatle, Mr. Romario Zenonbleck, and Dr. Ali El-Tahir Omer for their intellectual support, encouragement, and camaraderie. Working alongside such brilliant minds has been a true privilege.
- To my family, thank you for your steadfast emotional support, encouragement, and prayers. Your love has been my anchor through the highs and lows of this journey.
- The financial assistance of the National Research Foundation towards this research is acknowledged. Opinions expressed in this thesis and the conclusions arrived at are those of the author and are not necessarily to be attributed to the National Research Foundation.

DEDICATION

This thesis is lovingly dedicated to my parents, Aissata Diaby and Alain Ndjoubi Ossamy, whose unwavering support and guidance have been my greatest source of strength.

To my uncle, Cheikh Himela Sidibe and his wife, Irene Mouely Mouely, your encouragement and love have always been deeply cherished.

To my love, Dr.Yohan Mfoumboulou, and our precious son, Tahir Ayaan Mfoumboulou Ndjoubi, you are my inspiration, joy, and constant motivation to strive for excellence.

PREFACE

This thesis is divided into 10 chapters and follows an article-based format per university requirements and the guidelines of the journals to which the articles were submitted or published. Chapters One, Two, Five, Nine and Ten are written in normal thesis form, while Chapters Three, Four, Six, Seven and Eight are articles written in the style of the journal they will be submitted to

CHAPTER ONE: Introduction

This chapter overviews *L. frutescens, P. venus*, and *L. xanthoconus*, highlighting their significance and potential in medicinal research. It emphasises medicinal plants' importance, economic value, and role in modern medicine and drug discovery. Additionally, it discusses the challenges faced in exploring their therapeutic potential for pharmaceutical research and development. The chapter also outlines the study's aim, objectives, and rationale, underscoring the need to investigate these plants.

CHAPTER TWO: South African Neuroprotective and Cardioprotective Plants

This chapter discusses studies on the medicinal plants of South Africa, focusing on their neuroprotective and cardioprotective effects. It provides a comprehensive overview of the specific plant extracts studied, the experimental models used, the mechanisms of action, and the outcomes of these research studies. Additionally, the chapter highlights the ethnobotanical uses of these plants, their other pharmacological properties, and the protective effects of their bioactive compounds, demonstrating their potential in addressing cardiovascular and neurological disorders.

Chapter THREE: Phytochemistry, Ethnopharmacology and Phytotherapy of *Lessertia frutescens*: A Multifaceted Review of Cancer Bush

This chapter outlines *L. frutescens* botanical description, taxonomy, nomenclature and geographical distribution. It also delves into the phytochemical constituents, ethnobotanical uses, ethnopharmacological properties and pharmacological properties of the plant. The experimental models, mechanisms of action, clinical trials and outcomes of pharmacological studies conducted on the different plant extracts, fractions and bioactive compounds are also provided in detail.

CHAPTER FOUR: A Review of Phytochemical and Biological Activities of two Proteaceae genera: *Protea* and *Leucadendron*

This chapter explores the economic importance, ecological significance, ethnomedicinal uses as well as pharmacological and phytochemical investigations conducted on two key genera in South Africa's Proteaceae family: *Protea* and *Leucadendron*.

CHAPTER FIVE: General Methodology

This chapter overviews the extraction, chromatographic, and spectroscopic techniques used to extract, isolate, and characterise *L. frutescens*, *P. venus* and *L. xanthoconocus* secondary metabolites.

CHAPTER SIX: Isolation of Novel Lessertiosides A and B and Other Metabolites from *Lessertia frutescens* and their Neuroprotective Activity

This chapter provides an overview of the extraction, isolation, purification and characterisation of *L. frutescens* secondary metabolites. Additionally, it shows the mechanism of action by which *L. frutescens* bioactive compounds protect SH-SY5Y cells against MPP+-induced neurotoxicity.

CHAPTER SEVEN: Isolation of Secondary Metabolites from *Protea venus* and Evaluation of their Antioxidant, Cytotoxic and Cardioprotective Activities

This chapter explores the phytochemical analysis of *P. venus*, detailing the isolation and characterisation of its compounds as well as their antioxidant, cytotoxic, and cardioprotective effects.

CHAPTER EIGHT: Phytochemical Profiling and Therapeutic Potential of *Leucadendron xanthoconus*

This chapter provides an overview of the various phytochemical methods employed in the extraction, isolation, and characterisation of *L. xanthoconus*, along with an assessment of its pharmacological potential.

CHAPTER NINE: *In Silico* Approaches for Drug Discovery: Molecular Docking, Toxicological and ADME Profiling of Bioactive Compounds Isolated from *L. frutescens*, *P. venus* and *L. xanthoconocus*

This chapter explores the predicted toxicological profile, physiological and pharmacokinetic properties, drug-likeness, and lead-likeness of compounds isolated from *L. frutescens*, *P. venus*

and *L. xanthoconus*. From the 28 isolated compounds, (**6.3-6.11**, **7.3-7.6**, **7.9**, **8.3** and **8.5**) with adequate yields were selected for molecular docking studies.

CHAPTER TEN: Conclusion and Recommendations

This chapter concisely summarises the study's key findings. It also offers recommendations for future research, emphasising their role in advancing the exploration of medicinal plants.

TABLE OF CONTENTS

Contents

LIST OF FIGURES

LIST OF TABLES

APPENDICES

GLOSSARY

The list of terms/acronyms/abbreviations and their definitions is presented below

Terms/Acronyms/ Abbreviations	Definition/Explanation
ABTS	2,2′-azinobis(3-ethylbenzothiazoline-6-sulfonic acid
AChE	Acetylcholinesterase
ADMET	Absorption, Distribution, Metabolism, Excretion, And Toxicity
Ala	Alanine
ALS	Amyotrophic Lateral Sclerosis
AMPK	AMP-activated Protein Kinase
Arg	Arginine
Asn	Asparagine
Asp	Aspartic Acid
ATP	Adenosine Triphosphate
β_1-AR	Beta-1 adrenergic receptor
BBB	Blood-Brain Barrier
CAT	Catalase
CK-MB	Creatine Kinase-MB
CRP	C-Reactive Protein
Cys	Cysteine
DA	Dopamine
DMSO	Dimethylsulfoxide
eNOS	Endothelial Nitric Oxide Synthase
FFA	Free Fatty Acids
FRAP	Ferric Reducing Antioxidant Power
GABA	Gamma-Aminobutyric Acid
GI	Gastrointestinal
Glu	Glutamic Acid
Gln	Glutamine
Gly	Glycine
GSH	Glutathione
HA	Heavy atoms
HBA	Hydrogen-Bond Acceptors
HBD	Hydrogen-Bond Donors
HG	High glucose
His	Histidine
IL	Interleukin
Ile	Isoleucine
iNOS	Inducible Nitric Oxide Synthase
JNK	c-Jun N-terminal Kinases
KEAP1	Kelch-like ECH-associated protein 1
LD	Lethal dose
LDH	Lactate Dehydrogenase
Leu	Leucine
LPS	Lipopolysaccharide
Lys	Lysine
MnSOD	Manganese Superoxide Dismutase
Met	Methionine
MW	Molecular weight
N/A	Not applicable

NF-κB	Nuclear Factor kappa-light-chain-enhancer of activated B cells
NOS	Nitric Oxide Synthase
NRF2	Nuclear factor erythroid 2-related factor 2
Pal	Palmitate
PD	Parkinson's Disease
PDB	Protein data bank
P-gp	P-glycoprotein
Phe	Phenylalanine
Pro	Proline
QSAR	quantitative structure-activity relationships
RB	Rotatable bonds
ROS	Reactive Oxygen Species
Ser	Serine
SOD	Superoxide Dismutase
SSRI	Selective Serotonin Reuptake Inhibitor
TEAC	Trolox Equivalent Antioxidant Capacity
Thr	Threonine
TNF-α	Tumor Necrosis Factor-alpha
Trp	Tryptophan
Tyr	Tyrosine
UFF	Universal forcefield
Val	Valine
VEGF	Vascular Endothelial Growth Factor

CHAPTER ONE: Introduction

1.1 Introduction

Plants have long been integral to human life, providing essential resources such as food, medicine, dyes, gums, spices, oils, fuel, fibres, resins, wood, and timber. Medicinal plants play a vital role in traditional medicine, treating various ailments through decoctions, infusions, teas, powders, and tinctures (Dhanalekshmi et al., 2022; Balunas & Kinghorn, 2005; Balick & Cox, 1997; Samuelsson, 2004).

Globally, these plants significantly contribute to healthcare, especially in developing countries, where approximately 80% of the population relies on them for primary care due to their accessibility and affordability (Balogun & Ashafa, 2018; Dzoyem et al., 2013). However, despite their promising therapeutic potential, the journey from plant-based remedies to clinically validated drugs faces challenges. Addressing these challenges will facilitate the integration of traditional medicine into modern medicine, ultimately benefiting global health and well-being.

While natural products remain a vital source for drug discovery, many plant metabolites remain unexplored. The *Dictionary of Natural Products* lists approximately 200000 plant-based metabolites, with 60% originating from just ten taxonomic families. Comprehensive phytochemical and pharmacological studies are still needed for many species used in traditional medicine (Harvey et al., 2015).

In recent years, computational (*in silico*) approaches have emerged as valuable tools for investigating these metabolites. These methods help predict bioactive compounds' absorption, distribution, metabolism, excretion, and toxicity (ADMET) properties and binding affinity for therapeutic targets (Ekins et al., 2007).

South Africa's flora, especially within the Cape Floristic Region, offers a rich source of medicinal plants with therapeutic potential. Notable examples include *Lessertia frutescens* (cancer bush), known for immune-boosting and neuroprotective properties; *Aspalathus linearis* (rooibos), valued for its antioxidant and cardioprotective effects; and *Pelargonium sidoides*, widely used for respiratory infections (Street & Prinsloo, 2013). These plants highlight the unique therapeutic resources within South Africa's flora for treating neurodegenerative diseases like Parkinson's disease (PD) and cardiovascular conditions such as diabetic cardiomyopathy (DCM), both linked to oxidative stress and apoptosis.

L. frutescens is an indigenous South African plant renowned for its ethnopharmacological properties and traditional uses. *L. frutescens* is used to treat a wide range of ailments such as asthma, chronic bronchitis, colds, coughs, convulsion, diabetes mellitus, epilepsy, gastric, gout,

heart failure, heartburn, hypertension, kidney and liver infections, menopausal symptoms, osteoarthritis, pains, peptic ulceration, rheumatoid arthritis, reflux oesophagitis, varicose veins, and stress-related conditions linked to the endocrine system (Gericke et al., 2001; Prevoo et al., 2004; Mills et al., 2005; Ojewole, 2008). It is also used as drug support in the treatment of anorexia, cancer, influenza, HIV/AIDS, and tuberculosis (Gericke et al., 2001). Studies have shown that *L. frutescens* contains high levels of amino acids, saponins, phenolic compounds, and flavonoids, contributing to its anti-inflammatory, antioxidant, antiviral, antistress, cytotoxicity, and neuroprotective properties. However, most studies have focussed on the plant's various organic extracts rather than its secondary metabolites.

Protea venus, a hybrid of *P. repens* and *P. aristate*, and *Leucadendron xanthoconocus* are ornamental plants belonging to the Proteaceae family, valued for their commercial potential in cut flowers and cut stems. While neither species has been studied before, the Proteaceae family is known for its bioactive compounds. *Protea* species are traditional remedies for ailments such as dysentery, diarrhea, skin diseases, inflammation, fever, stomach pains, and menstrual problems. Research on various *Protea* species has demonstrated remarkable antioxidant (*P. cynaroides, P. elliottii, P. mundii,* and *P. nerifolia*), anti-tyrosinase (*P. madiensis*), anti-inflammatory (*P. simplex*), and antibacterial (*P. caffra*) properties, attributed to their high phenol and polyphenol content (Gadea et al., 2022). Moreover, despite the economic importance of the genus *Leucadendron*, its phytochemical composition is understudied, while its ethnobotanical and pharmacological potential remains unexplored.

Thus, studying the phytochemical composition and exploring the antioxidant potential of *L. frutescens*, *P. venus* and *L. xanthoconus* alongside the neuroprotective effects of *L. frutescens*, and the cardioprotective properties of *P. venus* and *L. xanthoconus* will significantly enrich the field of natural product chemistry.

1.2 Economic importance of medicinal plants

Medicinal plants are vital to the global economy, contributing significantly to international trade, job creation, and cultural heritage. Asia and Africa are the leading exporters of herbal products, with China and India trading over 7000 species annually, generating $2–5 billion in revenue (Dzoyem et al., 2013; Sofowora et al., 2013; Kuipers, 1997; Lange, 2006). Globally, 30% of pharmaceuticals are plant-derived, employing millions in developed and developing nations as well as supporting Indigenous communities and plant traders (Asigbaase et al., 2023). The global herbal medicine market, valued at $83 billion in 2019, is expected to grow to $550 billion by 2030 (Nath et al., 2023). China and India export over 120000 tonnes and 32000 tonnes annually, respectively. At the same time, Europe, Japan, and the United States dominate

the import market, with Europe being the largest importer, receiving approximately 400000 tonnes annually (Khan, 2014; Dzoyem et al., 2013; Briskin, 2000). In 2020, over-the-counter herbal remedies reached $73.4 billion in sales, with the U.S. market alone projected to grow from $230 billion in 2021 to $430 billion by 2028 (Nath et al., 2023).

The medicinal plant trade in South Africa operates at national, informal, and formal levels. National trade involves hundreds of species sold at regional herbal markets, while informal trade occurs between neighbouring countries (Van Wyk & Prinsloo, 2018). Formal trade focuses on large-scale international exports totalling 6497 tonnes in 2015. Of this, 6028 tonnes were exported to Europe, 387 to America, 58 to other African countries, and 24 to Asia (DAFF, 2016; Van Wyk & Prinsloo, 2018). Approximately 27 million South Africans use medicinal plants, creating 133000 jobs, primarily for women (Mander et al., 2007).

In 2006, South Africa's formal trade was estimated at R520 million per annum ($74.25 million at 2006 exchange rates), with traditional health practitioners prescribing an additional R2.6 billion ($371.4 million at 2006 exchange rates) worth of plant material (Van Wyk & Prinsloo, 2018). Total revenues from the trade, involving 700000 tonnes of plant material, were estimated at R2.9 billion ($414.2 million at 2006 exchange rates), representing 5.6% of the national health budget (Street & Prinsloo, 2013; Mander et al., 2007). However, most of this value did not enter the formal trade, contributing to South Africa's Gross Domestic Product.

Regionally, significant trade occurs in Eastern Cape (525 tonnes, R27 million annually), KwaZulu-Natal (4500 tonnes, R60 million annually), and Limpopo (1200 tonnes, R5000 per month) (Rasethe et al., 2019; Moeng & Potgieter, 2011; Botha et al., 2004). Johannesburg's trade is valued at $1-3 million (Delbanco et al., 2017). Additionally, folklore medicine plays a crucial role, with 128 million prescriptions annually consuming 20000 tonnes of plant material (Mander et al., 2007). This thriving sector reflects medicinal plants' cultural, economic, and health importance in South Africa.

1.3 Importance of medicinal plants in modern medicine and drug discovery

Developing new drugs is a complex, time-consuming, and expensive process that typically spans around 12 years and costs over $1 billion from discovery to clinical availability. The process begins with identifying new chemical entities through chemical synthesis or isolation from natural products (Katiyar et al., 2012). The isolation of bioactive compounds from plants has a long history, dating back to 1803 when Friedrich Sertuner first isolated morphine from Opium. This milestone paved the way for the discovery of several other significant compounds, such as atropine (*Atropa belladonna*), colchicine (*Colchicum autumate*), emetine (*Carapichea ipecacuanha*), papaverine (*Papaver somniferum*), quinine (*Cinchona officinalis*), salicin (Salix

ssp.) and strychnine (*Strychnos nux vomica*) (Süntar, 2020; Oliviera et al., 2015; Siddiqui et al., 2014). These discoveries revolutionised medicine, leading to the development of safer and more effective prescription drugs, eventually facilitating the advent of synthetic and semi-synthetic compounds in the 20th century. Between 1959 and 1980, approximately 25% of clinically used drugs were derived from extracts of 90 higher plant species. These drugs have been widely utilised globally, underscoring the significant role of medicinal plants in modern medicine (Gurib-Fakim, 2006; Farnsworth et al., 1985). Noteworthy discoveries in this period include the vinca alkaloids from the flowers of *Catharanthus roseus* in the 1950s and paclitaxel from the bark of *Taxus brevifolia* in 1967, both of which have been significant in anticancer drug discovery. Moreover, from 1994 to 2007, nearly 50% of synthesised drugs were derived from natural products, with 13 natural product-based drugs being approved between 2005 and 2007, highlighting the ongoing importance of plants and natural resources in drug development (Katiyar, 2012; Harvey, 2008). In a study from 2020, it was found that between 1981 and 2019, 32% (441 out of 1394) of approved small-molecule drugs were originated from natural products or their derivatives, categorised as N (71, natural product), NB (14, botanical natural product recently approved) and ND (356, derived from a natural product and is usually a semisynthetic modification). The remaining 68% (953 out of 1394) were synthetic drugs classified as S (464, synthetic drug, often found by random screening/modification of an existing agent), S* (217, made by total synthesis, but the pharmacophore is/was from a natural product), S/NM (65) and S*/NM (207) with /NM indicating mimic of a natural product as illustrated in Figure 1.1 (Newman & Cragg, 2020).

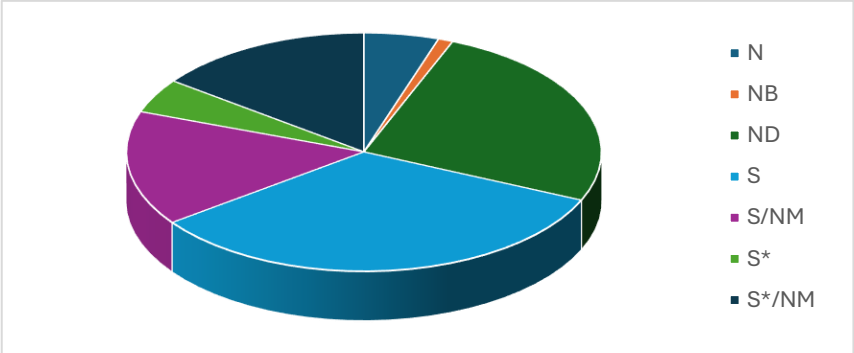

Figure 1.1: Approved small molecules drugs from 1981 to 2019 (Newman & Cragg, 2020)

In 2018, 22% (10 out of 46) of approved small drugs were classified as N, NB and ND. In 2017, 36% of the 39 approved drugs were in these categories, and in the first nine months of 2019, 28% of the 32 approved small-molecule drugs were derived from natural products. The study also exhibited natural products' substantial contribution to drug approvals across different

therapeutic areas, with the highest contribution observed in antibacterial drugs (78 out of 162) and the lowest in antiviral drugs (6 out of 185). Other categories such as antiparasitic (7 out of 20), anti-sclerosis (4 out of 13), and anti-glaucoma at 31.58% (6 out of 19) exhibited moderate reliance on natural products derived drugs. Additionally, anticancer drugs had 17.41% (43 out of 247) of approvals derived from natural products, antidiabetic drugs stood at 12.70% (8 out of 63), and antifungal drugs had 8.82% (3 out of 34), highlighting the varying dependency on natural sources across different therapeutic categories as shown in Figure 1.2 (Newman & Cragg, 2020).

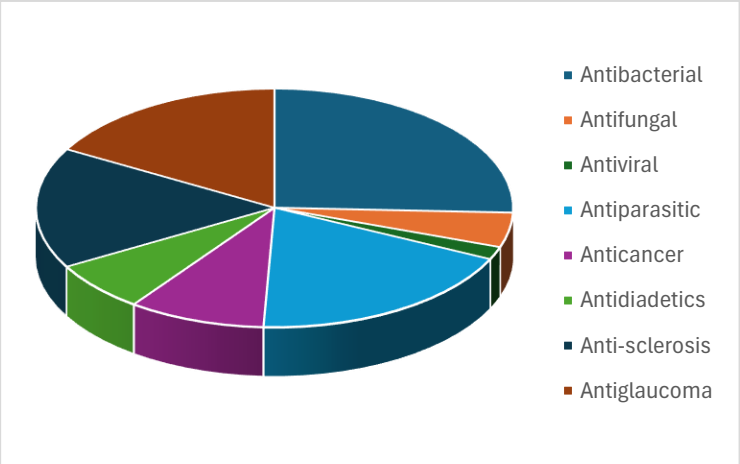

Figure 1.2: Percentage of small molecules approved drugs derived from natural products (Newman & Cragg, 2020)

Furthermore, Nguyen-Vo et al. (2020) noted that 83% of 1300 molecular cyclic structures are exclusively found in natural products, further confirming the pivotal role of natural products in drug design and development. In 2014, Butler (2014) reviewed 100 natural products and natural product-derived compounds, including 33 antibody-drug conjugates with natural product-derived cytotoxic agents in clinical trials, revealing the enduring value of natural products in cancer treatment. Natural resources offer more structural diversity and novelty than synthetic compounds. Plant-derived drugs typically have higher molecular weights, more oxygen atoms, and greater complexity, allowing for diverse and specific target binding. The use of structural chemical databases and computational modelling facilitates the creation of new chemical entities for pharmacological evaluation (Nisbet & Moore, 1997).

These advantages make plant-derived drugs excellent lead compounds for further drug development. The diverse structural features of natural products, including stereochemistry, functional groups, chiral centres, and saturation, have proven crucial in drug discovery as a starting point for optimising new or lead drugs. Several known compounds isolated from medicinal plants have demonstrated efficacy in targeting newly validated molecular targets, such as indirubin and kamebakaurin, which inhibit cyclin-dependent kinases and NF-K,

respectively (Balunas & Kinghorn, 2005; Eisenbrand et al., 2004; Lee et al., 2002). Despite natural products' significant contributions, pharmaceutical companies have often favoured synthetic and semi-synthetic compounds due to the advantages of large-scale production and the avoidance of issues related to plant collection, artefacts in extracts, lengthy resupply times, and compliance with biodiversity conservation regulations (Süntar, 2020; Flick et al., 2017). However, synthesising complex natural products with multiple chiral centers remains challenging and costly, leading to continued reliance on certain bioactive compounds such as podophyllotoxin and taxol from plants (Beutler, 2009).

Out of the 250000 flowering plant species found worldwide about 125000 are widespread in tropical forests. Remarkably, only 1% of the secondary metabolites derived from these tropical plant species have been thoroughly investigated and utilised for their pharmaceutical potential (Jachak & Saklani, 2015). This observation highlights the vast untapped reservoir within understudied plants, offering the potential for invaluable new lead drugs, novel pharmaceuticals, and innovative chemical entities.

In addition to drug discovery, modern techniques have been applied to standardise herbal medicines, aiding in identifying analytical marker compounds (Balunas & Kinghorn, 2005). The beneficial aspect of medicinal plants in discovering, developing, and producing drugs in many societies has resulted in the complementary use of modern and traditional medicine. Traditional medicine is typically used to treat chronic illness, alleviate symptoms, and cost-effectively enhance the quality of life. Approximately 80% of the world population relies on plant-based medicine as their primary health care, while the allopathic medical system is used to treat acute conditions. In countries like Mali, Zambia, Ghana, and Nigeria, herbal medicines are used as primary healthcare to treat 60% of children diagnosed with malaria. Similarly, in London, San Francisco, and South Africa, approximately 70% of HIV/AIDS patients turn to traditional medicine as an alternative therapy (Srivastava, 2018). The economic challenges many developing countries face, and the high costs of importing conventional medicines have compelled several nations in Asia and Africa to incorporate traditional medicines into their public healthcare programs. This integration is driven by folklore medicines' affordability and widespread availability (Parasuraman, 2018).

1.4 Medicinal plants in drug discovery: Challenges

In the late 20th century, the growth of high-throughput synthesis and combinatorial chemistry in drug development led to a sturdy decline in phytomedicine research. These advanced technologies resulted in an unlimited supply of potent combinatorial compounds targeting more than 10000 biological targets (McChesney et al., 2007). However, despite the greater diversity

of structural characteristics and physicochemical properties found in plant secondary metabolites compared to combinatorial compounds, many fail to meet drug-likeness criteria (Nguyen-Vo et al., 2020).

Drug discovery from medicinal plants is more complicated, challenging, and lengthier than modern drug discovery methods. This is primarily attributed to the limited quantity of isolated bioactive compounds, which may be insufficient for lead drug optimisation, development, and clinical trials. Additionally, there are hurdles associated with the bioactive compounds' intellectual property rights (Atanasov et al., 2021; Balunas & Kinghorn, 2005). Moreover, during the purification process, some plant components may lose their therapeutic potential due to alterations or decomposition caused by light exposure, extraction temperature, and storage conditions. Consequently, several pharmaceutical companies have scaled back their research efforts in herbal-based drug discovery. Furthermore, the lack of a record on the therapeutic efficacy of the existing 700000 medicinal plants and the illegal collection of protected or highly demanded plants (locally or internationally) contributes to these plants' rapid extinction or decline, which remains to be thoroughly studied. These unstainable harvesting practices impact drug discovery from medicinal plants and raise concerns among researchers and environmental conservationists (Rasethe et al., 2019).

1.5 Rationale of the study

The global medicinal use of plants highlights a significant opportunity to discover novel therapeutic agents. Approximately 70000 out of 250000 known higher plant species are utilised for their medicinal properties; however, only 15% have been studied for phytochemical composition, and a mere 6% have undergone biological screening (Iwu, 2013; Yuan et al., 2016; Suntan, 2019; Nath et al., 2022). This limited research underscores a need to explore plant-derived secondary metabolites, especially for their potential to treat oxidative stress-related diseases, including neurodegenerative and cardiovascular conditions.

South Africa presents a precious case, given its rich biodiversity. Home to over 30000 plant species, the country contributes 10% of the world's higher plant species (Bareetseng, 2022; Street & Prinsloo, 2013). Medicinal plants are central to the healthcare practices of 60-80% of the population, with over 200,000 traditional healers using more than 3000 species to treat various ailments (Mothibe & Sibanda, 2019). However, the increasing demand for these plants, combined with urbanisation and unsustainable harvesting, threatens biodiversity.

Given these factors, it is essential to investigate *L. frutescens*, *P. venus*, and *L. xanthoconus*. Despite being part of South Africa's rich and diverse flora, these plants remain largely unexplored regarding their chemical composition and pharmacological properties, particularly

P. venus and *L. xanthoconus*. Isolating and characterising their secondary metabolites could lead to the discovery of novel bioactive compounds with therapeutic effects. Such compounds may offer promising treatments for conditions like DCM and PD, addressing pressing health needs and underscoring the potential of plant-based research.

1.6 Problem statement

The rising prevalence of chronic diseases, such as PD and DCM, presents significant healthcare challenges, particularly in South Africa (Cairncross, 2019). Managing these conditions often requires prolonged and costly treatments, which are inaccessible to many of the population due to high poverty levels and healthcare disparities (Goudge et al., 2009; Statistics South Africa, 2020). South Africa faces additional barriers, including a severe shortage of neurologists (Smith & Francis, 2020), limited access to essential medications in public healthcare facilities, and a healthcare system strained by the dual burden of communicable and non-communicable diseases. These challenges disproportionately affect individuals in rural and low-income areas, exacerbating health inequities (Goudge et al., 2009).

PD and DCM are multifactorial conditions driven by oxidative stress, inflammation, and metabolic dysfunction, making them particularly difficult to treat effectively (Nguyen-Vo et al., 2020; Potashkin et al., 2019). With limited access to appropriate care and a growing number of affected individuals, there is an urgent need for alternative therapeutic strategies that are both effective and affordable.

This study investigates the phytochemical composition and bioactivities of *L. frutescens*, *P. venus*, and *L. xanthoconus*. By evaluating their potential neuroprotective and cardioprotective properties, the research aims to uncover novel, plant-derived treatments that could address the challenges of managing PD and DCM, while alleviating the associated healthcare and socioeconomic burdens in South Africa.

1.7 Aim of the research

The study aims to extract, isolate, and characterise the secondary metabolites from the methanolic extracts of *L. frutescens*, *P. venus*, and *L. xanthoconus*. It will evaluate their physicochemical and pharmacokinetic properties, assess their drug- and lead-likeness, and determine binding affinity to key therapeutic targets. Through phytochemical analysis, the study will investigate the compounds' antioxidant, neuroprotective, and cardioprotective effects to identify potential candidates for treating or preventing neurodegenerative and cardiovascular diseases.

1.8 Objectives of the research study

The objectives of this study include:

i. To collect and identify *P. venus*, *L. xanthoconus* and *L. frutescens*

ii. To document the ethnomedicinal uses of various parts of *P. venus*, *L. xanthoconus* and *L. frutescens*

iii. To extract *P. venus*, *L. xanthoconus* and *L. frutescens* plant materials secondary metabolites using methanol (*P. venus* and *L. xanthoconus*) and 70% aqueous methanol (*L. frutescens*)

iv. To isolate secondary metabolites from these plants using chromatographic techniques such as column chromatography and semi-preparative high-performance liquid chromatography (semi-prep-HPLC)

v. To characterise the isolated compounds using different spectroscopic techniques such as 1D and 2D nuclear magnetic resonance (NMR) spectroscopy, electrospray ionisation mass spectroscopy (ESI-MS), Fourier transform infrared spectroscopy (FTIR) and ultraviolet (UV) Spectroscopy

vi. To evaluate the bioactivities of plant extracts and isolated compounds, the neuroprotective properties of *L. frutescens* will be assessed using MTT, ATP, and caspase-3/7 assays. The antioxidant effects of *P. venus* and *L. xanthoconus* will be determined through FRAP and TEAC assays, while their cardioprotective potential will be investigated using ATP assays.

vii. To predict the toxicological profiles of the isolated compounds using ProTox 3.0 and evaluate their physicochemical and pharmacokinetic properties, as well as their drug- and lead-likeness, through SwissADME.

viii. To determine the binding affinities of the isolated compounds to key therapeutic targets, such as DJ-1 and MAO-B for neuroprotection, as well as KEAP1-NRF2, GPX4, and β_1-AR for cardioprotection, using AutoDock Vina and LigPlot.

References

Asigbaase, M., Adusu, D., Anaba, L., Abugre, S., Kang-Milung, S., Acheamfour, S. A., Adamu, I. & Ackah, D. K. (2023). Conservation and economic benefits of medicinal plants: Insights from forest-fringe communities of Southwestern Ghana. *Trees, Forests and People*, 14: 1-12.

Atanasov, A. G., Zotchev, S. B., Dirsch, V. M., Orhan, I. E., Banach, M., Rollinger, J. M., Barreca, D., Weckwerth, W., Bauer, R., Bayer, E. A., Majeed, M., Bishayee, A., Bochkov, V., Bonn, G. K., Braidy, N., Bucar, F., Cifuentes, A., D'Onofrio, G., Bodkin, M. & Supuran, C. T. (2021). Natural products in drug discovery: advances and opportunities. *Nature Reviews Drug Discovery*, 20(3): 200-216).

Balick, M.J. & Cox, P.A. (1997). *Plants, People, and Culture: Science of Ethnobotany*. New York: Scientific American Library.

Balogun, F. O. & Ashafa, A. O. T. (2019). A Review of Plants Used in South African Traditional Medicine for the Management and Treatment of Hypertension. In *Planta Medica*, 85(4): 312-334.

Balunas, M. J. & Kinghorn, A. D. (2005). Drug discovery from medicinal plants. *Life Sciences*, 78: 431-441.

Botha, J., Witkowski, E. T. F. & Shackleton, C. M. (2004). Market profiles and trade in medicinal plants in the Lowveld, South Africa. *Environmental Conservation*, 31(1): 38-46.

Butler, M, S., Robertson, A. A. & Cooper, M. A. (2014). Natural product and natural product derived drugs in clinical trials. *Nat Prod Rep*, 31(11): 1612-61.

Cairncross, C. A. (2019). *Prevalence of chronic diseases in the population covered by medical schemes in South Africa*. Research and Monitoring Unit, Council of Medical Schemes.

Dhanalekshmi, U. M., Alam, T. & Khan, S. A. (2022). 'The Folkloric Uses and Economic Importance of Some Selected Edible Medicinal Plants Native to Oman: A Brief Overview'. In Masoodi, M. H. & Rehman, M. U. (Eds.). *Edible Plants in Health and Diseases: cultural, Practical and Economic Value*. Springer.

Dold, A. P. & Cocks, M. L. (2001). Traditional veterinary medicine in the Alice district of the Eastern Cape Province, South Africa: Research in action. *South African Journal of Science*, 97: 375-379.

Dzoyem, J. P., Tshikalange, E. & Kuete, V. (2013). Medicinal Plants Market and Industry in Africa. In Kuete, V (Ed). *Medicinal Plant Research in Africa: Pharmacology and Chemistry*. Elsevier Inc.

Gadea, A., Khazem, M. & Gaslonde, T. (2022). Current knowledge on chemistry of Proteaceae family, and biological activities of their bis-5-alkylresorcinol derivatives. In *Phytochemistry Reviews,* 21(6): 1996-2005.

Gericke, N., Albrecht, C.F., Van Wyk, B., Mayeng, B., Mutwa, C. & Hutchings, A. (2001). *Sutherlandia frutescens*. A*ustralian Journal of Medical Herbalism*, 13: 9-15.

Goudge, J., Gilson, L., Russell, S., Gumede, T. & Mills, A. (2009). Affordability, availability and acceptability barriers to health care for the chronically ill: Longitudinal case studies from South Africa. *BMC Health Services Research*, 9(75): 1-18.

Gurib-fakim, A. (2006). Medicinal plants: Traditions of yesterday and drugs of tomorrow. *Molecular Aspects of Medicine*, *27*: 1-93.

Harvey, A. L. (2008). Natural products in drug discovery. *Drug Discov Today*, 13: 894-901.

Harvey, A. L., Edrada-Ebel, R. & Quinn, R. J. (2015). The re-emergence of natural products for drug discovery in the genomics era. *Nature Reviews Drug Discovery*, 14(2): 111-129.

Jachak, S. M. & Saklani, A. (2007). Challenges and opportunities in drug discovery from plants. *Current Science*, *2*(8): 1251-1257.

Katiyar, C., Kanjilal, S., Gupta, A. & Katiyar, S. (2012). Drug discovery from plant sources: An integrated approach. *International Quarterly Journal of Research in Ayurveda*, *33*(1): 1-10.

McChesney, J. D., Venkataraman, S. K. & Henri, J. T. (2007). Plant natural products: Back to the future or into extinction?. *Phytochemistry*, 68: 2015-2022.

Mills, E., Cooper, C., Seely, D. & Kanfer, I. (2005). African herbal medicines in the treatment of HIV: Hyoxis and Sutherlandia. An overview of evidence and pharmacology. *Nutr J*, 4: 19-24.

Mothibe, M. & Sibanda, M. (2019). African Traditional Medicine: South African Perspective. In *Traditional and Complementary Medicine*. IntechOpen.

Nath, R., Kityania, S., Nath, D., Das Talkudar, A., & Sarma, G. (2023). *An Extensive Review on Medicinal Plants in The Special Context of Economic Importance*. *16*, 6-11.

Newman, D. J. & Cragg, G. M. (2020). Natural Products as Sources of New Drugs over the Nearly Four Decades from 01/1981 to 09/2019. *Journal of Natural Products*, 83(3): 770-803.

Nisbet, L. J. & Moore, M. (1997). Will natural products remain an important source of drug research for the future?. *Curr Opin Biotechnol*, 8(6): 708-12.

Nguyen-Vo, T. H., Nguyen, L., Do, N., Nguyen, T. N., Trinh, K., Cao, H., & Le, L. (2020). Plant Metabolite Databases: From Herbal Medicines to Modern Drug Discovery. *Journal of Chemical Information and Modeling*, *60*(3): 1101-1110.

Ojewole, J. A. O. (2008). Anticonvulsant property of Sutherlandia frutescens R. BR. (variety Incana E. MEY.) [Fabaceae] shoot aqueous extract. *Brain Research Bulletin*, *75*(1): 126-132.

Parasuraman, S. (2018). Herbal Drug Discovery: Challenges and Perspectives. *Current Pharmacogenomics and Personalized Medicine*, *16*(1): 63-68.

Potashkin, J., Huang, X., Becker, C., Chen, H., Foltynie, T. & Marras, C. (2019). Understanding the links between cardiovascular disease and Parkinson's disease. *Movement Disorders*, 35(1): 55-74.

Prevoo, D., Smith, C., Swart, P. & Swart, A. C. (2004). The effect of Sutherlandia frutescens on steroidogenesis: Confirming indigenous wisdom. *Endocrine Research*, *30*(4): 745-751.

Rasethe, M. T., Semenya, S. S. & Maroyi, A. (2019). Medicinal Plants Traded in Informal Herbal Medicine Markets of the Limpopo Province, South Africa. *Evidence-Based Complementary and Alternative Medicine*, 2019: 1-11.

Samuelsson, G. 2004. *Drugs of Natural Origin: a Textbook of Pharmacognosy*. 5th Ed. Stockholm: Swedish Pharmaceutical Press.

Seidl, S. E. & Potashkin, J. A. (2011). The promise of neuroprotective agents in Parkinson's disease. *Frontiers in Neurology*, 2: 1-19.

Smith, M. & Francis, P. (2020). Parkinson's Diseases in Africa: A South African Perspective. *World Federation of Neurology*, 35(4): 11.

Sofowora, A., Ogunbodede, E., Onayade, A. & Dentistry, C. (2013). The Role and Place of Medicinal Plants in The Strategies For Disease. *Afr J Tradit Complement Altern Med*, 10(5): 210-229.

Srivastava, A. K. (2018). 'Significance of medicinal plants in human life'. In Tewari, A. & Tiwari, S (Eds). *Synthesis of Medicinal Agents from Plants*. Elsevier.

Street, R. A. & Prinsloo, G. (2013). Commercially Important Medicinal Plants of South Africa: A Review. *Journal of Chemistry*, 1-16.

Süntar, I. (2020). Importance of ethnopharmacological studies in drug discovery: role of medicinal plants. *Phytochemistry Reviews*, 19(5): 1199-1209.

Van Wyk, A. S. & Prinsloo, G. (2018). Medicinal plant harvesting, sustainability and cultivation in South Africa. *Biological Conservation*, 227: 335-342.

CHAPTER TWO: South African Neuroprotective and Cardioprotective Plants

2.1 Introduction

There is a growing interest in using medicinal plants to treat neurological and cardiovascular diseases, reflected in the increasing number of plants investigated for their potential neuroprotective and cardioprotective effects. These investigations have shown that the protective effects of medicinal plants on brain and heart tissues stem from their abilities to scavenge free radicals, inhibit pro-inflammatory cytokines and apoptosis, and enhance mitochondrial function (Ayeni et al., 2022; Dludla et al., 2017).

This chapter provides a detailed overview of the experimental models used, specific plant extracts or bioactive compounds investigated, and the observed outcomes for both disease areas, as summarised in Tables 2.1 and 2.2.

2.2 South African neuroprotective plants

Neuroprotection is the ability of a treatment to prevent the central nervous system from neuronal cell death caused by acute neurodegenerative or chronic ND diseases (Schapira, 2010; Elufioye, Berida & Habtemariam, 2017). Neurodegenerative diseases (ND) are neuronal diseases that impinge on the central and peripheral nervous systems of the brain's function and composition (Ayeni et al., 2022). Subsequently causing permanent brain damage, which limit patients' speech, mobility, bladder, bowel functions, and cognitive abilities (Lamptey et al., 2022). The prominent ND are PD, Alzheimer's disease, amyotrophic lateral sclerosis, dementia with Lewy bodies, Huntington's disease, multiple sclerosis, and spongiform encephalopathy (Elufioye et al., 2017). Age, cell signalling impairments, deposition of aggregated proteins, ethnicity, environmental exposures and climate, genetics, gender, inflammatory response, mitochondrial dysfunctions, neuronal apoptosis, and oxidative stress are associated with the etiological factors of ND (Ayeni et al., 2022). According to the WHO 2024 report, it is estimated that more than 3 billion people globally were living with a neurological condition in 2021, with over 80% of neurological deaths and health loss occurring in low- and middle-income countries, including those in sub-Saharan Africa (WHO, 2024). To address this issue, researchers have been working towards finding effective neuroprotective treatments to prevent the development and progression of these neurodegenerative diseases. One promising approach being explored is the use of medicinal plants such as *Annona senegalensis, Bidens pilosa, Boophone disticha, Brunsvigia bosmaniae, Boophone haemanthoides, Cassia singueana, Carpobrotus edulis, Crinum bulbispermum, Crossyne flava, Euphorbia hirta, Harpagophytum procumbens, Hypericum perforatum, Hibiscus asper, Lannea schweinfurthii, Lessertia frutescens, Scadoxus*

puniceus, Strumaria truncata, and Zanthoxylum capense. These South African plant species have been studied for their potential to protect the brain from various pathological challenges, as presented in Table 2.1.

Table 2.1: South African neuroprotective plants and their constituents

Plant name (Family)	Traditional uses of the plants	Extracts (parts used) and isolated compounds	Other pharmacological properties	Models	Mode or mechanisms of action (s)	References
Annona senegalensis **(Annonaceae)**	Used to treat convulsions, epilepsy, sterility, dysentery, gastrointestinal problems, diabetes, erectile dysfunction, snake bites, infection problems, memory loss, malaria, and skin disorders	Dichloromethane: methanol extract (bark)	Anxiolytic, anticonvulsant, antioxidant, anti-inflammatory, antibacterial, anticancer, antiparasitic, muscle relaxant, haemostatic and anti-sickling	U373MGsiGT6 cells	Protected against aminochrome-induced toxicity in human astrocytoma U373MGsiGT6 cells where GSTM2 expression was 74% silenced	Akah, 2023; Ngoungoure et al., 2019
Bidens pilosa **(Asteraceae)**	Used to treat dizziness, migraines, headaches, and rheumatism	Aqueous extract (whole plant)	Anxiolytic, anticonvulsant chemopreventive, and antidiabetic	superoxide dismutase-1 (SOD1G93A) transgenic mouse model of Amyotrophic lateral sclerosis (ALS): G93A mice	Protected motor neurons by suppressing the inflammatory activation of microglia and astrocytes in the spinal cord of the G93A ALS model mice after the onset of ALS symptoms	Kosuge et al., 2020; Taïwe & Kuete, 201
					Inhibited LPS-induced pro-inflammatory Cytokine (TNF-α, IL-1β, and IL-6) Production in BV-2 microglial cells and restored microglia/ macrophage balance by inhibiting the polarisation of microglia/macrophages to the M1-like phenotype and regulating cell proliferation	Tsuruta et al., 2023
Boophone disticha **(Amaryllidaceae)**	Used to induce hallucinations for divinatory and to treat hysteria, stress-related ailments, psychosis, anxiety and depression as well as age-related dementia	Methanol extract (bulb)	Antimicrobial, anti-inflammatory, anticancer, cytotoxic, antihypertensive, and anxiolytic	MPP^+-induced neurotoxicity model using SH-SY5Y cells	Enhanced antioxidant defence mechanisms, increased cell proliferation, restored cellular morphology, inhibited ATP degeneration and prevented MPP^+-induced increase in ROS and caspase 3/7 activities in the cells	Nair & Van Staden, 2014, 2022; Kangwa et al., 2024
				AChE (cholinesterase) enzyme assay	Possessed anticholinesterase effect	
				6-hydroxydopamine-induced toxicity in SH-SY5Y neuroblastoma cells	Inhibited ATP degeneration	Ibrakaw et al., 2020
Boophone haemanthoides	Used to treat asthma and knee pain	Methanol extract (bulb)	Antibacterial, and anticancer		Improved cell viability, increased ATP generation in the cells, and	

(Amaryllidaceae)				MPP^+-induced toxicity in SH-SY5Y neuroblastoma cells	inhibition of MPP^+-induced apoptosis	
	N/A	Distichamine	selective serotonin re-uptake inhibitors (SSRI), antibacterial, cytotoxic			Elgorashi, 2019; Ibrakaw et al., 2020
		Hippadine	Antifertility agent			Chattopadhyay et al., 1983; Ibrakaw et al., 2020
		Stigmast-4-ene-3,6-dione	Anti-inflammatory and antiallergic			Tsai et al., 1998, Ibrakaw et al., 2020
		3-hydroxy-1-(4′-hydroxyphenyl)-1-propanone	N/A			Ibrakaw et al., 2020
		Tyrosol	Antiatherogenic antioxidant, anti-inflammatory, and cardioprotective			Marković et al., 2019
		Cholest-4-en-3-one	Anti-obesity and lipid-lowering			Higuchi et al., 2024
Brunsvigia bosmaniae **(Amaryllidaceae)**	used as decoctions to enhance the accuracy of the dice thrown by local diviners	Methanol extract (bulb)	Weak antioxidant	MPP^+-induced toxicity in SH-SY5Y neuroblastoma cells	Enhanced antioxidant defence mechanisms, increased cell proliferation, restored cellular morphology, inhibited ATP degeneration, and prevented MPP+-induced increase in ROS and caspase 3/7 activities in the cells.	Kangwa et al., 2024; Nair & van Staden, 2022; SANBI, 2005
Cassia singueana **(Caesalpiniaceae)**	Used to treat fever, conjunctivitis, convulsions, gonorrhoea, bilharzia, stomach-ache, constipation, epilepsy, and syphilis	Methanol extract (leaf)	Anticonvulsant, antioxidant, and antipsychotic	Ketamine-induced cognitive impairment in murine models of schizophrenia (Adult male Swiss albino mice)	Ameliorated cognitive impairment and negative symptoms of schizophrenics modulatory effect on NMDAR, normalisation of dopamine and serotonergic neurotransmission, and reduced reactive oxygen species accumulation activities.	Alkali et al., 2022
Carpobrotus edulis **(Aizoaceae)**	Used in the treatment of diarrhoea, burn wounds, diabetes mellitus, high blood pressure, intestinal worms, constipation tuberculosis, and sore throat or gum wounds	Sequential extraction Hexane, dichloromethane, ethyl acetate and ethanol extracts (leaves)	Antioxidant, immune modulating, antimicrobial, and anti-tumoral	Rotenone-induced toxicity in SH-SY5Y neuroblastoma cells	Protected neuronal cells from oxidative stress imposed by H_2O_2 treatment and reduced NO production in LPS-stimulated microglia cells, with the methanol extract being the most active,	Rocha et al., 2017

					followed by dichloromethane, ethyl acetate, then hexane extracts	
				AChE enzyme assay	Possessed anticholinesterase effect (methanol extract)	
***Crinum bulbispermum* (Amaryllidaceae)**	Used in the treatment of aching joints, rheumatism, varicose veins and backache, kidney or bladder infections, malaria earache, cough, colds, septic sores, and stimulate breast milk	Methanol extract (bulb)	Antimicrobial, antinociceptive, antiplasmodial, antioxidant, cytotoxicity, and anti-apoptotic, as well as causing central nervous system depression	Rotenone-induced toxicity in SH-SY5Y cells	Inhibited apoptotic activity and restored intracellular glutathione content following rotenone treatment	Maroyi, 2016; Seoposengwe et al., 2013
***Crossyne flava* (Amaryllidaceae)**	N/A	Methanol extract (bulb)	N/A	MPP^+-induced toxicity in SH-SY5Y cells	Inhibited ROS generation, ATP depletion, and apoptosis induction in the SH-SY5Y cells	Omoruyi et al., 2021; Nair & van Staden, 2022
				AChE enzyme assay	Possessed anticholinesterase effect	
		Bufanidrine	N/A	MPP^+-induced toxicity in SH-SY5Y cells	Inhibited ROS generation, ATP depletion, and apoptosis induction in the SH-SY5Y cells	Omoruyi et al., 2021; Elgorashi, 2019
		Buphanisine	SSRI, cytotoxic			
		Pancratinine B	N/A			
		Epibuphanisine	SSRI	MPP^+-induced toxicity in SH-SY5Y cells	Inhibited ROS generation, ATP depletion, and apoptosis induction in the SH-SY5Y cells	
				AChE enzyme assay	Possessed anticholinesterase effect	
***Euphorbia hirta* (Euphorbiaceae)**	Used to treat convulsions, insomnia, epilepsy, and mental illness	Methanol extract (whole plant)	GABAergic, anti-inflammatory; antirheumatic antioxidant, and sedative	Rat	Inhibited pro-inflammatory mediators TNF-α, IL-6, IL-1β and oxidative stress biomarkers (TBARS, GSH, CAT and SOD)	Ahmad et al., 2018
***Harpagophytum procumbens* (Pedaliaceae)**	Used to treat indigestion, allergic reactions, fever, urinary infections, postpartum pain, ulcers and Inflammatory bowel diseases	Capsule powder (suspended in 1% CMC)	Antidiabetic antirheumatic, antioxidant and antiinflammation	Female rat expose to arsenic	Reduced anxiety behaviour caused by arsenic through its anti-inflammatory and antioxidant effects	Peruru et al., 2020; Taïwe & Kuete, 2014
		Ethanolic extract (whole plant)		Rat	Stimulated, in a dose-dependent manner, rat cortex superoxide dismutase, catalase, and glutathione peroxidase activities, with a concomitant reduction of tissue lipid peroxidation	Bhattacharya & Bhattacharya, 1998; Menghini et al., 2019
		70% ethanolic extract and ethyl acetate fraction (root)		Male Wistar rats	The ethanolic extract and ethyl acetate fraction improved the viability of slices challenged with pro-oxidant stimuli (Fe2+, nitroprusside).	Schaffer et al., 2013; Menghini et al., 2019

					Demonstrated protective effect by reducing the MDA level as an index of lipid peroxidation	
		Ethyl acetate extract (whole plant)		AChE and BChE enzyme assay	Inhibited acetylcholinesterase and butyrylcholinesterase (BChE) enzymes	Bae et al., 2014; Menghini et al., 2019
		Aqueous extract (whole plant)		Rat cortex synaptomes challenged with amyloid β-peptide (1–40)	Improved the reduction of oxidative stress and protected against the decline in cortical dopamine (DA), norepinephrine (NE) and serotonin (5-hydroxytryptamine,) levels induced by amyloid β-peptide	Ferrante et al., 2017; Menghini et al., 2019
		Harpagoside	Anti-inflammatory, anti-rheumatic, and analgesic effects	scopolamine-induced amnesic mice	Exerted potent cognitive-enhancing activity through both anti-acetylcholinesterase and antioxidant mechanisms	Georgiev et al., 2013;Sun et al., 2013; Menghini et al., 2019
				amyloid β-peptide (1–40) injected Alzheimer's Disease rat model	Exerted neuroprotective effects on learning and memory deficit through the up-regulation of brain-derived neurotrophic factor (BDNF) expression and the activation of MAPK/ERC and PI3K/Akt pathways	Li et al., 2015; Menghini et al., 2019
Hibiscus asper **(Malvaceae)**	Used to treat inflammation, anaemia, jaundice, leucorrhoea, poison antidote, depression and dysmenorrhea	Methanol extract (leaves)	Antioxidant, anxiolytic, anti-inflammatory, antidepressant and antiapoptotic	6-hydroxydopamine-lesion rodent model of PD in male Wistar rats	Increased antioxidant enzyme activities (SOD, GPX and CAT), total GSH content and reduced lipid peroxidation (MDA level) in rat temporal lobe homogenates, possessing antiapoptotic activity	Hritcu et al., 2011
Hypericum perforatum **(Clusiaceae)**	Used to treat attention-deficit-hyperactivity disorders, anxiety, convulsions, fever, and pain	Flowers (Methanol extract)	Analgesic; psychomotor disturbances; antidepressant	Aluminium-maltolate-induced toxicity in SH-SY5Y cells	APP gene expression levels decreased depending on $Al(mal)_3$ toxicity in SH-SY5Y cells.	Akkuş et al., 2022
		Standardised extract of Hypericum perforatum SHP1 rich in hyperforin (6 %)		Rotenone model of PD	Decreased in nerve damage in the extract-administered group reduced neuronal damage, diminishing substantia nigra dopaminergic cell death caused by the pesticide, as well as inhibited the apoptotic cascade by decreasing Bax levels	Del Rio et al., 2013
		Aerial part (Ethanolic extract)		Amyloid-β peptide (25–35)-induced cell death	Prevented the amyloid-ß peptide (25-35)-mediated neuronal	Silva et al., 2004

				in rat cultured hippocampal neurons	neurodegeneration through its antioxidant effect	
		Standardised extract (0.3%) of Hypericum perforatum		Trauma-induced by hydrogen peroxide in PC12 Cells	Blocked DNA fragmentation and prevented the cells from shrinking and turning around of H_2O2-induced apoptosis in PC12 cells at concentrations of 10~100 µg/ml by significantly reduced ROS levels.	Lu et al., 2004
		Aerial part (70% ethanol extract)		Intrastriatal 6-Hydroxydopamine rat Model of PD	Attenuation of DNA fragmentation, astrogliosis, inflammation, and oxidative stress that may be of benefit in protective strategies for PD at its early stages.	Kiasalari et al., 2016
	N/A	Quercetin	Antibacterial, cardioprotective, antioxidant, immunostimulant, anti-inflammatory, antihypertensive and antidiabetic	Rat-cultured hippocampal neurons	Reduced mitochondrial lipid peroxidation and loss of mitochondrial transmembrane electric potential caused by oxidative stress induced by ADP plus iron	El-Saber Batiha et al., 2020; Silva et al., 2008
		Kaempferol	antioxidant, anti-inflammatory, anti-cancer, cardioprotective, anti-allergic, and anti-diabetic			Xue et al., 2023; Silva et al., 2008
		Biapigenin	N/A		Affected mitochondrial bioenergetics and decrease the capacity of mitochondria to accumulate calcium	Silva et al., 2008
***Lannea schweinfurthii* (Anacardiaceae)**	Used to enhance memory and to treat reproductive system disorders, respiratory disorders, injuries, headaches, blood system disorders, infections, and gastrointestinal disorders	Root bark (Methanol extract)	Anti-apoptotic, antibacterial, antiviral, anti-giardia, anti-inflammatory, antioxidant, antiplasmodial, anti-trypanosomal, hepatoprotective, larvicidal, and cytotoxic	Rotenone-induced toxicity in SH-SY5Y	Inhibited apoptotic activity and restored intracellular glutathione content following rotenone treatment	Maroyi, 2019; Seoposengwe et al., 2013
				AChE enzyme assay	Possessed acetylcholinesterase	
***Lessertia frutescens* (Fabaceae)**	Used to treat asthma, chronic bronchitis, colds, coughs, convulsions, diabetes mellitus, epilepsy, gastric, gout, heart failure, heartburn, hypertension, kidney and liver infections, menopausal symptoms, osteoarthritis, pains, peptic	Leaves (Aqueous extract)	Anticancer, antibacterial, antiviral, anti-inflammatory, antioxidant, antistress, antidiabetic, and cytotoxic	MPP^+-induced neurotoxicity model using SH-SY5Y cells	Enhanced antioxidant defence mechanisms, increased cell proliferation, restored cellular morphology, inhibited ATP degeneration, and prevented MPP+-induced increase in ROS and caspase 3/7 activities in the cells.	Gericke et al., 2001; Prevoo et al., 2004; Enogieru et al., 2020

	ulceration, rheumatoid arthritis, reflux oesophagitis, varicose veins, and stress-related conditions linked to the endocrine system					
Mentha aquatic	Used to prevent diseases such as cancer, heart problems, and Alzheimer's	Aqueous and ethanol extract (Leaf)	Antimicrobial, antioxidant, allergenic, analgesic, antipyretic, antiseptic, antispasmodic, anxiolytic, carminative, decongestant, deodorant, diaphoretic, digestive, diuretic, antiemetic, insecticides, sedatives, stimulatory, and vermifuge	MAO enzymes	Inhibited MAO and MAO-B, AChE	Stafford et al., 2007; Vi Nguyen Phuong Truong et al., 2022
	N/A	(*S*)-Naringenin	Antibacterial, antiinflammation, antioxidant, antidiabetic, antitumor, antihypertension, antifibrotic	rotenone-induced animal model of PD	Inhibited apoptosis and promote neuronal survival reduce caspase activation while upregulating the heat shock proteins 60, 70 and 90 and have an affinity to the $GABA_A$ benzodiazepine receptor	Cai et al., 2023; Enogieru et al., 2018
Scadoxus puniceus **(Amaryllidaceae)**	Used to treat Ulcers, blood purifiers, pain, wounds, fertility, inflammation in the gastrointestinal tract, hepatotoxicity, diarrhoea, nausea, hallucination, central nervous system excitation, pneumonia, tonsillitis, anxiety, diabetes, arthritis, dysmenorrhea, urinary and kidney infections	Bulb (Methanol extract)	Antimicrobial, antiseptic, anticonvulsant, and antioxidant	Rotenone-induced toxicity in SH-SY5Y	Inhibited apoptotic activity and restored intracellular glutathione content following rotenone treatment	Das et al., 2022; Seoposengwe et al., 2013
Strumaria truncata **(Amaryllidaceae)**	Mainly centred around local diviners to enhance the accuracy of their readings, to influence and affect the behaviour and mind of the person to whom they were administered		Weak antioxidant	MPP+-induced neurotoxicity model using SH-SY5Y cells	Enhanced antioxidant defence mechanisms, increase cell proliferation, restore cellular morphology, inhibit ATP degeneration, and prevent MPP+-induced increase in ROS and caspase 3/7 activities in the cells.	Kangwa et al., 2024; Nair & van Staden, 2022
Zanthoxylum capense **(Rutaceae)**	Epilepsy	Root Methanol extract	anti-mycobacterial, anti-proliferative effects, and antioxidant	rotenone-induced toxicity in SH-SY5Y	Inhibit apoptotic activity and restore intracellular glutathione content following rotenone treatment	Adebayo et al., 2015; Seoposengwe et al., 2013

2.2 South African cardioprotective plants

Cardiovascular diseases (CVDs) are among the leading causes of morbidity and mortality, particularly in low and middle-income countries (Mounika et al., 2021). In 2020, approximately 523 million people were affected by CVDs, leading to around 19 million deaths. This represents about 32% of all global deaths and reflects an 18.7% increase from 2010, placing a significant burden on global health and impacting the quality of life for many individuals (Coronado et al., 2022).

Ischemic heart disease, characterized by reduced blood flow to the heart muscle due to narrowed or blocked coronary arteries, remains the leading cause of CVDs-related mortality, responsible for the 9.14 million deaths in 2019 (Roth et al., 2020). Diabetes Mellitus, a prevalent metabolic disorder characterised by impaired glucose tolerance, is strongly associated with increased cardiovascular morbidity and mortality (Davì et al., 2013). While coronary artery disease is a primary cause of these deaths, diabetic cardiomyopathy is a serious complication of diabetes and obesity, occurring independently of coronary artery disease or hypertension (Dlula et al., 2017; Song et al., 2023). The pathogenesis of diabetic cardiomyopathy involves hyperglycemia and elevated free fatty acids, which lead to oxidative and endoplasmic reticulum (ER) stress, myocardial insulin resistance, inflammation, and cardiomyocyte apoptosis (Wu et al., 2021; Inoue et al., 2013).

Despite advancements in treatment, there is still a lack of effective therapies to fully protect the myocardium from various insults associated with ischemia-reperfusion injury, myocardial infarction and diabetic cardiomyopathy (Ferdinandy et al., 2023; Dludla et al., 2017). In this regard, research into medicinal plants, including those from South Africa, such as *Aspalathus linearis, Tacoma anomala, Leonotis Leonurus, protorhus longifolia,* and *Tinospora cordifolia,* has been conducted to explore their potential for protecting the heart from various insults, as detailed in Table 2.2, and to identify possible new therapeutic plant-derived agents.

Table 2.2: South African cardioprotective plants and their constituents

Plant name (Family)	Traditional uses	Other pharmacological properties	Extracts and isolated compounds	Experimental Model	Mode of action/ mechanisms of action	References
Aspalathus linearis **(Fabaceae)**	Health/functional beverage (used as tea and to improve appetite)	Neuroprotection, antioxidant, anti-inflammatory, anti-hyperglycaemic, anti-hyperlipidaemic, anti-HIV, bronchodilatory, antispasmodic, antiviral, antimicrobial, chemoprotective, anticarcinogenic and antiallergic activities	Aqueous extract (fermented rooibos)	Cardiomyocytes isolated from diabetic rats	Prevented experimentally induced oxidative stress and ischemia	Akinmoladun et al., 2014; Dludla et al., 2014; Erlwanger & Ibrahim, 2017
			Aqueous extracts (fermented and unfermented rooibos)	Non-diabetic rats	Reversed ischemia-reperfusion injury	Pantsi et al., 2011
		Antidiabetic and antioxidant	Aspalathin	H9c2 cardiomyocytes exposed to high glucose cardiomyocytes isolated from insulin-resistant rats	Prevented cell apoptosis by reducing phosphorylation of AMPK; decreased inflammation and lipid accumulation, and attenuated oxidative damage by increasing *NRF2* expression	Johnson, 2016, 2017; Dludla, 2017
				H9c2 cardiomyoblasts	Prevented Doxorubicin-induced cardiotoxicity through amelioration of mitochondria membrane depolarisation and cellular apoptosis	Samukelisiwe et al., 2019
		Antioxidant, antiaging, antiviral, antibacterial, anti-inflammation, vasodilatation, radiation protective, neuroprotective, antidepressant-like, anti-adipogenesis, and antinociceptive	Orientin	Isolated hearts of nondiabetic rats, rabbits and guinea pigs as well as H9c2 cells	Prevented ischemia-reperfusion injury and platelet aggregation by inhibiting mPTP formation and apoptosis	Liu et al., 2016; Lu et al., 2011; Lam et al., 2016
				Rats	Prevented myocardial infarction	Ku et al., 2014
				Non-diabetic rats	Attenuated ventricular remodelling associated with myocardial infarction	Liu et al., 2013
		Anticancer, antioxidant, anti-inflammatory, anti-nociceptive, anti-Alzheimer's disease, anti-hypertensive, anti-spasmodic, anti-depressant-like actions and anti-viral	Vitexin	Adult male Sprague-Dawley rats	Prevented ischemia-reperfusion injury by enhancing the antioxidant defence system, inhibiting Ca^{2+} overload and suppressing myocardial apoptosis	Che et al., 2016; He et al., 2016
				Isolated rat hearts	Prevented ischemia-reperfusion injury by reducing the oxidative stress level and inhibiting the release of inflammatory cytokines via attenuating expression of NF-$_k$B	Dong et al., 2013

					p65 and TNF-α, as well as the up-regulation of p-ERK and the downregulation of p-c-Jun expression	
				Primary rat cardiomyocytes	Protected against cardiac hypertrophy through Ca2+-mediated calcineurin-NFATc3 and CaMKII signalling pathways	Lu et al., 2013
				Rats	Attenuated acute doxorubicin cardiotoxicity by reducing oxidative stress and apoptosis	Sun et al., 2016
		Antioxidant and antiinflammation	Luteolin	Rat cardiomyocytes,	Prevented ischemia-reperfusion injury via the downregulation of microRNA-208b-3p	Bian et al., 2015
				Diabetic rats	Prevented ischemia-reperfusion injury by upregulating the myocardial NOS pathway, and downstream effects include the enhancement of MnSOD and inhibition of mPTP.	Yang et al., 2015
				STZ-induced diabetic mice	protected heart tissues by modulating NRF2-mediated oxidative stress and NF-κB-mediated inflammatory responses	Li et al., 2019
				Diabetic heart	Prevented ischemia-reperfusion injury by enhancing eNOS-mediated S-nitrosylation of KEAP1, with subsequent upregulation of NRF2 and the NRF2-related antioxidative signalling pathway	Xiao et al., 2019
				EA.hy926 human endothelial cell line Rat heart.	Activated the mitoBKCa channel, both in cardiomyocytes and in vascular endothelial cells.	Kampa et al., 2022
				Rat	Enhanced antioxidant activity and reduced NO production.	Liao et al., 2011
		Antioxidant, antimicrobial, anticancer, and antiinflammatory	Chrysoeriol	Rats under anesthesia and H9c2 cells	Reduced arterial blood pressure and protected against doxorubicin-induced cardiotoxicity	Aboulaghras et al., 2022;Khan et al., 2006; Liu et al., 2009
		Antibacterial, cardioprotective, antioxidant, immunostimulant, anti-inflammatory, antihypertensive and antidiabetic	Quercetin	Rats	Protected against diabetic cardiomyopathy, autoimmune myocarditis, LDL-oxidation, and doxorubicin-induced lipid peroxidation	Dludla et al., 2017; El-Saber Batiha et al., 2020
				Either endothelial cells or rats	Presented antihypertensive potential and reduced cardiac hypertrophy by increasing antioxidant capacity	
		Anti-inflammatory, anti-depressant, neuroprotective, anti-diabetic, anticancer, anti-	Hyperoside	*In vitro* and *in vivo*	Protected against hyperglycemia induced inflammation	Raza et al., 2017;Ku et al., 2014

		fungal, radioprotective, gastroprotective, and antioxidant activities		Rat subjected to thoracic aortic constriction	Enhanced autophagy activity by increasing LC3II and Beclin-1 levels, while reducing p62 level	Guo et al., 2020
				AngII-induced H9C2 cells	Inhibited apoptosis effects	
				myocardial ischemia mice	Ameliorated left ventricular remodelling as well as cytokines of serum, such as Lactic dehydrogenase, creatine kinase-MB, and cardiac troponin, with elevation of autophagic flux	Yang et al., 2021
				Rat	Protected cardiomyocytes from ischemia-reperfusion-induced oxidative stress through the activation of ERK-dependent signalling pathway	Li et al., 2013
				ECV304 cells	Prevented advanced glycation end products and promoted via the c-Jun N-terminal kinases (JNK) pathway	Dludla et al., 2017
				Hyperoxide *in vitro* and *in vivo*	Hydrogen peroxide-induced cell damage and ischemia-reperfusion injury	
		anti-inflammatory, hypoglycemic, antioxidant, neuroprotective, renal protective, and hepatoprotective	Rutin	STZ-induced diabetics rats	Protected against advanced glycation end products, oxidative stress and myocardial infarction	Xue et al., 2023; Dludla et al., 2017
					Mediated via alteration in TNF-α, CRP, and BNP levels coupled with antioxidant effect	Saklani et al., 2016
				Rats exposed to pirarubicin toxicity	Reduced serum levels of MDA, BNP, CK-MB, CTnT, and LDH and increased serum SOD levels. Treatment with rutin and dexrazoxane increased the Bcl-2/Bax ratio and reduced JNK and Caspase-3 protein levels	Wang et al., 2018
				H9c2 cells	Decreased NF-κB, Bax, TGF-β1, p38 MAPK, caspase-9, caspase-7, and caspase-3. It also increased cell viability, PI3K/Akt/mTOR activity, VEGF, and FGF1	Rahmani et al., 2023
		Antidiabetic	Phenylpyruvic acid-2-*O*-β-D-glucoside (PPAG)	PPAG on high-glucose exposed H9c2 cells	Protected against substrate impairment, mitochondrial depolarisation and cell apoptosis	Dludla et al., 2016
			PPAG and aspalatin	H9c2 cardiomyocytes exposed to high glucose cardiomyocytes	Regulated cardiac substrate metabolism by improving FFA and glucose oxidation, reduced oxidative stress by suppressing ROS and iNOS activities and concomitantly strengthened intracellular antioxidants such as GSH.	Dludla et al., 2020

				isolated from insulin-resistant rats		
Dicoma anomala (Asteraceae)		Antioxidant Antidiabetic Cardioprotection	Aqueous extract (root)	isoproterenol–induced myocardial infarction in Wistar rats	Ameliorated isoproterenol–induced myocardial infarction	
Leonotis leonurus (Lamiaceae)	Treatment of coughs, colds, influenza, bronchitis, headaches, high Blood pressure, and other cardiovascular ailments	Anticonvulsant, anticoagulant, antiplatelet and antiinflammatory effects (cox-1), cardioprotective Antioxidant Antibacterial, antidiabetic	Marrubiin	Rats	Inhibited platelet aggregation, hypercoagulation and the inflammation	Mnonopi et al., 2011
Protorhus longifolia (Anacardiaceae)	N/A	N/A	3β-hydroxylanosta-9,24-dien-21-oate RA-3	Isoproterenol-induced myocardial injury in rats	Increased endogenous antioxidant capacity and prevent lipid peroxidation. It also increased serum GSH content and CAT activity, along with a decrease in MDA content	Mosa et al., 2016
				streptozotocin (STZ)-induced diabetic rats	Increased endogenous antioxidant capacity	Mosa et al., 2015
Tinospora cordifolia (Menispermaceae)	N/A	N/A	Ethanol extract	Isoprenaline-induced ischemia-reperfusion in rats	Strengthened the myocardial membrane by its membrane-stabilizing activity as well as reduced oxidative stress level by enhancing the endogenous antioxidant levels or by protecting Mg^{2+} dependant Ca^{2+} ATP enzyme or by antagonising free radical-mediated inhibition of sarcolemmal $Na^{+}K^{+}$ ATPase activity or by Ca^{2+}channel blocking activity	Vijaya Nirmala & Abinaya, 2019; Sharma et al., 2011

2.3 Conclusion

The medicinal plants in Table 2.1 exhibit promising neuroprotective potential against Parkinson's disease (PD) and Alzheimer's disease (AD). These effects are mediated through multiple mechanisms, including their potent antioxidant activity, which reduces reactive oxygen species (ROS) and enhances intracellular glutathione levels. Additionally, their anti-apoptotic properties involve the inhibition of caspase pathways. At the same time, their ability to mitigate neuroinflammation is evident through the suppression of pro-inflammatory cytokines such as TNF-α, IL-1β, and IL-6. Furthermore, these plants demonstrate their protective roles by improving mitochondrial function, enhancing ATP generation, and regulating cholinergic systems by inhibiting acetylcholinesterase AChE and BChE.

Similarly, the cardioprotective effects highlighted in Table 2.2 reveal the potential of these plants to shield myocardial tissues from apoptosis, oxidative damage, and ischemic stress. This cardioprotection is achieved through critical mechanisms such as the inhibition of mPTP formation, upregulation of NRF2 pathways, and reduction in inflammatory cytokines like TNF-α and IL-6.

Overall, the data presented in this study highlight the therapeutic potential of South African medicinal plants in protecting heart and brain tissues from a range of pathological insults while also showcasing the diverse mechanisms through which they mitigate the pathogenesis of neurodegenerative and cardiovascular diseases.

References

Adebayo, S. A., Dzoyem, J. P., Shai, L. J. & Eloff, J. N. (2015). The anti-inflammatory and antioxidant activity of 25 plant species used traditionally to treat pain in southern African. *BMC Complementary and Alternative Medicine, 15*(159): 1-10.

Ahmad, P., Adak, M., Hussain, A., Wahab, S., Singh, S., Mishra, C. & Sinha, R. (2018). Ameliorative Potential of Euphorbia hirta (Linn.) Extract against Lipopolysaccharide Induced-neuroinflammation and Oxidative Damage in Rats. *Biochemistry & Pharmacology*, *7*(3): 1-4.

Akah, P. A. (2023). Annona senegalensis Pers (Annonaceae): exploring the underutilized potentials of an African medicinal plant. *Journal of Ethnopharmacology and Toxicology*, *1*(1): 16-26.

Akinmoladun, A. C., Olaleye, M. T. & Farombi, E. O. (2014). Cardiotoxicity and Cardioprotective Effects of African Medicinal Plants. In Kuete, V. (Ed). *Toxicological Survey of African Medicinal Plants*. Elsevier Inc.

Akkuş, R. Y., Bitmez, B., Kuşoğlu Gültekin, S., Albayrak, İ. G., Özen, F., Deveci, Y., Sicak, Y., Akalin, E., Pirhan, A. F. & Atasever Arslan, B. (2022). Neuroprotective effect of Hypericum perforatum extract against Aluminum-maltolate induced toxicity in SH-SY5Y cells. *International Journal of Science Letters*, 4(2): 277-291.

Alkali, I. Y., Garba, M. M. & Ya'u, J. (2022). Ameliorative effect of Cassia singueana extract against acute ketamine induced cognitive impairment in murine models of schizophrenia. *GSC Biological and Pharmaceutical Sciences*, 21(2): 274-285.

Cai, J., Wen, H., Zhou, H., Zhang, D., Lan, D., Liu, S., Li, C., Dai, X., Song, T., Wang, X., He,

Y., He, Z., Tan, J. & Zhang, J. (2023). Naringenin: A flavanone with anti-inflammatory and anti-infective properties. In *Biomedicine and Pharmacotherapy*, 164: 1-16.

Chattopadhyay, S., Chattopadhyay, U., Mathur, P. P., Saini, K. S. & Ghosal, S. (1983). Effects of Hippadine, an Amaryllidaceae Alkaloid, on Testicular Function in Rats1. *Plantamedica*, 49: 252-254.

Che, X., Wang, X., Zhang, J., Peng, C., Zhen, Y., Shao, X., Zhang, G. & Dong, L. (2016). Vitexin exerts cardioprotective effect on chronic myocardial ischemia/reperfusion injury in rats via inhibiting myocardial apoptosis and lipid peroxidation. In *Am J Transl Res*, 8(8): 3319-28.

Chen, S., Yang, B., Xu, Y., Rong, Y. & Qiu, Y. (2018). Protection of Luteolin-7-O-glucoside against apoptosis induced by hypoxia/reoxygenation through the MAPK pathways in H9c2 cells. *Molecular Medicine Reports*, 17(5): 7156-7162.

Das, R., Barman, A. & Ray, S. (2022). Traditional knowledge, phytochemistry, and pharmacological properties of the African genus Scadoxus (Amaryllidaceae). In *South African Journal of Botany*, 151: 565-577.

Dludla, P. V., Joubert, E., Muller, C. J. F., Louw, J. & Johnson, R. (2017). Hyperglycemia-induced oxidative stress and heart disease-cardioprotective effects of rooibos flavonoids and phenylpyruvic acid-2-O-β-D-glucoside. In *Nutrition and Metabolism*, 14(45): 1-18.

Dludla, P. V., Muller, C. J. F., Louw, J., Joubert, E., Salie, R., Opoku, A. R. & Johnson, R. (2014). The cardioprotective effect of an aqueous extract of fermented rooibos (Aspalathus linearis) on cultured cardiomyocytes derived from diabetic rats. *Phytomedicine*, 21(5): 595-601.

Dludla, P. V., Muller, C. J. F., Louw, J., Mazibuko-Mbeje, S. E., Tiano, L., Silvestri, S., Orlando, P., Marcheggiani, F., Cirilli, I., Chellan, N., Ghoor, S., Nkambule, B. B., Essop, M. F., Huisamen, B. & Johnson, R. (2020). The combination effect of aspalathin and phenylpyruvic acid-2-*O*-*β*-*D*-glucoside from rooibos against hyperglycemia-induced cardiac damage: An *in vitro* study. *Nutrients*, 12: 1-12.

Dong, L. Y., Li, S., Zhen, Y. L., Wang, Y. N., Shao, X. & Luo, Z. G. (2013). Cardioprotection of vitexin on myocardial ischemia/Reperfusion injury in rat via regulating inflammatory cytokines and MAPK pathway. *American Journal of Chinese Medicine*, 41(6): 1251-1266.

Elgorashi, E. E. (2019). Phytochemistry and Pharmacology of the Family Amaryllidaceae: An Overview of Research at RCPGD. *Natural Product Communications*, 14(9): 1-11.

El-Saber Batiha, G., Beshbishy, A. M., Ikram, M., Mulla, Z. S., Abd El-Hack, M. E., Taha, A. E., Algammal, A. M. & Ali Elewa, Y. H. (2020). The pharmacological activity, biochemical properties, and pharmacokinetics of the major natural polyphenolic flavonoid: Quercetin. *Foods*, 9(3): 1-6.

Enogieru, A. B., Omoruyi, S. I., Hiss, D. C. & Ekpo, O. E. (2018). Potential antiparkinsonian agents derived from South African medicinal plants. *Journal of Herbal Medicine*, 13: 1-7.

Erlwanger, K. H. & Ibrahim, K. G. (2017). Aspalathin a unique phytochemical from the South African rooibos plant (*Aspalathus linearis*): A mini-Review. *Journal of African Association of Physiological Sciences*, 5(1): 1-6.

Georgiev, M. I., Ivanovska, N., Alipieva, K., Dimitrova, P. & Verpoorte, R. (2013). Harpagoside: From Kalahari Desert to pharmacy shelf. *Phytochemistry*, 92: 8-15.

Guo, X., Zhang, Y., Lu, C., Qu, F. & Jiang, X. (2020). Protective effect of hyperoside on heart failure rats via attenuating myocardial apoptosis and inducing autophagy. *Bioscience, Biotechnology and Biochemistry*, 84(4): 714-724.

Higuchi, M., Okumura, M., Mitsuta, S. & Shirouchi, B. (2024). Dietary Cholest-4-en-3-one, a Cholesterol Metabolite of Gut Microbiota, Alleviates Hyperlipidemia, Hepatic Cholesterol Accumulation, and Hyperinsulinemia in Obese, Diabetic db/db Mice. *Metabolites*, *14*: 1-14.

Hritcu, L., Foyet, H. S., Stefan, M., Mihasan, M., Asongalem, A. E. & Kamtchouing, P. (2011). Neuroprotective effect of the methanolic extract of *Hibiscus asper* leaves in 6-

hydroxydopamine-lesioned rat model of Parkinson's disease. *Journal of Ethnopharmacology*, 137(1): 585-591.

Ibrakaw, A. S., Omoruyi, S. I., Ekpo, O. E. & Hussein, A. A. (2020). Neuroprotective Activities of Boophone haemanthoides (Amaryllidaceae) Extract and Its Chemical Constituents. *Molecules*, 25: 1-17.

Kampa, R. P., Flori, L., Sęk, A., Spezzini, J., Brogi, S., Szewczyk, A., Calderone, V., Bednarczyk, P. & Testai, L. (2022). Luteolin-Induced Activation of Mitochondrial BKCa Channels: Undisclosed Mechanism of Cytoprotection. *Antioxidants*, 11: 1-20.

Kangwa, T. S., Hiss, D. C., Hussein, A. A., Ekpo, O. E. & Omoruyi, S. I. (2024). *In vitro* neuroprotective effects of *Boophone disticha*, *Brunsvigia bosmaniae* and *Strumaria truncata* extracts in SH-SY5Y cells. *South African Journal of Botany*, 166: 512-524.

Kiasalari, Z., Baluchnejadmojarad, T. & Roghani, M. (2016). *Hypericum Perforatum* Hydroalcoholic Extract Mitigates Motor Dysfunction and is Neuroprotective in Intrastriatal 6-Hydroxydopamine Rat Model of Parkinson's Disease. *Cellular and Molecular Neurobiology*, 36(4): 521–530.

Kosuge, Y., Kaneko, E., Nango, H., Miyagishi, H., Ishige, K., & Ito, Y. (2020). *Bidens pilosa* Extract Administered after Symptom Onset Attenuates Glial Activation, Improves Motor Performance, and Prolongs Survival in a Mouse Model of Amyotrophic Lateral Sclerosis. *Oxidative Medicine and Cellular Longevity*, 1-11.

Li, L., Luo, W., Qian, Y., Zhu, W., Qian, J., Li, J., Jin, Y., Xu, X. & Liang, G. (2019). Luteolin protects against diabetic cardiomyopathy by inhibiting NF-κB-mediated inflammation and activating the NRF2-mediated antioxidant responses. *Phytomedicine*, 59: 1-39.

Li, Z. L., Hu, J., Li, Y. L., Xue, F., Zhang, L., Xie, J. Q., Liu, Z. H., Li, H., Yi, D. H., Liu, J. C. & Wang, S. W. (2013). The effect of hyperoside on the functional recovery of the ischemic/reperfused isolated rat heart: Potential involvement of the extracellular signal-regulated kinase 1/2 signaling pathway. *Free Radical Biology and Medicine*, 57: 132-140.

Liao, P. H., Hung, L. M., Chen, Y. H., Kuan, Y. H., Zhang, F. B. Y., Lin, R. H., Shih, H. C., Tsai, S. K. & Huang, S. S. (2011). Cardioprotective effects of luteolin during ischemia-reperfusion injury in rats. *Circulation Journal*, *75*(2): 443-450.

Lu, Y.-H., Du, C.-B., Liu, J.-W., Hong, W. & Wei, D.-Z. (2004). Neuroprotective Effects of Hypericum perforatum on Trauma Induced by Hydrogen Peroxide in PC12 Cells. *The American Journal of Chinese Medicine*, 32(3): 397-405.

Marković, A. K., Torić, J., Barbarić, M. & Brala, C. J. (2019). Hydroxytyrosol, tyrosol and derivatives and their potential effects on human health. *Molecules*, 24(10): 1-10.

Maroyi, A. (2016). Ethnobotanical, phytochemical and pharmacological properties of crinum bulbispermum (Burm f) milne-redh and schweick (Amaryllidaceae). *Tropical Journal of Pharmaceutical Research*, 15(11): 2497-2506.

Menghini, L., Recinella, L., Leone, S., Chiavaroli, A., Cicala, C., Brunetti, L., Vladimir-Knežević, S., Orlando, G. & Ferrante, C. (2019). Devil's claw (Harpagophytum procumbens) and chronic inflammatory diseases: A concise overview on preclinical and clinical data. In *Phytotherapy Research*, 33(9): 2152-2162.

Mnonopi, N., Levendal, R. A., Davies-Coleman, M. T. & Frost, C. L. (2011). The cardioprotective effects of marrubiin, a diterpenoid found in Leonotis leonurus extracts. *Journal of Ethnopharmacology*, 138(1): 67-75.

Mosa, R. A., Hlophe, N. B., Ngema, N. T., Penduka, D., Lawal, O. A. & Opoku, A. R. (2016). Cardioprotective potential of a lanosteryl triterpene from Protorhus longifolia. *Pharmaceutical Biology*, 54(12): 3244-3248.

Nair, J. J. & Van Staden, J. (2014). Traditional usage, phytochemistry and pharmacology of the South African medicinal plant *Boophone disticha* (L.f.) Herb. (Amaryllidaceae). In *Journal of Ethnopharmacology*, 151(1): 12-26.

Ndam Ngoungoure, V. L., Muñoz, P., Tizabi, Y., Valdes, R., Fewou Moundipa, P. & Segura-Aguilar, J. (2019). Protective Effects of Crude Plant Extracts against Aminochrome-

induced toxicity in Human Astrocytoma Cells: Implications for Parkinson's Disease. *Clin Pharmacol Transl Med.*, 3(1): 125-133.

Omoruyi, S. I., Ibrakaw, A. S., Ekpo, O. E., Boatwright, J. S., Cupido, C. N. & Hussein, A. A. (2021). Neuroprotective activities of *Crossyne flava* bulbs and amaryllidaceae alkaloids: Implications for Parkinson's disease. *Molecules*, *26*(13): 1-14.

Peruru, R., Usha Rani, R., Thatiparthi, J., Sampathi, S., Dodoala, S. & Prasad, K. V. S. R. G. (2020). Devil's claw (*Harpagophytum procumbens*) ameliorates the neurobehavioral changes and neurotoxicity in female rats exposed to arsenic. *Heliyon*, 6(5): 1-8.

Rahmani, S., Naraki, K., Roohbakhsh, A., Hayes, A. W. & Karimi, G. (2023). The protective effects of rutin on the liver, kidneys, and heart by counteracting organ toxicity caused by synthetic and natural compounds. *Food Science and Nutrition*, 11(1): 39-56.

Rocha, M. I., Rodrigues, M. J., Pereira, C., Pereira, H., da Silva, M. M., da Neng, N. R., Nogueira, J. M. F., Varela, J., Barreira, L. & Custódio, L. (2017). Biochemical profile and *in vitro* neuroprotective properties of *Carpobrotus edulis* L., a medicinal and edible halophyte native to the coast of South Africa. *South African Journal of Botany*, 111: 222-231.

Saklani, R., Gupta, S. K., Mohanty, I. R., Kumar, B., Srivastava, S. & Mathur, R. (2016). Cardioprotective effects of rutin via alteration in TNF-α, CRP, and BNP levels coupled with antioxidant effect in STZ-induced diabetic rats. *Molecular and Cellular Biochemistry*, 420(1–2): 65-72.

SANBI, 2005. *Brunsvigia-bosmaniae* available at https://pza.sanbi.org/brunsvigia-bosmaniae

Seoposengwe, K., Van Tonder, J. J. & Steenkamp, V. (2013). *In vitro* neuroprotective potential of four medicinal plants against rotenone-induced toxicity in SH-SY5Y neuroblastoma cells. *BMC Complementary and Alternative Medicine*, 13: 1-16.

Sharma, A. K., Kishore, K., Sharma, D., Srinivasan, B. P., Agarwal, S. S., Sharma, A., Singh, S. K., Gaur, S. & Jatav, V. S. (2011). Cardioprotective activity of alcoholic extract of *Tinospora cordifolia* (Willd.) Miers in calcium chloride-induced cardiac arrhythmia in rats. *Journal of Biomedical Research*, 25(4): 280-286.

Silva, B. A., Dias, A. C. P., Ferreres, F., Malva, J. O. & Oliveira, C. R. (2004). Neuroprotective Effect of *H. perforatum* Extracts on β-Amyloid-induced Neurotoxicity. *Neurotoxicity Research*, 6(2): 119-130.

Silva, B., Oliveira, P. J., Dias, A. & Malva, J. O. (2008). Quercetin, Kaempferol and Biapigenin from Hypericum perforatum are Neuroprotective Against Excitotoxic Insults. *Neurotoxicity Research*, 13(3-4): 265-279.

Stafford, G. I., Pedersen, P. D., Jäger, A. K. & Van Staden, J. (2007). Monoamine oxidase inhibition by southern African traditional medicinal plants. *South African Journal of Botany*, 73(3): 384-390.

Taïwe, G. S. & Kuete, V. (2014). Neurotoxicity and Neuroprotective Effects of African Medicinal Plants. In Kuete, V. (Ed). *Toxicological Survey of African Medicinal Plants*. Elsevier.

Tsai, P.-L., Wang, J.-P., Chang, C.-W., Kuo, S.-C. & Chao, P.-D. L. (1998). Constituents And Bioactive Principles of *Polygonum Chinensis*. *Phytochemistry*, 49(6): 1663-1666.

Tsuruta, K., Shidara, T., Miyagishi, H., Nango, H., Nakatani, Y., Suzuki, N., Amano, T., Suzuki, T. & Kosuge, Y. (2023). Anti-Inflammatory Effects of Miyako Bidens pilosa in a Mouse Model of Amyotrophic Lateral Sclerosis and Lipopolysaccharide-Stimulated BV-2 Microglia. *International Journal of Molecular Sciences*, 24(18): 1-14.

Vijaya Nirmala, R. & Abinaya, R. (2019). An Effect of Cardioprotective Activity In Various Medicinal Plants–A Review. *International Journal of Current Pharmaceutical Research*, 11(2): 1-6.

Wang, Y. Di, Zhang, Y., Sun, B., Leng, X. W., Li, Y. J. & Ren, L. Q. (2018). Cardioprotective effects of rutin in rats exposed to pirarubicin toxicity. *Journal of Asian Natural Products Research*, 20(4): 361-373.

Xiao, C., Xia, M. L., Wang, J., Zhou, X. R., Lou, Y. Y., Tang, L. H., Zhang, F. J., Yang, J. T. & Qian, L. B. (2019). Luteolin Attenuates Cardiac Ischemia/Reperfusion Injury in Diabetic Rats by Modulating NRF2 Antioxidative Function. *Oxidative Medicine and Cellular Longevity*, 2019: 1-9.

Xue, J. C., Yuan, S., Meng, H., Hou, X. T., Li, J., Zhang, H. M., Chen, L. L., Zhang, C. H. & Zhang, Q. G. (2023). The role and mechanism of flavonoid herbal natural products in ulcerative colitis. *Biomedicine and Pharmacotherapy*, 158: 1-15.

Yang, J.-T., Qian, L.-B., Zhang, F.-J., Wang, J., Ai, H., Tang, L.-H. & Wang, H.-P. (2015). Cardioprotective Effects of Luteolin on Ischemia/Reperfusion Injury in Diabetic Rats Are Modulated by eNOS and the Mitochondrial Permeability Transition Pathway. *J Cardiovasc Pharmacol.*, 65: 349-356.

Yang, Y., Li, J., Rao, T., Fang, Z. & Zhang, J. (2021). The role and mechanism of hyperoside against myocardial infarction in mice by regulating autophagy via NLRP1 inflammation pathway. *Journal of Ethnopharmacology*, 276: 1-10.

Yao, H., Zhou, L., Tang, L., Guan, Y., Chen, S., Zhang, Y. & Han, X. (2017). Protective effects of luteolin-7-O-glucoside against starvationinduced injury through upregulation of autophagy in H9c2 Cells. *BioScience Trends*, 11(5): 557-564.

CHAPTER THREE: Phytochemistry, Ethnopharmacology and Phytotherapy of *Lessertia frutescens* (Cancer Bush): A Comprehensive Review

Kadidiatou O. Ndjoubi[1], Rajan Sharma[1] and Ahmed A. Hussein[1]
[1]Chemistry Department, Cape Peninsula University of Technology, Bellville Campus, Symphony Road, 7535 Bellville, South Africa
*Correspondence: mohammedam@cput.ac.za

Abstract

Lessertia frutescens, commonly known as cancer bush, is one of the most prominently used South African medicinal plants, with a rich history of traditional uses among indigenous communities. Its phytochemical investigations have led to the isolation of three amino acids (**3.1**-**3.3**), two non-protein amino acids (**3.5**-**3.6**), an essential fatty acid (**3.4**), a sugar (**3.7**), six flavonoid glycosides (**3.8**-**3.13**), thirteen cycloartenol glycosides (**3.14**-**3.31**), and an oleanane-type saponin (**3.32**).

Moreover, several research studies have highlighted the promising therapeutic effects of *L. frutescens* in combating various cancer cell lines. Beyond its anticancer properties, this medicinal plant demonstrated potent immunomodulatory, antioxidant, anti-inflammatory, antidiabetic, neuroprotective, anti-stress, and antimicrobial activities. These findings make *L. frutescens* a promising candidate for exploring and developing new or complementary drugs for treating various diseases and ailments.

Keywords: *Lessertia frutescens*, ethnopharmacology, phytochemistry, and phytotherapy.

3.1 Introduction

Lessertia frutescens, an indigenous Southern African medicinal plant belonging to the Fabaceae family, is prominent in traditional medicine (Van Wyk et al., 1997). Commonly referred to as “cancer bush”, it ranks among the foremost medicinal plants in South African herbal pharmacopoeia (Mncwangi et al., 2023). The leaves and stems are the most studied part of the plant. *L. frutescens* is widely spread in the Eastern Cape, KwaZulu Natal, Northern Cape, and Western Cape, where it plays a crucial role in ameliorating the body's ability to combat diseases and ailments. Moreover, it aids in reducing mental and physical stress by helping the body to mobilise its physiological and immunological resources (Ojewole, 2008; Van Wyk & Albrecht, 2008; Van Wyk et al., 1997). This results in the plant being regarded as an adaptogenic tonic which is safe to use since the only side effects are sporadic dry mouth, dizziness, mild diuresis, and diarrhoea in cachectic patients (Johnson et al., 2007; Ojewole, 2008). Decoctions of *L. frutescens* have been used to treat various diseases and ailments such as asthma, chronic

bronchitis, colds, coughs, convulsion, diabetes mellitus, epilepsy, gastric, gout, heart failure, heartburn, hypertension, kidney and liver infections, menopausal symptoms, osteoarthritis, pains, peptic ulceration, rheumatoid arthritis, reflux oesophagitis, varicose veins, and stress-related conditions linked to the endocrine system (Gericke et al., 2001; Prevoo et al., 2004; Mills et al., 2005; Ojewole, 2008). Furthermore, the plant has been used as drug support in the treatment of anorexia, cancer, influenza, HIV/AIDS, and tuberculosis (Gericke et al., 2001). In 2002, several clinical trials were conducted to verify the assertions made by indigenous regarding the safety, potency, and therapeutical uses of *L. frutescens*. Following a three-month clinical trial assessing the plant's toxicity using vervet monkeys, it was discovered that ingestion of the plant extract at human-equivalent dosages showed no toxicity or adverse effects. Consequently, the South African Medical Research Council (MRC) affirmed the safety of *L. frutescens* decoctions, infusions, and tinctures for consumption (Morris, 2001; Mills et al., 2005).

This review aims to provide a detailed overview of the ethnobotany, phytochemistry, ethnopharmacology, and therapeutic potential of *L. frutescens,* emphasising its rich history of traditional use and the advancements in modern research on its phytotherapeutic applications.

3.2 Taxonomy, nomenclature, and distribution

The *Lessertia* genus, belonging to the Fabaceae family, comprises 62 accepted species (POWO, 2023). Some of these species were formerly classified under the *Sutherlandia* genus, such as *Lessertia frustescens*, previously known as *Sutherlandia frutescens* (POWO, 2023; Van Wyk & Gorelik, 2017). Prior to the reclassification of the *Sutherlandia* species, 35 species within the *Lessertia* genus were endemic to South Africa (Balkwill & Balkwill, 1999).

L. frutescens stands out as one of the most extensively studied and utilised medicinal plants in South Africa. It is known by names such as umnwele in Xhosa, blaasbossie in Afrikaans, Insiswa in Zulu, and Musa-Pelo in Sotho (Jackson, 1990). It is also associated with around twenty-five common names in languages like Afrikaans, Zulu, Tswana, and Sotho, which often reflect aspects of its characteristics, including its seedpods (blaasbossie and blaas-ertjie), flower colour or shape (kalkoenbos, hoenderbelletjie, eendjie), appearance (unwele); taste (bitterbos), or medical uses (kankerbos, insiswa, phetola, and lerumo lamadi) (Aboyade et al., 2013).

3.3 Botanical Description

L. frutescens (Figure 3.1) is a perennial non-climbing shrub, typically reaching heights between 0.2 to 2.5 m (Schrire & Andrews, 1992). Its leaves are greyish-green pinnately compounds, with each leaflet measuring 4-10 mm. These leaflets vary from elliptic to narrowly oblong or

ovate-oblong, with the adaxial leaflets' surface ranging from glabrous to sericeous depending on the plant's cultivation region (Van Wyk & Albrecht, 2008). The prostate to erect stems is either sparsely pubescent or glabrous, with many leaves in terminal racemes (PlantzAfrica, 2013; Van Wyk & Albrecht, 2008). Its orange-red butterfly-shaped flowers (35 mm long) appear in short clusters within the leaf axils at branch tips from September to December (Adefuye, 2016). After flowering, the plant produces inflated bladder-like pod fruits that contain black seeds (Schrire & Andrews, 1992; Daghman, 2015).

Figure 3.1: *Lessertia frutescens*

3.4 Economic importance of *Lessertia frutescens*

In South Africa, the commercial value of *L. frutescens* lies in its renowned ethnopharmacological applications, particularly in treating internal cancers, HIV/AIDS, and diabetes. Additionally, it is prized for its immune-boosting and antioxidant properties and its use as a skincare product. Over the past decade, the plant has been sold in various forms, including capsules, tablets, teas, syrup, soap, cream, and raw materials products available in local shops and pharmacies, such as Dischem, Faithful to Nature, and Pharmadiv with prices ranging from R38 to R200 per unit (Table 3.1).

Table 3.1: The different forms of *L. frutescens* in the market (Picture sourced from Dischem, Faithful to Nature, and Pharmadiv)

Moreover, the global trade of *L. frutescens* extends to regions such as North and South America, Western and Eastern Europe, Asia-Pacific, the Middle East, and Africa, with Africa and the Middle East holding a significant share of the global trade. Companies such as Afriplex, Medico Herbs, Global Fusion Natural, Afrinaturals, and Geva SA are leading retailers and distributors of the various processed and semi-processed forms of *L. frutescens* (Persistence Market Research, 2024).

Its popularity in traditional medicine has sparked significant scientific interest in understanding the pharmacokinetics and pharmacodynamics of *L. frutescens* crude extracts and identifying the specific metabolites responsible for its ethnobotanical properties and its ability to treat conditions related to oxidative stress. These investigations have prompted companies and researchers to patent their formulations and extraction methods for sale (Marais et al., 2022; Visser, 2012).

3.6 Ethnomedicinal uses

In South Africa, *L. frutescens* has been a staple in traditional medicine, utilised by healers, herbalists, diviners, and local people to treat various ailments and diseases. Despite its bitterness, it has gained popularity as a medicinal tea due to its liquorice aftertaste (Van Wyk & Gorelik, 2017). Since 1895, the Khoisan and Cape Dutch have known this flowering shrub as a cancer bush due to its potency against internal cancers (Van Wyk & Albrecht, 2008; Drewes, 2012; Street & Prinsloo, 2012). Conversely, the Nama and Khoi-San communities traditionally use decoctions of the plant to treat fevers and wounds (Street & Prinsloo, 2012). Historically, Zulu warriors would consume a concoction of the plant to induce relaxation following the battle. In contrast, the widows of the deceased warriors used it as an antidepressant to help them navigate through their grief. In Van Wyk and Albrecht's (2008) review on the ethnobotany of *L. frutescens*, it was revealed that decoctions or infusions of the leaves were used in the treatment of diarrhoea, urinary tract infection, rheumatism, inflammation, intestinal pain, haemorrhoids, eyes diseases, chickenpox, and skin disorder. Moreover, the plant is a tonic that cleanses blood, stimulates appetite, and aids digestion (Aboyade et al., 2013; Van Wyk & Albrecht, 2008). Traditionally, an infusion made from three teaspoons of the plant stems and leaves taken daily was believed to cure some illnesses such as diabetes, stomach pain, fever, backache, kidney and liver disorders, influenza, colds, and bladder problems (Thring & Weitz, 2006).

3.5 Phytochemistry

The phytochemical studies conducted on *L. frutescens* have revealed that the leaves contain a high concentration of free amino acids such as *L*-asparagine (1.6-35.0mg/g, **3.1**), proline (0.7-7.5 mg/g, **3.2**) and *L*-arginine (0.5-6.7 mg/g, **3.3**) (Van Wyk & Albrecht, 2008). Additionally, the essential omega-3 fatty acid α-linolenic acid (**3.4**) was isolated from the dichloromethane: methanol (1:1) extract of the aerial part of the plant (Masoko et al., 2016). For the first time, Moshe (1998) isolated *L*-canavanine (**3.5**), a non-protein amino acid usually found in the seed, from the leaves of *L. frutescens*. Furthermore, γ-aminobutyric acid (GABA, **3.6**) was identified as another non-protein-free amino acid in the leaves. The cyclitol D-pinitol (**3.7**), known for its antidiabetic activity, was also isolated from the plant leaves. In addition to these compounds, researchers Fu and colleagues (2008, 2010a, 2010b and 2012) isolated and identified four flavonoid glycosides, named sutherlandins A–D (**3.8**-**3.11**) (Figure 3.2).

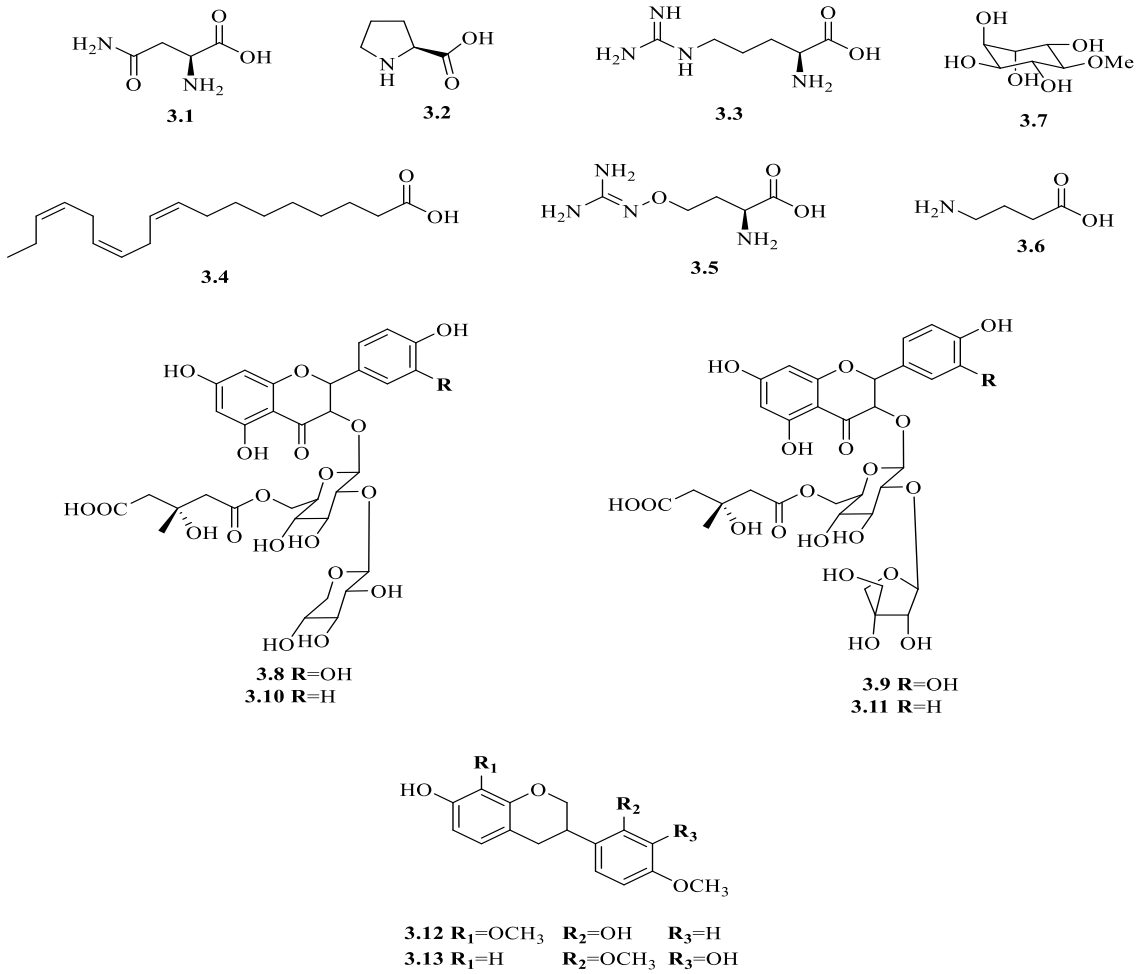

Figure 3.2: Chemical constituents of *L. frutescens* isolated compounds (**3.1- 3.13**)

Fu et al., (2010a, 2010b and 2012) reported the isolation of 8 cycloartane glycoside given the trivial name of sutherlandiosides A-H (**3.14-3.21**) (Figure 3.3). Compounds **3.20** and **3.21** exhibited novel rearrangements in their cycloartenol glycoside structures, featuring a rearranged five- and seven-membered A/B-ring system. This discovery marked the first observation of the hexadecahydro-1-H-indeno[5,4-f] azulene ring system in nature (Fu et al., 2010b). Recently, the oleanan-type saponin 3-*O*-[α-L-rhamnopyranosyl-(1→3)-*β*-*D*-glucuronopyranosyl]-22-epi-soyasapogenol B-22-*O*-*β*-*D*-glucopyranoside (**2.32**), along with seven cycloartane glycoside compounds named sutherlandiosides E-K (**3.22-3.27**) were isolated (Tchegnitegni et al., 2024). However, some of these trivial names, specifically sutherlandiosides E-H (**3.22**-**3.25**), have already been assigned by Fu (2012) to two 9,10-seco-cycloartane-type diglycosides with an unprecedented 5/7/6/5 ring skeleton (**3.20** and **3.21**) and two cycloartane-type diglycosides (**3.18** and`**3.19**). Moreover, the cycloartane glycoside sutherlandioside I reported as new by Tchegnitegni and co-workers (2024) had already been identified as sutherlandioside G (**3.18**) by Fu and colleagues (2010b). The IUPAC names of the sutherlandiosides E-H isolated by Fu (2012) and Tchegnitegni et al. (2024) are tabulated in

Table 3. 2 to highlight the duplication in sutherlandiosides naming. Recently, Ndjoubi and co-workers (2024) isolated two cycloartane glycoside namely Lessertiosides A (**3.29**) and B (**3.30**) as well as the flavonoids 8-methoxyvestitol (**3.12**) and mucronulatol (**3.13**).

Table 3.2: The IUPAC names of the sutherlandiosides E-H isolated by Fu (2012) and Tchegnitegni et al. (2024)

Compounds	Fu (2012)	Tchegnitegni et al. (2024)
Sutherlandioside E	24, 25-*O*-*β*-D-diglucopyranosyl-3S,24S,25-trihydroxy, 2(1-10)-abeo-9,10R-seco-cycloartanoic acid (**3.20**)	7*S*,24*S*,25-trihydroxy-9,10*R*-*seco*-9,19-cyclolanost-2(3),9(11)-diene-25-*O*-*β*-D-glucopyranoside (**3.22**)
Sutherlandioside F	24, 25-*O*-*β*-D-diglucopyranosyl-3R,24S,25-trihydroxy, 2(1-10)-abeo-9,10R-seco-cycloartanoic acid (**3.21**)	1*S*,3*R*,7 *S*,24 *S*,25-pentahydroxycycloartan-11-one-25-*O*- *β*-D-glucopyranoside (**3.23**)
Sutherlandioside G	(3 *R*,7 *S*,24 *S*,25)-[3-*O*-*β*-D-glucopyranosyl]-tetrahydroxycycloartan-1-one-25-*O*-*β*-D-glucopyranoside (**3.18**)	1*S*,3*R*,7 *S*,24 *S*,25-pentahydroxycycloartan-11-one-24-*O*- *β*-D-glucopyranosyl-25-*O*-*β*-D-glucopyranoside (**3.24**)
Sutherlandiosde H	3 *R*,24 *S*,25-trihydroxycycloartane-1,11-dione-24, 25-*O*-*β*-D-diglucopyranoside (**3.19**)	3*R*,24*S*,25-trihydroxycycloartan-1-one-25-*O*-*β*-D-glucopyranoside (**3.25**)

In 2019, Gonyela et al. (2019) reported the isolation of cycloartenol (**3.28**) and an acylated form of sutherlandioside D (**3.31**) from *L. frustecens* leaves. However, D-pinitol, *L*-canavanine, and sutherlandioside B are identified as the major components in the plant (Van Der Walt et al., 2016). Apart from these secondary metabolites, *L. frutescens* is known to biosynthesise tannins, as well as methyl and propyl parabens (Van Wyk & Gerick, 2000; Tai et al., 2004).

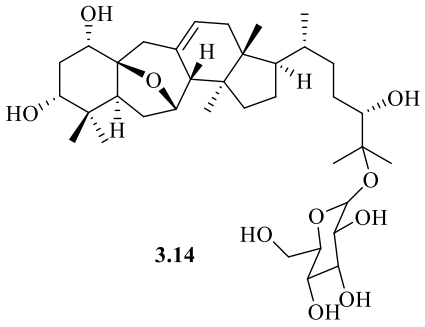

3.14

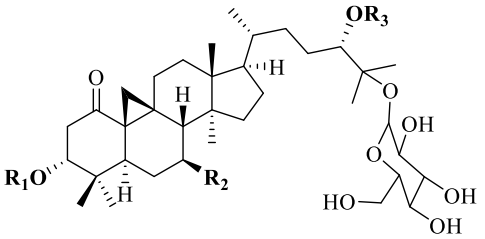

	R_1	R_2	R_3
3.15	H	OH	H
3.18	Glc	OH	H
3.25	H	H	H
3.26	H	OH	Glc

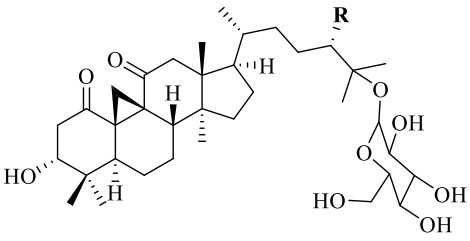

3.16 **R**=H
3.19 **R**=O-Glc
3.27 **R**=1-O-(4-coumaroyl)-*b*-*D*-glucose

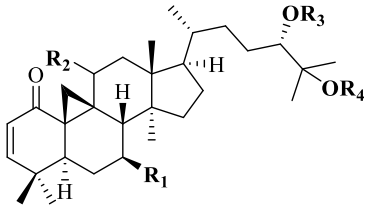

	R_1	R_2	R_3	R_4
3.17	OH	H	H	Glc
3.28	OH	H	H	H
3.29	H	H	H	Glc
3.30	H	=O	H	Glc
3.31	OH	H	H	

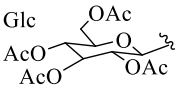

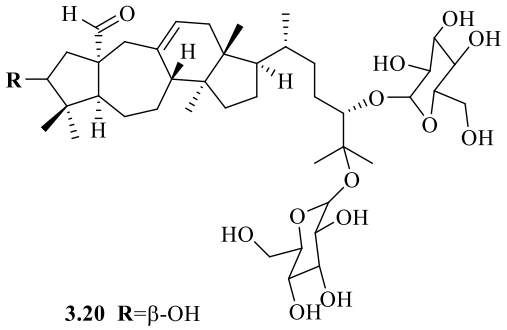

3.20 **R**=β-OH
3.21 **R**=α-OH

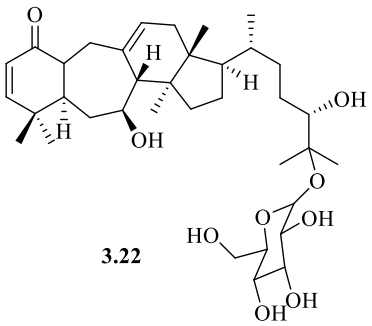

3.22

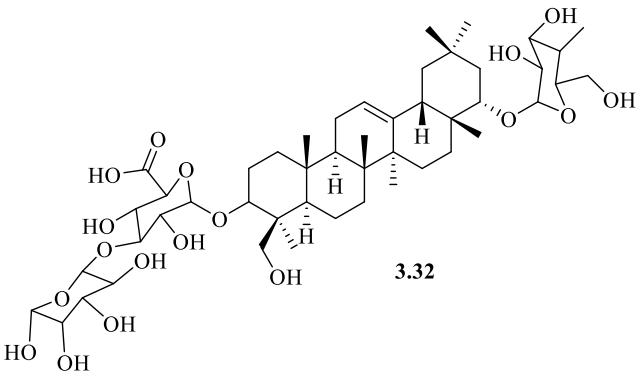

3.32

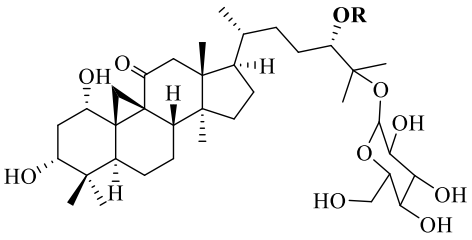

3.23 **R**=H
3.24 **R**=Glc

Figure 3.3: Chemical constituents of *L. frutescens* isolated compounds (**3.14**-**3.32**)

3.7 Ethnopharmacological and pharmacology properties of the plant extracts and bioactive compounds

L. frutescens, a medicinal plant native to Southern Africa, boasts diverse ethnomedicinal applications. In South Africa, the Khoisan and Cape Dutch people have historically used this perennial shrub for treating internal cancers, wounds, inflammation, stomach pains, diabetes, HIV/AIDS, and infections (Van Wyk & Albrecht, 2008). While the pharmacology and ethnomedicinal properties of *L. frutescens* (Table 3.3) have not been ascribed to a specific bioactive compound, it is believed that the synergy among the plant bioactive compounds contributes to its complex mechanism of action. *L*-canavanine, *D*-pinitol, and GABA are reported as the most bioactive elements within the plant (Table 3.4).

The following sections will discuss a more detailed exploration of the biological activity of different organic extracts and bioactive compounds.

Table 3.3: Summary of *L. frutescens* extracts ethnopharmacological and pharmacological properties.

Extracts	Activities	Experimental models	Tested concentrations and IC_{50}	Experimental outcomes	References
***IN VITRO* ASSAYS**					
70% Ethanol extract (tablet)	antiproliferative	MDA-MB-468, HL-60, MCF-7 and Jurkat cells	300 mg in 2.2 mL of ethanol	Reduced cell growth with IC_{50} of 1/250, 1/200, 1/150, and 1/200 dilution for MCF7, MDA-MB-468, Jurkat and HL60 cells, respectively. Additionally, it did not induce HL60 differentiation into either monocyte/macrophage or granulocyte pathway	Tai et al., 2004
	Antioxidant	LPS-activated NO production by RAW 264.7 cells	300 mg	Scavenge hydroxyl free radical in the TEAC assay, it did not suppress LPS induced NO production by RAW 264.7 cells over an extended range of concentration (1/200-1/2000 dilutions), nor did it stimulate NO production by RAW 264.7 cells. In comparison, canavanine at 0.5 mM and pinitol at 10 mM significantly inhibited LPS induced NO secretion by RAW 264.7 cells. l-Canavanine is a selective inhibitor of inducible nitric oxide synthase so the lack of inhibitory activity of Sutherlandia preparation on NO secretion by RAW 264.7 cells in this study could be concentration related	
Hot aqueous extract	Antioxidant	FMLP stimulated neutrophils	10 µg/ml	Decreased both the luminol and luciginin enhanced chemiluminescence response	Fernandes et al., 2004
		Xanthine/xanthine oxidase system	10 µg/mL	Scavenged neutrophil-derived oxidants effectively at concentrations as low as 10µg/mL for superoxide generated by the xanthine/xanthine oxidase system	
		Horseradish peroxidase/hydrogen peroxide system.	2.5 µg/mL	Scavenged neutrophil-derived oxidants effectively for the hydrogen peroxide/horseradish peroxidase-mediated chemiluminescence	
		horseradish peroxidase/hydrogen peroxide system.	0.62 µg/mL	Inhibited horseradish peroxidase/hydrogen peroxide-induced chemiluminescence	
Aqueous extract (leaves)	Anti-HIV	HIV-1 reverse transcriptase enzyme	0.2 mg/mL	Inhibited HIV-1 reverse transcriptase (RT) enzyme at ≥ 50%, with tannins being primarily responsible for the extract activity	Harnett et al., 2004
Aqueous extract without sulphated polysaccharides (leaves)		HIV-1 reverse transcriptase enzyme	0.2 mg/mL	Inhibited HIV-1 reverse transcriptase (RT) enzyme at ~30%	
Dichloromethane extract (leaves)	Anti-HIV and antidiabetic	HIV-II protease enzyme	0.2 mg/mL	Displayed little activity against HIV-II protease enzyme but significantly inhibit α- and β-glucosidase enzymes	
Methanol extract	Anti-stress	Ovine adrenal mitochondria and microsomes (0.78 mM P450 in binding studies and 0.33 mM P450 in conversion)	50 µL of 82 mg/mL	Inhibited the binding of DOC (59%) and PROG (17%) as well as the conversion of PROG and PREG by 52 and 72%, respectively	Prevoo et al., 2004

Chloroform extract		Ovine adrenal mitochondria and microsomes (0.78 mM P450 in binding studies and 0.33 mM P450 in conversion)	50 µL of 82 mg/mL	Inhibited the binding of DOC (80%), PROG (67%) and PREG (62%), as well as the conversion of PROG and PREG by 100 and 93 %, respectively It also showed a more significant inhibitory effect than the methanol extract on PROG and PREG and metabolism	
Aqueous extract		Ovine adrenal mitochondria (0.78 mM P450 in binding studies and 0.33 mM P450 in conversion),	50 µL of 48 mg/mL	inhibited substrate binding to CYP21 by 38% and CYP11B1 by 60%. PREG and PROG conversion was inhibited by 30% and 34%, respectively.	
Aqueous extract	Cytotoxic	CHO and cervical neoplastic cells	3.5 mg/mL	Activated apoptosis	Chinkwo, 2005
Hexane	Antibacterial	*Enterococcus faecali*, *Escherichia coli*, and *Staphylococcus aureus*		Inhibited the bacteria with IC_{50} of 2.50, 1.25 and 0.31 mg/mL, respectively	Katerere & Eloff, 2005
70% ethanolic extract (leaves and twigs)	Antiproliferation	MCF-7	1.5 mg/mL	Inhibited the proliferation of MCF-7 cells after 72 h of exposure. Additionally, a 50% decrease in malignant cell numbers after 24 h of exposure was observed, with increased effects over 36, 48, and 72 h, leading to a further reduction in cell density	Stander et al., 2007
Triterpenoid fraction	Anti-stress	P450 enzymes	0.6 mg/mL	Exhibited a 60% inhibitory effect on the binding of PROG to cytochrome P450	Prevoo et al., 2008
			1.5 mg/ ml	Exhibited a 50% inhibitory effect on the binding of PREG to cytochrome P450	
			1.5 mg/mL	Reduce both the PROG-induced and PREG-induced difference spectra	
Methanol		P450 enzymes	4.1mg/mL	inhibited the binding of PROG to the cytochrome P450 enzymes CYP17 and CYP21	
Methanol and aqueous extracts		P450 enzymes	4.1 mg/mL 2.4 mg/mL	Methanol (4.1 mg/ mL) and aqueous (2.4 mg/ mL) extracts inhibited the binding of PROG to the cytochrome P450 enzymes significantly ($p < 0.05$), while the inhibition of PREG binding was less than 10% ($p = 0.25$).	
Aqueous extract		P450 enzymes	2.4 mg/mL	Inhibited the binding of PROG to the cytochrome P450 enzymes CYP17 and CYP21	
		Adrenocortical microsomes	2.4 mg/mL	Inhibited 49% of PROG metabolism. Inhibited the formation of DOC (71%), 17-OH-PROG (21%) and deoxycortisol formation (46%), suggesting that the aqueous extract is a more potent inhibitor of CYP21 when compared to their inhibitory effects on CYP17	
		COS-1 cells	2.4 mg/mL	Inhibited PREG and PROG metabolism and the formation of the hydroxysteroid intermediates than DHEA and A4.	
70% ethanolic extract (leaves and twigs)	Cytotoxic	MCF-7and MCF-12A cell lines	10 mg/mL	Reduced cell growth in MCF-7 (26%) and MCF-12A (54%) cell lines after 72 h, causing cellular changes and increased apoptosis	Stander et al., 2009
Aqueous extract (tablet)	Immune modulatory	MDBK and LLC-PK1 cells	6 mg/mL	Reduced intracellular glutathione in MDBK and LLC-PK1 cells while lipid peroxidation augmented in the treated cells. It also promoted mitochondrial membrane depolarisation in 80% of the cells. At high concentrations, it increases oxidative stress to change	Phulukdaree et al., 2010

				mitochondrial membrane integrity and induce apoptosis in renal tubule epithelia	
100% Ethanol extract	Antiapoptotic	Normal human lymphocytes	7.5 mg/mL (IC_{50})	Decreased cell growth and viability with an IC_{50} of 7.5 mg/mL, thus increased apoptosis in total lymphocytes, with a more pronounced effect observed in the CD4+ sub-population. Additionally, it instigated lymphocyte activation in the CD4+ subpopulations and total lymphocytes, leading to activation-induced lymphocyte cell death. These results contradict preliminary clinical tests suggesting that the extract could potentially be used to treat HIV/AIDS	Korb et al., 2010.
70% Ethanol extract	Anti-HIV	LS180 cells	300 µg/mL	elevating the functional activity of CYP3A4	Minocha et al., 2011
70% Ethanol extract	Anticancer	SNO cells	2.5 and 5mg/mL	Extract A (from Colesberg) and extract B (from Platvei) significantly reduced ATP levels (~80 % reduction), with extract B causing the most considerable reduction	Skerman et al., 2011
			2.5 and 5 mg/mL	Extract A did not significantly reduce the cytochrome c level in the mitochondria, meaning it may induce apoptosis via the extrinsic pathway and exhibit early apoptosis. It increased the levels of caspase 3/7, indicating that the extract induced caspase-dependent cell death	
			2.5 and 5mg/mL	Extract B reduced cytochrome c in treated cells and displayed late apoptotic. It also decreased the levels of caspase 3/7 due to many cells being in the late stages of apoptosis	
70% Ethanol extract (tablet)	Antiapoptotic	Normal T-lymphocytes	2.5 mg/mL	Induced significant necrosis (95%), depletion of ATP (76%), and inhibition of caspase 3/7 activity (11%) after 24 h. DNA fragmentation was observed after 48 h	Ngcobo et al., 2012
Aqueous extract (tablet)		Normal T-lymphocytes	2.5 mg/mL	Induced necrosis (26%), depletion of ATP (91%), and inhibition of caspase 3/7 activity (15%) after 24 h. DNA fragmentation was observed after 48 h, and the water extract was less toxic than the ethanolic extract	
Methanolic and aqueous extracts	Anti-HIV	Human liver microsomes	10 mg/mL	Inhibited the metabolism of atazanavir in human liver microsomes, suggesting that *S. frutescens* could potentially alter the metabolism and absorption of atazanavir in a clinical setting	Müller et al., 2012
Aqueous extract		CaCo-2 cells	10 mg/mL	Decreased atazanavir accumulation, bioavailability and absorption	
The triterpenoid glycosides enriched fractions		CaCo-2 cells	500 µg/mL	Increased atazanavir accumulation and enhanced its bioavailability and absorption	
		Human liver microsomes	500 µg/mL	Decreased reduced the atazanavir present ($p < 0.001$) in human liver microsome	
40% aqueous methanolic	Anti-HIV	P 450 enzymes		Inhibited CYP1A2, CYP2A6, CYP2B6, CYP2C8, CYP2C9, CYP2C19, CYP3A4/5 and CYP3A4/5 with IC_{50} values of 41, 160, 20, 22.4, 23, 35.9, 17.5, and 28.3 µg/mL respectively. It also	Fasinu et al., 2012

				inhibited CYP3A4/5 with a KI of 296 µg/mL and a Kinact of 0.063 min-1	
		Hepatocytes	100 µg/mL	reduced midazolam clearance by 40% by delaying the production of midazolam metabolites	
		LLC-PK1 cells stably transfected with human P-gp	324.8 µg/mL (IC_{50})	Inhibit P-gp	
		Human embryonic kidney 293 cells stably transfected with human OATP1B1	10.4 µg/mL (IC_{50})	Inhibit OATP1B1	
		Human embryonic kidney 293 cells stably transfected with human OATP1B3	6.6 µg/mL (IC_{50})	Inhibited OATP1B3	
Aqueous extract	Antidiabetic	Hepatocytes	12.5 µg/mL	Prevented insulin resistance	Williams et al., 2013
Hot water extract	Protective	CHO, HepaRG, and A549	500 µg/mL	Protected the cells against t-BHP-induced oxidative stress by scavenging ROS and preserving GSH/GSSG levels	Tobwala et al., 2014
	Antioxidant		1 mg/mL	Potent scavenger of hydroxyl radicals followed by superoxide radicals, then hydrogen peroxide	
70% Ethanol extract	Antiinflammation	BV-2 microglial cells	0-80 µg/mL	Inhibited IFN-γ -induced p-ERK1/2 and p-STAT-1α expression as well as NO and filopodia production with significant inhibition starting at 40 µg/mL for p-ERK1/2 and filopodia and 20 µg/mL for both NO and p-STAT-1α	Jiang et al., 2014
		BV-2 microglial cells	0-80 µg/mL	Inhibited LPS+ IFN-γ induced ROS and NO production as well as iNOS expression with significant inhibition starting at 10 µg/mL for ROS and 20µg/mL for NO and iNOS	
		HAPI microglial cells	0-80 µg/mL	Inhibited LPS +IFN-γ induced ROS and NO production as well as iNOS expression with significant inhibition starting at 2.5 µg/mL for ROS, 20 µg/mL for NO and 80 µg/mL for iNOS	
	Antioxidant	Primary rat cortical neurons	0-7.5 µg/mL	Inhibited NMDA-induced ROS production in neurons without altering cell viability with maximum inhibition at 5 µg/mL.	
70% Ethanol extract	Antiapoptotic	CaCo-2 cells	300 mg	At 1/50 dilution, a significant reduction in cell viability (48.83 ± 7.976 %, $p < 0.01$) and an increase in the number of pyknotic cells (1.267 ± 0.1453 %, $p < 0.01$) and propidium iodide-positive cells (77.29 ± 4.775 %, $p < 0.001$) were observed	Leisching et al., 2015
		CaCo-2 cells	300 mg	At 1/50 dilution, a significant decrease in the endogenous levels of the p85 (69.63 ± 4.345 %, $p <0.01$) and p110 (75.6 ± 2.818 %, $p < 0.01$) phosphorylation led to a reduction in PI3-K activity	
		CaCo-2 cells	300 mg	At 1/50 dilution, Akt phosphorylation at Ser473 (94.83 ± 0.589%, $p < 0.01$) and Thr308 (65.10 ± 2.597 %, $p < 0.01$) significantly decrease. Additionally, a decrease in the phosphorylation of PTEN (65.97 ± 1.964 %, $p < 0.001$) at 1/50 dilution results in the activation of Akt in many tumour cell lines	

		CaCo-2 cells	300 mg	After treatment, a significant increase in PARP cleavage (85.57 ± 1.964 %, $p < 0.05$) and the endogenous levels of cleaved caspase-9 (255.33 ± 3.756%, $p < 0.05$) while the total Bax (74.53 ± 6.401%, $p < 0.05$) and c-IAP (60.77 ± 2.541%, $p < 0.001$) levels decreased significantly	
Polysaccharide-enriched fractions of the aqueous extract	Immune simulatroy	RAW 264.7 cells	200µg/mL	Activated macrophages via TLR4 receptors and the NF-kB signalling pathway	Lei et al., 2015a
Ethanolic extract	Anti-inflammation	RAW 264.7 cells	200 µg/mL	Decrease the production of NO to 36.4 ±7.4 and iNOS by 60%	Lei et al., 2015b
			200 µg/mL	Decreased the production of IL-6 and TNF-α by 65% and 28%, respectively and the activation of NF-κB by 26%	Lei et al., 2015b
			200 µg/mL	Reduced the phosphorylation of ERK1/2 and STAT1-α activated by LPS and IFN-γ up to 70% and 80% at 200µg/mL, respectively. These reductions were made without changing the expression of total p-ERK1/2 and p-STAT1-α and were observed in all doses used	
Sutherlandioside B-enriched fraction	Anti-inflammation	RAW 264.7	200 µg/mL	Reduced the production of ROS induced by LPS and IFNγ.	
Aqueous extract	Neuroinflammation in HIV context	Human astrocytes, HUVEC, primary human monocyte and BBB co-cultures stimulated with HIV-1 subtype B& C Tat protein and/or HL2/3 cell secretory protein	500 µg/mL	Decreased IL-1β secretion ($p < 0.0001$) but exacerbated the levels of MCP-1 ($p < 0.0001$) and the infiltration of CD14+ monocytes across the blood-brain barrier (BBB, $p < 0.01$). It also worsened HIV-associated neuroinflammation	Africa & Smith, 2015; Zonyane et al., 2019
Aqueous extract (leaves)	Anti-inflammation	NRK-52E cells	1:100 (10 g in 250 mL water)	Partially reduced TNF-α induced chemokine CCL5 expression	Grunz-borgmann et al., 2015
70% Ethanol extract	Anticancer	PC3, LNCaP, and TRAMP-C2 cells	25-250 µg/mL	Suppressed the growth of PC3, LNCaP, and TRAMP-C2 independent of androgen receptors with IC_{50} values of 167, 200 and 100 µg/mL, respectively. It also inhibited Gli/Hh signalling activity by reducing Gli1 and PTCH1 gene expression in TRAMP-C2 and PC3 cells, as well as suppressed poorly differentiated carcinomas formation in the prostate glands of TRAMP-C2 cells	Lin et al., 2016
70% ethanol extract (tablet)	Cytotoxic	A-375 and Colo-800 cells	0.625 mg/mL	Inhibited cells proliferation to 38% (A-375) and 59% (Colo-800) after 72h	Van Der Walt et al., 2016
		normal HDFα cells	0.3 mg/mL	Reduced normal HDFα cell viability to 19% after 72h	
Dichloromethane: methanol (1:1) extract (aerial part)	Antituberculosis	Mycobacterium tuberculosis shikimate kinase enzyme	0.1 µg/mL (IC_{50})	Inhibited shikimate kinase enzyme	Masoko et al., 2016
Aqueous extract (aerial part)	Antituberculosis	Mycobacterium tuberculosis shikimate kinase enzyme	5.1 µg/mL (IC_{50})	Inhibited shikimate kinase enzyme	
Ethanol extract (aerial part)	Antituberculosis	Mycobacterium tuberculosis shikimate kinase enzyme	1.7 µg/mL (IC_{50})	Inhibited shikimate kinase enzyme	

DCM fraction of DCM: MeOH extract (aerial part)	Antituberculosis	Mycobacterium tuberculosis shikimate kinase enzyme	2.5 µg/mL (IC_{50})	Inhibited shikimate kinase enzyme	
DCM: MeOH (7:3) fraction of DCM: MeOH (1:1) extract (aerial part)	Antituberculosis	Mycobacterium tuberculosis shikimate kinase enzyme	0.3 µg/mL (IC_{50})	Inhibited shikimate kinase enzyme	
DCM: MeOH (3:7) fraction of DCM: MeOH (1:1) extract (aerial part)	Antituberculosis	Mycobacterium tuberculosis shikimate kinase enzyme	1.5 µg/mL (IC_{50})	Inhibited shikimate kinase enzyme	
MeOH fraction of DCM: MeOH (1:1) extract (aerial part)	Antituberculosis	Mycobacterium tuberculosis shikimate kinase enzyme	94.3 µg/mL (IC_{50})	Inhibited shikimate kinase enzyme	
Methanol extract	Anti-stress	COS-1 cells	2.6 mg/mL	Inhibited PROG binding to CYP17A1 and CYP21A2 while not affecting 3β-HSD2	Sergeant et al., 2017
		Human H295R adrenal cells	1 mg/mL	Decreased total steroid production under basal steroidogenesis from 4.02 uM to 2.9 uM and under forskolin-stimulated Steroidogenesis from 10.79 um to 6.6 um after treatment. DHEAS levels increased significantly, while 16OH-PROG levels decreased significantly, indicating inhibition of CYP17A1 (basal and forskolin-stimulated Steroidogenesis). Deoxycortisol, cortisol, and corticosterone (CORT) levels were significantly decreased, while the precursor DOC increased significantly, suggesting an impact on the glucocorticoid pathway (basal). PROG, DOC, CORT, 17OH-PREG, 16OH-PROg, 11-DHC, 11OHA4 and A4 were significantly decreased. It inhibited CYP11B1 by considerably reducing cortisol and 11-OH-A4	
	MR antagonist	COS-1 cells	0.5 - 0.75 mg/mL	Antagonised the effects of aldosterone (ALDO) via the MR, similar to the known MR antagonist spironolactone, suggesting that the extract could be used as an anti-hypertensive treatment.	
	glucocorticoid receptor (GR) antagonist	COS-1 cells	0.5 - 0.75 mg/mL	Significantly repressed the IL-6 promoter after stimulation with PMA (10 ng/mL).	
Hot aqueous and ethanolic extracts (leaves)	Immune modulatory	RAW 264.7 cells	200 µg/mL.	Both extracts significantly inhibited LPS-induced ERK1/2 and p38 phosphorylation as well as LPS-induced production of GM-CSF	Camille & Dealtry, 2018
			From 100 µg/mL	Reduced LPS stimulated NO, and ROS production in a dose-dependent manner, with the ethanolic extract being a more potent regulator than the hot aqueous extract at 100 µg/mL	
			50 µg/mL	Reduced LPS-induced production of IL-1α	

Hot aqueous extract (leaves)	Immune modulatory	RAW 264.7 cells	200 µg/mL	Inhibited NFκB activation by attenuating NFκB p65 subunit phosphorylation on the Ser 536 residue (P< 0.05). it also reduced LPS-induced TNF-α (44.43 ng/mL to 33.99 ng/mL), IL-6 (8.52 ng/mL to 8.05 ng/mL), and G-CSF (116.85 ng/mL to 71.52 ng/mL), although this was not statistically significant. Downregulation of iNOS expression (P< 0.05) by 85-fold relative to the DMSO vehicle control (expressed as 1-fold expression) was observed	
			150 µg/mL	Reduced CD86 expression and Inhibited COX-2	
Ethanolic extract (leaves)	Immune modulatory	RAW 264.7 cells	200 µg/mL.	Decreased LPS-induced TNF-α, G-CSF (P< 0.05), and IL-6 production (P< 0.001) as well as downregulated iNOS expression (P< 0.01), compared to the DMSO vehicle control.	
			100, 150 and 200 µg/mL.	Inhibited NFκB activation by attenuating NFκB p65 subunit phosphorylation on the Ser 536 residue (100 and 150 µg mL−1, P<0.05; 200 µg/mL, P< 0.001)	
			100µg/mL	Reduced CD86 expression and increased the CD206 cell surface marker expression in a dose-dependent manner. It also inhibited COX-2 expression	
			50 µg/mL	reduced iNOS expression, although not significantly	
Ethyl acetate	Antimutagenic properties	TA97a, TA98, TA100 and TA102 strains	5,10 and 20% (w/w) of 100g in DMSO	exhibited antimutagenic effect against TA97a, TA98, TA100 and TA102	Ntuli et al., 2018
methanol	Pro-mutagenic	TA98 and TA100 strains	50% (w/w) of 100g in DMSO	showed Pro-mutagenic potential in the presence of the S9 in TA98 with 2-acetamidofluorene and TA100 with aflatoxin B1	
methanol			25 and 10% (w/w) of 100g in DMSO	showed antimutagenic potential in the presence of the S9 in TA98 with 2-acetamidofluorene and TA100 with aflatoxin B1	
Aqueous extract	Neuroprotection	(MPP+) induced toxicity in SH-SY5Y	20 µg/mL	Protected the cells by reducing ROS production	Enogieru et al., 2020
Aqueous extract	Anticancer	LS180	2.63 mg/mL (IC_{50})	Decreased cell growth and viability as well as the soluble protein content to 0.2 mg/mL.µg protein for (IC_{50})/2 and 0.4 mg/mL.µg protein for IC_{50} while decreasing ATP and AK per protein content below detectable limits after 24 hour exposure	Gouws et al., 2021
Aqueous extracts		P450 enzymes	2.63 mg/mL (IC_{50})	Inhibited the gene expression of CYP3A4 and CYP2D6 enzymes after treatment with IC_{50} and IC_{50}/2	
***IN VIVO* ASSAYS**					
Aqueous extract (Shoot)	Anti-analgesic	Hot-plate and acetic acid test models of pain in mice	50-800 mg/Kg	Produced significant ($p < 0.05$ - 0.001) analgesic effects against thermally and chemically induced nociceptive pain stimuli in mice	Ojowole, 2004.
	Antiinflammation	Fresh egg albumin-induced pedal (paw) edema	50-800 mg/Kg	Inhibited fresh egg albumin-induced acute inflammation ($p < 0.05$ - 0.001)	
	Antidiabetic	Streptozotocin-induced hyperglycemia in mice	50-800 mg/Kg	Inhibited streptozotocin-induced hyperglycemia ($p < 0.05$ - 0.001)	

Aqueous extract		Wistar rats fed a diabetogenic diet	0.01 ml/g rat weight, of the 2.5 g/100 ml tea extract, in their drinking water (equivalent to 3 cups/day for human consumption)	Showed promise as a type 2 antidiabetic drug by significantly increasing glucose uptake into muscle and adipose tissue while significantly decreasing intestinal glucose uptake ($p < 0.001$ after 1 hour). This indicates the extract's potential to normalise insulin levels and glucose uptake in peripheral tissues as well as suppress intestinal glucose uptake without causing weight gain	Chadwick et al., 2007
Aqueous extract (Shoot)	Anti-convulsion	Streptozotocin (PTZ)-induced seizures in mice	50-800 mg/Kg	Protected the mice against PTZ-induced seizures by significantly delayed ($p < 0.05$ - 0.001) the onset of antagonised PTZ-induced seizures with a 12.58 ± 2.43 ($p < 0.05$, 50 mg/kg), 14.69 ± 2.56 min ($p < 0.01$, 100 mg/kg), 17.73 ± 2.66 min ($p < 0.01$, 200 mg/kg), 21.56 ± 2.73 min ($p < 0.01$, 400 mg/kg)	Ojewole, 2008
Aqueous extract (Shoot)		Picrotoxin (PCT)-induced seizures in mice	50-800 mg/KG	Protected the mice against PCZ-induced seizures by significantly delayed ($p < 0.05$–0.001) the onset of, and antagonised, PTZ-induced seizures with a latency of tonic convulsion of 13.39 ± 2.41 min ($p < 0.05$, 50 mg/kg), 16.48 ± 2.60 min ($p < 0.01$, 100 mg/kg), 18.53 ± 2.77 min ($p < 0.01$, 200mg/kg), 21.60 ± 2.86 min ($p < 0.01$, 400 mg/kg) min	
70% Ethanol extract	Anti-HIV	Rat hepatic and intestinal tissues	12 mg/kg	Increased intestinal (200%) and hepatic (330%) rat CYP3A2 expression levels after 5 days of exposure	Minocha et al., 2011
		Rats	6 mg/kg	Altered the pharmacokinetics of nevirapine after 5 days of chronic exposure with the extract (oral administration) by reducing the AUC_{0-inf} of nevirapine from 60544.60 ± 6579.32 min.ng/mL to 33000.60 ± 7168.55 min.ng/mL (45% decrease) as well as its Cmax from 575.64 ± 51.60 ng/mL to 281.1 ± 62.80 ng/mL (51% decrease)	
Methanol	Antioxidant and spermatotoxic	Wistar rats	0.2% (corresponding to 2.5 mL of 40g/L solution diluted in 50 mL of water)	The infusion-treated animals showed a nonsignificant decrease in total motility (17.2%) and progressive motility (27.3%) compared to the control group. Additionally, rapid progressive motility was reduced by 37%, while there was a significant increase in the number of spermatozoa with slow speed ($p = 0.03$), catalase activity (23.7%) and SOD activity (23%). This increase in SOD was accompanied by a 45.9 % decrease in malondialdehyde (MDA) levels compared to the control group.	Omolaoye et al., 2023
CLINICAL TRIALS					
Aqueous extract	Anticancer	16 cancer patients (11 men and 5 women)	600 mg/day	Decreased fatigue in cancer patients (oral consumption)	Grandi et al., 2005
L. frutescens leaf powder capsules	Non-cytotoxic	A randomised, double-blind, placebo-controlled trial of Sutherlandia leaf powder in 25 healthy adults.	800 mg/day	There was no significant difference in adverse events or health indicators between the treatment and placebo groups except for improved appetite in the treatment group. Overall, healthy adults tolerated 800 mg/d of Sutherlandia leaf powder well for three months.	Johnson et al., 2007

Leaf powder	Anti-HIV	107 participants were analysed (54 in the L. frutescens 1,200 mg arm and53intheplaceboarm	2400mg/day (1200 mg twice daily)	*L. frutescens* did not alter the viral load, and the CD4 T-lymphocyte count remained the same in the two arms. The mean and total BOI were higher in the *L. frutescens* arm, primarily due to two tuberculosis cases in patients on IPT	Wilson et al., 2015

Table 3.4: Summary of *L. frutescens* compounds pharmacological properties

Compounds	Activity	Experimental model	Tested concentrations	Experimental outcomes	References
***IN VITRO* ASSAYS**					
L-canavanine and D-Pinitol	Antioxidant	LPS-activated NO production by RAW 264.7 cells	0.5 mM (*L*-canavanine) and 10 mM (D-pinitol)	Inhibited LPS-induced NO secretion without reducing the cell numbers	Tai et al., 2004
		TNF- and IL-1 mRNA expression in RAW 264.7 cells stimulated with LPS		Did not affect the mRNA expression of TNF- and IL-1 mRNA.	
Sutherlandioside B and D	Anticancer	Shh Light II cells	10 µg/mL	Sutherlandioside B and D inhibited the Gli-reporter activity by 22 and 89%, respectively	Lin et al., 2016
α-linolenic acid	Antitubular and antibacteria	Mycobacterium tuberculosis	3.7 µg/mL (IC_{50})	Inhibited the shikimate kinase enzyme	Masoko et al., 2016
Sutherlandioside B	Antistress	COS-1 cells	0.5 and 0.75 mg/mL	Suppressed NF-kB-driven gene expression while being unable to activate MR mediated gene transcription. It also antagonized the effects of ALDO via the MR, although its antagonism level ($P<0.05$) is lower than the extract level of antagonism ($P<0.001$)	Sergeant et al., 2017
		COS-1 cells	10 and 30 µM	Inhibited CYP17A1 towards PREG (at 30 µM) and PROG (at 10 and 30 µM) as well as 3β-HSD2 toward PROG (at 10 and 30 µM), signifying that the compound could disrupt steroidogenesis at the branch point. It also acted as selective glucocorticoid receptor agonists (SEGRAs)	
		In H295R cells	30 µM	Decreased cortisol and androgen precursors such as androstenedione (A4), 11-hydroxyandrostenedione (11OH-A4), 16-hydroxyprogesterone (16OH-PROG) significantly, while 11-dehydrocorticosterone (11-DHC) increased significantly at 30 µM.	
L-arginine, GABA, D-pinitol	antimutagenic	TA97a, TA98, TA100 and TA102 strains	L-arginine (0.05, 0.14 and 0.28 M); D-pinitol (0.05, 0.13 and 0.26 M); and	Exhibited antimutagenic activity against all four strains	Ntuli et al., 2018

			GABA (0.10, 0.24 and 0.49 M).		
L-canavanine	Co-mutagenic	TA97a, TA98, TA100 and TA102 strains	0.05, 0.13 and 0.26 M	Displayed co-mutagenic effect in the absence of S9 in TA97 with 9-aminoacridine	Ntuli et al., 2018
***IN VIVO* ASSAYS**					
D-pinitol	Anti-neuphroyoxicity	cisplatin-induced nephrotoxicity in mice	10 mg/kg/day for seven consecutive days after a single dose of cisplatin (20mg/Kg)	Prevented alterations in renal biomarkers expressed in mg/dl by decreasing the serum creatinine (1.14 ± 0.12), urine creatinine (4.42±0.68), serum blood urea nitrogen (23.8 ± 2.44) and NO (54.05 ± 6.20 µM) levels compared to cisplatin (2.06 ± 0.25), (6.21.8 ± 0.12), (37.6 ± 2.3), and (88.21 ± 11.41) respectively Prevented alterations in oxidative biomarkers by reducing MDA levels (48.4 ± 10.4 µg/mg) and increasing SOD (13.21 ± 0.75 U/mg), catalase (9.65 ± 1.06 U/mg) and GSH (8.43±1.78 µg/mg) levels compared to cisplatin (100.6 ± 19 µg/mg), (5.8 ± 0.71 U/mg), (3.94 ± 0.8 U/mg), and (6.16 ± 0.9 µg/mg) respectively Showed normalisation of kidney structure	Vasaikar et al., 2018
		cisplatin-induced nephrotoxicity in mice	20 mg/kg/day for seven consecutive days after a single dose of cisplatin (20mg/Kg)	Prevented alterations in renal biomarkers expressed in mg/dl by decreasing the serum creatinine (0.92 ± 0.01), urine creatinine (2.01 ± 0.09), serum blood urea nitrogen (25.8 ± 3.19) and NO (34.72 ± 6.93 µM) levels prevented alterations in oxidative biomarkers by reducing MDA levels (45.5±10.4 µg/mg) and increasing SOD (9.88 ± 0.39 U/mg), catalase (7.51 ± 0.95 U/mg) and GSH (13.4 ± 1.37 µg/mg) levels	
		cisplatin-induced nephrotoxicity in mice	40 mg/kg/day for seven consecutive days after a single dose of cisplatin (20mg/Kg)	Prevented alterations in renal biomarkers expressed in mg/dl by decreasing the serum creatinine (0.82±0.03), urine creatinine (1.16±0.09), serum blood urea nitrogen (23.5±2.10) and NO (31.02±3.22 µM) levels Prevented alterations in oxidative biomarkers by reducing MDA levels (33.2 ± 8.25 µg/mg) and increasing SOD (12.8 ± 0.80 U/mg), catalase (7.63 ± 0.54 U/mg) and GSH (14.9 ± 1.91 µg/mg) levels	
		cisplatin-induced nephrotoxicity in mice	10, 20, and 40 mg/kg/day for seven consecutive days after a single dose of cisplatin (20mg/Kg)	Altered cisplatin-induced changes in inflammatory markers by decreasing the levels of TNF-α, IL-1β, IL-6 and NO, indicating an inhibitory effect on the cytokine release and NO	
		cisplatin-induced nephrotoxicity in mice	20 and 40 mg/kg/day for seven consecutive days after a single dose of cisplatin (20mg/Kg)	Improved histopathological alterations by preventing severe and widespread necrosis with dilatation, ruptured glomerulus structure, widening urinary space and oedema.	
MOLECULAR DOCKING					
L-cavananine	COVID -19 inhibitor	SARS-Cov-2 3CL Pro	-5.2kcal/mol (molecular docking score)	Exhibit favourable binding modes in the active site of $3CL^{pro}$ Exhibited the favourable docking score of -5.2kcal/mol in binding to $3CL^{pro}$ Engaged in strong interactions with binding site residues of 3CLpro	Dwarka et al., 2020

3.7.1 Cancer

The ethanolic extract of *L. frutescens* has demonstrated a significant cytotoxic effect on normal T-lymphocytes, particularly at a concentration of 2.5 mg/mL. After 24 h, the extract induced necrosis in 95% of cells, depleted ATP levels by 76% and inhibited caspase 3/7 activity by 11%. In contrast, the deionised water extract at the same concentration caused milder effects, with necrosis at 26%, ATP levels at 91%, and caspase 3/7 inhibition at 15%. Both extracts exhibited time-dependent effects over 48 h, with the ethanolic extract showing more potent inhibition of cell growth through necrosis, ATP depletion, and reduced caspase activity. DNA fragmentation observed after 48 h confirmed the potential toxicity of the extracts, although the water extract appeared relatively safer (Ngcobo et al., 2012).

Ethanolic extracts of *L. frutescens* have also shown anticancer activity. Tai et al. (2004) reported that the ethanolic extract inhibited the proliferation of cancer cell lines, including Jurkat, MDA-MB-468 (malignant breast cancer), HL-60 (human leukaemia), and MCF-7 (breast cancer) with IC_{50} values of 0.91 mg/mL (1/150 dilutions), 0.68 mg/mL (1/200 dilutions),0.68 mg/mL (1/200 dilutions), and 0.55 mg/mL (1/250 dilutions), respectively. The active compound *L*-canavanine, a non-proteinogenic amino acid, was implicated in the antiproliferative effects by inhibiting enzyme function and inducing protein misfolding (Fowler & John, 2019). Interestingly, *L*-arginine at 1 mM mitigated the antiproliferative effects of 2 mM *L*-canavanine in MCF-7 cells, suggesting a potential pathway to modulate toxicity. Further studies by Stander et al. (2007) showed that a 70% ethanolic extract of *L. frutescens* (1.5 mg/mL) inhibited MCF-7 cell proliferation and induced apoptosis within 72 h. An aqueous extract at 10 mg/mL reduced cell growth by 26% in MCF-7 cells and 49% in MCF-12A cells. In MCF-7 cells, pronounced apoptotic changes, such as chromatin condensation and apoptotic bodies, were observed. Flow cytometry revealed a heightened sub-G1 apoptotic fraction and S-phase arrest. Transmission electron microscopy suggested that these effects were driven by autophagic and apoptotic processes, likely induced by L-canavanine's protein misfolding response (Stander et al., 2009). In contrast, Steenkamp and Gouws (2006) reported that an aqueous extract (50 µg/mL) exhibited minimal cytotoxicity against MCF-7, DU-145 (prostate cancer), MDA-MB-231, and MCF-12A cells, suggesting that concentrations ≤ 50 µg/mL, the plant do not exhibit antiproliferative properties.

Methanolic extracts of *L. frutescens* have demonstrated cytotoxic effects against prostate cancer cell lines (PC3, LNCaP, and TRAMP-C2), with IC_{50} values of 167, 200, and 100 µg/mL, respectively. These effects were independent of androgen receptor signalling and involved suppression of Gli/Hh signalling, as evidenced by reduced Gli1 and Ptch1 gene expression, which plays a role in prostate cancer tumorigenesis (Lin et al., 2016). Similarly, ethanolic

extracts have been shown to downregulate PI3K/Akt signalling, reduce FKHR phosphorylation, and activate mitochondrial apoptotic pathways in Caco-2 colon cancer cells, promoting apoptosis (Leisching et al., 2015). The aqueous extract at 2.63 mg/mL further induced cytotoxicity in LS180 colorectal cancer cells, depleting soluble protein content, intracellular ATP, and extracellular adenylate kinase within 24 h (Gouws et al., 2021).

In melanoma and cervical cancer models, ethanolic extracts reduced the viability of melanoma cells (A-375 and Colo-800) by 62% and 43%, respectively, after 72 h at 0.625 mg/mL. It showed even greater efficacy against human dermal fibroblast cells (HDFα), where viability decreased by 81% at 0.3 mg/mL after 72 h (Van Der Walt et al., 2016). Meanwhile, it was reported that the aqueous extract at 3.5 mg/mL induced apoptosis and cytotoxicity in Chinese hamster ovary (CHO) and cervical neoplastic cells (Chinkwo, 2005). Studies on oesophagal cancer (SNO cells) highlighted geographical variations in extract efficacy. Extracts from Colesberg induced apoptosis through caspase 3/7 activation, while extracts from Platvei triggered cytochrome c release, highlighting the influence of geographical variations on the phytochemical composition and biological activity of the plant (Skerman et al., 2011).

Phulukdaree et al. (2010) reported that *L. frutescens* aqueous extract (6 mg/mL) significantly reduced intracellular glutathione levels, increased lipid peroxidation, and induced mitochondrial membrane depolarisation (in 80% of the treated cells) in MDBK and LLC-PK1 cells. At higher concentrations (12 and 24 mg/mL), the extract increased oxidative stress, disrupted mitochondrial integrity, and promoted apoptosis. These findings suggest that *L. frutescens* aqueous extract has dose-dependent cytotoxic effects on MDBK and LLC-PK1 cells, mediated primarily through the induction of oxidative stress and mitochondrial damage.

3.7.2 COVID-19

A molecular docking investigation revealed that *L*-canavanine is a promising inhibitor of the SARS-Cov-2 $3CL^{Pro}$, showing favourable binding modes and strong interactions in the active site of $3CL^{Pro}$(Dwarka et al., 2020). Moreover, Akindele and co-authors (2022) also reported that apart from its antiviral, anti-inflammatory, and immunomodulatory properties, the plant also possesses COVID-19 symptoms-relieving activity.

3.7.3 Immune modulation and inflammation

Na et al. (2004) reported that the methanolic extract (10, 5 and 1 µg/mL) of *L. frutescens* inhibited 12-O-tetradecanoylphorbol-13-acetate (TPA)-induced cyclooxygenase-2 (COX-2) expression in human breast epithelial (MCF10A) cells by suppressing the DNA binding activity of nuclear factor kappa-light chain enhancer of activated B cells ($NF\text{-}_KB$) induced by TPA (10

nM). This inhibition of TPA-induced COX-2 expression achieved through suppressing NF_KB DNA binding may be responsible for the plant's chemo-preventive activity (Na et al., 2004). The aqueous extract also partially reduced tumour necrosis factor-alpha (TNF-α) induced chemokine CCL5 expression in NRK-52E cells (Grunz-Borgmann et al., 2015).

The transcriptome analysis has provided valuable insights into the role of *L. frutescens* in modulating the immune system. Lei et al. (2015a) discovered that the crude polysaccharide enriched fraction of *L. frutescens* aqueous extract influenced gene expression in activated murine macrophage cell lines (RAW 264.7), resulting in the differential expression of 547 genes (Adefuye, 2016). This fraction also exhibited immuno-stimulatory activity by activating macrophages via TLR4 receptors and the NF_KB signalling pathway (Lei et al., 2015a). Additionally, the ethanolic extracts enriched polysaccharide reduced the production of nitric oxide (NO) and reactive oxygen species (ROS), as well as inhibited the phosphorylated extracellular signal-regulated kinase ½ (p-ERK1/2), signal transducer, and activator of transcription 1-α (STAT1-α) and NF-κB induced by Lipopolysaccharides (LPS) and interferon-gamma (IFNγ) (Lei et al., 2015b). Furthermore, both ethanolic and aqueous extracts were found to significantly inhibit the pro-inflammatory cytokines granulocyte-macrophage colony-stimulating factor (GM-CSF), granulocyte colony-stimulating factor (G-CSF), Interleukin (IL)-1α, IL-6 and TNF-α, the production of inducible nitric oxide synthase (iNOS), NO, and ROS as well as the pro-inflammatory mediator COX-2 and the gene expression CD86 in a dose-dependent manner. The ethanolic extract also modified the M1 and M2 macrophage phenotypes' expressions by enhancing the M2 phenotype and downregulating the M1 phenotype (Camille & Dealtry, 2018). These findings corroborate the results of Lei et al. (2015b) regarding the plant anti-inflammatory macrophage markers.

L. frutescens was also shown to negatively regulate the NF-$_K$B signalling pathway by suppressing NF-$_K$B nuclear translocation following LPS induction. This further substantiates the plant's ability to inhibit NF-$_K$B activation through the attenuation of NF-$_K$B p65 subunit phosphorylation on the Ser 536 residue, which is essential for both NF-κB nuclear transcriptional and translocation activity (Camille & Dealtry, 2018). Likewise, Kirsten (2010) stated that the plant extract regulated the expression of IL-6, IL-10 and IFN-γ in phytohaemagglutinin (PHA) and LPS. However, it was reported that these immune modulation effects are donor-dependent (Kisten, 2010). Additionally, little effect of the ethanol extract on the stimulation of TNF-α and IL-8 by phorbol myristoyl acetate was observed (Faleschini et al., 2013; Jiang et al., 2014). Jiang et al. (2014) further demonstrated that the ethanol extract could mitigate N-methyl-D-aspartic acid (NMDA) induced neuronal oxidative responses and reduce ROS and NO production induced by LPS and IFN-γ in microglial cells (BV-2 and HAPI).

Moreover, the ability of the ethanolic extract to inhibit IFN-γ induced p-ERK1/2 pathway explains the extract's potential in preventing or treating inflammatory infections including HIV-associated neurocognitive disorders. *L. frutescens* shoot aqueous extract inhibited fresh egg albumin-induced acute inflammation, triggering hypoglycemia in rats (Ojewole, 2004; Akindele et al., 2022). Its efficacy as an antidiabetic and anti-inflammatory herbal remedy can be attributed to its inhibitory effects on cytokines and apoptosis (Choi et al., 2007; Sivakumar et al., 2010; Vasaikar et al., 2018). Furthermore, Gouws et al. (2021) also found that the aqueous extract inhibited the gene expression of CYP3A4 and CYP2D6 enzymes instead of inducing them.

3.7.4 Neuroprotection

Pre-treatment of 1-methyl-4-phenylpyridinium (MPP+) induced toxicity in SH-SY5Y neuroblastoma cells with the plant aqueous extract resulted in the protection of the cells from MPP+ induced toxicity and loss of MPP via the regulation of ROS, thus hinting at the extract's neuroprotective effect and its potential as an anti-Parkinson agent (Enogieru et al., 2020). In a study by Ndjoubi et al. (2024), several natural compounds, including 8-methoxyvestitol, mucronulatol, proline, D-pinitol, sutherlandin C, sutherlandiosides B, D, K, and 7*S*,24*S*,25-trihydroxy-9,10*R*-seco-9,19-cyclolanost-2(3),9(11)-diene-25-*O*-*β*-*D*- glucopyranoside, demonstrated significant neuroprotective effects through their antiapoptotic activity. The compounds were evaluated for their antiapoptotic potency, with sutherlandioside B, mucronulatol, proline, and D-pinitol, significantly restoring ATP levels from 51% (MPP^+-treated) to 73, 75, 74, and 75%, respectively, while inducing caspase 3/7 activity from 5-fold to 1.5-2.8-fold relative to controls, with mucronulatol exhibiting the most potent anti-apoptotic effect (1.5-fold) (Ndjoubi et al., 2024).

3.7.5 Antioxidant

The ethanolic extract of *L. frutescens* demonstrated significant hydroxyl radical scavenging in the TEAC assay but failed to modulate LPS-induced NO production in RAW 264.7 cells across various concentrations ranging from 0.068-0.68 mg/mL. In contrast, *L*-canavanine (0.5 mM) and D-pinitol (10 mM) significantly inhibited LPS-induced NO secretion. Given *L*-canavanine's role as a selective inhibitor of inducible nitric oxide synthase, the absence of inhibitory activity by *L. frutescens* may be concentration-dependent (Tai et al.,2004). Similarly, Fernandes et al. (2004) reported that a hot aqueous extract of *L. frutescens* at a concentration of 10 µg/mL reduced the luminol- and lucigenin-enhanced chemiluminescence response in FMLP-stimulated neutrophils and effectively scavenged neutrophil-derived oxidants in the

xanthine/xanthine oxidase system. In the hydrogen peroxide/horseradish peroxidase-mediated chemiluminescence, it scavenged neutrophil-derived oxidants at 2.5 µg/mL. Furthermore, at a concentration of 0.62 µg/mL, it inhibited horseradish peroxidase/hydrogen peroxide-induced chemiluminescence (Fernandes et al., 2004). Moreover, the antioxidant efficiency of *L. frutescens* varied significantly depending on the extraction solvent, as reported by Tobwala et al. (2014). This variation is primarily attributed to the solvent's impact on the composition of phenolics and flavonoids in the extract. Solvents with higher polarity yielded extracts with greater total phenolic and flavonoid content, resulting in greater reducing power and radical scavenging activity (Tobwala et al., 2014; Zonyane et al., 2020). The freeze-dried hot water extract of *L. frutescens* (500 µg/mL) demonstrated protective effects against tert-butyl hydroperoxide (t-BHP)-induced oxidative stress in CHO, human hepatoma (HepaRG), and human pulmonary alveolar carcinoma (A549) cells by effectively scavenging ROS and preserving intracellular glutathione (GSH/GSSG) levels (Tobwala et al., 2014). At a 1 mg/mL concentration, the extract exhibited potent scavenging activity, effectively neutralising hydroxyl radicals, followed by superoxide radicals and hydrogen peroxide.

3.7.6 Nephrotoxicity

The sugar D-pinitol improved histopathological alterations in cisplatin-induced nephrotoxicity in mice because of its anti-apoptotic, antioxidant, and anti-inflammatory properties (Vasaikar et al., 2018). Likewise, the reduction of histopathological and biochemical alterations, as well as decreasing levels of cytokines (TNF-α, IL-6, IL-1β) and oxidative stress in cisplatin-induced nephrotoxicity ameliorate nephrotoxic reaction of cisplatin in D-pinitol treated mice (Vasaikar et al., 2018).

3.7.7 HIV/AIDS

The aqueous extract (200 µg/mL) of the leaves was reported to inhibit the HIV-1 reverse transcriptase (RT) enzyme by ≥50% (Harnett et al., 2004). However, when tested with 0.2% (w/v) bovine serum albumin (BSA) to neutralise tannin effects, the inhibitory activity was reduced, indicating that tannins contributed significantly to the inhibition. Despite this, the extract retained approximately 30% of its activity (Harnett et al., 2004). On the other hand, the dichloromethane extract exhibited limited activity against the HIV-II protease enzyme but significantly inhibited α- and β-glucosidase enzymes (Harnett et al., 2004).

An ethanolic extract concentration equivalent to its calculated IC_{50} (7.5 mg/mL) was administered to normal human lymphocytes for 3, 6, and 12 h. At the 12-hour mark, the extract induced apoptosis in total lymphocytes, with a stronger effect on $CD4^+$ subpopulations. This

was supported by increased caspase-3/7 activity, phosphatidylserine (PS) translocation, and reduced ATP levels (Korb et al., 2010). Additionally, after 12 h, the extract doubled the number of lymphocytes expressing the CD69 activation marker, leading to activation-induced cell death. These findings contradicted earlier clinical suggestions that the extract might be useful in treating HIV/AIDS (Korb et al., 2010).

D-pinitol and GABA have been proposed to alleviate wasting conditions in cancer and HIV/AIDS patients by inhibiting inflammatory cytokines TNF-α and IL-1β, thus enhancing glucose availability for cell metabolism (Engelbrecht et al., 2010; Korb et al., 2010; Mombereau et al., 2004). Conversely, *L*-canavanine demonstrated antiviral properties against HIV and influenza by disrupting viral protein synthesis and function (Green, 1992; Korb et al., 2010).

Chronic oral administration of *L. frutescens* extract (12 mg/kg for 5 days) induced intestinal and hepatic CYP3A2 expression in rats, altering the pharmacokinetics of the antiretroviral drug nevirapine and increasing CYP3A4 activity in LS180 cells (Minocha et al., 2011). This suggests a potential drug-herb interaction when nevirapine is co-administered with *L. frutescens*. D-pinitol and the aqueous extract reduced atazanavir accumulation in Caco-2 cells at 10 mg/mL, potentially lowering its bioavailability, while a triterpenoid glycoside-enriched fraction enhanced atazanavir accumulation and absorption (Müller et al., 2012). Additionally, methanolic and aqueous extracts of *L. frutescens* inhibited atazanavir metabolism in human liver microsomes, indicating a potential impact on the drug's clinical metabolism and absorption (Müller et al., 2012).

Fasinu et al. (2012) also demonstrated the anti-HIV activity of *L. frutescens* against various cytochrome P450 isozymes. These include CYP1A2-mediated phenacetin demethylation, CYP2A6-mediated coumarin 7-hydroxylation, CYP2B6-mediated bupropion hydroxylation, CYP2C8-mediated paclitaxel 6α-hydroxylation, CYP2C9-mediated diclofenac 4'-hydroxylation, CYP2C19-mediated *S*-mephenytoin 4'-hydroxylation, CYP3A4/5-mediated midazolam 1'-hydroxylation, and CYP3A4/5-mediated testosterone 6β-hydroxylation in pooled human liver microsomes with IC_{50} values of 41, 160, 20, 22.4, 23, 35.9, 17.5, and 28.3 μg/mL respectively (Fasinu et al., 2012). The studied extract induced time-dependent (irreversible) inhibition of CYP3A4/5 with an inhibition constant (K_i) of 296 μg/mL and a maximal rate of enzyme inactivation (K_{inact}) 0.063 min^{-1} (Fasinu et al., 2012). The authors also indicated that plant inhibited the human ATP-binding cassette transporters P-gp as well as the organic anion transport polypeptide OATP1B1 and OATP1B3 with IC_{50} values of 324.8, 10.4, and 6.6 μg/mL respectively. This inhibition also led to a 40% reduction in the clearance of midazolam metabolites in hepatocytes. However, no activity was observed when treating the

efflux transporter BRCP (breast cancer resistance protein) as well as the enzymes CYP2D6 and CYP2E1 with *L. frutescens* (Fasinu et al., 2012).

Despite some therapeutic potential, *L. frutescens* also raised safety concerns. Africa and Smith (2015) found that the plant significantly reduced IL-1β secretion but increased monocyte chemoattractant protein-1 (MCP-1) levels, leading to greater infiltration of CD14+ monocytes across the blood-brain barrier. This exacerbated HIV-associated neuroinflammation, prompting warnings against its use by HIV patients at any stage of infection (Africa & Smith, 2015; Zonyane et al., 2019).

3.7.8 Diabetes

Studies have shown the effectiveness of *L. frutescens* extracts in managing diabetes through various mechanisms. Oral administration of the shoot aqueous extract strongly inhibited streptozotocin-induced hyperglycemia in mice at concentrations ranging from 50 to 800 mg/kg (Ojowole, 2004). Additionally, the aqueous leaf extract showed promise as a type 2 antidiabetic drug by significantly increasing glucose uptake into muscle and adipose tissue while significantly decreasing intestinal glucose uptake (after 1 hour). This indicates the extract's potential to normalise insulin levels and glucose uptake in peripheral tissues and suppress intestinal glucose uptake without causing weight gain (Chadwick et al., 2007; Adefuye, 2016). Studies on rats fed on a high-fat diet showed that the plant extracts prevent the development of insulin resistance by reducing plasma-free fatty acid levels (Mackenzie et al., 2009). It was also observed that rats on a high-fat diet exhibited a twelve-fold reduction in plasma-free fatty acid levels compared to those on a normal diet (Mackenzie et al., 2009). Moreover, Bates and co-workers (2000) stated that D-pinitol acted similarly to insulin by lowering blood sugar levels and augmenting glucose uptake for cellular metabolism. This resulted in its capacity to regulate cellular energy by boosting energy levels and reducing fatigue. In 2013, it was discovered that the aqueous extract could prevent insulin resistance in hepatocytes (Williams et al., 2013).

3.7.9 Stress

The warm water extract of *L. frutescens* leaves was revealed to efficiently reduce the corticosterone response to chronic stress in Wistar rats (Prevoo et al., 2008; Smith & Myburgh, 2004). This finding confirmed the traditional use of the plant in treating ailments associated with high levels of glucocorticoids. Investigations on the aqueous and methanolic extracts revealed these extracts inhibit progesterone (PROG) binding to CYP17A1 and CYP21A2 without affecting 3β-HSD2 (Prevoo et al., 2008). The methanolic extract containing sutherlandioside B (SUB) as its major component significantly inhibited pregnenolone (PREG)

and PROG conversion by CYP17A1. Interestingly, at lower concentrations, the extract could considerably affect the catalytic activity of CYP17A1 only by PROG conversion (Sergeant et al., 2017). The absence of an inhibitory effect on PREG metabolism suggests that the plant's bioactive compounds may bind to a site in the active pocket other than the one occupied by PREG (Prevoo et al., 2008). Changes observed in the inhibition of PROG and PREG metabolism and substrate binding imply that the extract's bioactive components probably act synergistically and interfere with the electron transport chain to inhibit CYP17A1 and CYP21A2 enzymes (Prevoo et al., 2008). Furthermore, SUB was reported to inhibit CYP17A1 towards PREG and PROG as well as 3β-HSD2, signifying that SUB could disrupt steroidogenesis at the branch point (Sergeant et al., 2017). In human H295R adrenal cells, the extract inhibited CYP11B1 by considerably reducing cortisol (CORT) and 11-hydroxy androstenedione (11-OHA4) levels, explaining the plant's anti-stress, anti-anxiety, and anti-hypertensive properties (Sergeant et al., 2017). Moreover, the methanol extract and SUB acted as selective glucocorticoid receptor agonists (SEGRAs) by not showing any transactivation ability on glucocorticoid response element-driven gene expression. SUB and the studied plant extract also suppressed NF-kB-driven gene expression while being unable to activate mineralocorticoid receptor (MR) mediated gene transcription, although both antagonised the effects of aldosterone via the MR (Sergeant et al., 2017).

The non-protein free amino acid GABA exhibits anti-neurotransmitter properties, which partly explain the use of *L. frutescens* for stress and anxiety disorders (Van Der Walt et al., 2016). The anti-anxiety activity of GABA has been linked to its ability to reduce glucocorticoid production (Engelbrecht et al., 2010).

3.7.10 Antimicrobial

The IC_{50} of *L. frutescens* hexane extract against *Enterococcus faecali, Escherichia coli*, and *Staphylococcus aureus* were found to be 2.50, 1.25 and 0.31 mg/mL respectively (Katerere & Eloff, 2005). Conversely, the dichloromethane: methanol (1:1) extract displayed a good inhibition against the shikimate kinase enzyme, an important drug target for *Mycobacterium tuberculosis* with an IC_{50} of 0.1 μg/mL, whereas the aqueous and ethanolic extracts had IC_{50} of 5.1 and 1.7 μg/mL, respectively (Masoko et al., 2016). The efficiency of the dichloromethane: methanol (1:1) extract as shikimate kinase inhibitor was attributed to the essential omega 3 fatty acid α-linolenic acid which is known for its antimicrobial activity against *Staphylococcus aureus*, *Bacillus subtilis*, *Helicobacter pylori*, *Rhizoctonia solani*, *Crinipellis perniciosa*, and hepatitis C virus (McGaw et al., 2002; Obonoyo et al., 2012; Leu et al., 2004; Masoko et al.,

2016). α-linolenic acid was found to possess antitubercular activity by inhibiting the shikimate kinase enzyme with an IC_{50} of 3.7 µg/mL (Masoko et al., 2016).

The ethyl acetate and 50% methanolic extracts were diluted to 5%, 10% and 20% (w/w) with DMSO and tested for their mutagenic and antimutagenic properties against *Salmonella typhimurium* strains TA97a, TA98, TA100 and TA102. After investigations, it was observed that the ethyl acetate extract significantly exhibited antimutagenic effects against TA97a, TA98, TA100, and TA102 (Ntuli et al., 2018). On the other hand, the methanolic extract showed pro-mutagenic and antimutagenic potential in the presence of the S9 in TA98 with 2-acetamidofluorene and TA100 with aflatoxin B1 (Ntuli et al., 2018). *L*-arginine, GABA, and D-pinitol exhibited antimutagenic activity against all four strains, whilst *L*-canavanine displayed a co-mutagenic effect in the absence of S9 in TA97 with 9-aminoacridine. Thus, the pro-mutagenic activity of the methanol extract cannot be ascribed to *L*-canavanine (Ntuli et al., 2018). The ethyl acetate extract, having a higher antimutagenic potential and total phenolic content than the methanolic extract, explains the correlation between the antioxidant and antimutagenic activities of the plant.

3.7.11 Toxicology

The traditional dosage involves daily infusions or decoctions of 2.5-5 g of dried material. The highest recorded dose, a decoction of 5 g of leaves, stems, and pods taken twice daily over six years, resulted in no adverse effects (Van Wyk et al., 2008). Furthermore, studies on the intraperitoneal administration of graded aqueous extracts of *L. frutescens* in fasted Balb C albino mice (20–25 g) established the lethal dose (LD_{50}) at 1280 ± 71 mg/Kg, suggesting that the crude extracts are likely to be relatively safe in mammals (Ojewole, 2004). A study on determining the toxicity of the aqueous and ethanolic leaf extracts on zebrafish embryos, focusing on their hatching rates and larval mortality at concentrations ranging from 5 to 300 µg/mL, exhibited lethal concentration (LC_{50}) values of 297.57 µg/ml (aqueous) and 40.54 µg/ml (ethanol), reaffirming the claim that the water extract is less toxic than the ethanol extract (Zonyane et al., 2029). However, further study on how the plant may interact with other drugs and diseases is essential to avoid fatal or detrimental side effects.

For commercial preparations, a recommended dose of 300 mg of dried leaves twice daily (600 mg/day) is advised, with the caution that it should be avoided during pregnancy and lactation. This conservative dosage was used for a safety study in vervet monkeys, where doses of 0, 9, 27, and 81 mg/kg body weight correspond to 0, 1, 3, and 9 times the recommended human dose. These doses were administered as part of a standard diet for three months, and the study showed no clinical side effects across 15 haematological, 21 clinical biochemical, 6 physiological, and

many behavioural variables, providing strong and reassuring evidence of the safety of *L. frutescens* at recommended human doses (Seier et al., 2002).

3.8 Clinical trials

Grandi et al. (2005) conducted a study with 16 cancer patients (11 men and 5 women) to evaluate the effect of 600 mg/day of aqueous *L. frutescens* extract. They found that the extract significantly decreased fatigue in cancer patients, with no other major adverse effects reported. In Johnson et al. (2007), a randomised, double-blind, placebo-controlled trial involving 25 healthy adults, examined the effects of 800 mg/day of *L. frutescens* leaf powder capsules. The study concluded that the powder was well tolerated over three months, with no significant adverse events observed, and there was a noted improvement in appetite in the treatment group. In 2002, the South African Ministry of Health recommended the aqueous extract as a drug support in the treatment of HIV/AIDS (Mills et al., 2005; SADC, 2002) as it decreased viral loads and improved CD4 counts (Chaffey & Stokes, 2002). However, preclinical studies done in 2011 have indicated that using *L. frutescens* extract alongside antiretroviral drugs or CYP3A4 substrates may cause harmful drug-herb interactions, treatment failure, and the development of viral resistance (Minocha et al., 2011; Mills et al., 2005). Wilson et al. (2015) performed a study on 107 participants, dividing them into two groups: one received 2400 mg/day of *L. frutescens* leaf powder (1200 mg twice daily), and the other received a placebo. The results showed that *L. frutescens* did not alter the viral load or CD4 T- lymphocyte count, but the treatment group had a higher burden primarily due to two tuberculosis cases in patients on isoniazid preventive therapy (IPT). While no other safety concerns related to *L. frutescens* consumption were detected, the study indicates the need for further investigation into the potential interaction between *L. frutescens* and IPT (Wilson et al., 2015).

3.9 Discussion

L. frutescens has been extensively studied for its anticancer, anti-inflammatory, immune booster and anti-HIV properties, with traditional usage suggesting minimal side effects. However, research studies highlight significant complexities and limitations in its application, particularly in anticancer and anti-HIV therapies, while revealing promise in other areas such as immune booster, metabolic, oxidative, and microbial conditions.

The cytotoxic effects of *L. frutescens* extracts have been demonstrated in various cancer cell lines, including breast (MCF-7), colon (Caco-2), melanoma (A-375, Colo-800), prostate (PC3, LNCaP, TRAMP-C2), ovary (CHO), cervical (HeLa), and oesophageal (SNO) cancers. These effects are primarily mediated through mechanisms such as PI3K/Akt inhibition, oxidative

stress, mitochondrial dysfunction, caspase activation, and suppression of the Gli/Hh signalling pathway. Despite these promising results, the therapeutic concentrations required (0.3-10 mg/mL) are significantly higher than those of standard chemotherapeutic drugs like doxorubicin (IC_{50}= 0.68±0.04 µg/ml for MCF-7) and paclitaxel (IC_{50}= 2.5 ng/mL for MCF-7 and 2.6 ng/mL for HeLa), raising concerns about the practical application of *L. frutescens* in cancer therapy (Fang et al., 2014; Liebmann et al., 1993). Additionally, the lack of selectivity is a major limitation, as both cancer and normal cells (e.g., T-lymphocytes, human dermal fibroblasts) exhibit toxicity at similar concentrations. This raises questions about the plant's therapeutic index and clinical safety

In HIV therapy, *L. frutescens* has shown inhibitory effects on HIV-1 RT, primarily due to its tannin content. However, tannins lack specificity, and their pharmacological efficacy is significantly lower than established antiretroviral drugs (Sieniawska, 2015). For instance, tenofovir, a nucleotide analogue RT inhibitor, exhibits highly specific activity by competing with the natural substrate, deoxyadenosine 5′-triphosphate, for incorporation into viral DNA at the active site of reverse transcriptase, ultimately causing premature termination of the DNA chain during replication with IC_{50} values of 0.5-2.2 µM with a highly specific mechanism of action (De Clercq, 2004; Paintsil & Cheng, 2009; Wassner et al., 2020). On the other hand, *L. frutescens* extracts require much higher concentrations (IC_{50} = 200 µM), limiting their practical utility.

Furthermore, the immunotoxicity of *L. frutescens* further complicates its potential use in HIV therapy. At an IC_{50} concentration of 7.5 mg/mL, the ethanolic extract induces apoptosis in lymphocytes and $CD4^+$ cells by increasing caspase-3/7 activity, promoting phosphatidylserine translocation, and depleting ATP levels. This activation-induced cell death significantly undermines the preservation of the $CD4^+$ T-cell population, a critical goal in HIV treatment (Okoye & Picker, 2013). The resulting loss of immune integrity heightens susceptibility to opportunistic infections, such as tuberculosis and fungal infections, presenting a substantial drawback for therapeutic application.

Its potential for drug-herb interactions poses significant challenges, as it may compromise the efficacy and bioavailability of antiretroviral drugs, creating risks for patients who require precise drug concentrations. Additionally, *L. frutescens* has been associated with exacerbating HIV-associated neuroinflammation, evidenced by increased MCP-1 levels and $CD14^+$ monocyte infiltration across the blood-brain barrier. These effects could worsen HIV-associated neurocognitive impairment, a condition affecting 42.6 % of patients (Wang et al., 2020; Okoye & Picker, 2013).

Despite the higher concentrations required for anticancer and anti-HIV activity, *L. frutescens* has demonstrated more promising potential in other therapeutic areas. Studies highlight significant anti-diabetic, antioxidant, neuroprotective, anti-inflammatory, and antimicrobial properties. Both aqueous and ethanolic extracts, along with bioactive compounds such as sutherlandioside B, mucronulatol, D-pinitol, and α-linolenic acid, exhibit potent biological activity at concentrations below 50 µg/mL (Tables 3.3 and 3.4). These findings suggest greater efficacy against metabolic, oxidative, and microbial conditions. For instance, D-pinitol is recognised for its insulin-sensitizing effects, while α-linolenic acid, sutherlandioside D, and mucronulatol contribute to anti-tubercular, antistress, and neuroprotective activities, respectively. Such properties underscore the plant's potential in addressing metabolic and oxidative stress-related disorders.

3.10 Conclusion

The phytochemical investigation on *L. frutescens* has highlighted its potential as a rich source of amino acids, flavonoid glycosides and cycloartane glycosides. The discovery of novel cycloartane glycosides and 9,10-seco-cycloartane-type diglycosides with an unprecedented 5/7/6/5 ring skeleton underlines the importance of *L. frutescens* in natural product chemistry. The therapeutic efficacy of *L. frutescens* is hindered by several limitations, including its high effective concentrations, lack of selectivity, potential drug-herb interactions, and immunotoxicity. Most observed activities occur at concentrations significantly higher than the widely accepted pharmacological threshold of 50 µg/mL, calling into question its clinical relevance for cancer and HIV treatment. However, its potency in diabetics, neurodegenerative, microbial and oxidative-related diseases presents an opportunity for further exploration.

Future research should focus on isolating and characterising the active compounds responsible for their therapeutic potential. Additionally, comprehensive investigations into drug-herb interactions are essential for safe integration with existing therapies.

References

Aboyade, O. M., Styger, G., Gibson, D. & Hughes, G. (2013). Sutherlandia frutescens: The meeting of science and traditional knowledge. *The Journal of Alternative and Contemporary Medicine*, 20(2): 71-76.

Adefuye, O.J. (2016). *Anti-Diabetic and Phytochemical analysis of Sutherlandia fruescens extracts*. PhD thesis. Nelson Mandela University.

Africa, L. & Smith, C. (2015). *Sutherlandia frutescens* may exacerbate HIV-associated neuroinflammation. *J Negat Results Biomed*., 14: 1-9.

Akindele, A. J., Sowemimo, A., Agunbiade, F. O., Sofidiya, M. O., Awodele, O., Ade-Ademilua, O., Orabueze, I., Ishola, I. O., Ayolabi, C. I., Salu, O. B., Akinleye, M. O. & Oreagba, I. A. (2022). Bioprospecting for Anti-COVID-19 Interventions From African

Medicinal Plants: A Review. *Natural Product Communications*, 17(5): 1-24.
Bates, S.H., Jones, R.B., Bailey, C.J. (2000). Insulin-like effect of pinitol. *Br. J. Pharmacol.*, 130: 1944-1948.
Camille, N. & Dealtry, G. (2018). Regulation of M1/M2 macrophage polarization by *Sutherlandia frutescens* via NFkB and MAPK signaling pathways. *South African Journal of Botany*, 116: 42–51.
CANSA. (2021). Fact Sheet And Position Statement on *Sutherlandia Frutescens.* Available at https://cansa.org.za/files/2021/07/Fact-Sheet-and-Position-Statement-on-Sutherlandia-Frutescens-July-2021.pdf (Accessed: 10 June 2023).
Chaffy, N. & Stokes, T. (2002). Aids herbal therapy. *Trends in Plant Scien*ce, 7: 57.
Chinkwo, K.A. (2005). *Sutherlandia frutescens* extracts can induce apoptosis in cultured carcinoma cells. *Journal of Ethnopharmacology*, 98: 163-170.
Choi, M. S., Lee, W. H., Kwon, E. Y., Kang, M. A., Lee, M. K., Park, Y. B. & Jeon, S. M. (2007). Effects of soy pinitol on the pro-inflammatory cytokines and scavenger receptors in oxidized low-density lipoprotein-treated THP-1 macrophages. *Journal of medicinal food*, 10: 594-601.
Daghman, M. I. (2015). *Comparison of the physicochemical characteristics and flavonoid release profiles of Sutherlandia frutescens phytosomes versus liposomes.* Master Thesis. University of Western Cape. Cape Town.
De Clercq, E. (2004). Antiviral drugs in current clinical use. *Journal of Clinical Virology*, 30(2):115-133.
Drewes, S.E. (2012). Natural products research in South Africa: 1890-2010. *S. Afr. J. Sci.*, 108: 1-8.
Dwarka, D., Agoni, C., Mellem, J.J., Soliman, M.E. & Baijnath, H. (2020). Identification of potential SARS-CoV-2 inhibitors from South African medicinal plant extracts using molecular modelling approaches. *S Afr J Bot.*, 133:273-284.
Engelbrecht, A., Smith, C., Neethling, I., Thomas, M., Mattheyse, M., Myburgh, K. H., Smith, C., Neethling, I., Thomas, M., Mattheyse, M., Myburgh, K. H., Engelbrecht, A., Smith, C., Neethling, I. A. N., Thomas, M., Ellis, B., Mattheyse, M. & Myburgh, K. H. (2010). Daily brief restraint stress alters signaling pathways and induces atrophy and apoptosis in rat skeletal muscle induces atrophy and apoptosis in rat skeletal muscle. *Stress*, 13(2): 132-141.
Enogieru, A. B., Omoruyi, S. I. & Ekpo, O. E. (2020). Aqueous leaf extract of *Sutherlandia frutescens* attenuates ROS-induced apoptosis and loss of mitochondrial membrane potential in MPP+-treated SH-SY5Y cells. *Tropical Journal of Pharmaceutical Research*, 19(3): 549-555.
Faleschini, M. T., Myer, M. S., Harding, N. & Fouchè, G. (2013). South African Journal of Botany Chemical pro fi ling with cytokine stimulating investigations of *Sutherlandia frutescens* L . R . (Br .) (Fabaceae). *South African Journal of Botany*, 85: 48–55.
Fang, X. J., Jiang, H., Zhu, Y. Q., Zhang, L. Y., Fan, Q. H. & Tian, Y. (2014). Doxorubicin induces drug resistance and expression of the novel CD44st via NF-κB in human breast cancer MCF-7 cells. *Oncology Reports*, 31(6): 2735–2742.
Fasinu, P. S., Gutmann, H., Schiller, H., James, A. & Bouic, P. J. (2012). The Potential of *Sutherlandia frutescens* for Herb-Drug Interaction. *Drug Metabolism And Disposition*, 41: 488–497.
Fernandes, A. C., Cromarty, D., Albrecht, C. & Van Rensburg, C. E. J. (2004). The antioxidant potential of *Sutherlandia frutescens*. *J. Ethnopharmacol.*, 95: 1-5.
Fu, X., Li, X.C., Smillie, T.J., Carvalho, P., Mabusela, W., Syce, J., Johnson, Q., Folk, W., Avery, M.A. & Khan, I. A. (2008). Cycloartane glycosides from Sutherlandia frutescens. *Journal of natural products*, 71(10):1749-1753.
Fu, X., Li, X. C., Wang, Y. H., Avula, B., Smillie, T. J., Mabusela, W., Syce, J., Johnson, Q., Folk, W. & Khan, I. A. (2010a). Flavonol glycosides from the South African medicinal

plant *Sutherlandia frutescens*. *Planta Medica*, 76(2): 178-181.
Fu, X., Li, X.C., Smillie, T.J. & Khan, I. A. (2010b). Rearranged Cycloartanol Glycosides from *Sutherlandia frutescens*. *Planta Medica*, 76(5): 47.
Fu, X. (2012). *Phytochemical studies on the medicinal plant Sutherlandia frutescens*. PhD thesis. University of Mississipi.
Gericke, N., Albrecht, C.F., Van Wyk, B., Mayeng, B., Mutwa, C. & Hutchings, A. (2001). *Sutherlandia frutescens*. A*ustralian Journal ofMedical Herbalism*, 13: 9-15.
Gonyela, O., Peter, X., Dewar, J. B., Westhuyzen, C. Van Der, Steenkampa, P. & Fouchee, G. (2019). Cycloartanol and Sutherlandioside C peracetate from *Sutherlandia frutescens* and their immune potentiating effects Natural Product Research Cycloartanol and Sutherlandioside C peracetate from Sutherlandia frutescens and their immune potentiating effects. *Natural Product Research*, 1: 1-9.
Gouws, C., Smit, T., Willers, C., Svitina, H., Calitz, C., & Wrzesinski, K. (2021). Anticancer potential of sutherlandia frutescens and xysmalobium undulatum in ls180 colorectal cancer mini-tumors. *Molecules*, 26(3): 1-18.
Grandi, M., Roselli, L. & Vernay, M. (2005). *Lessertia* (*Sutherlandia frutescen*s) and fatigue during cancer treatment [*Lessertia* (*Sutherlandia frutescen*s) et la fatigue en cancérologie]. *Phytotherapie*, 3: 110-113.
Green, M. H. (1988). *Method of treating viral infections with amino acid analogs*. United States Patent no. 5,110,600.
Grunz-borgmann, E., Mossine, V., Fritsche, K. & Parrish, A. R. (2015). Ashwagandha attenuates TNF- α - and LPS- induced NF- κ B activation and CCL2 and CCL5 gene expression in NRK-52E cells. *BMC Complementary and Alternative Medicine*, 2: 1-8.
Harnett, S. M., Oosthuizen, V. & Venter, M. Van De. (2004). *Anti-HIV activities of organic and aqueous extracts of Sutherlandia frutescens and Lobostemon trigonus*. 96: 113-119.
Jackson, W.P.U. (1990). *Origins and meanings of names of South African plant genera*. U.C.T. Printing Department, Cape Town.
Jiang, J., Chuang, D. Y., Zong, Y., Patel, J., Brownstein, K., Lei, W., Lu, H., Simonyi, A., Gu, Z., Cui, J., Rottinghaus, G. E., Fritsche, K. L., Lubahn, D. B., Folk, W. R. & Sun, G. Y. (2014). Sutherlandia frutescens Ethanol Extracts Inhibit Oxidative Stress and Inflammatory Responses in Neurons and Microglial Cells. *PloS One*, 9(2): 1-9.
Johnson, Q., Syce, J., Nell, H., Rudeen, K. & Folk, W. R. (2007) A Randomized, Double-Blind, Placebo-Controlled Trial of *Lessertia frutescens* in Healthy Adults. *PLOS Clin Trial*, 2(4): 1-16
Katerere, D. R. & Eloff, J. N. (2005). Antibacterial and Antioxidant Activity of Sutherlandia frutescens (Fabaceae), A Reputed Anti-HIV / AIDS Phytomedicine. *Phytotherapy Research*, 19: 779-781.
Kisten, N. (2020). *The immune-modulating activity of Sutherlandia frutescens*. Master thesis. University of Western Cape. Cape Town.
Korb, V. C., Moodley, D. & Chuturgoon, A. A. (2010). Apoptosis-promoting effects of *Sutherlandia frutescens* extrActs on normAl humAn lymphocytes *in vitro*. *South African Journal of Science*, 106(1/2): 64-69.
Lei, W., Browning, J. D., Eichen, P. A., Lu, C. H., Mossine, V. V., Rottinghaus, G. E., Folk, W. R., Sun, G. Y., Lubahn, D. B. & Fritsche, K. L. (2015a). Immuno-stimulatory activity of a polysaccharide-enriched fraction of *Sutherlandia frutescen*s occurs by the toll-like receptor-4 signaling pathway. *Journal of Ethnopharmacology*, 172: 247-253.
Lei, W., Browning, J. D., Eichen, P. A., Brownstein, K. J., Folk, W. R., Sun, G. Y., Lubahn, D. B., Rottinghaus, G. E. & Fritsche, K. L. (2015b). Unveiling the anti-inflammatory activity of *Sutherlandia frutescens* using murine macrophages. *Int. Immunopharmacol.* 29: 254-262.
Leisching, G., Loos, B., Nell, T. & Engelbrecht, A.-M. (2015). *Sutherlandia frutescens* treatment induces apoptosis and modulates the PI3-kinase pathway in colon cancer cells.

South African J. Bot., 100: 20-26.
Leu, G., Lin, T. & John, T. A. (2004). Anti-HCV activities of selected polysaturated fatty acids. *Biochem Biophys Res Commun*., 318: 275-80.
Liebmann, J. E., Cook, J. A., Lipschultz, C., Teague, D., Fisher, J. & Mitchell, J. B. (1993). Cytotoxic studies of pacfitaxel (Taxol®) in human tumour cell lines. *Br. J. Cancer*, 68: 1104-1109.
Lin, L. G., Ung, C. O. L., Feng, Z. L., Huang, L. & Hu, H. (2016). Naturally occurring diterpenoid dimers: Source, biosynthesis, chemistry and bioactivities. *Planta Medica*, 82(15): 1309-1328.
Lu, Y., Starkey, N., Lei, W., Li, J. & Cheng, J. (2015). Inhibition of Hedgehog-Signaling Driven Genes in Prostate Cancer Cells by Sutherlandia frutescens Extract. *PLoS ONE*, 10(12): 5-7.
Mackenzie, J., Koekemoer, T., Venter, M. & van De Dealtry, G. (2009). *Sutherlandia frutescen*s Limits the Development of Insulin Resistance by Decreasing Plasma Free Fatty Acid Levels. *Phytother Res*. 23: 1609-1614.
Masoko, P., Mabusa, I. H. & Howard, R. L. (2016). Isolation of alpha-linolenic acid from Sutherlandia frutescens and its inhibition of Mycobacterium tuberculosis ' shikimate kinase enzyme. *BMC Complementary and Alternative Medicine*, 1-8.
McGaw, L. J., Jäger, A. J. & van Staden, J. (2002). Antibacterial effects of fatty acids and related compounds from plants. *S Afr J Bot*., 68:417-23.
Mills, E., Cooper, C., Seely, D. & Kanfer, I. (2005). African herbal medicines in the treatment of HIV: Hyoxis and Sutherlandia: An overview of evidence and pharmacology. *Nutr J*, 4: 19-24.
Minocha, M., Mandava, N. K., Kwatra, D., Pal, D., Folk, W. R., Earla, R. & Mitra, A. K. (2011). Effect of short term and chronic administration of Sutherlandia frutescens on pharmacokinetics of nevirapine in rats. *Internatonal Journal of Pharmaceutics*, 413: 44-50.
Morris, K. (2001). Treating HIV in South Africa–a tale of two systems.*The Lancet*, 357: 1190.
Moshe, D., Van der Bank, H., Van der Bank, M. & Van Wyk, B. E. (1998). Lack of genetic differentiation between 19 populations from seven taxa of Sutherlandia Tribe: Galegeae, Fabaceae. *Biochem. Syst. Ecol.*, 26: 595-609.
Mncwangi, N., Viljoen, A., Mulaudzi, N. & Fouche, G. (2023). *Lessertia frutescens*. *The South African Herbal Pharmacopoeia*. Academic Press: 321-344.
Müller, A. C., Patnala, S., Kis, O., Bendayan, R. & Kanfer, I. (2012). Interactions between Phytochemical Components of Sutherlandia Frutescens and the Antiretroviral , Atazanavir *In Vitro* : Implications for Absorption and Metabolism. *Journal of Pharmacy and Pharmaceutical Sciences*, 15(1): 221-233.
Na, H.-K., Mossanda, K.S., Lee, J.-Y. & Surh, Y.-J. (2004). Inhibition of phorbol ester-induced COX-2 expression by some edible African plants. *Biofactors*, 21: 149-53.
Ndjoubi, K. O., Omoruyi, S. I., Luckay, R. C., & Hussein, A. A. (2024). Isolation of Lessertiosides A and B and Other Metabolites from Lessertia frutescens and Their Neuroprotection Activity. *Plants*, 13(21): 1-14.
Ngcobo, M., Gqaleni, N., Chelule, P. K., Serumula, M. & Assounga, A. (2012). Effects of Sutherlandia frutescens extracts on normal t-lymphocytes *in vitro*. *African Journal of Traditional, Complementary and Alternative Medicines*, 9(1): 73-80.
Ntuli, S. S. B. N., Gelderblom, W. C. A. & Katerere, D. R. (2018). The mutagenic and antimutagenic activity of Sutherlandia frutescens extracts and marker compounds. *BMC Complementary and Alternative Medicine*, 18(1): 1-10.
Obonyo, M., Zhang, L., Thamphiwatana, S., Pornpattananangkul, D., Fu, V. & Zhang, L. (2012). Antibacterial activities of Liposomal linolenic acids against antibiotic-resistant helicobacter pylori. *Mol Pharm*., 9: 2677-85.
Ojewole, J. (2004). Analgesic, antiinflammatory and hypoglycemic effects of *Sutherlandia*

frutescens R. BR. (variety Incana E. MEY.) [fabaceae] shoot aqueous extract. *Methods and findings in exp. Clin Pharmacol.*, 26: 409-416.

Ojewole, J. A. O. (2008). Antinociceptive, anti-inflammatory and antidiabetic properties of Hypoxis hemerocallidea Fisch. & C.A. Mey (Hypoxidaceae) corm ['African Potato'] aqueous antidiabetic properties of Hypoxis hemerocallidea Fisch. & C.A. Mey (Hypoxidaceae) corm ['African Potato'] aqueous extracts in mice and rats. *J Ethnopharmacol*, 103: 126-134.

Okoye, A. A. & Picker, L. J. (2013). $CD4^+$ T-Cell Depletion In Hiv Infection: Mechanisms Of Immunological Failure. *Immunological Reviews*, 254: 54-64.

Omolaoye, T. S., Skosana, B. T. & du Plessis, S. S. (2023). The effect of *Aspalathin linearis*, *Cyclopia intermedia* and *Sutherlandia frutescens* on sperm functional parameters of healthy male wistar rats. *Frontiers in Physiology*, 14: 1-10.

Ortega, A. (2003). A new role for GABA: inhibition of tumor cell migration. *Trends Pharmacol. Sci*., 24: 151-154.

Paintsil, E. & Cheng, Y. C. (2009). Antiviral Agents. In Moselio Schaechter (Ed.). *Encyclopedia of Microbiology*. 3rd Ed. Academic Press: 223-257.

Phulukdaree, A., Moodley, D. & Chuturgoon, A. A. (2010). The effecTs of Sutherlandia fruteScenS exTracTs in culTured renal proximal and disTal Tubule epiThelial cells. *South African Journal of Science*, 106(1/2): 54-58.

PlantzAfrica. (2013). *Sutherlandia frutescens herba*. Available at http://www.plantzafrica.com/medmonographs/sutherlfrut.pdf [03/02/2023].

Prevoo, D., Smith, C., Swart, P. & Swart, A.C. (2004). The Effect of *Sutherlandia frutescens*on Steroidogenesis: confirming Indigenous Wisdom. *Endocr. Res.*, 30: 745-751.

Prevoo, D., Swart, P. & Swart, A. C. (2008). The influence of *Sutherlandia frutescens* on adrenal steroidogenic cytochrome P450 enzymes. *Journal of Ethnopharmacology*, 118: 118-126.

Reid, K.A., Maes, J., Maes, A., Van Staden, J., De Kimpe, N., Mulholland, D.A. & Verschaeve, L. (2006). Evaluation of the mutagenic and antimutagenic effects of South African plants. *J. Ethnopharmacol*., 106: 44-50.

Schrire, B. D. & Andrews, S. (1992). *Sutherlandia*: gansies or balloon peas: Part 1 . *The Plantsman*, 14: 65-69.

Seier, J.V., Mdhluli, M., Dhansay, M.A., Loza, J. & Laubscher, R. (2002). A toxicity study of *Sutherlandia* leaf powder (*Sutherlandia microphylla*) consumption. Final report: April 2002. Medical Research Council of South Africa and National Research Foundation. available at: www.sa-healthinfo.org/traditionalmeds/firststudy.htm

Sergeant, C. A., Africander, D., Swart, P. & Swart, A. C. (2017). *Sutherlandia frutescens* modulates adrenal hormone biosynthesis , acts as a selective glucocorticoid receptor agonist (SEGRA) and displays anti- mineralocorticoid properties. *Journal of Ethnopharmacology*, 202: 290–301.

Sivakumar, S., Palsamy, P. & Subramanian, S. P. (2010). Impact of D-pinitol on the attenuation of proinflammatory cytokines, hyperglycemia-mediated oxidative stress and protection of kidney tissue ultrastructure in streptozotocin-induced diabetic rats. *Chemico-biological interactions*, 188: 237-245.

Smith, C. & Myburgh, K. H. (2004). Treatment with *Sutherlandia frutescens* ssp. microphylla alters the corticosterone response to chronic intermittent immobilization stress in rats. *South African Journal of Science*, 100(3-4): 229-232.

Stander, B. A., Marais, S., Steynberg, T. J., Theron, D., Joubert, F., Albrecht, C. & Joubert, A. M. (2007). Influence of *Sutherlandia frutescens* extracts on cell numbers, morphology and gene expression in MCF-7 cells. *Journal of Ethnopharmacology*, 112(2): 312-318.

Stander, A., Marais, S., Stivaktas, V., Vorster, C., Albrecht, C., Lottering, M. L. & Joubert, A. M. (2009). In vitro effects of *Sutherlandia frutescens* water extracts on cell numbers, morphology, cell cycle progression and cell death in a tumorigenic and a non-tumorigenic

epithelial breast cell line. *Journal of Ethnopharmacology*, 124(1): 45-60.
Steenkamp, V. & Gouws, M.C. (2006). Cytotoxicity of six South African medicinal plant extracts used in the treatment of cancer. *South African Journal of Botany,* 72: 630-633.
Street, R. A. & Prinsloo, G. (2012). Commercially important medicinal plants of South Africa: A review. *J Chem*, 2013: 1-16.
Tai, J., Cheung, S., Chan, E. & Hasman, D. (2004). In vitro culture studies of *Sutherlandia frutescens* on human tumor cell lines. *J. Ethnopharmacol*., 93: 9-19.
Tchegnitegni, B. T., Lerata, M. S., Beukes, D. R., & Antunes, E. M. (2024). Sutherlandiosides E−K: Further cycloartane glycosides from *Sutherlandia frutescens*. *Phytochemistry Letters*, 61: 66-74.
Thring, T.S. & Weitz, F.M. (2006). Medicinal plant use in the Bredasdorp/Elim region of the Southern Overberg in the Western Cape Province of South Africa. *J. Ethnopharmacol.*, 103: 261-75.
Tobwala, S., Fan, W., Hines, C.J., Folk, W.R. & Ercal, N. (2014). Antioxidant potential of *Sutherlandia frutescens* and its protective effects against oxidative stress in various cell cultures. *BMC Complement Altern Med*., 14: 271.
Van Der Walt, N. B., Zakeri, Z. & Cronjé, M. J. (2016). The induction of apoptosis in A375 malignant melanoma cells by *Sutherlandia frutescens*. *Evidence-Based Complementary and Alternative Medicine*, 2016: 1-14.
Van Wyk, B. E., Van Oudtshoorn, B. & Gericke, N. (1997). *Medicinal plants of South Africa*. Pretoria: Briza Publications.
Van Wyk, B. E. & Gericke, N. (2000). *Peoples plants: a guide to useful plants of southern Africa*. Pretoria: Briza Publications.
Van Wyk, B. E. & Albrecht, C. (2008). A review of the taxonomy, ethnobotany, chemistry and pharmacology of Sutherlandia frutescens (Fabaceae). *Journal of Ethnopharmacology*, 119(3): 620-629.
Van Wyk, B. E. & Gorelik, B. (2017). The history and ethnobotany of Cape herbal teas. *South African Journal of Botany*, 110: 18-38.
Vasaikar, N., Mahajan, U., Patil, K. R., Suchal, K., Patil, C. R., Ojha, S. & Goyal, S. N. (2018). D-pinitol attenuates cisplatin-induced nephrotoxicity in rats: Impact on pro-inflammatory cytokines. *Chemico-Biology Interactions*, 1: 1-23.
Wang, Y., Lui, M., Lu, Q., Farrell, M., Lappin, J., Shi, J., Lu, L. & Bao, Y. (2020). Global prevalence and burden of HIV-associated neurocognitive disorder: a meta-analysis. *Neurology*, 95(19): 1-18.
Wassner, C., Bradley, N. & Lee, Y. (2020). A Review and Clinical Understanding of Tenofovir: Tenofovir Disoproxil Fumarate versus Tenofovir Alafenamide. *Journal of the International Association of Providers of AIDS Care*, 19: 1-10.
Williams, S., Roux, S., Koekemoer, T., Venter, M. & Van Dealtry, G. (2013). *Sutherlandia frutescens* prevents changes in diabetes-related gene expression in a fructose-induced insulin-resistant cell model. *Journal of Ethnopharmacology*, 146(2): 482–489.
Wilson D, Goggin K, Williams K, Gerkovich MM, Gqaleni N, Syce J, et al. (2015) Consumption of *Sutherlandia frutescens* by HIV-Seropositive South African Adults: An Adaptive Double-Blind Randomized Placebo Controlled Trial. PLoS ONE 10(7): e0128522
Xaba, P. (2007). The cancer bush, a timeless remedy. *Veld & Flora*, 1: 234–235.
Zonyane, S., Chen, L., Xu, M. J., Gong, Z. N., Xu, S. & Makunga, N. P. (2019). Geographic-based metabolomic variation and toxicity analysis of *Sutherlandia frutescens* L. R.Br. – An emerging medicinal crop in South Africa. *Industrial Crops and Products*, *133*: 414–423.
Zonyane, S., Fawole, O.A., la Grange, C., Stander, M.A., Opara, U.L. & Makunga, N.P. (2020). The implication of chemotpic variation on the anti-oxidant and anti-cancer activities of *Sutherlandia frutescens* (L.) R.Br. (Fabaceae) from different geographic locations.

Antioxidants, 9(2): 152.

CHAPTER FOUR: A review of phytochemical and biological activities of *Protea* and *Leucadendron* Species

Kadidiatou O. Ndjoubi[1], Masande Yalo[1], Ahmed A. Hussein[1*]

[1]Chemistry Department, Cape Peninsula University of Technology, Symphony Rd., Bellville 7535, South Africa; dickakadi@yahoo.fr (K.O.N), masandeyalo@gmail.com (M.Y.), mohammedam@cput.ac.za (A.A.H.)
*Correspondence: mohammedam@cput.ac.za

Abstract

The Proteaceae family, renowned for its remarkable diversity and distinctive ecological adaptations, holds immense botanical significance. Prominent in regions with Mediterranean climates like Australia and South Africa, these plants also contribute to local economies by trading cut flowers, cut stems, and potted plants. Around 1800 species are distributed across 80 genera, and Protea and Leucadendron are the most prominent among the 14 Proteaceae genera that are endemic to the Cape floral region.

Only 30% of Proteaceae species have been subjected to phytochemical analysis, with less than 10% having their compounds isolated and purified. Among these, the genus *Protea* has received more attention, with approximately 53 compounds identified, 48 of which have been isolated. In contrast, research on *Leucadendron* species lags, with only 5 compounds isolated. Phytochemical studies of both genera have revealed the presence of cyanogenic glycosides and bislactonic spiro compounds in certain *Leucadendron* species. In contrast, aromatic esters of aryl glycosides, phenolic and flavonoid glycosides have been isolated and identified from *Protea* species.

The bioactive properties demonstrated by *Protea* species, such as antioxidant, anti-inflammatory, antibacterial, and anti-tyrosinase activities, are attributed to their high phenol and polyphenol content. Nevertheless, *Leucadendron* species' ethnobotanical and pharmacological potential remains unexplored, presenting an area ripe for further investigation and potential discovery.

Keywords: Proteaceae, *Protea*, *Leucadendron*, Phytochemistry, and pharmacological properties.

4.1 Introduction

The Proteaceae family is the most diverse and unique family in the fynbos region (Lamont et al., 1985; Cowling & Lamont, 1998). The family is made of shrubs and trees that crop up in rainforest to xeric habitats spreading in tropical and subtropical regions, especially in regions with Mediterranean climates like Australia, South Africa, South America, Central America,

Asia, India, Fiji, Indonesia, Japan, New Zealand, New Caledonia, Sri Lanka, Vanuatu, Micronesia, Madagascar, Solomon Islands, and Papua New Guinea (Simpson, 2010; Zhang et al., 2023). This botanical family consists of approximately 1800 species distributed across 80 genera, divided into five subfamilies: Bellendenoideae (1 genus), Grevilleoideae (47 genera), Persoonioideae (5 genera), Proteoideae (25 genera), and Symphionematoideae (2 genera) (Zhang et al., 2023). Australia hosts a significant portion, with over 1100 species distributed among 45 genera, 37 of which are endemic. In contrast, Southern Africa is home to 360 species within 14 genera, including *Aulax*, *Brabejum*, *Diastella*, *Faurea*, *Leucadendron*, *Leucospermum*, *Mimetes*, *Orothamnus*, *Paranomus*, *Protea*, *Serruria*, *Sorocephalus*, S*patalla*, and *Vexatorella* (Rebelo, 1995). Furthermore, 330 species out of the 360 found in Southern Africa are concentrated in the southwestern Cape region, known as the Cape Floral Kingdom (Blomerus et al., 2010; Newton et al., 2021). *Protea* (136 species) and *Leucadendron* (85 species) emerge as the preeminent genera in the Cape Floral region. Remarkably, approximately 60% (87 species) of *Protea* species and 90% (80 species) of *Leucadendron* species are endemic to this floral region (Leonhardt & Criley, 1999; Rebello, 1995; Verotta et al., 1999; Schnitzler et al., 2011).

Perennial and woody in nature, *Protea* and *Leucadendron* species exhibit diverse structural forms, ranging from shrubs (0.2 m) to tall trees (40 m). Most Proteaceae plants are bisexual, with flower parts ranging from actinomorphic to strongly zygomorphic. Many taxa within the family tend to have self-pollinating flowers, leading to a reduced flower-to-fruit ratio due to inbreeding depression (Zhang et al., 2023). Moreover, Proteaceae flowers are renowned for their intricate beauty and distinctive structure, typically arranged in dense clusters known as inflorescences. These flowers come in various shapes, sizes, and colours, ranging from small and inconspicuous, like *Leucadendron,* or to large and showy, like *Protea* (Zhang et al., 2023). Beyond their ornamental value, Proteaceae plants play crucial roles in their native ecosystems, providing food and habitat for diverse wildlife, including birds, insects, and mammals. Birds, insects, and rodents contribute to pollination across different species within the family, facilitating reproduction and genetic diversity. Moreover, many Proteaceae species hold cultural significance within indigenous communities as they are used for food, medicine, and ceremonial purposes. This underscores the multifaceted significance of Proteaceae plants as ecological contributors and integral components of cultural heritage and traditional practices (Leonhardt & Criley, 1999).

Only 30% of Proteaceae species have been subjected to phytochemical analysis, with less than 10% having their compounds isolated and purified (Gadea et al., 2022). The genera *Grevillea* and *Protea* are the most studied. Within the family, less than 400 compounds have been

identified, mainly phenolic compounds (69%), quinones (8%), and alkaloids (13%) (Gadea et al., 2022; Yang, 2017). These species are noted for their bioactive properties, such as antioxidant, anti-inflammatory, antibacterial, antiallergic, anti-cancer, and antiviral effects, attributed to their high phenol and polyphenol content. The prominent phytochemical groups in Proteaceae are phenolic glucosides, alkylresorcinols, their derivatives, and tropane alkaloids (Zhang et al., 2023).

This review aims to explore the economic importance, ecological significance, ethnomedicinal uses as well as pharmacological and phytochemical investigations conducted on two key genera in South Africa's Proteaceae family: *Protea* and *Leucadendron.*

4.2 Economic Importance of *Protea* and *Leucadendron*

The Proteaceae family, comprising woody plants like *Protea* and *Leucadendron*, holds symbolic significance within the fynbos biome, enriching its remarkable biodiversity (Goldblatt & Manning, 2002). In the fynbos biome, Proteaceae species play pivotal roles in ecological balance, serving as significant sources of nectar that attract various bird species, butterflies, and bees, thereby aiding in pollination and supporting biodiversity (Schurr et al., 2012). They also significantly play a crucial role in carbon, water, and nutrient cycling as well as providing essential resources for herbivores and pollinators. Moreover, *Protea* species contribute substantially to the economic value generated by the fynbos wildflower industry and serves as a flagship species for conservation (Schurr et al., 2012).

The commercial exploitation of Proteaceae likely commenced in South Africa during the late 18th century. During this era, *P. nitida* was extensively harvested for timber, while *Leucadendron* plantations were established to cater to the growing demand for firewood and tanning bark (Weston, 2007). Today, the South African Proteaceae industry encompasses two primary sectors: veld harvesting and cultivated production. Veld harvesting covers approximately 200,000 ha, mainly in the Western and Eastern Cape Provinces. Conversely, data on cultivated products from 2017 revealed a minor reduction in cultivated land area from the previously estimated 1,009 ha in 2014 to 996 ha in 2017, with *Protea* (595 ha), *Leucadendron* (134 ha), and *Leucospermum* (201 ha) being the primary species under cultivation (Reinten et al., 2018). Prominent export species from the *Protea* and *Leucadendron* genera (Table 4.1) majorly contribute to South Africa's floral export market. *Protea* and *Leucadendron* contribute 23.8% and 32.7% of the exported fynbos products during the 2015/2016 period (Reinten et al., 2018). Furthermore, in the cut-flower industry, *Protea* species commercialisation have evolved from wild harvesting to the commercial plantings of highly specialised hybrids with much less dependence on wild harvesting (Louw, 2024). Export

destinations for South African Proteaceae species encompass Central Europe (43%), the Middle East (30%), the United Kingdom (22%), the Far East and Asia (3%), the Americas (2%), and other African nations (1%). Despite the advantageous exchange rate for South African producers, pricing pressures persist in the European Union (EU) market. The Middle East and the Netherlands also serve as critical transit hubs facilitating product distribution to East Asian and European markets, respectively (Reinten et al., 2018).

Promoting *Protea* species in the export market as cut flowers has contributed to biodiversity conservation and spurred cultivation, resulting in the establishment of numerous nurseries. Recognised as South Africa's flagship cut flower, *Protea* species have significantly boosted employment rates and generated substantial revenue, reaching R240 million domestically and R280 million internationally (Baudoin et al., 2007; Netnou-Nkoana & Eloff, 2012). This assertion is supported by the 2007 International Society for Horticultural Science (ISHS) report, which highlights *Protea* species as one of the most commercialised proteaceous ornamentals plants (ISHS, 2007, Reinten et al., 2011). Additionally. The cut-flower industry in South Africa may have developed from the wild harvesting of proteas and fynbos but has since evolved to the commercial plantings of highly specialised hybrids with much less dependence on wild harvesting.

Moreover, beyond their ornamental value, some *Protea* species, such as *P. cynaroides, P. neriifolia*, *P. laurifolia*, *P. repens*, and *P. compacta*, exhibit resistance to phytophthora root rot, a significant fungal pathogen affecting various plants (Leonhardt & Criley, 1999). Consequently, commercial growers have capitalised on these desirable traits of *Protea* species by cultivating clonal selections and hybrids sourced from South African fynbos to meet market demands (Mathews, 1981).

Similarly, *Leucadendron* species, especially hybrids such as *'Silvan Red'*, *'Inca Gold'*, *'Kam-ee-lion'*, and *'Rosette'*, have gained commercial significance due to their long-lasting cut stems, high productivity potential, vibrant colours, and aesthetic appeal (Leonhardt & Criley, 1999). Cultivars such as *'Safari Sunset'* demonstrate impressive yields under intensive management, with *'Safari Sunset'* yielding over 600000 marketable stems per hectare annually in Israel (Littlejohn et al., 1998; Leonhardt & Criley, 1999). Furthermore, pruned and managed '*Silvan Red'*, which produces an average of 265 marketable stems per plant annually, can be harvested during autumn when the stems display red foliage and in winter when they exhibit tricolour stems adorned with green, red, and yellow foliar bracts (Barth et al., 1996).

Beyond their commercial use in cut stems, *Leucadendrons* can be cultivated as potted flowering plants. Research suggests that the male *L. discolor* can be induced to flower within 3 to 5 months by propagating large-branched cuttings already initiated with flowers, which will significantly

reduce the traditional two-year period required for flowering potted plants (Leonhardt & Criley, 1999; Ben-Jaacov et al., 1986). These advancements in cultivation techniques have expedited the flowering process of potted *Leucadendron* plants, offering promising prospects for the commercial nursery trade.

Table 4.1: List of some commercialised South African *Protea* and *Leucadendron* species (Pictures sourced from SANBI website)

Scientific Name	Common Name	Image	Commercial Uses
***PROTEA* SPECIES**			
***P. burchellii* Stapf**	Burchell's Sugarbush		Popular in the cut flower industry for its unique floral structure
***P. compacta* R.Br.**	Bot River Protea		Grown for the cut flower market for its vibrant colours and long vase life
***P. cynaroides* (L.) L.**	King Protea		Widely used in cut flower arrangements and bouquets
***P. eximia* (Salisb. Ex Knight) Fourc.**	Broad-leaf Sugarbush		Used in floral displays due to its robust, long-lasting flowers
***P. grandiceps* Tratt**	Rooisuikerbos		Used in floral arrangements for its decorative large flowers
***P. magnifica* Link**	Queen Protea		Valued for its large, attractive flower heads in floral arrangements
***P. neriifolia* R.Br.**	Oleander-leaf Protea		Popular in the cut flower industry for its distinctive appearance

***P. obtusifolia* H. Buek ex Meisn.**	Limestone Protea		Adapted for horticulture, particularly in coastal areas, due to its hardiness
***P. repens* L.**	Common Sugarbush		Cultivated for cut flowers and for honey production ("sugarbush syrup")
***LEUCADENDRON* SPECIES**			
***L. argenteum* (L.) R.Br.**	Silver Tree		Prized for its silvery foliage in floral arrangements and also used as an ornamental tree in gardens
***L. discolor* E. Phillips & Hutch.**	Piketberg Conebush		Valued for its striking yellow to orange bracts and extensively used in the cut flower industry
***L. laureolum* (Lam.) Fourc.**	Golden Conebush		Known for its bright yellow bracts and foliage and used for bouquets and landscaping purposes
***L. salignum* P.J. Bergius**	Common Sunshine Conebush		Used as filler material in floral arrangements

4.3 *Protea*

4.3.1 The genus *Protea*

Protea, a large genus of flowering plants commonly known as sugarbushes, consists of 136 species, primarily indigenous to the African continent, with 117 species residing there and a significant concentration of 90 species localised in South Africa (Vogts, 1982; Robelo, 1995). The genus *Protea* derives its name from the Greek god Proteus, renowned for his shapeshifting abilities, reflecting the diverse morphological characteristics observed across *Protea* species (Robelo, 1995). Their leaves display a variety of shapes, sizes, and textures, often characterised by lignification, hardness, and a leathery texture, adapted for water conservation and resilience against drought. These remarkable attributes and a high carbon-to-nitrogen ratio in the leaves

contribute significantly to their resistance against most insect pests, making commercial *Protea* plantings relatively pest-resistant (Leonhardt & Criley, 1999).

The genus *Protea* holds cultural significance as South Africa's national emblem. Its species are renowned for their distinctive flower heads surrounded by a conspicuous involucre of scales, primarily displaying shades of pink, occasionally featuring albino variations, as well as reds and, more rarely, greens (Werner, 1951). Among its notable species, *P. cynaroides*, commonly referred to as the King Protea or South Africa's national flower, stands out for its large, hemispherical heads that come in a spectrum of colours ranging from silvery pink to deep rose or creamy white, depending on the variety (Werner, 1951). Natural variations of *P. cynaroides* are classified into three eco-types found in the Eastern Cape and Southern Coastal Plain, the Outeniqua Mountains Region and the Western Cape, further emphasising *protea* species' ecological adaptability and geographic diversity (Leonhardt & Criley, 1999; Vogts, 1980). Other remarkable species include those adorned with striking beard-like scales, such as *P. lepidocarpodendron*, *P. marginata*, *P. neriifolia*, *P. stokoei*, and *P. speciosa*, as well as those without such scales, like *P. grandiceps*, *P. compacta*, *P. mellifera*, *P. obtusifolia*, and *P. pulchella* (Werner, 1951). These species vary in height and flowering seasons, offering a diverse range from tall tree like *P. lepidocarpodendron* to shrub like *P. pityphylla*. Hence, it provides a rich array of species that bloom throughout the year, most flourishing during spring and winter.

Moreover, while most *Protea* species thrive in temperate zones, some extend their habitat into sub-tropical and tropical regions, with a few even reaching the northern tropics (Rao, 1971). In South Africa, they thrive in well-drained, moderately acidic soils with low fertility, primarily composed of granite (Leonhardt & Criley, 1999). Their natural habitat extends from the coastal splendour of Cape Town to the majestic Table Mountain regions, reaching elevations of up to 1300 m above sea level (Leonhardt & Criley, 1999; Parvin et al., 1973). Natural hybrids within the *Protea* genus emerge where the geographical ranges of different species intersect, yielding novel genetic combinations. Studies conducted at South Africa's Fynbos Research have shed light on these natural hybrids (Table 1), paving the way for further innovation and progress in the *Protea* industry. Dr. Littlejohn's groundbreaking work in *Protea* breeding has opened avenues for controlled hybridisation, promising exciting prospects for *Protea* cultivation and conservation (Leonhardt & Criley, 1999).

Table 4.2: Example of South Africa *Protea* hybrids

Names	**Protea Hybrids**
Brenda	*P. compacta X P. burchelli*
Candida	*P. magnifica* X *P. obtusifolia*
King Grand	*P. cynaroides* X *P. grandiceps*
Liebencherry	*P. repens* X *P. longifoli*
Pink Duke	*P. compacta* X *P. susannae*
Robijn	P. glabra X P. laurifolia
Sheila	*P. magnifica* X *P. burchelli*
Valentine	*P. cynaroides* X *P. compacta*
Venetia	*P. magnifica* X *P. neriifolia*
Venus	*P. repens* X *P. aristata*

4.3.2 Ethnomedicinal uses of *Protea* species

4.3.2.1 *Protea angolensis Welw.*

P. angolensis, commonly known as Angola *protea*, is a 3m tall shrub native to Angola, Namibia, and Zambia (Tropical Plants Database, 2023). In Angola, the shoot tips and flowers are consumed as a source of nourishment, while the root powder and decoction are used to treat diarrhoea and cough in Zimbabwe. The stem bark, trunk, and branch powder are used in the same region for treating schistosomiasis (Gelfland et al., 1985). Intriguingly, in Cameroon, *P. angolensis* takes on a unique role associated with traditional beliefs or practices. Specifically, it is used in a ritual to create a "nymphomaniac cow" believed to bring prosperity to the herd (Dupiré, 1957). Overall, *P. angolensis* is a versatile plant with multiple uses and cultural significance in various parts of Africa.

4.3.2.2 *Protea caffra* Meisn.

P. caffra, commonly known as the Common *Protea*, is a Southern African shrub valued for its medicinal uses and found mainly in South Africa, Mozambique, and Zimbabwe (Vambe et al., 2020). Its roots are prepared as a decoction to heal broken bones, manage bleeding and stomach ulcers, and treat calves as well as haemorrhagic diarrhoea (Hutchings et al., 1996; Janick, 2007; Zukhulu, 2012). The plant's seed infusion is also used to treat chlamydia (Semenya et al., 2013), while the bark and fruits are utilised to manage symptoms of dizziness (Mabogo, 1990), making it a staple in traditional medicinal practices.

4.3.2.3 *Protea cynaroides*

P. cynaroides, commonly known as the King *Protea*, is South Africa's national flower. Beyond its striking beauty, it has been a staple in South African traditional medicine for generations (Paterson-Jones, 2000). Traditionally, it is used to treat bladder and kidney issues, as well as

cancer. Medicinal tea is prepared by steeping its leaves in boiling water, cooling, straining, and then drinking it for at least a day, tailored to the ailment treated (Arendse, 2003).

4.3.2.4 *Protea elliottii* Phill.

P. elliottii known as Madagascan or Buru protea, is a hardwood shrub from tropical Africa, appreciated for its beauty and medicinal uses (Udeozo et al., 2018). In Cameroon, the bark decoction of *P. elliottii* is used to treat sores eyes, worm diseases, haemorrhoids, and dental caries (Jiofack et al., 2010). In Nigeria, its leaves and the root of *Ricinus communis* are mashed together to remove the juice before putting the extract on the sanitary towel to reduce menstrual flow (Fasola, 2015).

4.3.2.5 *Protea gaguedi* J.F. Gmel.

P. gaguedi, also known as African sugarbush, plays a significant role in East and Central African traditional medicine (Beard, 1959; Gradé et al., 2009). In Ethiopian folklore medicine, infusion of the grounded fresh leaf of *P. gaguedi* has been used to treat animal jaundice (Kefalew et al., 2015). Meanwhile, in Uganda, the aqueous extracts of the plant barks and leaves are used to cure calves suffering from anthrax and lice (Gradé et al., 2009).

4.3.2.6 *Protea madiensis* Oliv.

P. madiensis, one of the four most abundant *Protea* species in tropical Africa alongside *P. gaguedi, P. welwitschii,* and *P. angolensis,* is renowned for its extensive medicinal uses (Beard, 1963). Traditionally, the plant has been used to treat fever, skin diseases, wounds, malaria and diarrhoea. For instance, the leaves in powdered form are used in treating wounds, diarrhoea, headache, and kwashiorkor, as well as to remove evil spirits and bad luck in Burundi (Baerts & Lehmann, 1989). Furthermore, decoction or powder of the plant leaves, stem bark, trunk and branches are used to cure some skin diseases such as dermatomycosis and tinea as well as gastrointestinal disorders, emetic, worm diseases, rachitis and psychological problems (stem) (Baerts & Lehmann, 1989). *P. madiensis* exhibits an extensive spectrum of uses, with the stem barks being employed to alleviate conditions such as malaria, amenorrhoea, fever, dysentery and headache (Udegbunam et al., 2012). In Rwandese traditions, dried leaves serve as a remedy for bronchitis, while the roots are used for their laxatives, anti-hyperpigmentation, and anti-depigmentation properties (Desouter, 1991; Kamagaju et al., 2013a, b). Nigerians also used the roots to treat epilepsy, while Cameroonians traditionally used the plant to cure haemorrhoids, eye worm diseases, and carious teeth (Tagne et al., 2014). In Tanzania, decoctions of the leaves or barks are used to cure cough (Kokwaro, 1976), while in Congo, the plant is used in the

treatment of mammary gland inflammation in animals (Defour, 1954) and bronchitis in goats (Balagizi et al., 2005).

4.3.2.7 *Protea nitida* Mill.

P. nitida, commonly known as wagon tree, is the only *Protea* species forming large trees yielding usable timber (Germishuizen & Meyer, 2003). Historically, the woody part was used in the construction of wagons by the Europeans settlers (Verotta *et al.*, 1999) and latter for crafting ornamental furniture and producing charcoal (Rebello, 1995). Its tannin-rich bark was used for tanning leather and making medicinal infusions to treat diarrhoea, while its leaves were used for ink and remedies for tuberculosis and pneumonia (Rebello, 1995; Hulley & Van Wyk, 2019).

4.3.2.8 *Protea petiolaris* Andrews

P. petiolaris is a small straggling tree to 10 m tall with petiolate leaves of 1-3 cm broad, native to Angola, the Democratic Republic of Congo, and Zambia (Bingham et al., 2023). In folklore medicine, a decoction of the roots has been used as an enema in the treatment of stomach pains, menstruation problems, infertility and diarrhoea (Lautenschläger et al., 2018). The leaves were used as fodder plants for animals and as a remedy for conditions such as rheumatism and headaches (Lautenschläger et al., 2018).

4.3.2.9 *Protea repens* L.

P. repens is an evergreen shrub used in the early Cape Colony to treat chest disorders (Pappe, 1847). Its nectar was processed into a syrup known as "bossiestroop," which formed the basis of traditional cough remedies (Van Wyk, 1997).

4.3.2.10 *Protea roupelliae* Meisn subsp. hamiltonii Beard ex Rourke

P. roupelliae is significant in traditional medicine, with its roots used in concoctions for urethral discharge and its stem bark for treating chronic penile ulcers (Amusan, 2009).

4.3.2.11 *Protea simplex* E.Phillips

P. simplex, a flowering shrub, holds medicinal significance as its decorticated bark and root infusions are utilised to treat diarrhoea and dysentery in humans and calves (Hutchings et al., 1996).

4.3.2.12 *Protea welwitschia* Engl.

P. welwitschia is a small tree 1-3m tall, native to South Africa. Its decorticated bark and root infusions are orally administrated as remedies for diarrhoea and dysentery in calves (Watt & Breyer-Brandwijk, 1962).

4.3.3 Pharmacological properties of *Protea* species extracts

Makhafola et al. (2016) investigations highlighted the remarkable antioxidant properties of *P. mundii*, *P. cynaroides*, and *P. neriifolia* with IC_{50} values of 1.45±0.64, 1.48±0.30 and 3.25±2.15 µg/mL, respectively. It was also noticed that *P. mundii* and *P. cynaroides* are better antioxidant agents than ascorbic acid (2.28±0.02 µg/mL), while *P. nitida* showed weaker antioxidant effects with an IC_{50} of 12.14±1.11 µg/mL. These strong antioxidant effects were attributed to the high phenolic content in the plants, with over 11 phenolic compounds identified through TLC autobiography assay. The antimutagenic activities of the four extracts against *S. typhimurium* ATCC TA100 and TA98 showed variable results. For TA100, *P. nitida* displayed the strongest antimutagenic effect, reducing revertants by 51.09±7.23 % (583.33±20.82 revertants), followed by *P. cynaroides* at 17.13±2.75 % (911±20.05 revertants). *P. neriifolia* and *P. mundii* exhibited negative effects, with -4.63±4.31 % (1031.67±10.41 revertants) and -13.16±2.66 % (1203±26.17 revertants), respectively. For TA98, the extracts generally showed weak antimutagenic effects. *P. mundii* had a slight positive effect of 9.30±5.44 % (194.67±6.66 revertants), while *P. nitida* also showed a small positive effect of 6.01±8.82 % (200±13.23 revertants). However, *P. cynaroides* and *P. neriifolia* showed negative effects of -6.56±1.13% (233.33±17.01 revertants) and -54.16±8.70% (261.67±13.05 revertants), respectively. The positive control 4-nitroquinoline 1-oxide had reduced 211.67±7.57 revertants for TA98 and 1076.33±26.95 revertants for TA100 at a concentration of 5 mg/mL (Makhafola et al., 2016).

The petroleum ether (PE), dichloromethane (DCME), ethanol and water extracts of *P. simplex* bark showed great anti-inflammatory activity against COX-1 with percentage inhibition of 94.2±3.7, 86.1±7.1, 89.2±7.8, and 90.5±1.2 at 250 µg/mL, respectively (Fawole et al., 2009). However, the extracts showed moderate to little activity against COX-2 with percentage inhibition of 41.0±7.4, 35.8±2.4, 20.0±2.1, and 16.7±0.3 µg/mL, respectively. On the other hand, the PE and DCME extracts of *P. simplex* leaves showed good anti-inflammatory activity against COX-1 (100.1±0.8 and 80.6±8.7 µg/mL) and COX-2 (72.4±1.1 and 68.4±3.7 µg/mL). The leaves of the ethanolic extract displayed little to no activities against COX-1 (23.7±6.1 µg/mL) and COX-2 (0.0). The water extract displayed moderate activity against COX-1 (57.8±14.4) but exhibited a poor inhibition effect against COX-2 (20.9±6.9 µg/mL) (Fawole et al., 2009).

PE and DCME extract of *P. caffra* flower showed antibacterial activity against the MDR *K. pneumoniae* ATCC 700603 with IC_{50} of 1.25 mg/mL for both extracts. The seed's methanolic, DCME and PE extracts and the plant twig PE and methanolic extract displayed IC_{50} of 1.25 mg/mL against MDR *K. pneumoniae*. The methanolic extract of *P. caffra* twig showed activity against MDR *E. coli* ATCC 25218 with an IC_{50} of 1.25 mg/mL (Vambe et al., 2018).

The study conducted by Kamagaju et al. (2013) demonstrated that the root bark of *P. madiensis* significantly inhibited melanogenesis by modulating pigmentation in normal melanocytes (LOCE-NM034). The percentage inhibition of pigmentation by the hexane (5±4 %), chloroform (12±4 %), methanol (3±3 % at 10 µg/mL and 4±2 % at 50 µg/mL), and water (22±3 % at 10 µg/mL) extracts were higher than the control kojic acid, which showed < 3% inhibition at 142 µg/mL and 68±6 % at 1420 µg/mL. The extracts also inhibited mushroom tyrosinase (MT) activity, with IC_{50} values of 40±13 µg/mL (hexane), >320 µg/mL (chloroform), 31±4 µg/mL (methanol), and >640 µg/mL (water), compared to kojic acid's IC_{50} of 14±1 µg/mL. For tyrosine hydroxylase activity (THA), the IC_{50} values were >16.7 µg/mL (hexane), 74±7 µg/mL (chloroform), <16 µg/mL (methanol), and <52 µg/mL (water), while kojic acid showed an IC_{50} of <42 µg/mL. These results highlight the water and methanol extracts of *P. madiensis* as particularly promising inhibitors of melanogenesis.

Moreover, the methanolic extract of *P. elliotti* exhibited very weak antiproliferative activity against NCI H460, MCF-7, PC3, Hela, and 3T3 cell lines, with GI_{50} values of 24.44±0.90, 87.00±1.22, 47.00±1.33, 66.46±0.37 and 81.60±0.70 µg/ml, respectively (Tagne et al.,2014). These values were compared to the control doxorubicin, which exhibited GI_{50} values of 0.020±0.001 (NCI H460), 0.220±0.053 (MCF-7), 0.29±0.12 (PC3), 0.62±0.15 (Hela), and 0.70±0.19 (3T3) µg/mL, respectively. Additionally, the methanolic crude extract of *P. elliottii* demonstrated significant antioxidant activity against DPPH free radicals with IC_{50} of 14.20±0.27µg/mL and a very weak inhibitory effect against NO with IC_{50} of 306.00±2.50 µg/mL. Given its excellent free radical scavenging ability compared to gallic acid (22.67±0.40 µg/mL), the extract was partitioned into hexane, DCME, ethyl acetate, *n*-butanol and methanol fractions. All fractions, except for the hexane and DCME fractions, showed good free radical scavenging ability with IC_{50} of 24.10±0.18 (ethyl acetate), 16.50±0.70 (*n*-butanol), and 15.30±0.20 (methanol) (Tagne et al., 2014).

4.3.4 Phytochemistry and pharmacological properties of *Protea* species secondary metabolites

Phytochemical investigations done on many *Protea* species revealed that the main secondary metabolites isolated or identified from *Protea* species are aromatic esters of aryl glycosides

(Perold & Carlton, 1989). The genus secondary metabolites consist of cinnamate and benzoate esters, D-allose and D-glucose as pyranoses as well as 3,4-dihydroxybenzyl alcohol and hydroquinone as aglycones (Perold & Carlton, 1989). The natural products (Figure 4.1) isolated from the studied *Protea* species are mentioned below.

4.3.4.1 *Protea cynaroides* (L.) L.

The phytochemical investigation of the 70% aqueous acetone extracts of *P. cynaroides* stems resulted in the isolation of the allelopathic agent 3,4-dihydroxybenzoic acid (**4.1**), caffeic acid (**4.2**), salicylic acid (**4.3**), ferulic (**4.4**) and gallic acids (**4.5**) (Wu et al., 2007). Recent work on *P. cynaroides* ethyl acetate and butanol extracts led to the isolation of eight compounds (**4.6-4.13**). Compounds **4.6** (3,4-bis(4-hydroxybenzoyl)-1,5-anhydro-D-glucitol) and **4.11** (4-hydroxybenzoic acid) were isolated from the ethyl acetate extracts, whereas compounds **4.7-4.10 (**4-hydroxybenzoyl-1,5-anhydro-D-glucitol, 2-(hydroxymethyl)-4-oxo-4*H*-pyran-3-yl-6-*O*-benzoate-D-glcopyranoside, 2-hydroxy-7,8-dihydro-ionone-3-*O*-D-glucopyranoside, 1,5-anhydro-D-glucitol) as well as compounds **4.1** and **4.12** (3-hydroxykojic acid) were isolated from the butanol extracts (Yalo *et al.*, 2022). Yalo and co-workers (2022) also demonstrated that compounds **4.1** (0.8776±0.12 μg/mL) and **4.12** (0.7215±0.09 μg/mL) are good anti-tyrosinase inhibitors, with **4.12** showing a better inhibitory effect than the positive control kojic acid (0.8347±0.093 μg/mL). Compounds **4.10** and **4.11** displayed weak anti-tyrosinase activity with IC_{50} of 274.5±2.12 and 149.2±1.06 μg/mL, respectively. Boeyens and co-workers (1983) state that the polygalatol 1,5-anhydro-D-glucitol is the major carbohydrate constituent of the methanolic extracts of *P. cynaroides*, *P. arborea, P. repens*, *P. obtustjolia, P. aurea*, *P. hybrid, P. pityphylla*, *P.neriifolia*, *P. compacta,* P. *lepidocarpodendron* and *P. eximia*. This statement was corroborated by Bieleski and Briggs (2005) who identified and quantified the polygalatol content in the leaf extracts of *P. repens, P. aurea*, *P. cynaroides*, *P. neriifolia*, *P. compacta*, and P. eximia. Bieleski and Briggs (2005) investigations also revealed the presence of glucose, sucrose, and inositol in the leaf extracts.

The hydroxycinnamic acid polygalatol ester, caffeoyl-*O*-polygalatol (1,5-anhydro-[6-*O*-caffeoyl]-sorbitol (glucitol)) (**4.13**) was isolated from the plant aqueous methanol extract (Masike et al., 2020). Whereas protocatechuic acid (**4.14**), rutin (**4.15**), quercetin-*O*-galactoside (**4.16**), quercetin-3-*O*-glucoside (**4.17**), Isorhamnetin (**4.18**) and Diosmetin (**4.19**) were identified from the plant extracts by ultrahigh-pressure liquid chromatography hyphenated to photodiode array and ion mobility-high resolution mass spectrometric (UHPLC-PDA-IM-HR-MS) (Masike et al., 2020).

4.3.4.2 *Protea susara* (*P. compacta* X *P. susannae*)

Stigmasterol (**4.20**), β-sitosterol (**4.21**), 2-ethoxy-4-(hydroxymethyl)-phenol (**22**), *p*-hydroxy ethylbenzoate (**4.23**), *p*-hydroxy acetophenone (**4.24**), hydroquinone (**4.25**), 6-ethoxy-3,5-dihydroxy-4-oxotetrahydro-2*H*-pyran-2-yl)-methyl-4-hydroxybenzoate (**4.26**), 4-ethoxy-2,3-dihydroxy-4-oxobutyl 4-hydroxybenzoate (**4.27**) as well as compounds **4.2**, **4.10** and **4.11** were isolated from *P. susara* (León et al., 2014). Among the isolated compounds tested (**4.10**, **4.22**, **4.26** and **4.27**) for their antioxidant property at 0.5 mg/mL. Compound **4.22** showed the highest inhibitory effects against DPPH radical with a percentage inhibition of 98±0.1%. Whereas compounds **4.10**, **4.26** and **4.27** displayed little activity (3.9±0.9, 24±0.3, and 7.1±0.2 %, respectively) (León et al., 2014).

4.3.4.3 *Protea eximia* (Salisb. ex Knight) Fourc.

The glycoside eximin (**4.46**) was isolated for the first time from *P. eximia* (Perold et al., 1979).

4.3.4.4 *Protea lacticolor* Salisb.

The phenolic compounds p-hydroxybenzoic acid (**4.11**), 3,4- dihydroxybenzyl alcohol (**4.28**) and benzoic acid (**4.29**) are biosynthesised by *P. lacticolor* in addition to the glucoside ester lacticolorin (**4.30**) (Perold et al., 1973). Additionally, compound **4.30** significantly inhibited histamine release in human mast cells and pro-inflammatory cytokines TNF-α and IL-6 (Kim et al., 2013).

4.3.4.5 *Protea neriifolia* R.Br.

The polyphenolic compounds neriifolin (**4.31**, Perold & Carlton, 1989), 3,4-dihydroxyphenyl-(6`-*O*-benzoyl)-*O*-β-D-glucopyranoside (**4.32**), 2,4-dihydroxyphenyl-(6`-*O*-benzoyl)- *O*-β-D-glucopyranoside (**4.33**), 2,4-dihydroxyphenyl-(6`-*O*-benzoyl)-*O*-β-D-allopyranoside (**4.34**), and 2,4 dihydroxyphenyl-[6`-*O*-(3-hydroxy,3`-phenylpropanoyl)]-*O*-β-D-allopyranoside (**4.35**) were identified and isolated from *P. neriifolia* methanolic extracts (Verotta *et al.*, 1999). Compounds **4.32**, **4.33** and **4.52** showed their ability to stimulate proliferation of human fibroblast cells at concentrations between 1 and 5 μg/mL (Verotta et al., 1999). Compounds **4.14**-**4.18,** as well as B-type procyanidin (**4.36**), (+)-catechin (**4.37**), kaempferol-3-*O*-glucoside (**4.38**), isorhamnetin-*O*-glucoside (**4.39**), 3-*p*-coumaroyl-*O*-quinic acid (**4.40**) and 3-feruloyl-*O*-quinic acid (**4.41**), were identified from the aqueous methanol extracts by UHPLC-PDA-IM-HR-MS (Masike et al., 2020).

4.3.4.6 Limelight (*P. neriifolia* X *P. burchelli*)

Many known phenolic compounds and flavonoids were identified from the aqueous methanol extracts of the hybrid leaves extracts. Among the identified compounds, compounds **4.15**, **4.16**-**4.18**, **4.46** and **4.36**-**4.41** were found to be biosynthesised by the plant. β-arbutin (**4.42**), vanillic acid (**4.43**), 5-caffeoyl-*O*-quinic acid (**4.44**), 3-caffeoyl-*O*-quinic acid (**4.45**), and isorhamnetin-*O*-galactoside (**4.47**) were also identified from the leaf's extract (Masike et al., 2020).

4.3.4.7 Black beauty (*P. magnifica* X *P. burchelli*)

Compounds **4.16**, **4.17**, **4.36**-**4.38**, **4.40**, **4.41**, **4.44**-**4.46** were identified from this hybrid using UHPLC-PDA-IM-HR-MS (Masike et al., 2020).

4.3.4.8 *Protea obtusifolia* H.Buek ex Meisn.

It was revealed that compounds **4.2**, **4.11**, **4.14**, **4.28** and **4.48** (methyl 3,5-dihydroxybenzyl ether), as well as quercetin (**4.49**), were isolated from *P. obtusifolia* (Verotta et al., 1999).

4.3.4.9 *Protea roupelliae* Meisn subsp. hamiltonii Beard ex Rourke

The phytochemical studies of the ethanolic extract of the heartwood of *P. roupelliae* resulted in the isolation of two long-chain phenolic compounds. The isolated compounds are 5-[8(*Z*)-tridecenyl] resorcinol (**4.50**) and 5-[8(*Z*)-tridecenvl]-2-methylresorcinol (**4.51**), with compound **2** being the major constituents of the plant (Bullock & Drewes, 1989).

4.3.4.10 *Protea rubropilosa* Beard

Studies done *P. rubropilosa* led to the isolation of the alloside ester rubropilosine (**4.52**) and pilorubrosine.(**4.53**) (Perold et al., 1973a).

Figure 4.1 represents the chemical structures of the phytochemical constituents present in *Protea* species.

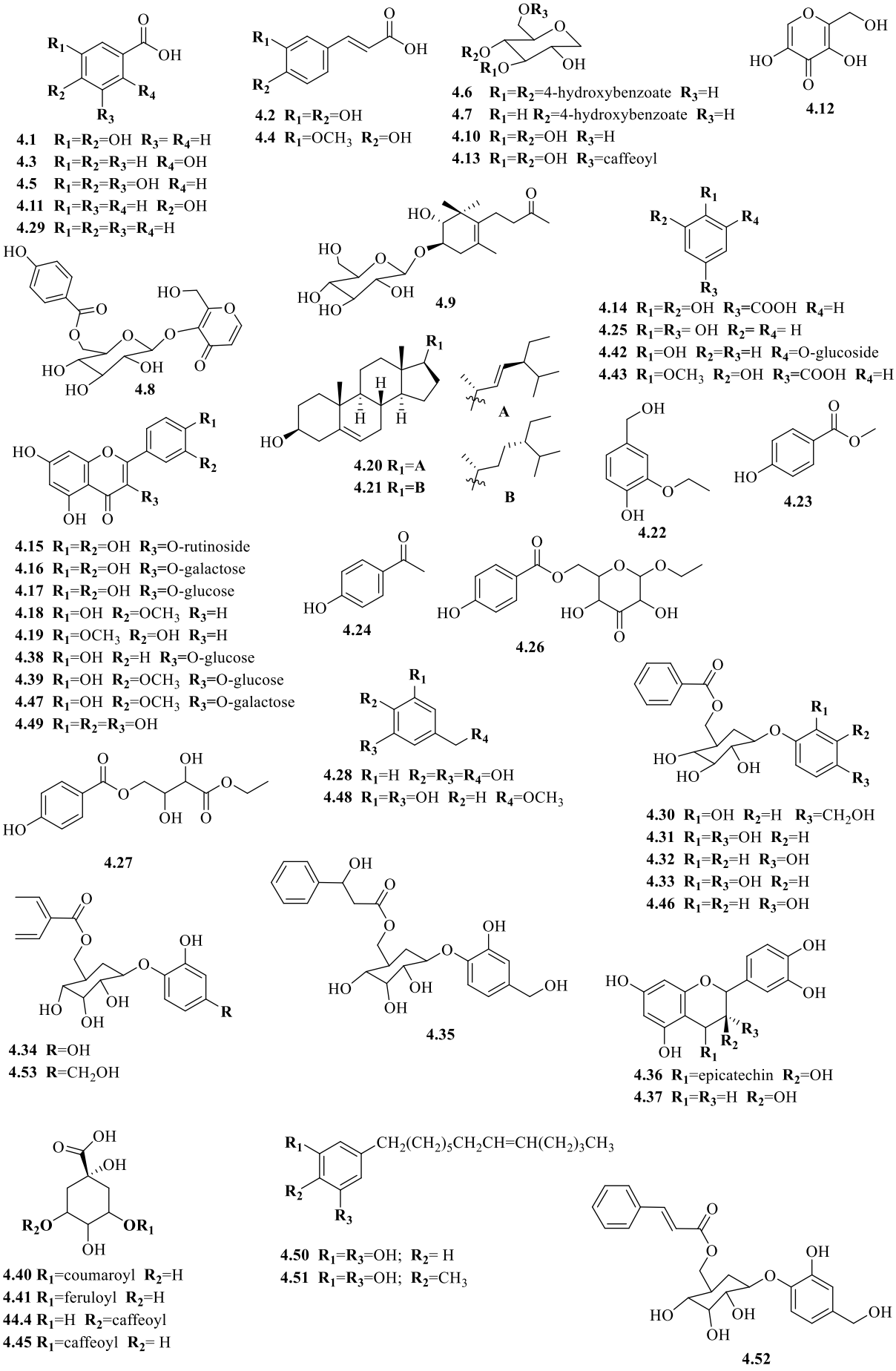

Figure 4.1: Chemical compounds isolated and reported from *Protea* species (**4.1-4.53**)

4.4 *Leucadendron*

4.4.1 The genus *Leucadendron*

The genus *Leucadendron* comprises approximately 85 species of flowering plants, categorised into two sections: Alatosperma and Leucadendron (Pharmawati et al., 2012). These sections were established based on fruit characteristics, with Leucadendron section consisting of 7 subsections (Villosa, Membranaceae, Nervosa, Leucadendron, Cuncata, Nucifra, and Ventriosa) and the Alatoserma section of 4 subsections (Trigona, Brunneobracteata, Alata, and Compressa) (Perold, 1983; Williams, 1972).

However, 51 taxa within this genus face extinction threats, and an additional 13 taxa are considered near-threatened, according to the 2017 South African National Biodiversity Institute report (SANBI, 2017). These *Leucadendron* species are renowned for the beauty of their upper leaves, which enlarge and display vibrant colours during flowering (Werner, 1951). Most of these species display their striking beauty during the winter and spring seasons, such as *L. argenteum*, *L. discolor*, *L. galpinii*, *L. laureolum*, *L. salicifolium*, *L. salignum*, *L. tinctum*, and *L. uliginosum*, cultivated for their attractive foliage (Vogts, 1980; Kepler, 1988).

These flowering plants, also known as conebushes, exhibit a dioecious nature, wherein male and female reproductive organs are borne on separate plants (Werner, 1951). Female *Leucadendron* plants produce woody cones containing fruits and seeds, while males do not. Female cones are characterised by spirally arranged floral bracts that partially cover the cone, whereas male plants tend to be larger, more robustly branched, and may exhibit smaller leaves (Leonhardt & Criley, 1999; Rebelo, 1995).

Dioecious species like *Leucadendron* tend to exhibit higher seed set percentages, facilitated by all flowers on female plants being reproductively functional, thus ensuring more effective seed production in environments with severely nutrient-deficient soils. Moreover, approximately 47% of *Leucadendron* species release their seeds upon maturation, while others retain seeds in cones. The degree of serotiny or seed retention, is relatively moderate, typically lasting 1–4 years compared to other fire-prone flora (Midgley & Enright, 2000). Even among serotinous *Leucadendron* species, significant seed release may occur without fire, particularly in older plants (Mustart et al., 1994).

Leucadendron fruits come in two main forms: flattened, winged achenes dispersed by wind, or rounded nutlets that fall to the ground upon release. Post-fire, these seeds are often dispersed into litter microsites, where they become covered by soil, ash, and charred plant remains. In contrast, non-serotinous fruits typically consist of nutlets that are collected from the soil surface and stored underground by ants, beetles, and rodents (Newton et al., 2021).

These plants thrive in light, well-drained soils with low salt levels, ample freshwater availability, moderate temperatures (7-27 °C), and occasional light winds. Additionally, acidic soil with a pH below 5.0 is essential for their growth (Vogts, 1980).

4.4.2 Ethnobotanical uses and Pharmacological properties of *Leucadendron* species

Despite the widespread use of *Leucadendron* species in horticulture, no information is reported regarding any specific attributes, characteristics, or applications associated with their ethnomedicinal uses and pharmacological properties.

4.4.3 Phytochemistry

The genus *Leucadendron* has been identified as a source of cyanogenic glycosides and bislactonic spiro compounds (Figure 4.2). Various species of *Leucadendron* have been found to contain the phenolic bislactonic spiro Leucodrin (**4.54**) as well as its hydroxylated analogue leudrin (**4.55**); its glycoside analogue Leucoglycodrin (**4.56**), and its diastereoisomeric analogue conocarpin (**4.57**; Perold, 1983; Gadea et al., 2022). Additionally, the cyanogenic glycoside dhurrin (**4.58**) has been isolated from the leaves of *L. sessile* (Swenson et al., 1989).

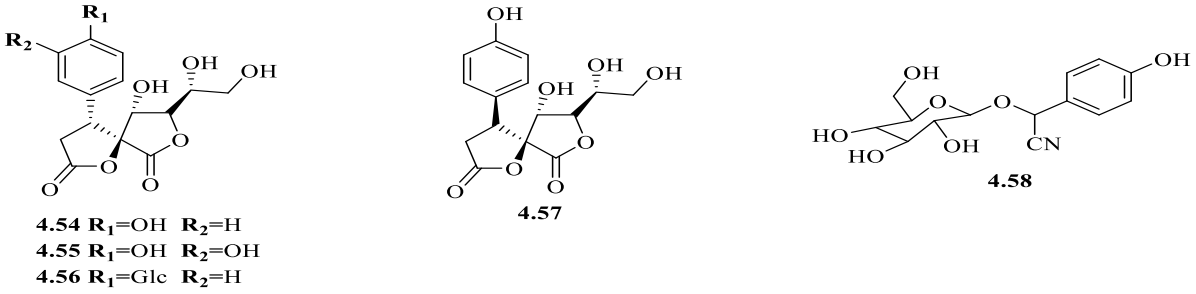

Figure 4.2: Chemical structure of compounds isolated from *Leucadendron* species (**4.54-4.58**)

4.5 Conclusion

The Proteaceae family is a cornerstone of biodiversity in Mediterranean climates worldwide, with its diverse species embodying ecological, cultural, medicinal, and economic significance. South African emblematic Proteaceae genera, *Protea* and *Leucadendron* exemplify this multifaceted importance.

Protea species are traditionally used as remedies to treat ailments such as dysentery, diarrhoea, skin diseases, inflammation, fever, stomach pains, and menstrual problems. Research on their phytochemical and pharmacological properties has revealed that only 21 out of 117 species have undergone chemical or biological investigations. For instance, extracts from *P. cynaroides, P. elliottii, P. mundii*, and *P. nerifolia*, alongside compound **4.22**, demonstrated

remarkable antioxidant activity. Furthermore, anti-tyrosinase effects were observed in extracts from *P. madiensis*, along with compounds **4.1** and **4.12**, while leaf extracts of *P. simplex*, as well as compound **4.30,** exhibited anti-inflammatory properties. Additionally, flower extracts of *P. caffra* exhibit antibacterial activity, whereas compound **4.30** suppressed the histamine release in human mast cells.

On the other hand, *Leucadendron* species, valued for its commercial potential in cut stem production and potted plant cultivation, remains unexplored chemically and biologically. These findings highlight the need for further research into *Protea* and *Leucadendron* species. Extensive phytochemical and biological investigations on these genera's phytochemical constituents and phytotherapy are essential to uncover their therapeutic potential.

References

Amusan, O. O. (2009). Some ethno-remedies used for HIV/AIDS and related diseases in Swaziland. *The African Journal of Plant Science and Biotechnology*, 3(1): 20-26.

Arendse, M. L. (2013). Medicinal plant use in the Dwarsrivier Valley. PhD thesis. Stellenbosch University, Cape Town.

Baerts, M. & Lehmann, J. (1989). *Guérisseurs et plantes médicinales de la région des crêtes Zaïre-Nil au Burundi*. Vol 18. Musée royal de l'Afrique centrale.

Balagizi, I., Cihyoka, A. & Mapatano, S. (2005). *Lexique et recueil des quelques pratiques en ethno-pharmacopée agro-vétérinaire au Kivu.* Plate forme Diobass au Kivu.

Barth, G. E., Maier, N. A., Cecil, J. S., Chyvl, W. L. & Bartetzko, M. N. (1996). Yield and seasonal growth flushing of Protea 'Pink Ice' and Leucadendron 'Silvan Red' in South Australia. *Austral. J. Expt. Agr.*, 36: 869-875.

Ben-Jaacov, J., Shillo. R. & Avishai, M. (1986). Technology for rapid production of flowering pot-plants of *Leucadendron discolor* E. Phillips, S. Hutch. *Scientia Horticulturae,* 28(4): 301-389.

Bieleski, R. L. & Briggs, B. G. (2005). Taxonomic patterns in the distribution of polyols within the *Proteaceae*. *Australian Journal of Botany*, 53(3): 205-217.

Bingham, M. G., Willemen, A., Wursten, B. T., Ballings, P. and Hyde, M. A. (2023). *Flora of Zambia: Species information: Protea petiolaris subsp. petiolaris*. Available at https://www.zambiaflora.com/speciesdata/species.php?species_id=190530 (Accessed 17 April 2023).

Brown, N., Kotze, D. & Botha, P. (1998). *Grow proteas*. Cape Town: Trident Press.

Brown, N.A.C. & Duncan, G.D. (2006). *Grow fynbos plants*. Kirstenbosch Gardening Series. South African National Biodiversity Institute. Cape Town.

Boeyens, J. C. A., Marais, J. L. C. & Perold, G. W. (1983). The occurrence, conformation and crystal structure of 1,5-anhydro-d-glucitol in Protea spp. *Phytochemistry*, 22(9): 1959-1960.

Bullock, L. M. & Drewes, S. E. (1989). Long-chain phenols from the heartwood of *Protea roupelliae*. *South African Journal of Chemistry*, 42(2): 76-80.

Coates Palgrave, K. (2002). *Trees of southern Africa*. Cape Town: Struik.

Cowling, R. M. & Lamont, B. B. (1998). On the nature of Gondwanan species flocks: diversity of Proteaceae in Mediterranean south-western Australia and South Africa. *Australian Journal of Botany,* 46(4): 335-355.

Desouter, S. (1991). *Pharmacopée humaine et vétérinaire du Rwanda*. Vol 22. Musée royal de l'Afrique centrale.

Dongo, E., Hussain, H., Miemanang, R. S., Tazoo, D., Schulz, B. & Krohn, K. (2009). Chemical Constituents of Klainedoxa gabonenses and Paullinia pinnata. *Records of Natural Products*, 3(3): 1.

Duncan, G., Brown, N. & Nurrish, L. (2013). *Grow proteas*. Kirstenbosch Gardening Series. South African National Biodiversity Institute, Cape Town.

Dupiré, M. (1957). Pharmacopée Peule du Niger et du Cameroun. *Bull. IFAN, XIX*, sér. B (3-4): 382-417.

Fawole, O. A., Ndhlala, A. R., Amoo, S. O., Finnie, J. F. & Van Staden, J. (2009). Anti-inflammatory and phytochemical properties of twelve medicinal plants used for treating gastro-intestinal ailments in South Africa. *Journal of Ethnopharmacology*, 123(2): 237-243.

Fasola, T. R. (2015). An Ethnobotanical Survey of Plants Used in the Management and Treatment of Female Reproductive Health Problems in Ibadan, Southwestern Nigeria. *Journal of Biology, Agriculture and Healthcare*, 5(3): 7-12.

Gadea, A., Khazem, M. & Gaslonde, T. (2022). Current knowledge on chemistry of Proteaceae family, and biological activities of their bis-5-alkylresorcinol derivatives. *Phytochemistry Reviews*, 21: 1969-2005.

Gelfland, M., Mavi, S., Drummond, R. B. & Ndemera, B. (1985). *The traditional medical practitioner in Zimbabwe: his principles of practice and pharmacopoeia*. Mambo press.

Germishuizen, G. & Meyer, N.L. (2003). *Plants of southern Africa*. Strelitzia 14. National Botanical Institute, Pretoria.

Goldblatt, P. (1997). Floristic diversity in the Cape Flora of South Africa. *Biodiversity and Conservation*, 6(3): 359-377.

Goldblatt, P. & Manning, J.C. (2000). *Cape plants: A conspectus of the Cape flora of South Africa*. Strelitzia 9. National Botanical Institute. Pretoria & Missouri Botanical Garden Press: Missouri.

Goldblatt, P. & Manning, J. C. (2002). Plant diversity of the Cape region of southern Africa. *Ann Missouri Bot Gard*, 89: 281-302.

Gradé, J. T., Tabuti, J. R. S. & Van Damme, P. (2009). Ethnoveterinary knowledge in pastoral Karamoja , Uganda. *Jounal of ethnopharmacology*, 122: 273-293.

Hulley, I. M. & Van Wyk, B. E. (2019). Quantitative medicinal ethnobotany of Kannaland (western Little Karoo, South Africa): Non-homogeneity amongst villages. *South African Journal of Botany, 122*: 225-265.

Hutchings, A., Lewis, G. & Cunningham, A. (1996). *Zulu Medicinal Plants: An Inventory*. University of Natal press, Pietermeritzburg.

Janick, J. (2007). *Proteaceous ornamentals: Banksia, Leucadendron, Leucospermum, and Protea*. International Society for Horticultural Science (ISHS).

Jiofack, T., Fokunang, C., Guedje, N., Kemeuze, V., Fongnzossie, E., Nkongmeneck, B., Mapongmetsem, P. M & Tsabang, N. (2010). Ethnobotanical uses of medicinal plants of two ethnoecological regions of Cameroon. *Journal of Medicine and Medical Sciences*, 2(1): 60-79.

Kamagaju, L., Bizuru, E., Minani, V., Morandini, R., Stévigny, C., Ghanem, G. & Duez, P. (2013a) An ethnobotanical survey of medicinal plants used in Rwanda for voluntary depigmentation. *J Ethnopharmacologyy*, 150: 708-717.

Kamagaju, L., Morandini, R., Bizuru, E., Nyetera, P., Nduwayezu, J. B., Stévigny, C., Ghanem, G. & Duez, P. (2013b). Tyrosinase modulation by five Rwandese herbal medicines traditionally used for skin treatment. *J. Ethnopharmacolology*, 146: 824-834.

Kefalew, A., Asfaw, Z. & Kelbessa, E. (2015). Ethnobotany of medicinal plants in Ada ' a District , East Shewa Zone of Oromia Regional State. *Journal of Ethnopharmacology*, 11(25): 1-28.

Kepler, A. K. (1988). *Proteas in Hawaii*. Honolulu: Mutual Publishing.

Blomerus, L., Joshua, S. & Williams, J. (2010). Breeding Proteaceae varieties for changing

market trends. *Acta Horticulturae*, 869: 173-181.
Kokwaro, J. O. (1976). *Medicinal plants of East Africa*. University of Nairobi Press, Kampala.
Lamont, B. (1985). The significance of flower colour change in eight co-occurring shrub species. *Botanical Journal of the Linnean Society*, 90(2): 145-155.
Lautenschläger, T., Monizi, M., Pedro, M., Mandombe, J. L., Bránquima, M. F., Heinze, C. & Neinhuis, C. (2018). First large-scale ethnobotanical survey in the province of Uíge , northern Angola. *Journal of Ethnobiology and Ethnomedicine*, 14(51): 1-73.
León, F., Alfayate, C., Batista, C. V., López, A., Rico, M. & Brouard, I. (2014). Phenolic compounds, antioxidant activity and ultrastructural study from *Protea hybrid* "Susara" *Industrial Crops and Products*, 55: 230-237.
Leonhardt, K. W. & Criley, R. A. (1999). Proteaceae floral crops: cultivar development and underexploited uses. In: Janick J (ed.). *Perspectives on new crops and new uses*. Alexandria, Virginia: ASHS Press. 410-430.
Littlejohn, G. M., van den Berg, G. C. & Brits, G. J. (1998). A yellow, single-stem Leucadendron, 'Rosette'.*Hort. Sci.*, 33(6): 1092-1093.
Mabogo, D. E. N. (1990). *The ethnobotany of the Vhavenda*. Magister Scientiae in the Faculty of Science (Department of Botany) Thesis. University of Pretoria. Pretoria.
Makhafola, T. J., Elgorashi, E. E., McGaw, L. J., Verschaeve, L. & Eloff, J. N. (2016). The correlation between antimutagenic activity and total phenolic content of extracts of 31 plant species with high antioxidant activity. *BMC Complementary and Alternative Medicine*, 16(1): 1-13.
Masike, K., De Villiers, A., Hoffman, E. W., Brand, D. J., Causon, T. & Stander, M. A. (2020). Detailed Phenolic Characterization of Protea Pure and Hybrid Cultivars by Liquid Chromatography-Ion Mobility-High Resolution Mass Spectrometry (LC-IM-HR-MS). *Journal of Agricultural and Food Chemistry*, 68(2): 485-502.
Mathews, P. (1981). *The growing and marketing of proteas. Report of the First Int. Conf. of Protea growers*. Proteaflora Enterprises Pty. Ltd., Melbourne, Australia.
Midgley, J.J & Enright, N.J. (2000) Serotinous species show correlation between retention time for leaves and cones. *J. Ecol.*, 88: 348-351.
Mustart, P. J., Cowling, R. M. & Dunne, T. T. (1994). Reproductive traits of two closely related species-pairs on adjacent, different soil types in South African Fynbos. *Vegetatio*, 111: 161-171.
Netnou-Nkoana, N. & Eloff, J. N. (2012). The South African floricultural industry and the plant breeders rights act: a short review. *World Patent Information*, 34(3): 224-228.
Newton, R. J., Mackenzie, B.D.E., Lamont, B. B., Gomez-Barreiro, P., Cowling, R. M. & He, T. (2021) Fire-mediated germination syndromes in Leucadendron (Proteaceae) and their functional correlates. *Oecologia*, 196: 589-604.
Pappe, K. W. L. (1847). *A list of South African indigenous plants used as remedies by the colonists of the Cape of Good Hope*. GJ Pike.
Paterson-Jones, C. (2000). *Protea family in southern Africa*. Struik. Cape town.
Perold, G. W., Rosenberg, M. E. K., Howard, A. S. & Huddle, P. A. (1979). Metabolites of *Proteaceae*. Part 9.l Eximin (6-0-Benzoylarbutin) and the Synthesis of Aryl Glycoside Esters. *J. Chem. Soc. Perkin Trans I*, 239-243.
Perold, G. W., Beylis, P. & Howard, A. S. (1973a). Metabolites of *Proteaceae*. Part VIII.l The Occurrence of (+)-D-Allose in Nature : Rubropilosin and Pilorubrosin from *Protea rubropiosa* Beard. *J. Chem. Soc. Perkin Trans I*, 643-649.
Perold, G. W., Beylis, P. & Howard, A. S. (1973b). Metabolites of *Proteaceae*. Part Vl1.l Lacticolorin, a Phenolic Glucoside Ester, and Other Metabolites of *Protea lacticolor* Salisb. *J. Chem. Soc. Perkin Trans I*, 638-643.
Perold, G. W. (1983). Phenolic lactones as chemotaxonomic indicators in the genera Leucadendron and Leucospermum (Proteaceae). *South African Journal of Botany*, 3(2): 103-107.

Perold, G. W. & Carlton, L. (1989). Neriifolin, an ester glucoside of benzene-1,2,4-triol. *J. Chem. Soc. Perkin Trans I,* 1215-1217.

Pharmawati, M., Yan, G. & Finnegan, P. M. (2012). The conservation of mitochondrial genome sequence in Leucadendron (Proteaceae). *J of Biological Diversity*, 13(2): 53-58.

Press, C. T. (1982). The proteas of southern Africa.

ProteaAtlas. (1999). *DM KwaZulu-Natal - African Sugarbush - Protea gaguedi*. Available at: https://www.proteaatlas.org.za/knprgagu.htm (Accessed 15 April 2023).

Rao, C. V. (1971). *Proteaceae, botanical monograph No. 6.* Sree Saraswaty Press Lt., Calcutta, India.

Rebelo, A. 2000. *Field guide to the proteas of the Cape Peninsula*. Pretoria: Protea Atlas Project xiii, 130p.-illus. ISBN, 1919684220.

Rebelo, A., 2001. *PROTEAS: A Guide to the Proteas of Southern Africa*.

Reinten, E. Y., Coetzee, J. H. & Van Wyk, B. E. (2011). The potential of South African indigenous plants for the international cut fl ower trade. *South African Journal of Botany*, 77(4): 934-946.

Reinten, E., Hoffman, E. W., Bezuidenhout, K. & Gerber, A. (2018). Sustainable globalization within international markets for the Proteaceae ornamental industry. *Acta Horticulturae*, 1201: 485-492.

Rourke, J. P. (1982). *The Proteas of Southern Africa*. 2nd edition. CENTAUR Publications (Pty) Ltd, Johannesburg.

SANBI. (2017). *Protea species and their conservation in South Africa.* Pretoria.

Schurr, F. M., Esler, K. J., Slingsby, J. A. & Allsopp, N. (2012). Fynbos *Proteaceae* as model organisms for biodiversity research and conservation. *South African Journal of Science*, 108 (11–12): 4-7.

Semenya, S. S., Potgieter, M. J. & Erasmus, L. J. C. (2013). Indigenous plant species used by Bapedi healers to treat sexually transmitted infections: Their distribution, harvesting, conservation and threats. *South African Journal of Botany*, 87: 66-75.

Simpson, M. G. (2010). Diversity and Classification of Flowering Plants: Eudicots. In *Plant Systematics*.Cambridge: Academic Press.

Swenson, W. K., Dunn, J. E. & Conn, E. E. (1989). Cyanogenesis in the Proteaceae. Phytochemistry, 28(3): 821-823.

Tagne, R. S., Telefo, B. P., Nyemb, J. N., Yemele, D. M., Njina, S. N., Goka, S. M. C., Lienou Lienou, L., Kamdje, A. H. N., Moundipa, P. F. & Farooq, A. (2014). Anticancer and antioxidant activities of methanol extracts and fractions of some Cameroonian medicinal plants. *Asian Pacific Journal of Tropical Medicine*, 7: 442-447.

Twine, M. (2007). *Protea nitida*. Available at: http://pza.sanbi.org/protea-nitida (Accesssed 17 April 2023).

Udegbunam, S. O., Udegbunam, R. I., Okpo, O. S. & Muogbo, C. J. (2012). Evaluation of the wound healing potential of Protea madiensis Oliv leaf extract in rats. *African Journal of Biotechnology*, 11(90): 15719-15727.

Udeozo, I. P., Udeozor, P. A., Uwa, C. U. & Odinachi. L. (2018). International Digital Organization for Scientific Research The Efficacy of Protea Elliotti Timber: An Important Study. *Journal of scientific research*, 3(2): 89-99.

Vambe, M., Aremu, A. O., Chukwujekwu, J. C., Finnie, J. F. & Van Staden, J. (2018). Antibacterial screening, synergy studies and phenolic content of seven South African medicinal plants against drug-sensitive and -resistant microbial strains. *South African Journal of Botany*, 114: 250-259.

Van Wyk, B.E., Oudtshoorn, B.V. & Gericke, N. (1997). *Medicinal Plants of South Africa*. Briza.

Van Wyk, B. E. (2008). A review of Khoi-San and Cape Dutch medical ethnobotany. *Journal of Ethnopharmacology*, 119: 331–341.

Verotta, L., Orsini, F., Pelizzoni, F., Torri, G. & Rogers, C. B. (1999). Polyphenolic glycosides

from african. *Proteacea*. *Journal of Natural Products*, 62(11): 1526–1531.
Vogts, M. M., Paterson-Jones, C. & Slingsby, P. (1982). *South Africa's' Proteaceae': know them and grow them*. Struik Publishers, Cape Town, South Africa.
Vogts, M. M. (1980). *Species and variants of protea. Farming in South Africa Ser.: Flowers and Ornamental Shrubs*. B.1. Dept. Agr. Water Supply.
Watt, J. M. & Breyer-Brandwijk, M. G. (1962). *The Medicinal and Poisonous Plants of Southern and Eastern Africa being an Account of their Medicinal and other Uses, Chemical Composition, Pharmacological Effects and Toxicology in Man and Animal*. 2nd edition. E. & S. Livingstone Ltd., Edinburg and London.
Werner, H. F. (1951). South African Proteaceae and their Cultivation. *The journal of the botanical society of South Africa*, 1-7.
Williams, I. J. M. (1972). *A revision of the genus Leucadendron (Proteaceae)*. Bolus Herbarium University of Cape Town, Cape Town.
Wood, H. . L. D. (1977). The commercial utilisation of fynbos for ornamental purposes and the influence on the natural habitat. *Veld & Flora*, 24-26.
Wu, H. C., Du Toit, E. S., Reinhardt, C.F., Rimando, A. M., Van der Kooy, F. & Meyer, J.J.M., (2007). The phenolic, 3, 4-dihydroxybenzoic acid, is an endogenous regulator of rooting in Protea cynaroides. *Plant Growth Regulation*, 52: 207-215.
Yalo, M., Makhaba, M., Hussein, A. A., Sharma, R., Koki, M., Nako, N. & Mabusela, W. T M. (2022). Characterization of four new compounds from *Protea cynaroides* leaves and their tyrosinase inhibitory potential. *Plants*, 1-12.
Yang, F. (2017). *Chemotaxonomy Study of Plants from the Family Proteaceae Based on Its Natural Product Profile (Alkaloid)*. PhD Thesis, Griffith University, Brisbane.
Zhang, J., Netzel, M. E., Pengelly, A. & Sultanbawa, Y. (2023). A Review of Phytochemicals and Bioactive Properties in the Proteaceae Family: A Promising Source of Functional Food. *Antioxidants*, 12(11): 1-32.
Zukulu, S., Dold, T. & Abbott, T. (2012). *Medicinal and charm plants of Pondoland*. South African National Biodiversity Institute.

CHAPTER FIVE: General Methodology

5.1 Chemicals and Reagents

The study utilised various solvents, reagents, and chemicals, each sourced from various suppliers. Methanol (HPLC grade, Merck, Cape Town, South Africa) was used for semi-preparative HPLC. In contrast, hexane, methanol, n-butanol, and ethyl acetate (AR grades, Kimix, Cape Town, South Africa) were employed for extraction and chromatography. For compound detection on TLC, sulphuric acid and vanillin (Sigma-Aldrich, Cape Town, South Africa) were used. Deuterated chloroform, deuterated dimethyl sulfoxide, and deuterated methanol (Merck, Cape Town, South Africa) were utilized in NMR spectroscopy to minimize background proton signals and provide a deuterium lock signal for stable spectra.

Chemicals for bioassays included Minimum Essential Medium (MEM) with Earle's salts, without L-glutamine (Capricorn Scientific, Ebsdorfergrund, Germany); Dulbecco's Modified Eagle's Medium (DMEM, Capricorn Scientific, Ebsdorfergrund, Germany); fetal bovine serum (Gibco, Thermo Fisher Scientific, Johannesburg, South Africa); L-glutamine (Lonza, Basel, Switzerland); 3-(4,5-dimethylthiazol-2-yl)-2,5-diphenyltetrazolium bromide (MTT, Sigma-Aldrich, Cape Town, South Africa); dimethyl sulfoxide (DMSO, Sigma-Aldrich, Cape Town, South Africa); palmitate, mannitol, and glucose (Sigma-Aldrich, Cape Town, South Africa); bovine serum albumin (Gibco, Thermo Fisher Scientific, Johannesburg, South Africa); and the ViaLight Plus Kit (Lonza, Walkersville, United States).

5.2 Chromatographic methods

5.2.1 Thin-layer chromatography (TLC)

TLC analysis was done on precoated silica gel 60 F_{254} aluminium plates (Merck, Germany). A small amount of each sample was diluted in methanol and spotted on the TLC plates. The plates were developed using mobile phases of varying polarity to separate the compounds. After development, the plate was exposed to ultraviolet (UV) light at 254 and 366 nm wavelengths using a CAMAG UV lamp to detect compounds with conjugated double bonds and isolated double bonds (C=C and C=O). The plate was sprayed with a vanillin/sulfuric acid reagent and heated at 100°C for five minutes to visualise and identify terpenoids and flavanoids based on their reaction to the reagent and UV light.

5.2.2 Preparation of the developing reagent

The vanillin/sulfuric acid reagent spray was prepared by dissolving 15 g of vanillin in 250 mL of absolute ethanol and then adding 2.5 mL of concentrated sulfuric acid with caution.

5.2.3 Column chromatography

Glass columns of varying diameters and lengths were packed with either silica gel 60 (0.040–0.063 µm, 230–400 mesh) or Sephadex LH-20. Sephadex LH-20 was utilised for size-exclusion chromatography, whereas silica gel 60 was used for normal-phase chromatography. Solvent systems of different polarities were selected as the mobile phase (eluent) to optimise the separation process. The volume of eluent collected was adjusted based on the starting material used in the procedure.

5.2.4 Semi-preparative high-performance liquid chromatography (semi-prep HPLC)

A Shimadzu HPLC system, equipped with an SPD-M20A UV/VIS detector and an LC-20AB binary pump, was employed for profiling crude extracts and purifying their chemical constituents. The purification process began with filtering the sample, dissolved in 100% HPLC-grade methanol, through 0.2-micron Whatman GD/X syringe filters to remove insoluble residues and particles. A 50 µL aliquot of the filtered sample was injected onto a Supelco C18 column (25 x 1 cm, 5 µm), with a flow rate of 1.5 mL/min maintained for one hour. Target compounds were detected at 254, 272, and 366 nm wavelengths, and the corresponding peaks were manually collected for further analysis.

5.3 Spectroscopic methods

5.3.1 Nuclear Magnetic Resonance Spectroscopy (NMR)

NMR analysis was conducted at 25°C using a Bruker 400 MHz FT-NMR spectrometer equipped with a 5mm BBO probe in the Cape Peninsula University of Technology Chemistry Department. Deuterated solvents, including methanol (CD_3OD), dimethyl sulfoxide (DMSO-d_6), and chloroform ($CDCl_3$), were used. Chemical shifts for both ^{13}C and ^{1}H nuclei were reported in parts per million (ppm) relative to tetramethylsilane (TMS) as a standard reference. The splitting patterns of proton signals from isolated compounds were described as singlet (*s*), doublet (*d*), triplet (*t*), quartet (*q*), multiplet (*m*), doublet of triplets (*dt*), etc. Coupling constants (*J*) were reported in Hertz (Hz), providing insights into the coupling between neighbouring nuclei in the molecule.

5.3.2 Electrospray ionisation mass spectroscopy (ESI-MS)

High-resolution mass spectrometry (HRMS) analysis used the Waters Quattro micro-API, featuring an electrospray ionisation (ESI) interface operating in positive mode. This setup determined the mass-to-charge ratio (m/z) of ions derived from isolated compounds, enabling precise identification and characterisation with exceptional detail and efficiency.

5.3.3 Fourier Transform Infrared Spectroscopy (FTIR)

A PerkinElmer Fourier Transform Infrared Spectrophotometer (UATR two) was used to validate compound structures and ascertain the presence or absence of specific functional groups within the analysed samples.

5.3.4 Optical Rotation Measurements

The Anton Paar MCP 200 Polarimeter was utilised to gauge the optical activity of the isolated compounds, dissolved at a concentration of 0.1 g/mL in methanol at a temperature of 25°C. Measurements were conducted at a wavelength of 589 nm, providing insights into the compounds' chiral properties and molecular configuration.

5.3.5 Ultraviolet (UV) Spectroscopy

The UV-visible absorbance maxima of each compound were determined using the SPECTROstar Nano Absorbance Reader from BMG LABTECH. This instrument allowed for precise measurement across a wide range of wavelengths, from 200 to 950 nm, providing valuable information about the compounds' electronic transitions and molecular structure.

5.4 Extraction, isolation and characterisation of *L. frutescens, P. venus* and *L. xanthoconus* secondary metabolites

The general procedure for extraction, isolation and characterisation of the studied plants' secondary metabolites are illustrated in Figures 5.1 and 5.2.

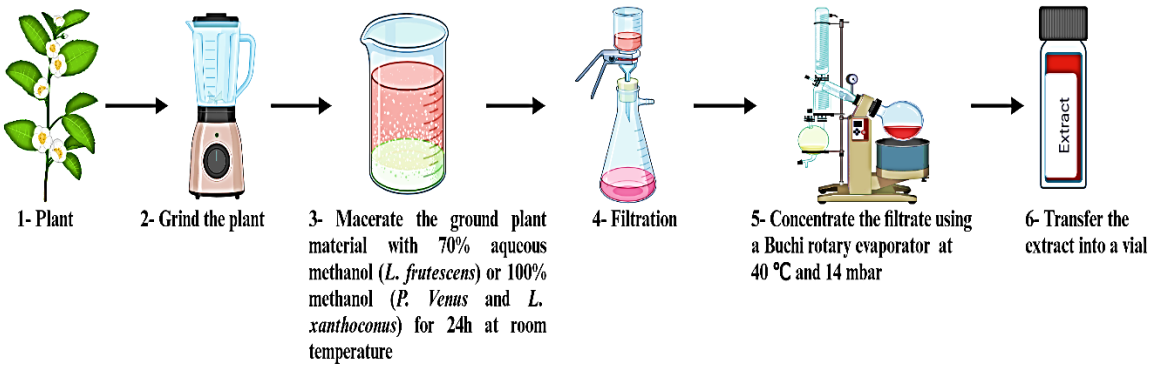

Figure 5.1: General scheme procedure of the extraction of *L. frutescens*, *P. venus* and *L. xanthoconus* secondary metabolites

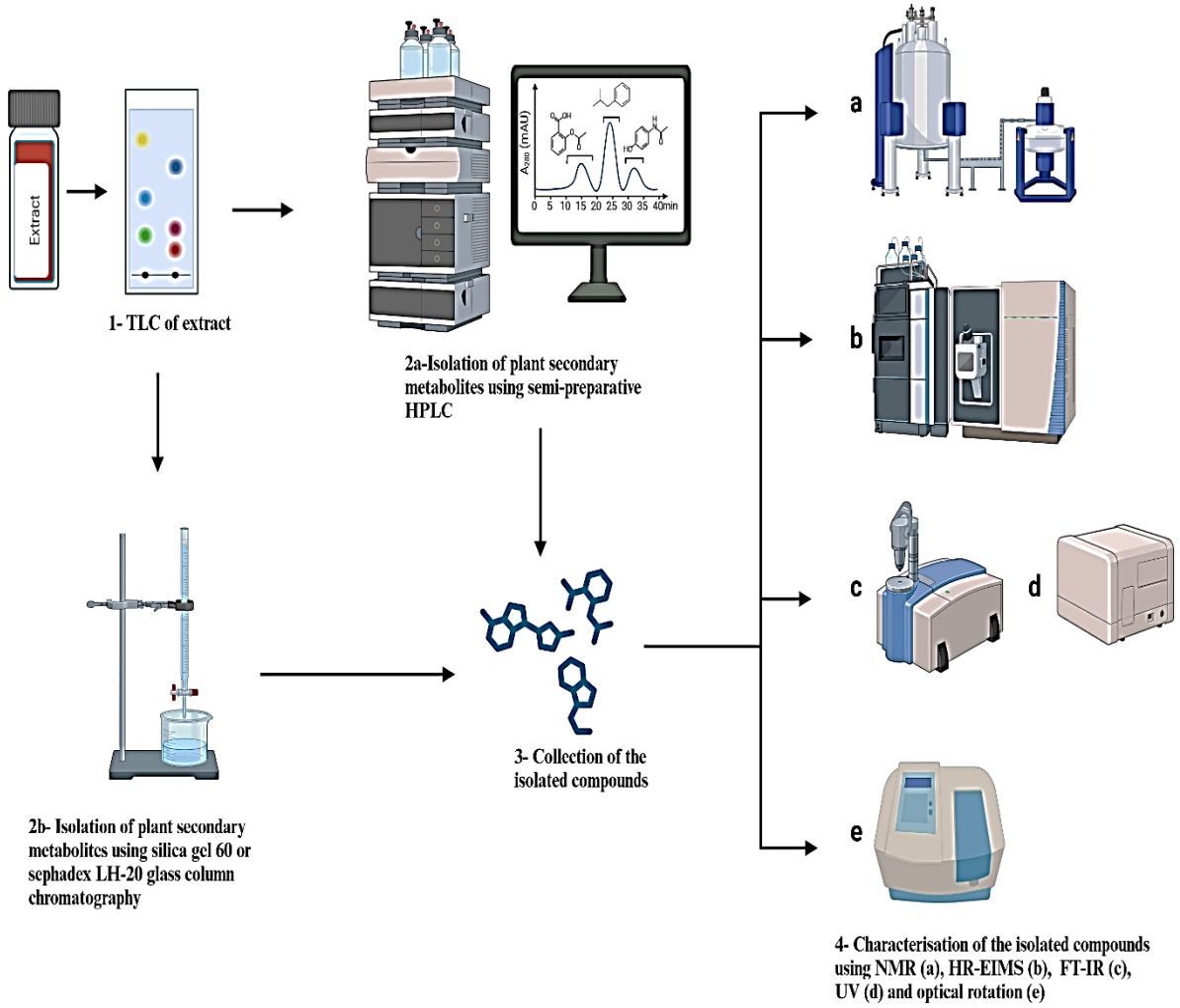

Figure 5.2: General scheme procedure of the purification and characterisation of *L. frutescens*, *P. venus* and *L. xanthoconus* secondary metabolites

5.5 Biological assays

5.5.1 Total phenolic content

50 mg of the sample was accurately weighed and placed into a 50 mL screw-cap tube. A volume of 50 mL of either distilled water or ethanol was added using a Gilson pipetting aid, and the mixture was thoroughly mixed to facilitate the extraction of phenolic compounds. The solution was centrifuged at 4000 rpm for 5 minutes to separate the solid residues from the liquid extract. The supernatant was collected and analysed using the Folin-Ciocalteu reagent, with gallic acid as the calibration standard. The absorbance of the reaction mixture was measured at 765 nm using a spectrophotometer.

5.5.2 FRAP assay

In a 96 well plate, 10 µL of the 100 µg/mL of the isolated compounds and total extracts stock solutions were added to 300 µL of FRAP reagent. The FRAP reagent was prepared by mixing 30 mL of acetate buffer (300 mM, pH 3.6), 3mL of tripyridyl triazine (TPTZ) (10 mM in 40 mM HCl) and 3mL of $FeCl_3.6H_2O$ (20 mM) in a 50 mL conical tube. After adding the samples' stock solutions to the FRAP reagent, the 96 well plate was incubated at room temperature for 30 minutes. The antioxidant potential was read at a wavelength of 593 nm in a Multiskan (Thermo Fisher Scientific) spectrum plate reader.

5.5.3 TEAC assay

The stock solution used is a mixture of 88 µL of 140mM of potassium peroxodisulphate ($K_2S_2O_8$) and 5 mL of 7 mM of 2,2'-azino-bis (3-ethylbenzothiazoline-6-sulfonic acid (ABTS) in a 15 mL screw cap. The prepared ABTS solution was kept in a dark place at room temperature for 24 h before use. The following day the prepared ABTS solution was diluted with ethanol (about 1 mL of ABTS solution mixed with 20 mL of ethanol) to be able to read the absorbance of approximately 2.0 (± 0.1). Trolox was the standard, with concentrations ranging between 0-500 µM. In a 96 well plate, 25 µL of the standards and isolated compounds were added to 300 µL of ABTS mixture and incubated at room temperature for 30 minutes. The absorbance was recorded by a Multiskan spectrometer plate reader at wavelength 734 nm.

5.5.4 High glucose and palmitate media preparation:

A palmitate stock concentration of 100 mM was prepared by dissolving 0.256 g palmitic acid in a 15 mL tube containing 10 mL ethanol (100%). The palmitate (PAL) solution was warmed to 70°C to dissolve the crystals completely. High glucose (HG) media was prepared by topping

up a 500 mL bottle of 25 mM DMEM (4.5 g/L) with 1.35g glucose and 3.64 g of mannitol to make a final concentration of 40 mM. 2 % fatty acid-free BSA was added to the high glucose media to facilitate palmitate conjugation. Subsequently, the treatment media was prepared by conjugating 100 µM palmitate in the high glucose/BSA media in the water bath (37°C) for at least an hour or until no precipitates remained. Once conjugated, the stress induction media was filter-sterilised. The combination of the high glucose (40 mM) and palmitate (150 µM) media was prepared to mimic a hyperglycemic and hyperlipidemic state.

5.5.5 Thawing C3A, H9c2 and MCF-7 cells

Cryopreserved cells were thawed by briefly placing the vial in a 37°C water bath, followed by complete thawing in a Class II biological safety cabinet (tissue culture hood). Once thawed, the cells were transferred into a T75 flask containing 14 mL of pre-warmed culture medium (DMEM with 10% FBS) and incubated under standard tissue culture conditions (37°C, 5% CO_2), and a water-saturated atmosphere) for 24 h. After incubation, the medium was refreshed with a fresh pre-warmed culture medium, and the cells were allowed to proliferate until reaching 80–90% sub-confluency (Figure 5.3). The cells should not reach 100% confluency, which could compromise cell integrity and affect subsequent experiments. To minimise experimental variation, cells were not sub-cultured beyond 10 passages.

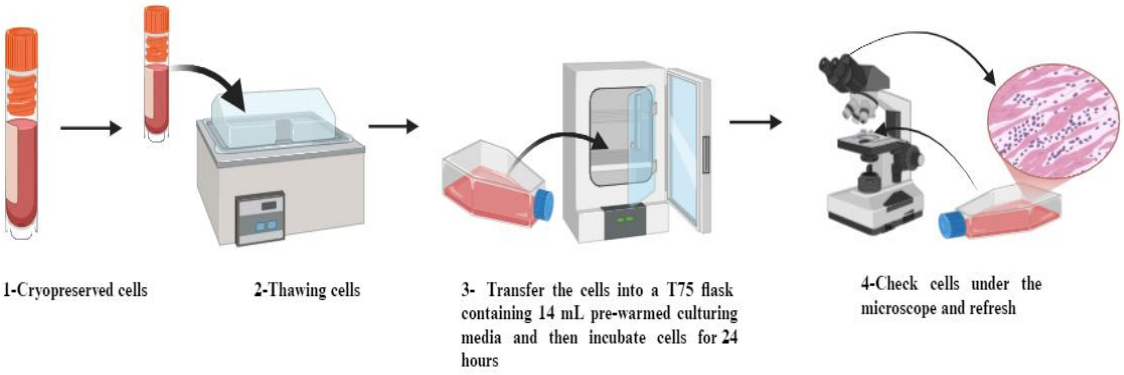

Figure 5.3: General scheme procedure of thawing cells

5.5.6 Sub-culturing cells

- **For cell maintenance:** Cells were refreshed by replacing the old medium with fresh pre-warmed culturing media (the volume should be between 15 – 20 mL, never more than 20 mL)
- **To split cells:** The culture medium in the flask was aspirated, and the cells were washed with 5 mL of pre-warmed DPBS to remove the residual medium. Next, 2.5 mL of pre-warmed trypsin was added, and the flask was incubated for 4-5 minutes at 37°C under

standard tissue culture conditions. Care was taken to avoid tapping or striking the flask to prevent mechanical damage to the cells; instead, the incubation time was extended as needed while observing the cells. Once the cells detached, 8 mL of culture medium was added to the cell-trypsin solution, and the cells were gently rinsed off the flask surface using a 10 mL serological pipette. The cell suspension was then transferred to a clean centrifuge tube and centrifuged at 1500 rpm for 5 minutes (for H9c2 and MCF-7 cells) or 800 rpm for 5 minutes (for C3A cells). After centrifugation, the supernatant was carefully aspirated without disturbing the pellet, and the cells were resuspended in 7 mL of fresh culture medium (Figure 5.4).

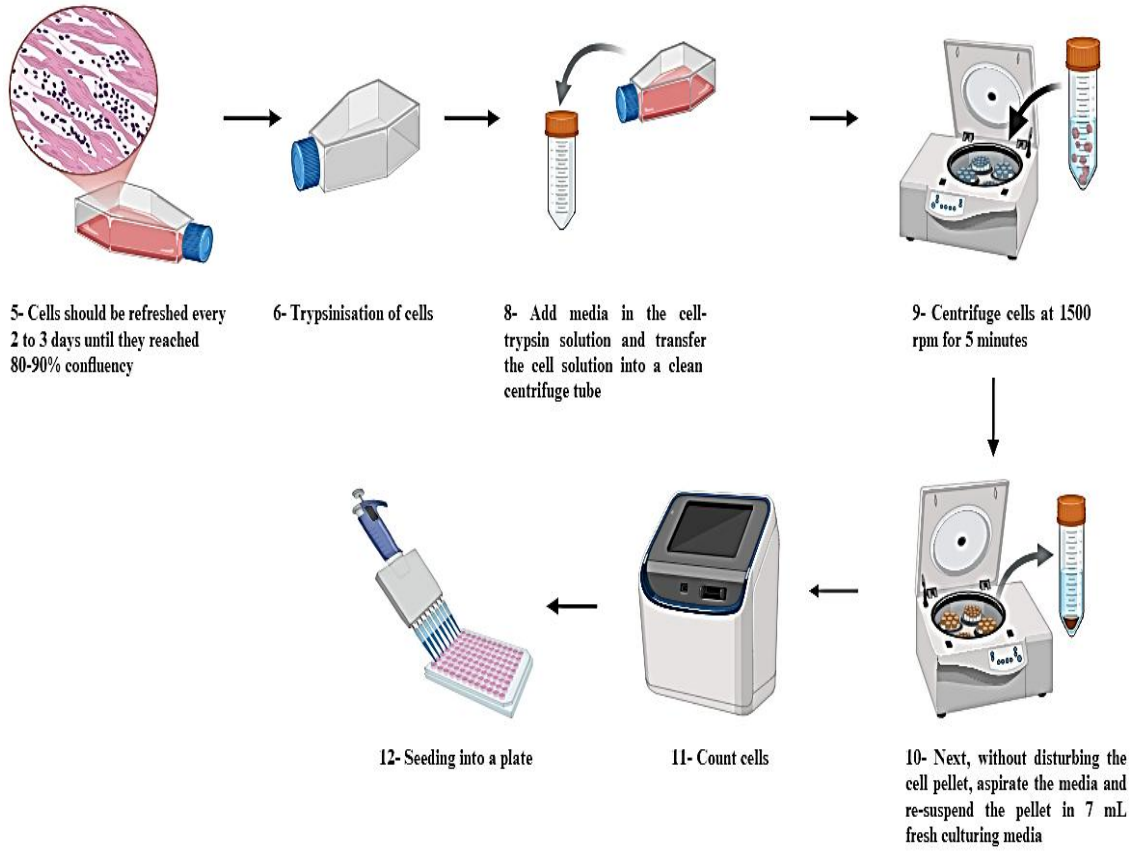

Figure 5.4: General scheme procedure of cell maintenance

- **If seeding into a flask (splitting)**: 1 mL of the resuspended cells was added to 14 mL of fresh culture medium in a new T75 flask. The flask was gently swirled to ensure even distribution of the cells before being incubated under standard tissue culture conditions.
- **If seeding onto plates**:

10 µL of the re-suspended cells was pipetted into a 1 mL Eppendorf tube containing 10 µL of 0.4% (w/v) trypan blue solution. The mixture was thoroughly mixed, and 10 µL of the solution was pipetted into a cell counting chamber for analysis. Cells were then counted using an

automated Countess cell counter. After determining the cell count, cells were seeded into the desired plates according to the specifications provided in Table 5.1. It is important to note that variations in seeding density will impact the time required for cells to reach sub-confluency, which may, in turn, influence the consistency and reproducibility of experiments. Once seeded, the culture media should be refreshed every two days until the cells are ready for an experiment.

Table 5.1: Seeding densities relevant to H9c2 and MCF-7 cells

Plate	Volume per well	Seeding density
96 well	0.2 mL	0.8×10^5
24 well	1 mL	1×10^5
6 well	3 mL	2×10^5

5.5.7 Treatment of H9c2 cardiomyocytes with compounds and crude extracts

Once the cells reach confluency in the plate, the hyperglycemia and hyperlipidemia phenotype characteristic of DCM will be induced by exposing the cells to high glucose (40 mM) and palmitate-BSA (0.15 mM) for 24 h. Cells exposed to normal glucose (25 mM) will serve as controls. Following this induction, cells will be treated with compounds and crude extract at a concentration of 10 µg/mL

5.5.8 Cell viability assay

5.5.8.1 MTT assay

A 3-(4,5-dimethylthiazol-2-yl)-2,5-diphenyltetrazolium bromide tetrazolium (MTT) colourimetric assay was used to assess the cell viability of C3A, H9C2 and MCF7 cells following treatment. After 24 h of treatment, the culture medium was aspirated and replaced with 50 µL MTT reagent (2 mg/mL in DPBS) into each well and incubated for 1 hour under standard tissue culture conditions. The purple formazan product was solubilised in 200 µL DMSO followed by 25 µL of Sorenson`s glycine buffer (pH 10.5) and quantified at OD_{570nm} using a Biotek ELx800 plate reader (Figure 5.5).

5.5.8.2 ATP assay

Cells were plated in a white-walled 96-well plate, and after reaching confluency, they were treated as described in Section 5.5.4. ATP levels were then quantified using the ViaLight Plus ATP Kit, following the manufacturer's instructions. Luminescence was measured with the SpectraMax i3x® Multi-Mode Microplate Reader.

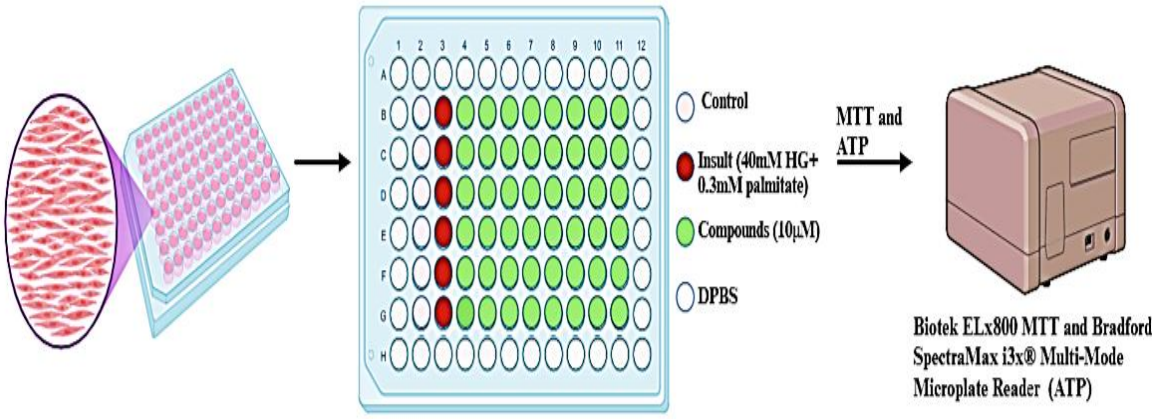

Figure 5.5: General scheme procedure of MTT and ATP assays

plants

MDPI

Article

CHAPTER SIX: Isolation of Lessertiosides A and B and Other Metabolites from *Lessertia frutescens* and Their Neuroprotection Activity

Kadidiatou O. Ndjoubi [1], Sylvester I. Omoruyi [2], Robert C. Luckay [3] and Ahmed A. Hussein [1,*]

[1] Chemistry Department, Cape Peninsula University of Technology, Symphony Rd. Bellville,
Cape Town 7535, South Africa; dickakadi@yahoo.fr
[2] School of Anatomical Sciences, Faculty of Health Sciences, University of the Witwatersrand, Parktown,
Johannesburg 2193, South Africa; sylvester.omoruyi@wits.ac.za
[3] Department of Chemistry and Polymer Science, Stellenbosch University, Matieland,
Stellenbosch 7602, South Africa; rcluckay@sun.ac.za
* Correspondence: mohammedam@cput.ac.za

Abstract: *Lessertia frutescens* (synonym *Sutherlandia frutescens*) is an important South African medicinal plant used traditionally to treat different human pathologies and is considered an adaptogenic plant. This study sought to isolate compounds from the plant and determine their protective potentials using SH-SY5Y cells and MPP+ (1-methyl-4-phenylpyridinium) to mimic Parkinson's disease. The phytochemical analysis of a 70% aqueous methanolic extract of *L. frutescens* leaves resulted in the isolation and identification of 11 pure compounds (**6.1–6.11**), among which compounds **6.1** and **6.2** were identified as new metabolites. The new compounds were characterised using IR, UV, NMR, and HRESIMS and were given the trivial names lessertiosides A (**6.1**) and B (**6.2**). Additionally, the flavonoids 8-methoxyvestitol (**6.7**) and mucronulatol (**6.8**) were isolated for the first time from the plant. The biological actions show that the isolated compounds had negligible toxicity on SH-SY5Y cells and improved cell viability in the cells exposed to MPP^+. Furthermore, as a mechanism of action, the compounds could sustain cellular ATP generation and prevent MPP^+-induced apoptotic cell death. Our findings provide evidence for the neuroprotective properties of compounds isolated from *L. frutescens* in MPP^+- prompted neuronal damage for the first time and create an avenue for these compounds to be further investigated to elucidate their molecular targets.

Keywords: *Lessertia frutescens*; terpenoids; lessertiosides A and B; SH-SY5Y cells; neurotoxicity; neuroprotection

check for updates

Citation: Ndjoubi, K.O.; Omoruyi, S.I.; Luckay, R.C.; Hussein, A.A. Isolation of Lessertiosides A and B and Other Metabolites from *Lessertia frutescens* and Their Neuroprotection Activity. *Plants* **2024**, *13*, 3076. https://doi.org/10.3390/plants13213076

Academic Editor(s): Carlos Gamarra-Luques

Received: 11 October 2024
Revised: 28 October 2024
Accepted: 29 October 2024
Published: date

6.1 Introduction

Neuroprotection is associated with the capacity of treatment to mitigate neuronal cell death in short-term and long-term neurodegenerative conditions affecting the central nervous system [1,2]. Neurodegenerative diseases (ND) impact the function and composition of the entire nervous system [3], often leading to permanent brain damage. This damage limits various functions, including speech, mobility, bladder and bowel functions, and cognitive abilities, which is evident in Parkinson's disease (PD) [4]. PD is a complicated neurological condition defined by the gradual and selective depletion of A9 midbrain dopaminergic (DA) neurons localised in the substantia nigra pars compacta (SNpc), accompanied by the collection of aggregated α-synuclein deposits known as Lewy bodies [3,5]. It ranks as the second most prevalent ND and affects about 1% of individuals between the ages of 65 and 70, with a higher prevalence of 4-5% among those over 80 [6]. By 2030, the number of PD patients is expected to surge by 30%, impacting not only the patients' lifestyles but also the economy and society [7].

Although PD presents non-motor symptoms, clinical diagnosis typically involves observing motor symptoms, including bradykinesia, postural instability, resting tremors, and muscle rigidity [8]. Motor symptoms become evident at a later stage of the disease, often after patients have already lost approximately 80% of their striatal dopamine, equivalent to a 50% loss of DA neurons within the bulb, years before the SNpc of PD patients is affected [9–11]. The actual aetiology underscoring PD occurrence is not fully elucidated. However, age environment, genetics, iron accumulation, glutamate excitotoxicity, lipid peroxidation, lysosomal and mitochondrial dysfunction, neuroinflammation, nitrosative stress, oxidative stress, and proteasomal alterations contribute to its development [11–14]. While preclinical studies have identified potential therapies successful in PD animal models, translating these findings into successful clinical trials remains challenging [11].

At the moment, curative medication for PD is lacking. While the dopaminergic drug Levodopa effectively manages symptoms, its prolonged use often leads to adverse effects such as dyskinesia, drowsiness, low blood pressure, nausea, vomiting, and psychosis [15]. Thus, to combat neuronal cell loss and seek a cure for PD, researchers have been diligently searching for novel and efficient anti-Parkinson treatments, including plant-derived drugs. One promising area of research centres on *L. frutescens*, formerly known as *S. frutescens*, among others (*Colutea grandiflora*; *C. frutescens*, *C. frutescens*) [16]. This widely used South African medicinal plant is recognised for its potential therapeutic properties in treating various diseases such as diarrhoea, urinary tract infection, rheumatism, inflammation, intestinal pain, haemorrhoids, internal cancers, eye diseases, chickenpox, and skin disorders, as well as alleviating physical and mental stress [17–19]. While our previous work demonstrated the neuroprotective activity of *L. frutescens* extract [20], the current study evaluates the neuroprotective effects of compounds isolated from L. frutescens. These compounds were tested against the neurotoxin 1-methyl-4-phenylpyridinium (MPP^+), which induces PD motor symptoms by limiting the function of

mitochondrial complex I, which results in reduced cellular adenosine triphosphate (ATP) and augmentation of oxidative stress [21,22].

6.2 Results

6.2.1 Purification of L. frutescens Secondary Metabolites

Sequential silica gel 60, Sephadex LH-20 column chromatography, and semi-preparative HPLC were used to isolate eleven compounds (Figure 6.1) from the aqueous methanolic extract of *L. frutescens*. The structure elucidation of the new compounds (**6.1**-**6.2**) was accomplished by interrogating NMR spectroscopic data and complementary analyses such as IR and HR-ESIMS data. The known compound (**6.3**-**6.11**) structures were confirmed by comparing their NMR data with the reported ones. ^{1}H and ^{13}C NMR data of compounds **6.1** and **6.2** are provided in Table 6.1.

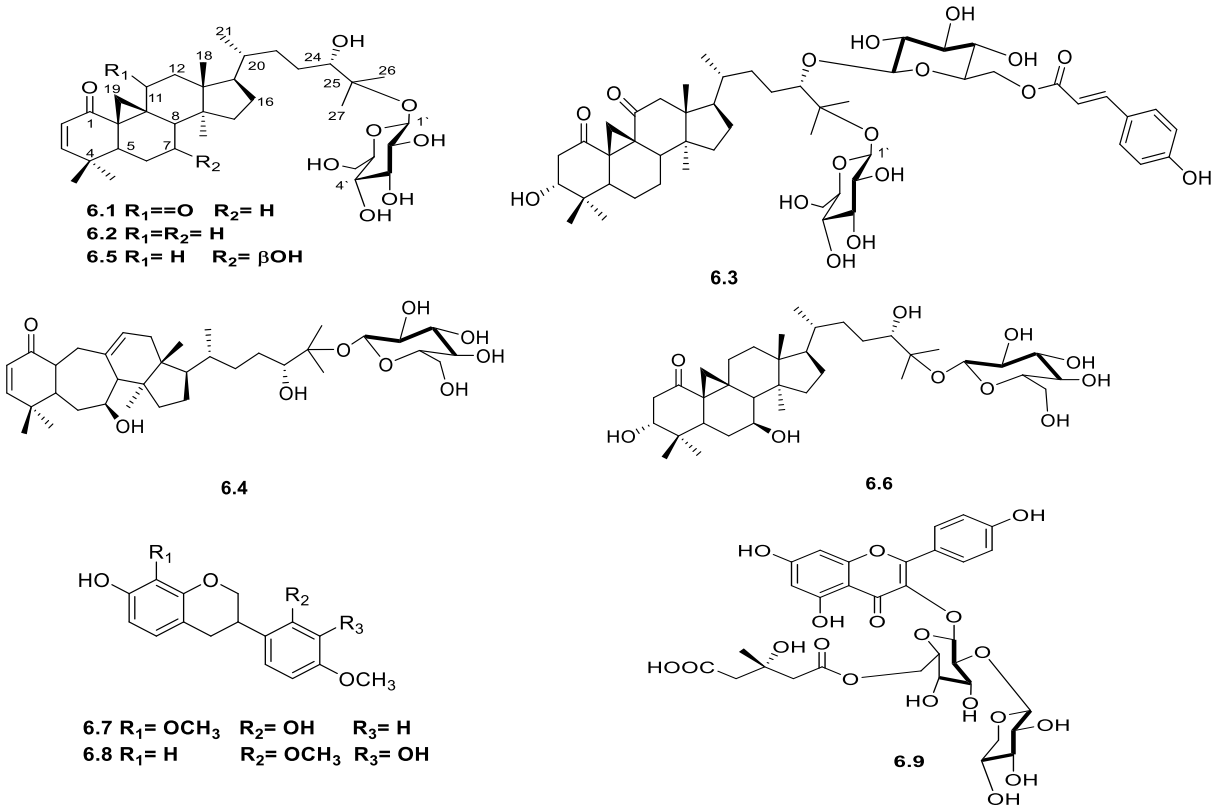

Figure 6.1 Chemical structure of *L. frutescens* isolated compounds (**6.1**-**6.9**)

Table 6.1 ^{1}H and ^{13}C NMR data of compounds **6.1** and **6.2**

	6.1		**6.2**	
No	**^{13}C**	**^{1}H, *muti.* (*J* = Hz)**	**^{13}C**	**^{1}H, *multi.* (*J* = Hz)**
1	199.8		204.3	
2	126.8	5.72, *d* (10.3)	129.5	5.69, *d* (10.1)
3	161.8	6.62, *d* (10.3)	161.5	6.61, *d* (10.1)
4	39.2		38.8	
5	45.7	2.14, *dd* (12.5, 4.3)	46.2	2.18, *dd* (12.8. 4.5)
6	22.6	1.59 *; 1.41	25.1	1.41 *; 1.20 *
7	19.5	1.57 *; 1.33 *	29.2	1.84 *; 1.24 *
8	39.3	2.25, *t* (7.9)	48.0	1.81*
9	36.2		31.8	
10	39.5		36.9	
11	212.6		26.8	2.25 *; 2.09 *
12	53.2	2.78, *d* (15.2) 2.52, d (15.2)	34.5	1.52* 1.23 *
13	45.0		46.4	
14	50.6		50.8	
15	34.2	1.41 *; 1.36 *	36.4	1.51 *; 1.21 *
16	22.8	1.41 *	22.0	1.60 *
17	52.2	1.79, *m*	54.0	1.51 *
18	16.6	0.74, *s*	18.2	0.87, *s*
19	34.9	1.79 *; 0.93 *	34.7	1.24 *; 0.95, *d* (4.5)
20	37.8	1.36 *	38.1	1.30 *
21	19.0	0.86, *d* (6.1)	19.4	0.81, *d* (6.7)
22	28.8	1.92, *m*; 1.40 *	35.3	2.24 *; 1.74 *
23	29.3	1.57 *; 1.08 *	29.7	1.52 *; 1.02 *
24	79.5	3.31, *t* (7.0)	79.8	3.27, *d* (7.4)
25	82.0		82.2	
26	21.5	1.14, *s*	21.6	1.10, s
27	23.9	1.17, *s*	24.2	1.13, *s*
28	28.7	1.08, *s*	28.4	1.02, *s*
29	21.5	1.02, *s*	21.4	0.89, *s*
30	19.1	1.10, s	19.7	0.88, *s*
1`	98.6	4.46, *d* (8.2)	98.8	4.40, *d* (7.4)
2`	75.2	3.10, *t* (8.2)	75.4	3.16, *t* (8.5)
3`	78.1	3.30 *	78.3	3.20 *
4`	71.1	3.22 *	71.8	3.18 *
5`	77.7	3.21 *	77.9	3.17 *
6`	62.7	3.58 *dd* (11,1; 4.5) 3.76, *d* (11.1)	62.9	3.59, *dd* (12.3, 4.3) 3.71, *d* (12.3)

* Partially or fully overlapped signals.

6.2.2 Dose–Response of L. frutescens Compounds

To determine the optimal concentrations of compounds that will not be cytotoxic and, in turn, show neuroprotection in the cells following neurotoxicity, the cells were treated with compounds numbered **6.3–6.11** at concentrations of 2.5, 5, and 10 μg/mL for 24 h, and an MTT cell viability assay was performed. The results showed that all compounds did not significantly induce cytotoxicity to the cells (Figure 6.2). Indeed, some compounds, including **6.4**, **6.5**, **6.6,** and **6.10**, had a concentration-dependent decrease in cell viability, with the 2.5 μg/mL concentration

showing the highest viability. On the other hand, compound **6.7** had a concentration-dependent increase in cell viability. Altogether, these results indicate that the compounds showed minimal cytotoxicity effects on the SH-SY5Y cells under the current treatment conditions. Nevertheless, it should be acknowledged that 2.5 µg/mL had the least effect on the viability of cells for most of the compounds.

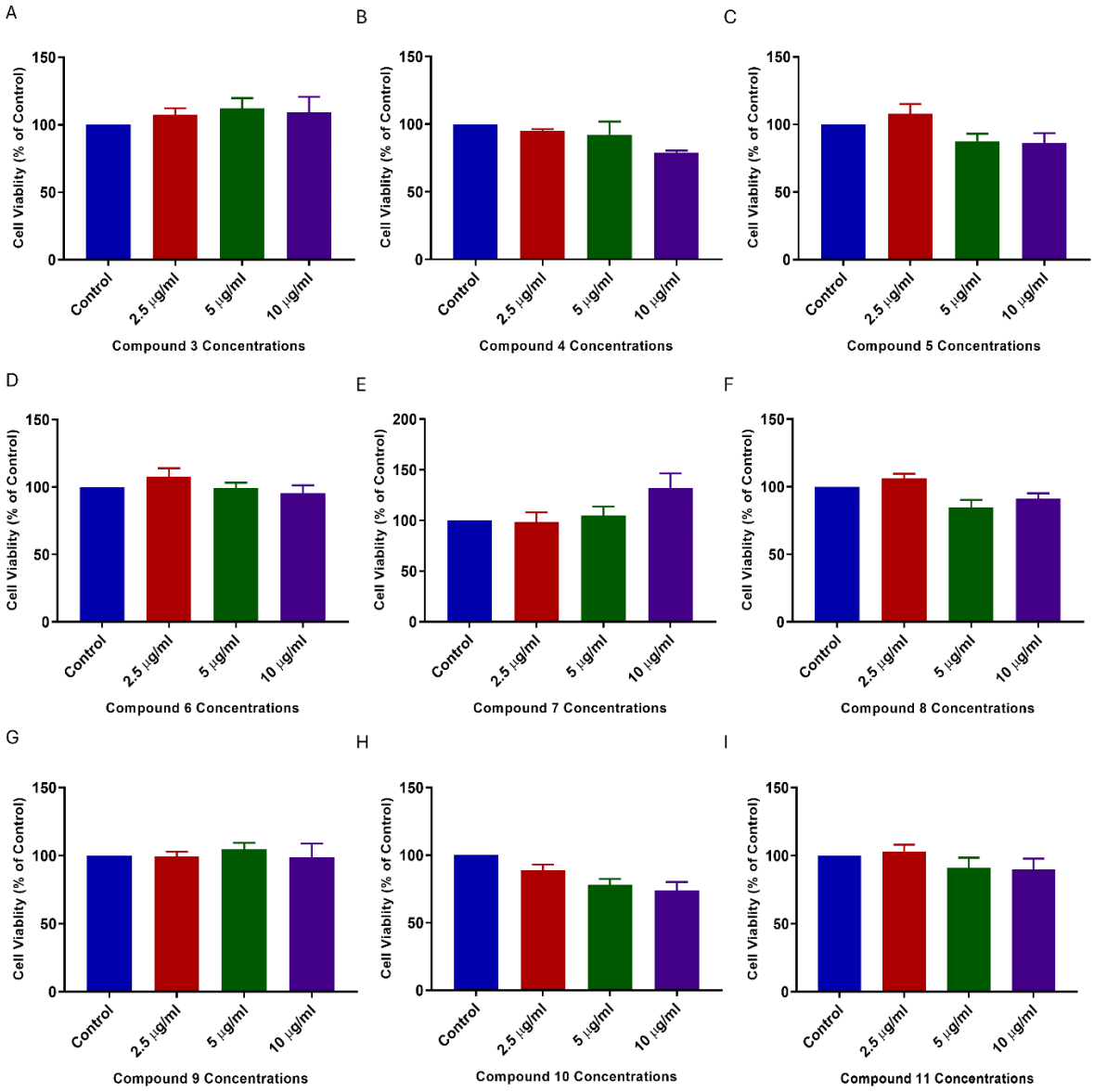

Figure 6.2 Cytotoxicity of *L. frutescens* compounds (**6.3–6.11**) on SH-SY5Y cells. SH-SY5Y cells were treated with concentrations of 2, 5, and 10 µg/mL of compounds for 24 h. After treatment, MTT assays were performed. The absorbance values obtained from quadruplicate wells were expressed as a percentage of the control. The bars in the graphs represent the means ± SEM of experiments performed in triplicates.

6.2.3 L. frutescens Compounds Protect SH-SY5Y Cells Following MPP⁺ Toxicity

Following optimisation of the concentration to be used for the neuroprotection studies, the neuroprotective potentials of the compounds (**6.3**-**6.11**) were evaluated in the SH-SY5Y cells co-treated with compounds and MPP⁺. Figure 6.3 confirms that under the concentrations utilised, all compounds significantly increased the viability of SH-SY5Y cells following MPP⁺ toxicity except for the cells treated with compound **6.4** (Figure 6.3) at the 10 µg/mL concentration. Indeed, MPP⁺ reduced cell viability to about 37 to 48%, while treatment with concentrations of the compounds rescued the cells from MPP⁺ toxicity. Since the 2.5 µg/mL concentration for the majority of the compounds showed the most increased cell viability, this concentration was selected for further evaluation of the neuroprotective effects of the compounds.

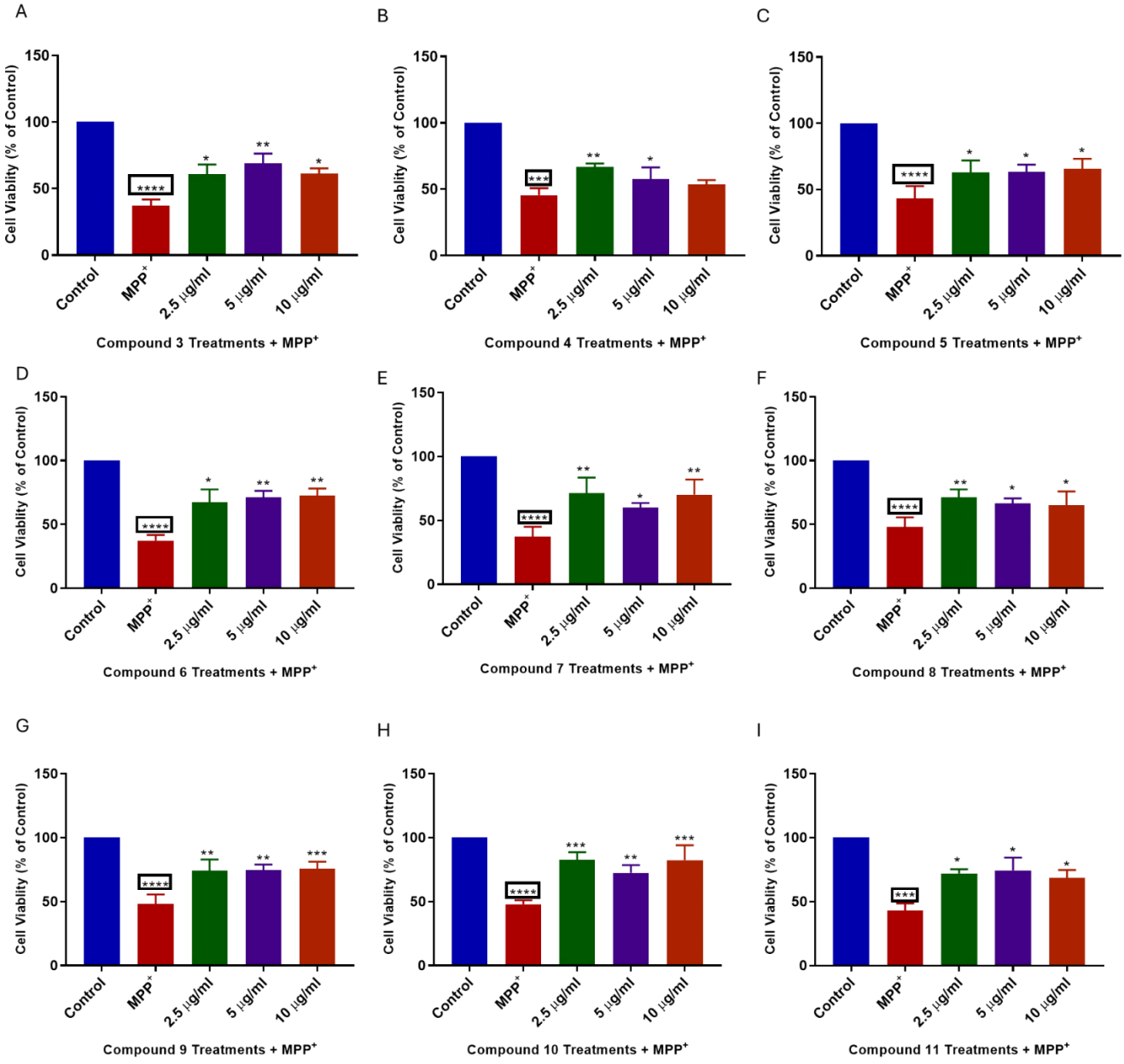

Figure 6.3 *L. frutescens* compounds (**6.3**-**6.11**) protect SH-SY5Y cells from MPP+ toxicity. SH-SY5Y cells were treated with 2, 5, and 10 µg/mL concentrations compounds for 2 h before the addition of MPP^+ and cells were incubated for 24 h, followed by MTT assays. Absorbance values obtained from quadruplicate wells were calculated as a percentage of control. Bars represent the means ± SEM of three independent experiments, and the significance of difference indicated with * $p <$ 0.05, ** $p < 0.01$, *** $p < 0.001$ and **** $p < 0.0001$ when cells pre-treated with compounds were compared to MPP+ and the boxed asterisks represent the comparison between MPP^+ and the control cells.

6.2.4 Effects of L. frutescens Compounds in ATP Production Following MPP^+ Toxicity

To further assess the neuroprotective potentials of compounds **6.3**-**6.11** isolated from *L. frutescens*, their impact on ATP production was determined in SH-SY5Y cells pre-treated with compounds before exposure to MPP^+. The results highlight that whereas MPP^+ significantly inhibited ATP production, pre-treatment with compounds showed an increase in ATP production (Figure 6.4). However, this increase was only significant for the cells treated with compounds **6.6**, **6.8**, **6.9,** and **6.10**. Indeed, MPP^+ reduced ATP production to about 51%, but pre-treatment with compounds **6.6**, **6.8**, **6.9,** and **6.10** increased ATP production to 73, 75, 74, and 75%, respectively. Altogether, these results suggest that the prevention of ATP degeneration induced by MPP^+ is involved in the neuroprotection mechanisms of compounds isolated from *L. frutescens*.

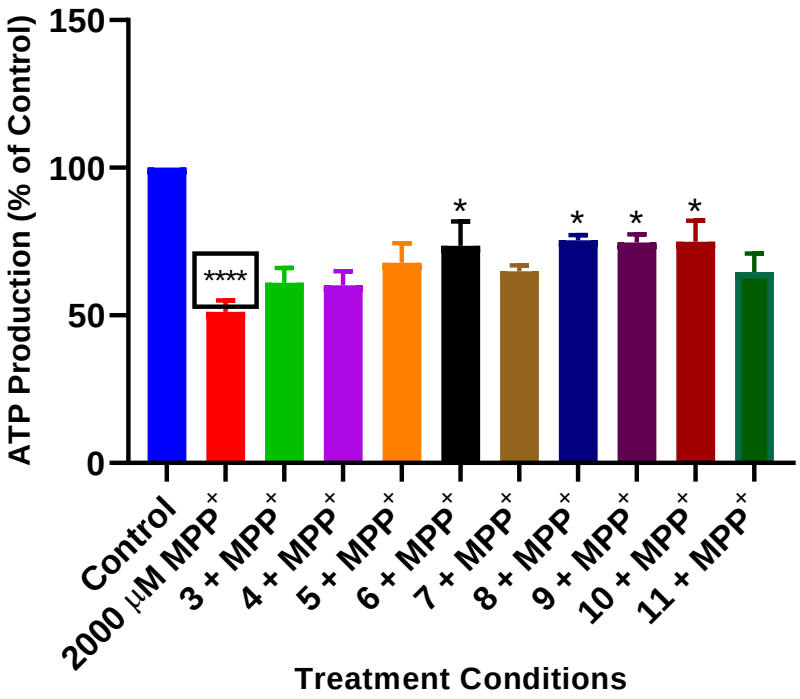

Figure 6.4 Impact of *L. frutescens* compounds (**6.3**-**6.11**) on ATP production. SH-SY5Y cells were treated with 2, 5, and 10 µg/mL concentrations compounds for 2 h before the addition of MPP+ and cells were incubated for 24 h, followed by ATP assays. Luminescence values obtained were expressed as a percentage of control. Bars represent means ± SEM of three independent experiments, and the

significance of difference is indicated with * $p < 0.05$ and **** $p < 0.0001$ when cells pre-treated with compounds were compared to MPP+, and the boxed asterisks represent the comparison between MPP^+ and the control cells.

6.2.5 L. frutescens Compounds Rescue Cells from MPP^+-Induced Apoptosis

Apoptosis is a mechanism of cell death, and caspase 3/7 activities in the cells can indicate apoptosis. Thus, to investigate apoptosis in the cells, the activities of caspase 3/7 were measured using the Promega caspase assay kit in cells pre-treated with compounds before exposure to MPP^+. The results showed that compounds **6.3**-**6.11** significantly mitigated the apoptosis-inducing effects of MPP+ by attenuating the elevated levels of caspase 3/7 activities in the cells. When caspase 3/7 activities were expressed as a fold of the control, which control cells set to 1, MPP^+ increased caspase 3/7 activities to approximately 5-fold of the control while the compounds ranged from 1.5- to 2.8-fold of the control (Figure 6.5). It is important to highlight that compound **6.8** inhibited apoptosis the most to about 1.5-fold of the control. These results suggest that the studied compounds might carry out their neuroprotective effects by mitigating MPP^+-induced apoptosis in the cells.

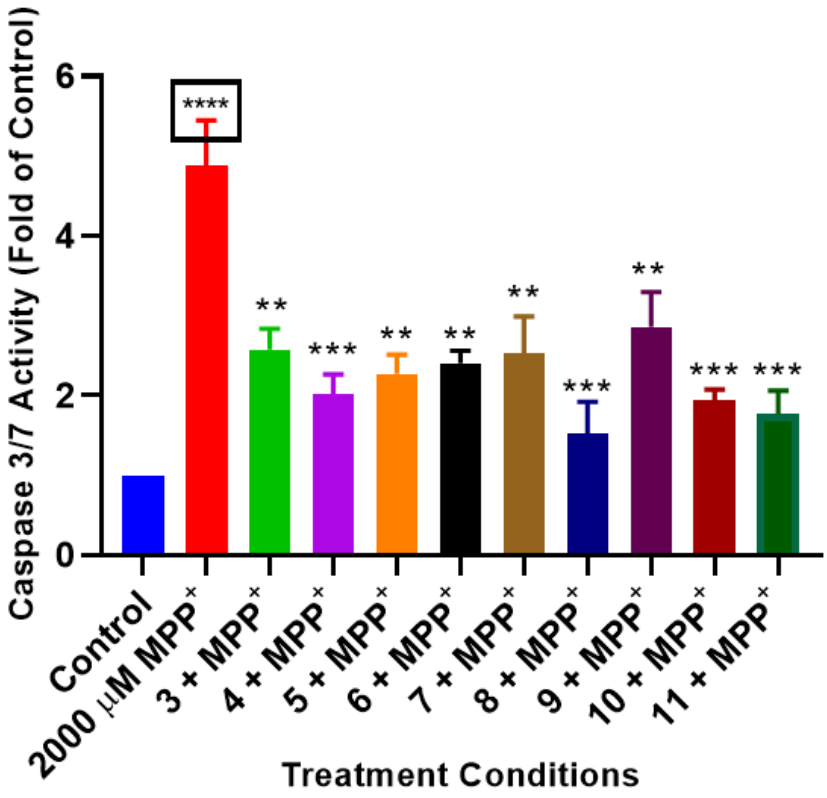

Figure 6.5 Impact of *L. frutescens* compounds (**6.3**-**6.11**) on ATP production. SH-SY5Y cells were treated with 2, 5, and 10 µg/mL concentrations compounds for 2 h before the addition of MPP^+ and cells were incubated for 24 h, followed by caspase 3/7 Glo assays. Luminescence values obtained were represented as fold of control. Bars represent means ± SEM of three independent experiments, and the significance of the difference is indicated with ** $p < 0.01$, *** $p < 0.001$, and **** $p <$

0.0001 when cells pre-treated with compounds were compared to MPP^+, and the boxed asterisks represent the comparison between MPP^+ and the control cells.

6.3 Discussion

The chromatographic purification of a methanolic extract from *L. frutescens* yielded eleven compounds (**6.1**-**6.11**). Compounds **6.3** and **6.4** were recently reported as sutherlandiosides K and E, respectively [23]. However, the trivial name sutherlandioside E was already assigned to the 9,10-seco-cycloartane-type diglycoside bearing an unprecedented 5/7/6/5 ring skeleton isolated earlier by Fu et al. (2012) [24]. Compound **6.7** was identified as 8-methoxyvestitol and previously isolated from *Astragalus trigonus* [25], while compound **6.8** was identified as mucronulatol and previously isolated from *Machaerium mucronularum* [26], both **6.7** and **6.8** were isolated for the first time from *L. frutescens*. On the other hand, compound **6.6** (sutherlandioside B), compound **6.9** (sutherlandin C), compound **6.10** (proline), and compound **6.11** (D-pinitol) are well-known *L. frutescens* compounds.

The neuroprotective effects of these compounds were evaluated against MPP^+-induced toxicity in SH-SY5Y cells. The study investigated ATP production and caspase 3/7 activity, which are critical indicators of cell viability and apoptotic pathways, respectively. Our findings suggest that the *L. frutescens* compounds confer neuroprotection against MPP+-induced neurotoxicity in SH-SY5Y cells, a model often used to mimic PD pathology.

6.3.1 Structure Elucidation

Compound **6.1** (lessertioside A), HR-ESIMS exhibited a molecular ion peak of 633.39 *m/z* corresponding to a molecular formula of $C_{36}H_{56}O_9$. The IR absorptions display characteristic bands at 3354, 2959, 1660, 1457, and 1143 cm^{-1}, revealing the presence of alkoxyl, carbonyl, hydroxyl, alkyl, and olefin groups. The ^1H NMR showed the signals of six tertiary methyl groups at δ_H 0.74 (*s*, Me-18), 1.14 (*s*, Me-26), 1.17 (*s*, Me-27), 1.08 (*s*, Me-28), 1.02 (*s*, Me-29), and 1.10 (*s*, Me-30) as well as one secondary methyl group at δ_H 0.86 (*d*, *J* = 6.1 Hz, Me-21). In addition, an isolated methylene group was observed at δ_H 0.93 (H-19α) and 1.79 (H-19β) as well as resonances of seven methylene groups at δ_H 1.41 (H-6α), 1.59 (H-6β), 1.33 (H-7α), 1.57 (H-7β), 2.52 (*d*, *J* = 15.2 Hz, H-12α), 2.78 (*d*, *J* = 15.2 Hz, H-12β), 1.36 (H-15α), 1.41 (H-15β), 1.41 (H-16), 1.40 (H-22α), 1.92 (*m*, H-22β), 1.08 (H-23α), and 1.57 (H-23β). The spectrum also showed a low field proton attached to an oxygenated carbon at δ_H 3.31 (*t*, *J* = 7.0 Hz, H-24); two olefinic protons at δ_H 5.72 (*d*, 10.3, H-2) and 6.62 (*d*, 10.3, H-3) as well as the signals of three methine groups 2.14 (*dd*, *J* = 12.5; 4.3 Hz, H-5), 2.25 (*t*, *J* = 7.9 Hz, H-8), and 1.36 (H-20) revealing the aglycon to be a cycloartane-type triterpenoid. The ^1H NMR also displayed a signal of an anomeric proton at δ_H 4.46 (*d*, *J* = 8.2 Hz, H-1`) and a cluster of protons ranging from δ_H 3.10 to 3.76, indicating the presence of a glucose unit.

The ^{13}C NMR signals showed 36 peaks which were categorised according to DEPT-135 into seven methyls at δ_C 16.6 (C-18), 19.0 (C-21), 21.5 (C-26), 23.9 (C-27), 28.7 (C-28), 21.5 (C-29), 19.1 (C-30); nine methylene at δ_C 22.6 (C-6), 19.5 (C-7), 53.2 (C-12), 34.2 (C-15), 22.8(C-16), 34.9 (C-19), 28.8 (C-22), 29.3 (C-23), 62.7 (C-6`); thirteen methines at $\delta_C$ 126.8 (C-2), 161.8 (C-3), 45.7 (C-5), 39.3 (C-8), 52.2 (C-17), 37.8 (C-20), 79.5 (C-24), 98.6 (C-1`), 75.2 (C-2`), 78.1 (C-3`), 71.1 (C-4`), 77.7 (C-5`); and seven quaternary

carbons at δ_C 199.8 (C-1), 39.2 (C-4), 36.2 (C-9), 39.5 (C-10), 212.6 (C-11), 48.7 (C-13), 50.6 (C-14), 82.0 (C-25).

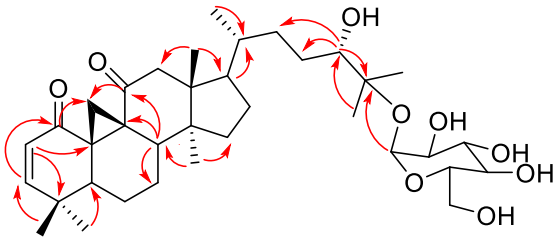

HMBC correlations of compound **6.1** (H→C)

Based on the HMBC spectrum, the correlation between the anomeric proton H-1′ and C-25 further confirms the attachment of the glucose group to C-25. It was also observed that the hydroxymethine moiety (C-24) correlated with the methyl groups at C-26 and C-27 as well as the quaternary carbon C-25, which in turn was linked to H-23, H-22 in the ^{1}H-^{1}H COSY spectrum. Moreover, the chemical shift of C-24, located within the range typical for *S* stereoisomers (77.1 to 78.6 ppm), suggests that C-24 is in the *S* configuration [23,27,28]. The chemical shifts observed for the side chain (C-20 to C-27) attached to C-17 were similar to those reported for sutherlandioside A-D. The ^{1}H-^{1}H COSY and HMBC spectra indicated correlations between H-5, H-6, and H-8 with the methylene signal at C-7. HMBC correlations from H-28/H-29 to C-3, H-3 to C-1, and H-2 to C-4 indicated the presence of an olefinic bond between C-2 and C-3. These findings suggest a structural resemblance between sutherlandioside D (compound **6.5**) and compound **6.1** [28]. The glucose unit was confirmed as β-configuration according to the coupling constants of the anomeric proton (*J* = 8.2 Hz). The chemical shifts of the protons and the carbons were compared carefully with similar compounds isolated from the same source [23,24,27,28].

However, unlike sutherlandioside D, compound **6.1** does not have a hydroxymethine at C-7 but a methylene group. Additionally, an extra carbonyl group at C-11 was found to be linked to the protons at position 19. The chemical shifts of H-12 were detected in the lower field compared to the resonance of H-12 at δ_H 1.62 (H-12α) and δ_H 1.35 (H-12β) in compound 5, further confirming the second carbonyl group to be attached to C-11. A carbonyl group at position 11 indicates that compound **6.1** is also similar to sutherlandioside C [28]. However, unlike sutherlandioside C, compound **6.1** features a double bond between C-2 and C-3 instead of a hydroxyl group at C-3. Following the data from HRESIMS, IR, and NMR analyses, compound **6.1** has been characterised as 24*S*,25-dihydroxycycloart-2-en-1,11-dione-25-*O*-*β*-*D*-glucopyranoside (lessertioside A).

Furthermore, compound **6.2** (lessertioside B) HR-ESIMS displayed a molecular ion peak of 619.41 *m*/*z*. The molecular formula of compound **6.2** was deduced as $C_{36}H_{58}O_8$, which corroborated with the HR-ESIMS and The IR absorption bands at 3292, 2938, 1674, 1457, and 1209, 3292 cm^{-1}, showing the presence of hydroxyl, olefin, and carbonyl groups. The ^{1}H NMR showed the signals of seven methyl groups at δ_H 0.87 (*s*, Me-18), 0.81 (*d*, *J* = 6.7 Hz, Me-21), 1.10 (*s*, Me-26), 1.13 (*s*, Me-27), 1.02 (*s*, Me-28), 0.89

(*s*, Me-29) and 0.88 (*s*, Me-30). Additionally, the resonance of nine methylene groups at δ_H 1.20 (H-6α), 1.41 (H-6β), 1.24 (H-7α), 1.84 (H-7β), 2.09 (H-11α), 2.25 (H-11β), 1.23 (H-12α), 1.52 (H-12β), 1.21 (H-15α), 1.51 (H-15β), 1.60 (H-16), 1.24 (H-19α), 0.95 (*d*, *J* = 4.5 Hz, H-19β), 1.74 (H-22α), 2.24 (H-22β), 1.02 (H-23α), and 1.52 (H-23β) were observed. The ^{1}H NMR spectrum also showed six methine groups at δ_H 5.69 (*d*, *J* = 10.1 Hz, H-2), 6.61 (*d*, *J* = 10.1 Hz, H-3), 2.18 (*dd*, *J* = 12.8; 4.5 Hz, H-5), 1.81 (H-8), 1.30 (H-20), and 3.27 (*d*, *J*= 7.4 Hz, H-24). The presence of a glucose unit was confirmed by the anomeric proton signal at δ_H 4.40 (d, *J* = 7.4 Hz, H-1′) and the cluster of protons at δ_H 3.16 (*t*, *J* = 8.5 Hz, H-2′), 3.20 (H-3′), 3.18 (H-4′), 3.17 (H-5′), 3.59 (*dd*, *J* = 12.3; 4.3 Hz, H-6α′), and 3.71 (*d*, *J* = 12.3 Hz, H-6β′).

The ^{13}C NMR signals showed 36 peaks; 30 were attributed to the triterpenoid nucleus, while the remaining 6 displayed a glucose unit. These peaks were categorised according to DEPT-135 and HSQC into seven methyls at δ_C 18.2 (C-18), 19.4 (C-21), 21.6 (C-26), 24.2 (C-27), 28.4 (C-28), 21.4 (C-29), 19.7 (C-30); nine methylene at δ_C 25.1 (C-6), 26.8 (C-11), 34.5 (C-12), 36.4 (C-15), 22.0 (C-16), 34.7 (C-19), 35.3 (C-22), 29.7 (C-23), 62.9 (C-6′); thirteen methines at δC 129.5 (C-2), 161.5 (C-3), 46.2 (C-5), 29.2 (C-7), 48.0 (C-8), 54.0 (C-17), 38.1 (C-20), 79.8 (C-24), 98.8 (C-1′), 75.4 (C-2′), 78.3 (C-3′), 71.8 (C-4′), 77.9 (C-5′); and seven quaternary carbons at δ_C 204.3 (C-1), 38.8 (C-4), 31.8 (C-9), 36.9 (C-10), 46.4 (C-13), 50.8 (C-14), 82.2 (C-25).

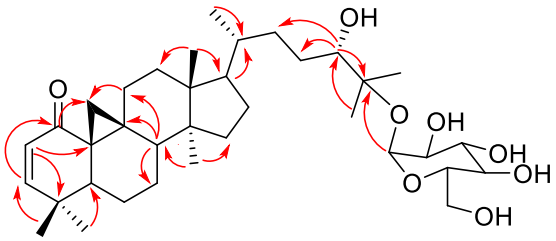

HMBC correlations of compound **6.2** (H→C).

The chemical shifts of the glucose unit are identical to compound **6.1**. According to the ^{1}H and ^{13}C NMR spectra, compounds **6.2** and **6.1** exhibit striking structural similarities with one notable distinction: the absence of a carbonyl group at C-11. This discrepancy has been thoroughly corroborated by the HMBC and COSY spectra, which showed the correlation between H-19 and H-11, which in turn was connected to C-11 in the HSQC spectrum, indicating the carbonyl group at C-11 in compound **6.1** has been reduced to a methylene group in compound **6.2**. Thus, the structure of compound **6.2** was characterised as 24*S*,25-dihydroxycycloart-2-en-1-one-25-*O*-*β*-*D*-glucopyranoside (lessertioside B).

6.3.2 Neuroprotective Effects of the Isolated Compounds

Their impact on cellular ATP was investigated to elucidate the mechanism of action of the compounds. ATP is the primary energy currency of the cell, and its depletion is a hallmark of mitochondrial dysfunction, which is closely linked to neurodegenerative diseases such as PD [29,30]. MPP^+ causes a significant decrease in ATP levels by blocking complex I of the mitochondrial electron transport chain, resulting in reduced cellular energy and subsequent cell death [31–33]. In this study,

treatment with *L. frutescens* compounds (**6.3–6.11**) resulted in substantial preservation of ATP levels in SH-SY5Y cells exposed to MPP^+. This suggests that these compounds may mitigate mitochondrial dysfunction, potentially through direct interaction with mitochondrial components or by scavenging free radicals that exacerbate oxidative stress and energy failure. Furthermore, the maintenance of ATP levels in the presence of MPP^+ implies that *L. frutescens* compounds help sustain cellular energy metabolism, which is crucial for neuronal survival [34,35]. This effect could be attributed to the enhancement of mitochondrial biogenesis, protection of mitochondrial integrity, or activation of alternative energy-generating pathways. Further investigation is warranted into the precise mechanisms by which *L. frutescens* compounds may impact ATP levels following MPP^+ toxicity.

Following the depletion of ATP in cells, cells may proceed to cell death [36,37]. Caspase 3/7 are central executors of apoptosis, activated during the terminal stages of the intrinsic/extrinsic apoptotic pathway, often triggered by mitochondrial dysfunction and energy deficits [38,39]. MPP^+ exposure triggered increased levels of caspase 3/7 activities, consistent with the induction of apoptosis in SH-SY5Y cells [40,41]. However, pre-treatment with *L. frutescens* compounds significantly reduced caspase 3/7 activation, indicating an anti-apoptotic effect. The inhibition of caspase 3/7 activities suggests that *L. frutescens* compounds may interfere with upstream events leading to caspase activation, such as cytochrome c release, apoptosome formation, or other pro-apoptotic signalling pathways [39,42]. By preventing the activation of these caspases, *L. frutescens* compounds likely help preserve cellular integrity and function, thereby offering a protective effect against MPP^+-induced neurotoxicity. In conjunction with preserving ATP levels, this anti-apoptotic action highlights the potential of *L. frutescens* compounds in maintaining neuronal viability in the face of mitochondrial stress.

6.4 Materials and Methods

6.4.1 Chemicals, Materials, and Reagents

The leaves powder of *L. frutescens* was donated by Afriplex in 2018. The Silica gel 60 (0.063–0.200 mm), Sephadex (LH-20), and aluminium thin layer chromatography plate supplied by Merck (Cape Town, South Africa) were used. Hexane, ethyl acetate, and methanol AR grades were purchased from the local market (Kimix, Cape Town, South Africa). The Shimadzu LC-20 HPLC system has a quaternary pump (LC-20AD), a diode array detector (DAD, SPD-M20A), and a manual injector. HPLC grade methanol and a reversed-phase C18 column (25 × 1 cm, 5 μm, Supelco, Merck, South Africa) were used for purification. The detector was operating at wavelengths 254, 272, and 366 nm. The 1D NMR (^1H, ^{13}C, and DEPT-135) and 2D NMR (HMBC, HSQC, and COSY) spectra were measured using a Bruker spectrometer (Rheinstetten, Germany) operating at 400/100 MHz for ^1H and ^{13}C NMR, respectively.

6.4.2 Extraction of Plant Sample

The ground plant material (1.0 kg) underwent maceration in 70% aqueous methanol for 24 h at room temperature, followed by filtration.

The process was repeated twice. The combined filtrates were evaporated using a Rotavapor, producing 64.6 g of total extract.

6.4.3 Isolation of L. frutescens Secondary Metabolites

The purification and isolation of secondary metabolites from the aqueous methanol extract were carried out using a combination of Sephadex LH-20 column chromatography, silica gel 60 column chromatography, and semi-preparative HLPC. All semi-preparative HPLC was conducted using HPLC grade methanol and deionised water as eluent at a flow rate of 1.0 mL/min, following a gradient of 60% to 80% methanol over 45 min, and 80% to 100% methanol for 15 min.

The total extract was fractionated using silica gel column chromatography. A gradient of hexane/ethyl acetate, followed by ethyl acetate/methanol with increasing polarity, was used, yielding twenty-seven fractions (I-XXVII), of which only fractions IX, X, XI, XII, XV, XVII, XIX, XX, XXII, and XXV were subjected to further purification. The remaining fractions were not considered due to their similarities with the selected fractions, except for fractions I to VII, which mainly contained fatty acids and chlorophyll components.

Fractions IX to XII were combined (4.2 g) and subjected to isocratic silica gel column chromatography using hexane: ethyl acetate (90:10), followed by Sephadex LH-20 column chromatography using 40% aqueous methanol. This purification process resulted in isolating compounds **6.7** (45.4 mg) and **6.8** (4.1 mg).

Fraction XV (500 mg) was subjected to Sephadex LH-20 column chromatography using 20% aqueous methanol, followed by semi-preparative HPLC, leading to the isolation of compounds **6.4** (5.9 mg) and **6.2** (4.1 mg) at retention times (R_t) of 36 min and 62 min, respectively. Fraction XVII (1.0 g) underwent the same conditions to yield compounds **6.3** (R_t 35 min, 6.7 mg), **6.5** (R_t 36 min, 12.1 mg), and **6.6** (R_t 32.5 min, 8.9 mg).

Fractions XIX and XX were combined and subjected to silica gel column chromatography, followed by semi-preparative HPLC, resulting in the isolation of compound **6.1** (R_t 47.5 min, 9.8 mg). Fraction XXII (250 mg) was subjected to Sephadex LH-20 column chromatography using 30% aqueous methanol, followed by semi-preparative HPLC, leading to the isolation of compound **6.9** (R_t 29 min, 8.2 mg). Fraction XXV (500 mg) was chromatographed on Sephadex LH-20 using 30% aqueous methanol, resulting in the isolation of compounds **6.10** (43.3 mg) and **6.11** (17.8 mg).

6.4.4. Spectroscopic Data of Lessertiosides A and B

Lessertioside A ($C_{36}H_{56}O_9$): colourless powder, $[\alpha]_{25}^{D}$ = −2.51 (*c* 0.3, MeOH); IR: 3354 cm^{-1} (OH), 2959 cm^{-1} (CH), 1660 cm^{-1} (C=O), 1457 cm^{-1} (C=C), 1143 cm^{-1} (C-O); UV: 316 nm; HRESIMS: *m*/*z* 633.3991 $[M+H]^+$ (calculated for $C_{36}H_{57}O_9$, 633.3997); ^1H NMR ($CDCl_3$) and ^{13}C NMR ($CDCl_3$): see Table 6.1

Lessertioside B ($C_{36}H_{58}O_8$): colourless powder, $[\alpha]_{25}^{D}$ = +3.06 (*c* 0.4, MeOH); IR: 3292 cm^{-1} (OH), 2938 cm^{-1} (CH), 1674 cm^{-1} (C=O), 1457 cm^{-1} (C=C), 1209 cm^{-1} (C-O); UV: 320 nm; HRESIMS: *m*/*z* 619.4190; $[M+H]^+$

(calculated for $C_{36}H_{59}O_8$, 619.4204); ^{1}H NMR ($CDCl_3$) and ^{13}C NMR ($CDCl_3$): see Table 6.1

6.4.5 Cell Culture and Maintenance

The human neuroblastoma SH-SY5Y cells were generously provided by the Blackburn Laboratory at the University of Cape Town. The SH-SY5Y cells were chosen for this study as they are widely used in neuroscience research to model neurodegenerative diseases, including PD, due to their dopaminergic characteristics. The cells exhibit functional dopamine receptors and neurotransmitter uptake, mimicking the dopaminergic system's physiology. The cells were cultured in Dulbecco's Modified Eagle's Medium (DMEM, Gibco, Life Technologies Corporation, Paisley, UK), with 10% fetal bovine serum (FBS, Gibco, Life Technologies Corporation, Paisley, UK), 100 U/mL penicillin, and 100 μg/mL streptomycin (Lonza Group Ltd., Verviers, Belgium) as supplements. Cultures were maintained at 37 °C in a humidified incubator with 5% CO_2, with the cell growth medium being routinely replaced every three days. When the cells reached 70-80% confluency, they were sub-cultured using a 0.25% trypsin EDTA solution (Lonza Group Ltd., Verviers, Belgium).

6.4.6. Treatments

A 10 mg/mL stock solution of the individual compounds (**3**–**11**) was made in dimethyl sulfoxide (DMSO) (Sigma-Aldrich, St Louis, MO, USA). These solutions were diluted further in the growth medium to achieve the desired final concentrations. To optimise the concentration of compounds that will be neuroprotective, 10,000 cells were grown/well in the 96-well plate, followed by treatment with 2.5, 5, and 10 μg/mL concentrations. Control cells were treated with the same amount of DMSO as contained in the 10 μg/mL concentration of the compounds, and treatments lasted for 24 h. To establish neurotoxicity, 2000 μM MPP+ was used, consistent with our previous research [22]. For neuroprotective studies, the cells were similarly grown as mentioned above and pre-treated with the 2.5, 5, and 10 μg/mL concentrations of compounds for 2 h, followed by adding 2000 μM MPP+. The treatments were left for 24 h, and the vehicle-treated cells were used as controls.

6.4.7. Cell Viability Assay

The MTT [3-(4, 5-dimethylthiazol-2-yl)-2, 5-diphenyltetrazolium bromide] assay (Sigma-Aldrich, St Louis, MO, USA) was utilised to assess cell viability following treatment with either compound or after pre-treatment with compounds followed by MPP+. After treatment of cells as mentioned above, 10 or 20 μL (depending on well volume) of a 5 mg/mL MTT solution in PBS (Lonza Group Ltd., Verviers, Belgium) was added to each well and kept in the incubator for an additional 4 h at 37 °C. After the incubation period, the medium with the MTT dye was removed, and the MTT formazan was dissolved using 100 μL of DMSO. The absorbance was then read at 570 nm in a spectrophotometer (BMG Labtech Omega® POLARStar) and the percentage of viable cells was determined with the control cells as reference.

6.4.8. Adenosine Triphosphate Levels (ATP) Assay

The Mitochondrial ToxGlo ATP assay kit (Promega, Madison, WI, USA) was utilised to determine ATP production in the cells. Summarily, the cells were plated in a white-walled 96-well plate, and treatment was similar to what was previously outlined for the neuroprotection studies. Post-treatment, cells were processed per the manufacturer's instructions by adding an equal volume of ATP detection reagent to each well and incubating at 37 °C for 30 min. After incubation, luminescence intensity was measured using the BMG Labtech Omega® POLARStar multimode microplate reader, and the luminescence values were expressed as percentages of the control.

6.4.9 Caspase 3/7 Apoptosis Assay

To investigate cell apoptosis, the Caspase 3/7 assay kit (Promega, Madison, WI, USA) was used to measure caspase 3/7 activity following the manufacturer's instructions. Briefly, cells were seeded in a white 96-well plate at a density of 10,000 cells per well and allowed to attach overnight. Subsequently, cells were pre-treated with compounds before adding 2000 μM MPP+. After 24 h of treatment, equal volumes of the caspase 3/7 assay mix were added to each well, and the luminescence intensity was measured using the BMG Labtech Omega® POLARStar multimode microplate reader. The luminescent values of the treated cells were expressed as fold changes compared to the control.

6.4.10 Statistical Analysis

Graph Pad Prism Version 8 was used to analyse the data obtained from three independent experiments. The data were represented as means ± SEM (standard error of means), and a one-way analysis of variance (ANOVA) was used to analyse the differences between the treated cells and vehicle control cells, and a p-value < 0.05 was considered significant.

6.5 Conclusions

The discovery of new cycloartane glycosides highlights the significance of this plant as a source of bioactive compounds. It supports its widespread use in treating various human diseases in Southern Africa. The neuroprotective effects observed in this study underscore the potential of *L. frutescens* compounds as potential therapeutic agents in neurodegenerative diseases that warrant further investigation. By preserving ATP levels and inhibiting caspase 3/7 activation, these compounds could help counteract the energy deficits and apoptotic processes contributing to neurodegeneration. In the future, the molecular targets of the compounds and more investigation into the mechanisms of action should be carried out. In addition, *in vivo* studies and clinical trials will be necessary to determine the efficacy and safety of these compounds in a physiological context.

Supplementary Materials:

The following supporting information can be downloaded at https://www.mdpi.com/article/10.3390/plants13213076/s1, Figure S1.1. ^{1}H NMR of compound **6.1**. Figure S1.2. ^{13}C NMR of compound **6.1**. Figure S1.3. DEPT-135 of compound **6.1**. Figure S1.4. HSQC of compound **6.1**. Figure S1.5. HMBC of compound **6.1**. Figure S2.1. ^{1}H NMR of compound **6.2**.

Figure S2.2. ^{13}C NMR of compound **6.2**. Figure S2.3. DEPT-135 of compound **6.2**. Figure S2.4. HSQC of compound **6.2**. Figure S2.5. HMBC of compound **6.2**.

References:

1. Schapira, A.H.V. Neuroprotection in Parkinson's Disease. *Blue Books Neurol.* **2010**, *34*, 301–320.
2. Elufioye, T.O.; Berida, T.I.; Habtemariam, S. Plants-Derived Neuroprotective Agents: Cutting the Cycle of Cell Death through Multiple Mechanisms. *J. Altern. Complement. Med.* **2017**, *2017*, 3574012.
3. Ayeni, E.A.; Aldossary, A.M.; Ayejoto, D.A.; Gbadegesin, L.A.; Alshehri, A.A.; Alfassam, H.A.; Afewerky, H.K.; Almughem, F.A.; Bello, S.M.; Tawfik, E.A. Neurodegenerative Diseases: Implications of Environmental and Climatic Influences on Neurotransmitters and Neuronal Hormones Activities. *Int. J. Environ. Res. Public Health* **2022**, *19*, 12495.
4. Lamptey, R.N.L.; Chaulagain, B.; Trivedi, R.; Gothwal, A.; Layek, B.; Singh, J.A.A. Review of the Common Neurodegenerative Disorders: Current Therapeutic Approaches and the Potential Role of Nanotherapeutics. *Int. J. Mol. Sci.* **2022**, *23*, 1851.
5. Kim, K.S. Toward neuroprotective treatments of Parkinson's disease. *Proc. Natl. Acad. Sci. USA* **2017**, *114*, 3795–3797.
6. Tansey, M.G.; McCoy, M.K.; Frank-Cannon, T.C. Neuroinflammatory mechanisms in Parkinson's disease: Potential environmental triggers, pathways, and targets for early therapeutic intervention. *J. Exp. Neurol.* **2007**, *208*, 1–25.
7. Chen, R.C.; Chang, S.F.; Su, C.L.; Chen, T.H.; Yen, M.F.; Wu, H.M. Prevalence, incidence, and mortality of PD: A door-to-door survey in Ilan county, Taiwan. *Neurology* **2001**, *57*, 1679–1686.
8. Kouli, A.; Torsney, K.M.; Kuan, W.L. Parkinson's disease: Etiology, Neuropathology, and Pathogenesis. In *Parkinson's Disease: Pathogenesis and Clinical Aspects*; Stoker, T.B., Greenland, J.C., Eds.; Codon Publications: Brisbane, Australia, 2018; pp. 1–45.
9. Braak, H.; Del Tredici, K.; Rüb, U.; de Vos, R.A.; Jansen Steur, E.N.; Braak, E. Staging of brain pathology related to sporadic Parkinson's disease. *Neurobiol. Aging* **2003**, *24*, 197–211.
10. Vingerhoets, F.J.G.; Snow, B.J.; Tetrud, J.W.; Langston, J.W.; Schulzer, M.; Calne, D.B. Positron emission tomographic evidence for progression of human MPTP-induced dopaminergic lesions. *Ann. Neurol.* **1994**, *36*, 765–770.
11. Devos, D.; Hirsch, E.; Wyse, R. Seven Solutions for Neuroprotection in Parkinson's disease. *J. Mov. Disord.* **2021**, *36*, 306–316.
12. Dauer, W.; Przedborski, S. Parkinson's disease: Mechanisms and models. *Neuron* **2003**, *39*, 889–909.
13. Bové, J.; Zhou, C.; Jackson-Lewis, V.; Taylor, J.; Chu, Y.; Rideout, H.J.; Wu, D.C.; Kordower, J.H.; Petrucelli, L.; Przedborski, S. Proteasome inhibition and Parkinson's disease modeling. *Ann. Neurol.* **2006**, *60*, 260–264.
14. Michel, P.P.; Hirsch, E.C.; Hunot, S. Understanding dopaminergic cell death pathways in Parkinson's disease. *Neuron* **2016**, *90*, 675–691.
15. Mallah, K.; Couch, C.; Borucki, D.M.; Toutonji, A.; Alshareef, M.; Tomlinson, S. Anti-inflammatory and Neuroprotective Agents in Clinical Trials for CNS Disease and Injury: Where Do We Go From Here? *Front. Immunol.* **2020**, *11*, 2021.
16. WFO. Available online: https://wfoplantlist.org/taxon/wfo-0001274560-202406?matched_id=wfo0000212662&page=1 (accessed on 8 July 2024).
17. Van Wyk, B.E.; Van Oudtshoorn, B.; Gericke, N. *Medicinal Plants of South Africa*; Briza Publications: Pretoria, South Africa, 1997; pp. 205–515.
18. Ojewole, J. Analgesic, antiinflammatory and hypoglycemic effects of Sutherlandia frutescens R. BR. (variety Incana E. MEY.) [fabaceae] shoot aqueous extract. *Methods Find. Exp. Clin. Pharmacol.* **2004**, *26*, 409–416.
19. Van Wyk, B.E.; Albrecht, C. A review of the taxonomy, ethnobotany, chemistry and pharmacology of Sutherlandia frutescens (Fabaceae). *J. Ethnopharmacol.* **2008**, *119*, 620–629.
20. Enogieru, A.B.; Omoruyi, S.I.; Ekpo, O.E. Aqueous leaf extract of Sutherlandia frutescens attenuates ROS-induced apoptosis and loss of mitochondrial membrane potential in MPP+-treated SH-SY5Y cells. *Trop. J. Pharm. Res.* **2020**, *19*, 549–555.
21. Fernagut, P.O. Etiology and Progression of Parkinson's Disease: Cross-Talk Between Environmental Factors and Genetic Vulnerability. In *Handbook of Basal Ganglia Structure and Function*, 2nd ed.; Steiner, H., Tseng, K., Eds.; Handbook of Behavioral Neuroscience: Bordeaux, France, 2016; Volume 24, pp. 803–819.
22. Omoruyi, S.I.; Ibrakaw, A.S.; Ekpo, O.E.; Boatwright, J.S.; Cupido, C.N.; Hussein, A.A. Neuroprotective activities of Crossyne flava bulbs and Amaryllidaceae alkaloids: Implications for Parkinson's disease. *Molecules* **2021**, *26*, 3990.
23. Tchegnitegni, B.T.; Lerata, M.S.; Beukes, D.R.; Antunes, E.M. Sutherlandiosides E−K: Further cycloartane glycosides from Sutherlandia frutescens. *Phytochem. Lett.* **2024**, *61*, 66–74.
24. Fu, X. Phytochemical Studies on the Medicinal Plant Sutherlandia Frutescens. Ph.D. Thesis, University of Mississippi, Oxford, MS, USA, 12 October 2012.
25. EL-Sebakhy, N.A.; Asaad, A.M.; Abdallah, R.M.; Toaima, S.M.; Abdel-Kader, M.S.; Stermitz, F.R. Antimicrobial isoflavans from Astragalus species. *Phytochemistry* **1994**, *36*, 1387–1389.
26. Kurosawa, K.; Ollis, W.D.; Suthwland, I.O.; Gorr, O.R.; De Oliveira, A.B. Mucroquinone and mucronucarpan, isoflavonoids from *Machaerium mucronulatum* and *M. villosum*. *Phytochemistry* **1978**, *17*, 1405–1411.
27. Meng, F.C.; Yuan, C.; Huang, X.J.; Wang, W.J.; Lin, L.G.; Zhang, X.T.; Jiao, H.-Y.; Zhang, Q.W. New cycloartane triterpene glycosides from Thalictrum ramosum. *Phytochem. Lett.* **2016**, *15*, 108–112.
28. Fu, X.; Li, X.C.; Smillie, T.J.; Carvalho, P.; Mabusela, W.; Syce, J.; Johnson, Q.; Folk, W.; Avery, M.A.; Khan, I.A. Cycloartane glycosides from Sutherlandia frutescens. *J. Nat. Prod.* **2008**, *71*, 1749–1753.
29. Vos, M. Mitochondrial Complex I deficiency: Guilty in Parkinson's disease. *Signal Transduct. Target. Ther.* **2022**, *7*, 136.

30. Choong, C.J.; Mochizuki, H. Involvement of Mitochondria in Parkinson's Disease. *Int. J. Mol. Sci.* **2023**, *24*, 17027.
31. Dionísio, P.A.; Amaral, J.D.; Rodrigues, C.M.P. Oxidative stress and regulated cell death in Parkinson's disease. *Ageing Res. Rev.* **2021**, *67*, 101263.
32. Pfab, A.; Belikov, S.; Keuper, M.; Jastroch, M.; Mannervik, M. Inhibition of mitochondrial transcription by the neurotoxin MPP^+. *Exp. Cell Res.* **2023**, *425*, 113536.
33. Li, H.; Zhang, J.; Shen, Y.; Ye, Y.; Jiang, Q.; Chen, L.; Sun, B.; Chen, Z.; Shen, L.; Fang, H.; et al. Targeting Mitochondrial Complex I Deficiency in MPP+/MPTP-induced Parkinson's Disease Cell Culture and Mouse Models by Transducing Yeast NDI1 Gene. *Biol. Proced. Online* **2024**, *26*, 9.
34. Moon, H.E.; Paek, S.H. Mitochondrial Dysfunction in Parkinson's Disease. *Exp. Neurobiol.* **2015**, *24*, 103–116.
35. Johnson, T.A.; Jinnah, H.; Kamatani, N. Shortage of cellular ATP as a cause of diseases and strategies to enhance ATP. *Front. Pharmacol.* **2019**, *10*, 98.
36. Pöltl, D.; Schildknecht, S.; Karreman, C.; Leist, M. Uncoupling of ATP-depletion and cell death in human dopaminergic neurons. *Neurotoxicology* **2012**, *33*, 769–779.
37. Qi, H.; Shen, D.; Jiang, C.; Wang, H.; Chang, M. Ursodeoxycholic acid protects dopaminergic neurons from oxidative stress via regulating mitochondrial function, autophagy, and apoptosis in MPTP/MPP+-induced Parkinson's disease. *Neurosci. Lett.* **2021**, *741*, 135493.
38. Svandova, E.; Lesot, H.; Sharpe, P.; Matalova, E. Making the head: Caspases in life and death. *Front. Cell Dev. Biol.* **2023**, *10*, 1075751.
39. Svandova, E.; Vesela, B.; Janeckova, E.; Chai, Y.; Matalova, E. Exploring caspase functions in mouse models. *Apoptosis* **2024**, *29*, 938–966.
40. Prommahom, A.; Dharmasaroja, P. Effects of eEF1A2 knockdown on autophagy in an MPP+-induced cellular model of Parkinson's disease. *Neurosci. Res.* **2021**, *164*, 55–69.
41. Li, Q.; Zhang, P.; Cai, Y. Genkwanin suppresses MPP^+-induced cytotoxicity by inhibiting TLR4/MyD88/NLRP3 inflammasome pathway in a cellular model of Parkinson's disease. *Neurotoxicology* **2021**, *87*, 62–69.
42. Mcilwain, D.R.; Berger, T.; Mak, T.W. Caspase functions in cell death and disease. *Cold Spring Harb. Perspect. Biol.* **2013**, *5*, a008656.

CHAPTER SEVEN: Isolation of secondary metabolites from *Protea venus* and evaluation of their antioxidant, cytotoxicity and cardioprotective activities

Kadidiatou O. Ndjoubi [1], Nonhlakanipho Sangweni [2], Rabia Johnson [2, 3], Fanie Rautenbach [4], Jeanine Marnewick [4] and Ahmed A. Hussein [1*]

[1] Chemistry Department, Cape Peninsula University of Technology, Symphony Rd. Bellville, Cape Town 7535, South Africa
[2] Biomedical Research and Innovation Platform (BRIP), South African Medical Research Council (SAMRC), Tygerberg, 7505, South Africa
[3] Division of Medical Physiology, Faculty of Health Sciences, Stellenbosch University, Tygerberg, South Africa
[4] Department of Biomedical Sciences and, Oxidative Stress Research Centre, Cape Peninsula University of Technology, South Africa
*Correspondence: mohammedam@cput.ac.za

Abstract

Protea venus, a hybrid of *Protea repens* and *Protea aristata*, is primarily valued as an ornamental plant and cut flower, with no prior studies investigating its phytochemical composition or biological effects. The phytochemical analysis of the methanolic extract led to the isolation of 11 compounds (**7.1**-**7.11**), including a novel metabolite, namely *p*-coumaroylcalleryanin (**7.1**). Among these compounds, **7.3**, **7.5**, **7.6**, and **7.9** exhibited significant antioxidant activity, with IC_{50} values of 0.018±1.11, 0.033±1.27, 0.048±0.53, and 0.018±0.39 mg/mL, respectively, outperforming vitamin E (IC_{50}= 0.152±0.67 mg/mL). Additionally, in the FRAP assay, compound **7.9** demonstrated higher antioxidant capacity (6175.19±0.63 µmol AAE/g) compared to vitamin C (5743.56±0.27 µmol AAE/g).

Cytotoxicity assessments revealed that the isolated compounds and crude extract had minimal effects on H9c2, MCF-7, and C3A cell viability, with compounds **7.3** and **7.5** exhibiting only weak cytotoxic effects against MCF-7 breast cancer cells. The ATP levels in H9c2 cells were significantly reduced after exposure to high-glucose (40 mM) and palmitate (0.150 mM). However, treatment with the methanolic extract (*$p < 0.05$) and compound **7.6** (**$p < 0.01$) significantly increased ATP levels, suggesting potential cardioprotective effects.

These findings provide the first insight into the phytochemical components and bioactivity of the plant's secondary metabolites, revealing their promising antioxidant and moderate cardioprotective properties.

Keywords: *Protea venus,* Protea, antioxidant, phytochemical, cytotoxicity, cardioprotection

7.1 Introduction

Protea, a large genus of flowering plants commonly known as sugarbushes, consists of 136 species primarily indigenous to the African continent. Of these, 117 species are found in Africa,

with a significant concentration of 90 species in South Africa (Vogts, 1982; Robelo, 1995). The genus holds cultural significance as South Africa's national emblem. *Protea species* are renowned for their distinctive flower heads surrounded by conspicuous involucre of scales. These flowers are primarily of pink with occasional albino and red varieties, and more rarely greens (Werner, 1951).

One notable species is *Protea Venus*, a hybrid of *P. repens* and *P. aristate*. This evergreen shrub within the Proteaceae family typically grows to heights ranging from 1.5-3 m and spreads outwards from 1.5-2 m in width. Blooming from May to September, *P. venus* attracts numerous pollinators such as butterflies, bees, and birds. This woody shrub is cultivated specifically for global cut flower markets due to its showy red flowers adorned with contrasting feathery white edges made of numerous small florets densely packed in spherical to conical shapes. Unlike its parent plant *P. aristate*, *P. venus* does not emit an unpleasant sulfuric scent when its leaves and stems are picked, enhancing its marketability (Duncan et al., 2013). Its low maintenance nature further elevates its desirability, making it a popular choice for coastal areas and native gardens worldwide.

P. venus is native to the Cape Florist region, particularly the mountainous regions of South Africa, where it typically grows in well-drained acidic soils. It is often found in fynbos vegetation, characterised by diverse shrubs and heathland plants adapted to a Mediterranean climate with hot summers and wet winters (Leonhardt & Criley, 1999).

Recently, there has been growing interest in the phytochemical and biological properties of *Protea* species. Some isolated secondary metabolites from species such as *P. cynaroides*, *P. sussara*, *P. elliotii*, *P. caffra*, *P. madiensis*, *P. nerifolia*, and *P. lacticolor* have shown promising antioxidant, anti-inflammatory, antibacterial, and anti-tyrosinase properties. Despite these findings, many *Protea* species, including *P. venus*, remain underexplored.

This research study aims to extract, isolate, and characterise the secondary metabolites of *P. venus* and evaluate their cytotoxicity effects against MCF-7, H9c2, and C3A cell lines. The isolated compounds and crude extract were assessed for their cardioprotective potential against H9c2 cells-induced high glucose and palmitate stress.

7.2 Methodology

7.2.1 Extraction

The fresh leaves of *P. venus* were first cut into pieces and ground. The ground material was then subjected to maceration in methanol for 24 h at room temperature. After maceration, the mixture was filtered using Whatman filter paper in a Buckner funnel to remove any solid particles. This maceration and filtration process was done twice, and the resulting filtrates were combined. The combined filtrates were then concentrated to dryness using Buchi Rotavapor R-300 at 45 ℃ and 14 mbar, resulting in the obtention of a dark green extract weighing 70 g. The extract was carefully stored in airtight sample vials until further analysis.

7.2.2 Isolation

The fractionation of the methanolic crude extract (70 g) yielded 15 fractions (Ip-XVp). Through TLC analysis, fractions exhibiting similar characteristics were combined and weighed. Fractions with similar retention factor values were combined and further purified except for fractions Ip to IVp, which primarily contained fatty acids and chlorophyll components.

7.2.2.1 Processing of fractions VIp-VIIIp and isolation of compounds 7.1-7.7 and 7.9-7.11

Fractions VIp to VIIIp (12.5872 g) were combined and produced crystalline solid precipitates separated from its surfactant. The surfactant was concentrated (8.6615 g) and subjected to sequential isocratic column chromatography using ethyl acetate (95%) and methanol (5%), followed by semi-preparative HPLC. This resulted in the isolation of ten compounds **7.2** (3.1 mg, R_t 18.2 min), **7.9** (4.8 mg, R_t 22 min) and **7.10** (3.2 mg, R_t 24.4 min), **7.1** (3.5 mg, R_t 30 min), **7.4** (36.3 mg, R_t 31.5 min), **7.3** (24.4 mg, R_t 38.5 min), **7.6** (9.5 mg, R_t 40.5 min), **7.7** (3.1 mg, R_t 41.5 min). At last, the crystalline solid precipitate was found to be the pure compound **7.5** (2.1778 g).

7.2.2.2 Processing of fraction XIp and isolation of compound 7.11

Fraction XIp (20.7997 g) produced a white crystalline precipitate that was separated from its surfactants. The white crystal was identified and characterised as the pure compound **7.11** (5.85 g). Moreover, the surfactant was found to have compounds similar to fractions VIp- VIIIp.

7.2.2.3 Processing of fraction XIIIp and isolation of compounds 7.8

Fraction XIIIp (100 mg) was subjected to sequential sephadex LH-20 column chromatographic with 80% aqueous methanol resulting in the isolation of compound **7.8** (3.3 mg).

7.2.3 Cell culture

7.2.3.1 Cytotoxicity

C3A liver cells were cultured in Minimum Essential Medium (MEM) with Earle's Salts, without *L*-Glutamine supplemented with 10% fetal bovine serum (FBS) and 1% *L*-glutamine at 37 ^{o}C, 5% CO_2 (standard tissue culture conditions). Cells were then seeded into a 96-well clear plate with a seeding density of 4.4 x 10^4 cells/well. Once cell confluency of 80% was reached, cells were treated with *P. venus* isolated compounds and crude extract diluted in complete growth media at concentrations of 0.01, 0.1, 1, 10 and 100 μg/mL for 24 h.

MCF-7 human breast cancer cells and H9c2 cardiomyoblasts were cultured in Dulbecco's Modified Eagle's Medium (DMEM) supplemented with 10% FBS under standard tissue culture conditions (37^{o}C, 5% CO_2 and humidified air). Cells were then seeded into a 96-well clear plate with a seeding density of 0.8 x 10^5 cells/well and then treated with the isolated compounds diluted in complete growth media at a concentration of 0.01, 0.1, 1, 10 and 100 μg/mL for 24 h.

7.2.3.2 Cardiotoxicity

Rat heart-derived myoblasts (H9c2) were cultured in DMEM with 10% FBS under standard tissue culture conditions (37°C in humidified air and 5% CO2). Cells were seeded into a white-walled 96-well plate with a seeding density of 0.8 x 10^5 cells/well. Upon reaching 80% confluency cells, the hyperglycaemia and hyperlipidaemia phenotype (DCM) were induced by exposing cells to high glucose (40 mM) and 0.15 mM palmitate for 24 h. Cells exposed to normal (25 mM) glucose were used as control. Afterwards, the cells were treated with *P. venus* compounds and crude extract diluted in high glucose media at 10 μg/mL for 24 h.

7.2.4 Cell viability

After treatment with *P. venus* compounds and extract, the cell viability was measured using MTT and ATP assays

7.2.5 Statistical analysis

To remove any experimental bias, 3 independent biological experiments were conducted (each biological had 3 technical replicates). A one-way ANOVA with Dunnett's multiple comparisons and a t-test with Mann-Whitney's test were assessed to identify statistical significance using GraphPad Prism version 9.5.

7.3 Results

7.3.1 Purification of *P. venus* secondary metabolites

The phytochemical analysis of the methanolic leaf extracts of *P. venus* resulted in the isolation of twelve (**7.1**-**7.11**) distinct compounds (Figure 7.1). Notably, compound **7.1**, which is a derivative of calleryanin, has been identified and isolated for the first time. Compounds **7.2**, **7.3**, **7.6**, and **7.7** are being reported here for the first time from the genus *Protea.*

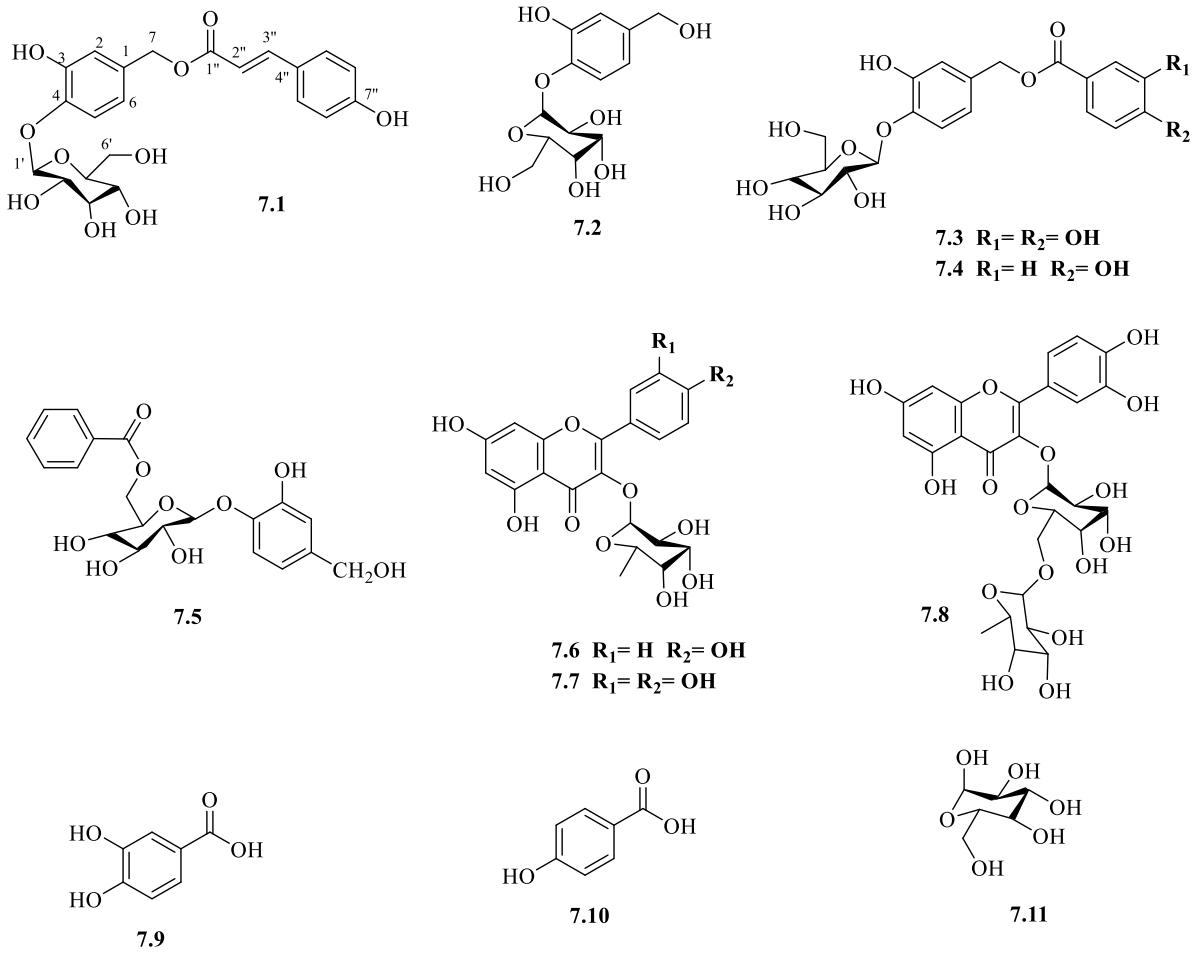

Figure 7.1: *Protea venus* isolated compounds (**7.1**-**7.11**)

Detailed ^{1}H and ^{13}C NMR data of compounds **7.1**-**7.5** and **7.6**-**7.11** are presented in Tables 7.1 and 7.2, respectively.

Table 7.1: ^{1}H and ^{13}C NMR of compounds **7.1**-**7.5**

	7.1		**7.2**		**7.3**		**7.4**		**7.5**	
No	**^{13}C**	**^{1}H, *muti.* (*J*= Hz)**	**^{13}C**	**^{1}H, *muti.* (*J*= Hz)**	**^{13}C**	**^{1}H, *muti.* (*J*= Hz)**	**^{13}C**	**^{1}H, *muti.* (*J*= Hz)**	**^{13}C**	**^{1}H, *muti.* (*J*= Hz)**
1	131.7		146.9		131.3		131.3		100.6	5.02, d (7.9)
2	115.7	6.89, s	144.9		116.2	6.88, s	116.2	6.89, s	72.2	4.07, t (8.2)
3	147.0		114.6	6.86, s	145.8		145.9		68.1	3.57. d (7.7)
4	145.5		137.1		147.1		147.2		70.7	3.57, d (7.7)
5	117.1	7.19, d (8.2)	117.1	7.17, d (8.0)	116.8	7.11, d (8.0)	117.1	7.11, d (8.4)	71.5	4.02, s
6	119.6	6.83, d (8.4)	118.1	6.78, d (8.0)	119.7	6.82, d (8.0)	119.7	6.81, s	66.2	4.61, d (11.4)
7	65.5	5,10, s,	63.4	4.48, s	65.9	5.13, s	65.9	5.16, s		
1′	100.6	5.16, d (8.4)	100.9	5.11, d (8.0)	100.5	5.00, d (7.9)	100.6	4.99, d (8.0)	166.1	
2′	74.5	3.8	74.6	3.80	75.4	3.60*	75.4	3.67*	130.2	
3′	67.1	3.59, d (2.3)	67.0	3.61	67.5	3.41, d (10.2)	67.5	3.45, m	129.7	8.02, d (7.5)
4′	70.8	3.61, d (2.3)	70.7	3.63	70.8	3.49, d (10.2)	70.8	3.45, m	129.2	7.57, t (7.9)
5′	71.4	4.15, brs	71.5	4.19, s	71.5	3.97, brs	71.5	3.95, s	133.9	7.69, t (7.9)
6′	61.3	3.85, d (12) 3.68, dd (6.3; 17.0)	61.3	3.86, d (10.8) 3.70 dd (16.4; 7.5)	61.5	3.68, t (13.0; 7.5) 3.47	61.5	3.67* 3.45, m	129.2	7.57, t (7.9)
7′									129.7	8.02, d (7.5)
1′′	167.64				166.0		165.9		144.5	
2′′	132.2	7.54, d (9.1)			121.0		120.6		146.9	
3′′	145.4	7.64, d (15.7)			116.7	7.37, s	132.0	7.82, d (8,4	117.6	6.76, s
4′′	125.8				145.5		115.9	6.85, d (10.1)	137.7	
5′′	129.8	7.46, d (8.2)			151.0		162.7		116.3	7.02, d (8.2)
6′′	115.4	6.79, d (8.6)			115.9	6.82, d (8.0)	115.9	6.85, d (10.1)	114.7	6.51, d (8.2)
7′′	159.9				122.4	7.34, d (8.3)	132.0	7.82, d (8.4)	63.00	4.33, s
8′′	115.4	6.79 d (8.6)								
9′′	129.8	7.46, d (8.2)								

***** Overlapping peaks

Table 7.2: ^{1}H and ^{13}C NMR of compounds **7.6-7.11**

	7.6		**7.7**		**7.8**		**7.9**		**7.10**		**7.11**	
No	**^{13}C**	**^{1}H, *muti.* (*J*= Hz)**	**^{13}C**	**^{1}H, *muti.* (*J*= Hz)**	**^{13}C**	**^{1}H, *muti.* (*J*= Hz)**	**^{13}C**	**^{1}H, *muti.* (*J*= Hz)**	**^{13}C**	**^{1}H, *muti.* (*J*= Hz)**	**^{13}C**	**^{1}H, *muti.* (*J*= Hz)**
1							121.8		122.0		82.0	4.92, d (11.8)
2	148.4		157.9		159.9		116.4	7.44, s	131.6	7.87, d (7.2)	78.9	3.41, d (7.5)
3	134,8		134.8		133.7		144.9		114.6	7.82, d (7.2)	69.9	3.11, t (7.5)
4	178.2		178.2		177.7		150.1		161.8		70.3	3.26, m
5	157.2		157.2		157.0		114.7	6.81, d (8.0)	114.6	7.82, d (7.2)	70.7	3.02, m
6	98.5	6.19, s	98.5	6,20, s	99.2	6.12, s	122.9	7.44, d (8.0)	131.6	7.87, d (7.2)	61.9	3.67, d (11.8) 3.74, dd (16.1; 7.5)
7	164.9		164.5		164.8		169.1		169.0			
8	93.3	6.36, s	93.4	6.38, s	94.1	6.32, s						
9	161.9		161.5		161.6							
10	104.5		104.5		104.3							
1´	121.6		121.2		121.5							
2´	115.5	7.33, s	130.5	7.78, d (8.8)	122.0	7.48, s						
3´	145.0		115.1	6.94, d (8.8)	115.7	6.78, d (7.8)						
4´	157.9		160.2		145.2							
5´	115.0	6.90, d (8.8)	115.1	6.94, d (8.8)	149.1							
6´	121.5	7.30, d (8.8)	130.5	7.78, d (8.8)	116.7	7.46, s						
1´´	102.1	5.34, s	102.1	5.37, s	101.7	5.27, d (6.2)						
2´´	70.6	4.2 s	70.6	4.2 s	74.5	3.15*						
3´´	70.7	3.76, dd (2.8; 12.4)	70.7	3.70, d (5.7)	71.0	3.21*						
4´´	71.9	3.32*	71.8	3.32*	70.4	3.00, t*(9.3)						
5´´	70.5	3.41*	70.5	3.34*	76.3	3.15*						
6´´	16.2	0.92, d (6.0)	16.3	0.92, d (3.2)	67.4	3.64, d (12.2)						
1´´´					101.2	4.31, s						
2´´´					70.8	3.33*						
3´´´					71.0	3.21*						
4´´´					72.3	3.00, t* (9.3)						
5´´´					68.7	3.20*						
6´´´					18.2	0.93, d (6.1)						

* Overlapping peaks

7.3.2 Antioxidant activity of *P. Venus* crude extract and isolated compounds

The antioxidant activities of the crude extract and isolated compounds (**7.3**-**7.6**, and **7.9**) were assessed using two assays: Ferric Ion Reducing Antioxidant Power (FRAP) and Trolox Equivalent Absorbance Capacity (TEAC), as presented in Table 7.3. These assays provide insight into the antioxidant potential of each compound, which was selected based on their quantities (more than 3.5 mg).

Table 7.3: Antioxidant activities of the crude extract and isolated compounds

	FRAP (µmol AAE/g)	**TEAC (µmol TE/g)**	**TEAC (IC_{50} - mg/mL)**
Extract	1720.57±0.34	1207.19±0.73	0.042±0.07
7.3	4192.87±1.50	2420.92±0.06	0.018±1.11
7.4	1420.77±0.47	2165.57±0.42	0.124±2.03
7.5	1602.96±0.93	2380.98±0.38	0.033±1.27
7.6	1748.73±0.12	2418.98±0.16	0.048±0.53
7.9	6175.19±0.63	2419.89±0.08	0.018±0.39
Controls	5743.56±0.27 (vitamin C)	4010.17±0.21 (vitamin E)	0.152±0.67 (vitamin E)

7.3.3 Cytotoxicity assessment of *P. venus* crude extract and isolated compounds in C3A, MCF-7, and H9c2 cell lines

The crude extract, as well as compounds **7.3**-**7.6** and **7.9**, were investigated for their cytotoxic potential against C3A (Human liver cell line), MCF-7 (Human breast cancer cell line) and H9c2 (Rat cardiomyoblast cell line) cells. In contrast, compounds **7.1**, **7.2**, **7.7**, **7.8**, and **7.10** were not assessed due to their small quantities. The percentage of cell viability after treatment is illustrated in Figures 7.2, 7.3 and 7.4. The Data were normalised to the vehicle control (0.53% DMSO) labelled ‘control’ in the data below.

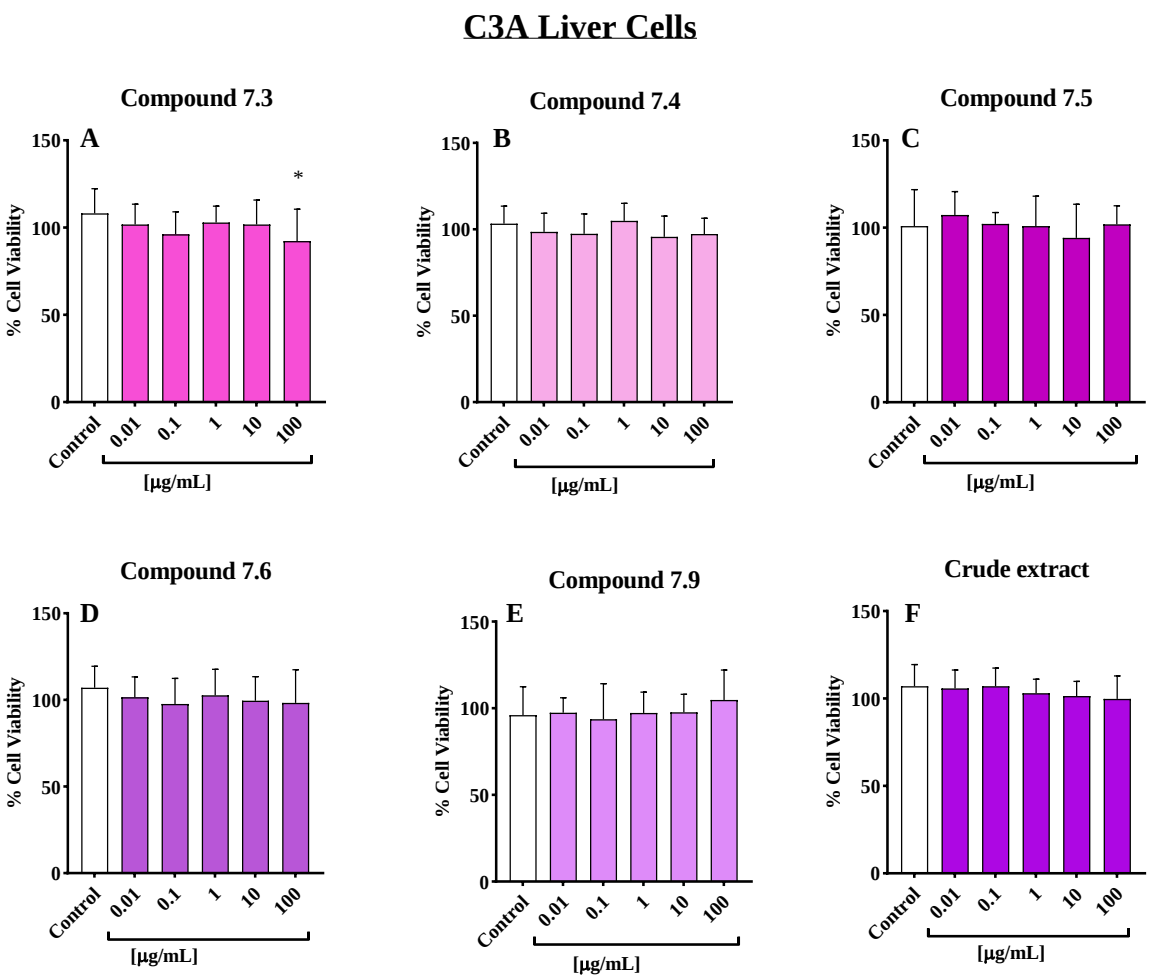

Figure 7.2: Cell viability assessment using the MTT assay. C3A liver cells were treated for 24 h with *P. venus* isolated compounds and crude extract. Data presented as mean ± SD, n = 3. Control = 0.53% DMSO. Significance is indicated as *p < 0.05 compared to the control.

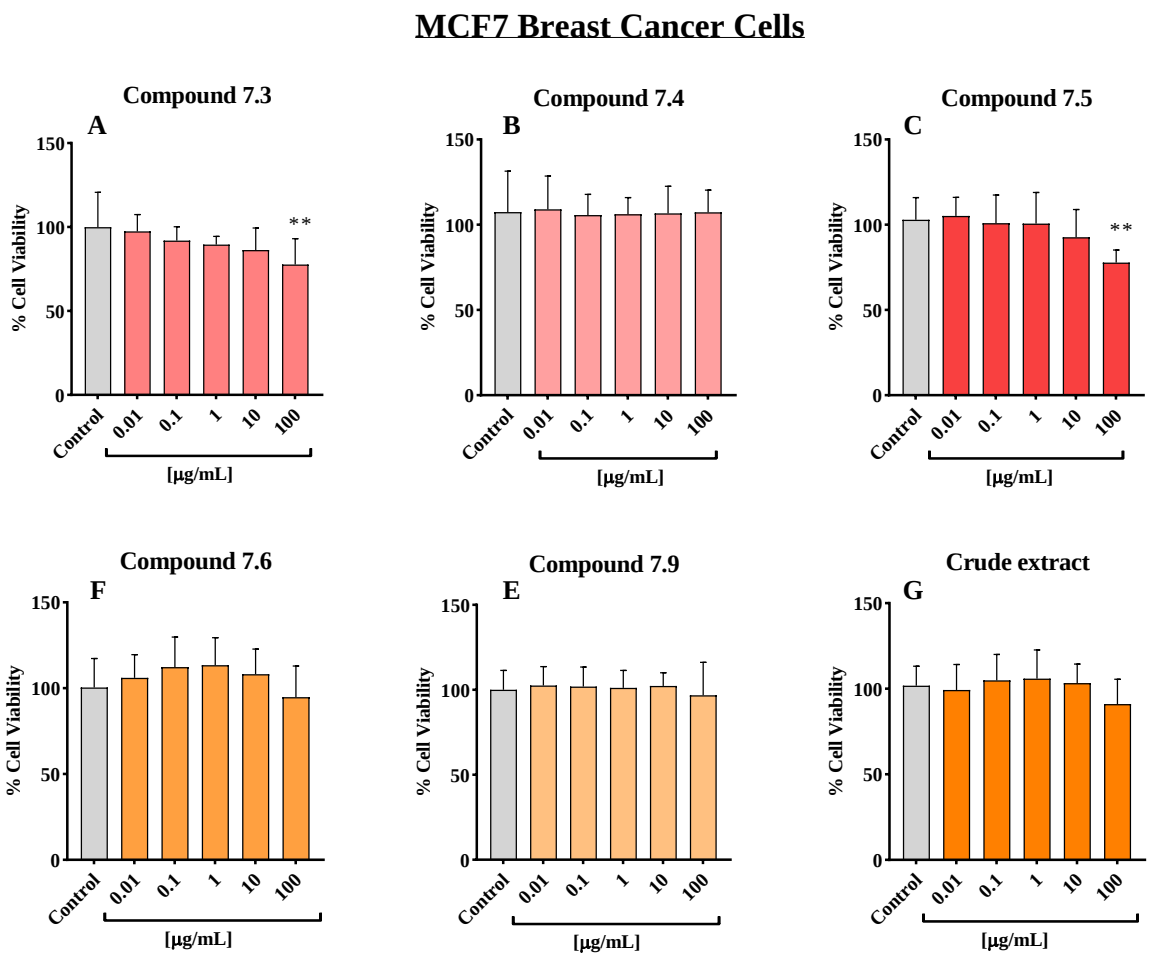

Figure 7.3: Cell viability assessment using the MTT assay. MCF7 breast cancer cells were treated for 24 h with *P. venus* isolated compounds and crude extract. Data presented as mean ± SD, n = 3. Control = 0.53% DMSO. Significance is indicated as *p < 0.05 and **p < 0.01 compared to the control.

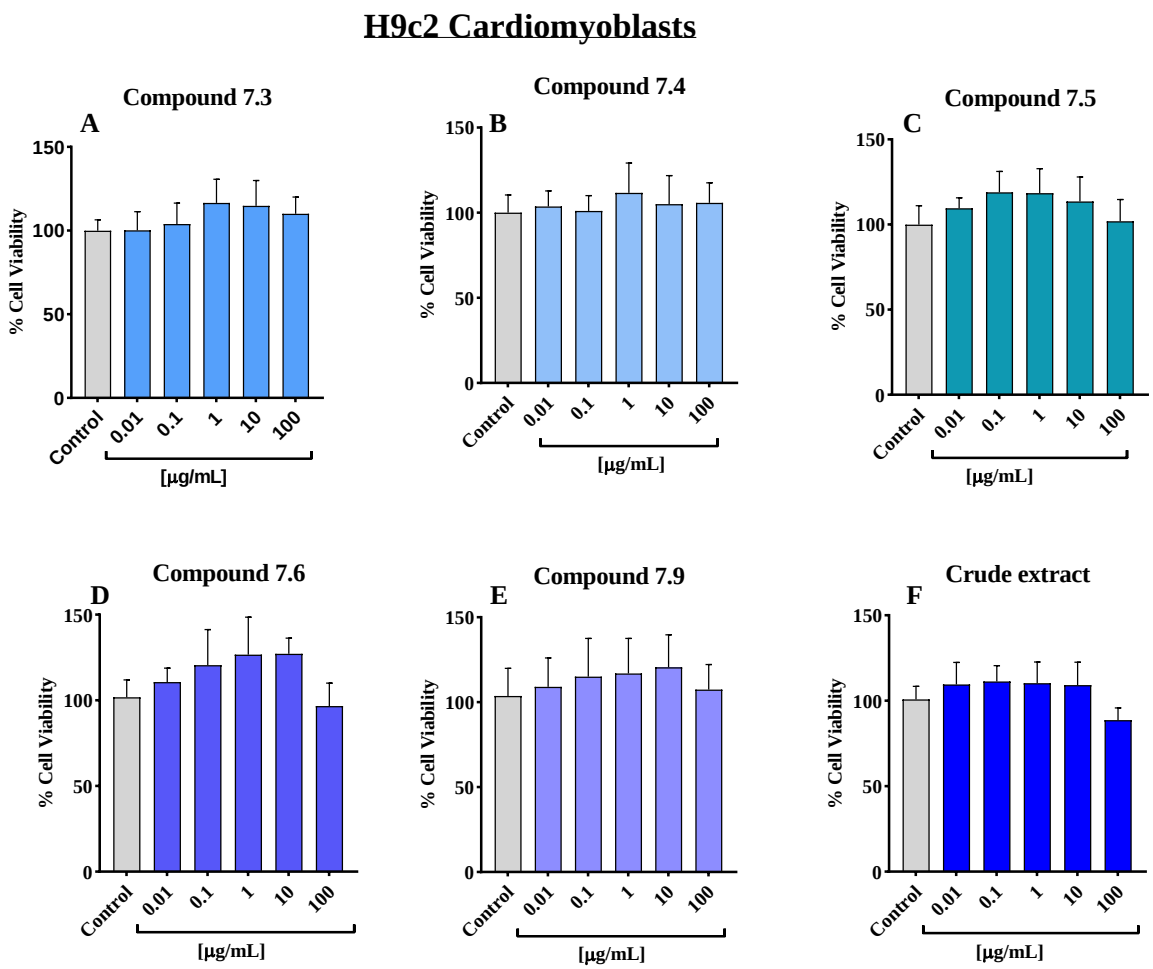

Figure 7.4: Cell viability assessment using the MTT assay. H9c2 cardiomyoblasts were treated for 24 h with *P. venus* isolated compounds and crude extract. Data presented as mean ± SD, n = 3. Control = 0.53% DMSO.

7.3.4 Effects of *P. venus* isolated compounds and crude extract on ATP Production in H9c2 cells exposed to high glucose and palmitate

The cardioprotective potential of selected compounds (**7.3-7.6** and **7.9**), along with the crude extract, was evaluated against H9c2 induced high glucose (HG) and palmitate (Pal) stress at a concentration of 10 µg/mL. The Data were normalised to the control as shown in Figure 7.5. The results showed a significant reduction in ATP production to 53%, but treatment with the extract and compound **7.6** increased ATP production to 70 and 73%, respectively.

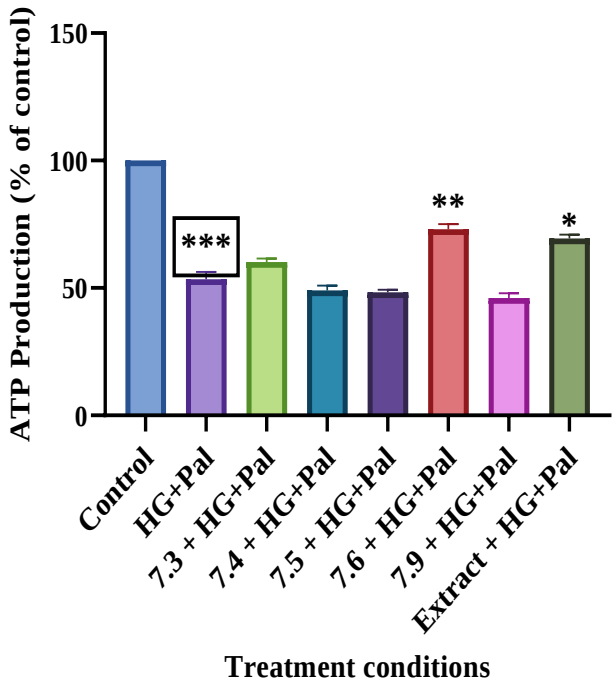

Figure 7.5: Impact of *P. venus* compounds on ATP production. H9c2 cells were exposed to HG and Pal for 24 h, followed by treatment with 10 µg/mL of each tested compound for an additional 24 h. ATP levels were then assessed using luminescence-based assays. Luminescence values were presented as a percentage of the control. Data represent means ± SEM of three independent experiments. Statistical significance is indicated as follows: * $p < 0.05$, **$p < 0.01$ and *** $p < 0.001$, comparing treated cells to the insult HG+Pal. Boxed asterisks represent the significance difference between HG+Pal and control cells

7.4 Discussion

7.4.1 Structure elucidation of isolated compounds

The following lines will provide an in-depth discussion of the structural elucidation of compounds **7.1-7.11.**

7.4.1.1 *p*-coumaroylcalleryanin (7.1)

Compound **7.1** HR-ESIMS exhibited a molecular ion peak of 448.4233 *m/z* corresponding to a molecular formula of $C_{22}H_{24}O_{10}$. The IR absorptions display characteristic bands at 3452, 2925, 1643, 1432, and 1216 cm^{-1}, revealing the presence of OH, C-H, C=C, and C-O functional groups

The ^{1}H NMR spectrum displayed the presence of an anomeric proton at δ_H 5.16 (*d*, *J*= 8.4 Hz, H-1´) and a cluster of hydroxymethine groups in the sugar region ranging from δ_H 3.59-4.15 which are characteristics of a *β-D*-glucopyranosyl moiety. Seven distinctive aromatic protons

peaks were observed at δ_H 6.89 (*s*, H-2), 7.19 (*d*, *J*= 8.2 Hz, H-5), 6.83 (*d*, *J*= 8.2 Hz, H-6), 7.46 (*d*, *J*= 8.2 Hz, H-5´´ and H-9´´), and 6.79 (*d*, *J*= 8.6 H-6´´ and H-8´´). Moreover, two olefinic protons peaks at δ_H 6.36 (*d*, *J*= 16.0 Hz, H-2´´) and 7.64 (*d*, *J*= 16.0 Hz, H-3´´) with vicinal coupling constants of 16.0 Hz, typical of a trans-orientated double bond was detected. A methylene unit at δ_H 5.10 (*s*, H-7) was observed in the downfield region.

The ^{13}C NMR spectrum displayed 22 distinctive signals consisting of a carbonyl unit at δ_C 167.6 (C-1´´); fourteen methine groups at δ_C 115.7 (C-2), 117.1 (C-5), 119.6 (C-6), 113.7 (C-2´´), 145.4 (C-3´´), 129.8 (C-5´´ and C-9´´), 115.4 (C-6´´ and C-8´´), 100.6 (C-1´), 74.5 (C-2´), 71.4 (C-3´), 67.1 (C-4´), and 70.8 (C-5´); two methylene groups at δ_C 65.5 (C-7), and 61.3 (C-6´), as well as five quaternary carbons at δ_C 131.7 (C-1), 147.0 (C-3), 145.5 (C-4), 125.8 (C-4´´), and 159.9 (C-7´´).

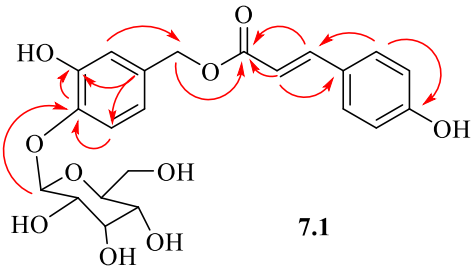

7.1

HMBC correlations of compound **7.1**

The HMBC spectrum revealed that the anomeric proton H-1´ correlated with C-4, indicating that the *β-D*-glucopyranosyl moiety is attached to ring A at position 4. The ^{1}H-^{1}H COSY spectrum showed connections between H-2, H-5, and H-6, confirming that ring A is a trisubstituted benzene ring. Furthermore, the HMBC spectrum demonstrated that the aromatic protons H-2 and H-6 correlated with C-1, C-3 and C-4, identifying the aglycone as 3,4-dihydroxybenzyl alcohol 4-O-β-D-monoglucopyranoside, commonly known as calleryanin (Challice et al., 1968).

The chemical shifts of C-5´´, C-6´´, C-8´´, and C-9´´ suggested the presence of a *p*-benzene ring. This was further supported by HMBC correlations between H-5´´, H-9´´, C-5´´, and C-9´´. Peaks associated with the *p*-benzene ring also correlated with H-2´´, H-3´´, C-7, C-1´´, and C-4´´, confirming the presence of a *p*-coumaryol moiety.

The oxymethylene proton (H-7) correlated with C-1, C-2, and C-6, indicating that the *p*-coumaryol unit is attached to C-1. Together, these findings confirm that compound **7.1** is a benzylic ester of calleryanin, characterised as *p*-coumaroylcalleryanin.

7.4.1.2 Calleryanin (7.2)

Compound **7.2,** ^{1}H NMR signals showed an anomeric proton at δ_H 5.11 (*d*, *J*= 8.0 Hz, H-1´) and five oxygenated methine groups at δ_H 3.80 (H-2´), 3.61 (H-3´), 3.63 (H-4´) and 4.19 (*s*, H-5´). Furthermore, two oxygenated methylene groups at δ_H 4.48 (*s*, H-7), 3.86 (*d*, *J*= 10.8 Hz, H-6α´) and 3.70 (*dd*, *J*= 16.4; 7.5 Hz, H-6β´) as well as three aromatic proton resonances at 6.86 (*s*, H-3), 7.17 (*d*, *J*= 8.0 Hz, H-5), and 6.78 (*d*, *J*= 8.0 Hz, H-6).

The ^{13}C NMR spectrum displayed thirteen peaks consisting of three quaternary at δ_C 146.9 (C-1), 144.9 (C-2), and 137.1 (C-4); two methylene groups at δ_C 63.4 (C-7) and 61.3 (C-6´); as well as eight methine groups at δ_C 114.6 (C-3), 117.1 (C-5), 118.1 (C-6), 100.9 (C-1´), 74.6 (C-2´), 67.0 (C-3´), 70.7 (C-4´), and 71.5 (C-5´).

Based on these NMR signals, compound **7.2** was characterised as calleryanin, a compound previously isolated from *Pyrus calleryana* (Challice et al., 1968).

7.4.1.3 Protocatechuoylcalleryanin (7.3)

The ^{1}H-^{1}H COSY spectrum showed the correlation between H-2, H-5 and H-6 as well as connections between H-3´, H-6´´ and H-7´´. Additionally, the HMBC spectrum revealed that H-3´´ correlate with C-1´´, C-2´´, C-4´´, C-5´´ and C-7´´. Meanwhile, H-2 correlates with C-1, C-3, C-4, C-6 and C-7, confirming that rings A and B are trisubstituted benzene rings. The chemical shifts of C-1 to C-7 closely resemble those of the aglycone calleryanin, while the chemical shifts of C-1´ to C-7´ are consistent with a protocatechuoyl moiety. These chemical shifts are similar to those observed for compound **7.1**, except that compound **7.3** has a protocatechuoyl group attached to the aglycone instead of a *p*-coumaroyl group at C-1. Based on the NMR data, compound **7.3** is characterised as protocatechuoylcalleryanin, a compound previously identified from *Pyrus calleryana* (Challice et al., 1968).

7.4.1.4 *p*-hydroxybenzoylcalleryanin (7.4)

The ^{1}H-^{1}H COSY spectrum showed correlations between H-3´´/H-7´´ and H-4´´/H-6´´, which were connected to C-3´´/C-7´´and C-4´´/C-6´´, respectively. This revealed that the mono-oxygenated quaternary carbon C-3´´ in compound **7.3** has been reduced to an aromatic carbon in compound **7.4** due to the absence of a hydroxyl group at C-3´´. This confirms that compound **7.4** possesses a *p*-hydroxybenzoyl moiety attached to the aglycon at C-1. Consequently,

compound **7.4** is *p*-hydroxybenzoylcalleryanin, a compound previously identified from *Pyrus calleryana* (Challice et al., 1968).

7.4.1.5 Lacticolorin (7.5)

The ^{1}H NMR signals of compound **6** displayed eight aromatic protons peaks at δ_H 8.02, (*d*, *J*= 7.5 Hz, H-3′ and H-7′), 7.57 (*t*, *J*= 7.9 Hz, H-4′ and H-6′), 7.69 (*t*, *J*= 7.9 Hz, H-5′), 6.76 (*s*, H-3′′), 7.02 (*d*, *J*= 8.2 Hz, H-5′′) and 6.51 (*d*, *J*= 8.2 Hz, H-6′′). An anomeric proton resonance at δ_H 5.02 (*d*, *J*= 7.9 Hz, H-1) and five oxygenated methine protons in the sugar region was detected at 4.07 (*t*, *J*= 8.2 Hz, H-2), 3.57 (*d*, *J*= 7.7 Hz, H-3), 3.57 (*d*, *J*= 7.7 Hz, H-4), and 4.02 (*s*, H-5). Two oxygenated methylene groups were observed at δ_H 4.33 (*s*, H-7′′) and 4.61 (*d*, *J*= 11.4 Hz, H-6).

The ^{13}C NMR spectrum displayed nineteen signals comprising a carbonyl at δ_C 166.1 (C-1′), four quaternary carbons at δ_C 130.2 (C-2′), 144.5 (C-1′′), 146.9 (C-2′′) and 137.7 (C4′′); two methylene at δ_C 66.2 (C-6) and 63.0 (C-7′′) as well as thirteen methine groups at δ_C 129.7 (C-3′ and C-7′), 129.2 (C-4′ and C-6′), 133.9 (C-5′), 117.6 (C-3′′), 116.3 (C-5′′), 114.7 (C-6′′), 100.6 (C-1), 72.2 (C-2), 68.1 (C-3), 70.7 (C-4), and 71.5 (C-5).

Compound **7.5** was characterised as lacticolorin, a compound previously isolated from *P. lacticolor* (Perold, 1973).

7.4.1.6 Kaempferol-3-O-rhamnoside (7.6)

The ^{1}H NMR spectrum of compound **7.6** showed a methyl group at δ_H 0.92 (*d*, *J*= 3.2 Hz, H-6′′); an anomeric proton at δ_H 5.37 (*s*, H-1′′); and four oxygenated methine groups at δ_H 4.2 (*s*, H-2′′), 3.70 (*d*, *J*= 5.7 Hz, H-3′′), 3.32 (H-4′′), and 3.34 (H-5′′) characteristic of α-*L*-rhamnopyranosyl moiety. Furthermore, the ^{1}H NMR spectrum also displayed six aromatic proton resonances at δ_H 6,20 (*s*, H-6), 6.38 (*s*, H-8), 7.78 (*d*, *J*= 8.8 Hz, H-2′ and H-6′), and 6.94 (*d*, *J*= 8.8 Hz, H-3′and H-5′) characteristic of a flavonoid skeleton.

The ^{13}C NMR spectrum displayed twenty-two signals consisting of a carbonyl group at δ_C 178.2 (C-4), eight quaternary carbons at δ_C 157.9 (C-2), 134.8 (C-3), 104.5 (C-10), 157.2 (C-5), 164.5 (C-7), 161.5 (C-9), 121.2 (C-1′), and 160.2 (C-4′); a methyl at δ_C 16.3 (C-6′′); as well as eleven methine groups at δ_C 98.5 (C-6), 93.4 (C-8), 130.5 (C-2′), 115.1 (C-3′), 115.1 (C-5′), 130.5 (C-6′), 102.1 (C-1′′), 70.6 (C-2′′), 70.7 (C-3′′), 71.8 (C-4′′), and 70.5 (C-5′′).

This compound is characterised as kaempferol-3-*O*-rhamnoside, a compound previously isolated from *Schima wallichii* (Diantini et al., 2012)

7.4.1.8 Quercetin-3-O-rhamnoside (7.7)

Compound **7.7** differs from compound **7.6** by the presence of an additional hydroxyl group at C-3. Based on the NMR data, compound **7.7** is characterised as quercetin-3-*O*-rhamnoside, a compound previously isolated from *Euphorbia hirta* (Gopi et al., 2016).

7.4.1.7 Rutin (7.8)

The ^{1}H NMR spectrum of compound **7.8** showed two anomeric protons at δ_H 5.27 (*d*, *J*= 6.2 Hz, H-1´´) and 4.31 (*s*, H-1´´´), along with a methylene at δ_H 3.64 (*d*, *J*= 12.2 Hz, H-6´´) and a methyl group at δ_H 0.93 (*d*, *J*= 6.1 Hz, H-6´´´), characteristic of a rutinose moiety. The HMBC spectrum confirmed the 1→6 linkage between the *β-D*-glucopyranosyl and *α-L*-rhamnopyranosyl units, with the disaccharide correlating to C-4 and C-2. This indicates that the rutinose moiety is attached to the aglycone quercetin at position 3. Additionally, compound **7.8** resembles compound **7.7,** differing only in the substitution of a rutinose moiety in place of the *α-L*-rhamnopyranosyl unit at position 3. Based on this, compound **7.8** is characterised as rutin, a compound previously isolated from *Hakea megadenia* (Zarfos et al., 2023).

7.4.1.9 3,4-dihydrobenzoic acid (7.9)

The ^{1}H NMR signals displayed three aromatic proton resonances at 7.44 (*s*, H-2), 6.81 (*d*, *J*= 8.0 Hz, H-5), and 7.44 (*d*, *J= 8.0* Hz, H-6).

The ^{13}C NMR spectrum displayed seven peaks consisting of four quaternary carbons at δ_C 169.1 (C-7), 121.8 (C-1), 144.9 (C-3) and 150.1 (C-4); as well as three methine groups at δ_C 116.4 (C-2), 114.7 (C-5), and 122.9 (C-6).

Compound **7.9** was characterised as 3,4-dihydrobenzoic acid, a phenolic compound isolated from *P. cynaroides* (Wu et al., 2007).

7.4.1.10 *p*-hydroxybenzoic acid (7.10)

Compound **7.10** resembles compound **7.9**, with the only difference being the absence of the hydroxyl group at position 3. Compound **7.9** is characterised as *p*-hydroxybenzoic acid, a phenolic compound previously isolated from *P. cynaroides* (Yalo et al., 2022).

7.4.1.11 *D*-Glucose (7.11)

Compound **7.11** ^{1}H NMR signals showed an anomeric proton at δ_H 4.92 (*d*, *J*= 11.8 Hz, H-1); five oxygenated methine groups at δ_H 3.26 (*m*, *J*= Hz, H-4), 3.02 (*m*, H-5), 3.11 (*t*, *J*=7.5 Hz, H-3) and 3.41 (*d*, *J*= 7.5 Hz, H-2); as well as an oxygenated methylene groups at δ_H 3.67 (*d*, *J*= 11.8 Hz, H-6α) and 3.74 (*dd*, *J*= 16.1; 7.5 Hz, H-6β).

The ^{13}C NMR spectrum displayed six peaks consisting of five methine groups at δ_C 82.0 (C-1), 78.9 (C-2), 70.7 (C-3), 70.3 (C-4), and 69.9 (C-5), as well as a methylene group at δ_C 61.9 (C-6).

Based on the NMR data, compound **7.11** is characterised as *D*-glucose, a compound previously isolated from *P. cynaroides* (Bieleski & Briggs, 2005).

7.4.2 Spectroscopy data

***p*-coumaroylcalleryanin** ($C_{22}H_{24}O_{10}$): yellowish solid, IR: 3452 cm^{-1} (OH), 2925 cm^{-1} (CH), 1643 cm^{-1} (C=O), 1432 cm^{-1} (C=C), 1216 cm^{-1} (C-O); HRESIMS: *m*/*z* 448.4233 $[M^+H]^+$ (calculated for $C_{22}H_{24}O_{10,}$ 448.4240); ^{1}H NMR (DMSO-$D_{6,}$) and ^{13}C NMR (DMSO-d_6): see Table 7.1

7.4.3 Total phenolic content and antioxidant potential of *P. venus* crude extract and compounds

The total phenolic content of the crude extract expressed as milligram gallic acid equivalents (GAE) per gram was found to be 199.05±1.64 mg GAE/g.

The FRAP assay was conducted based on Benzie and Strain's (1996) method, which expresses antioxidant activity in terms of µmol ascorbic acid equivalents per gram (µmol AAE/g). Vitamin C (5743.56±0.27 µmol AAE/g) was a control in this assay. Compounds **7.3** (4192.87±1.50 µmol AAE/g), and **7.9** (6175.19±0.63 µmol AAE/g) exhibited strong antioxidant potential, with compound **7.9** surpassing Vitamin C in antioxidant capacity. Compounds **7.4-7.6** and the crude extract showed weak antioxidant effects in the FRAP assay.

The TEAC assay used the Pellegrini et al. (1999) method, expressing antioxidant activity as µmol Trolox equivalents per gram (µmol TE/g). The tested compounds' inhibition concentration was also measured at 50% (IC_{50}). Vitamin E (4010.17±0.21 µmol TE/g; IC_{50}= 0.152±0.67) was used as a control. The crude extract (1207.19±0.73 µmol TE/g) exhibited a weak scavenging

power with an IC_{50} of 0.042±0.07 mg/mL. Compounds **7.3, 7.5, 7.6** and **7.9** exhibit strong radical scavenging potential with IC_{50} values of 0.018±1.11, 0.033±1.27, 0.048±0.53 and 0.018±0.391 mg/ml, respectively. In contrast, compound **7.4** demonstrates a moderate antioxidant effect, with an IC_{50} value of 0.124±2.03 mg/mL and a scavenging power of 2165.57±0.42 µmol TE/g.

Put together, compounds **7.3** and **7.9** also displayed significant antioxidant potential (FRAP). However, their ABTS radical scavenging power was moderate, indicating that these two compounds eliminate free radicals more in the single electron transfer (SET) than in the hydrogen electron transfer (HAT) mechanism of action. The crude extract and compounds **7.4-7.6** showed weak activities for FRAP and strong activities for TEAC, suggesting their preferred mechanism of action to reduce free radicals is through HAT. These results suggest that the isolated compounds may operate through SET or HAT, exhibiting varying efficacy levels across different radicals.

7.4.4 Interpretation of cytotoxic effects of the isolated compounds in C3A, MCF-7 and H9c2 cells.

The C3A liver cells were exposed to the isolated compounds and crude extract. After exposure, compound **7.3** at 100µg/mL was observed to have slightly affected the MTT activity (*$p < 0.05$, 92.26±18.30 vs control 108.2±14.10). According to López-García et al, (2014), percentages of cell viability above 80% are considered non-cytotoxic. This statement was based on the ISO 10993-5:2009, which describes in-vitro cytotoxicity testing. Therefore, compound **7.3** at 100 µg/mL is non-cytotoxic to the C3A liver cells.

MCF-7 cells growth significantly decreased when treated with compounds **7.3** and **7.5**, both at concentrations 100 µg/mL (**$p < 0.01$, 77.70±15.40 vs control 100.0±20.73 and 77.87±7.28 vs control 102.9±12.94, respectively). Based on the cytotoxicity ranges by López-García et al, (2014), compounds **7.3** and **7.5** have weak cytotoxic effects.

On the other hand, the tested secondary metabolites did not show any cytotoxicity on cultured H9c2 cardiomyoblasts after 24 h of treatment.

7.4.5 Cardioprotective potential of *P. venus* isolated compounds and crude extract

Diabetic cardiomyopathy (DCM) is a ventricular dysfunction observed in diabetic individuals. It is characterised by impaired myocardial structure and function, independent of coronary

artery disease or hypertension, and often culminates in heart failure (Duncan, 2011). A hallmark of DCM pathogenesis is mitochondrial dysfunction, where impaired ATP synthesis, oxidative stress, and mitochondrial uncoupling converge to exacerbate cardiac energy deficits and cellular damage (Gollmer et al., 2020). Addressing mitochondrial dysfunction is, therefore, a critical therapeutic strategy to mitigate the progression of DCM.

In this study, the DCM phenotype was modelled *in vitro* by exposing H9c2 cardiomyoblasts to high glucose (40 mM) and palmitate (0.15 mM), simulating the hyperglycemic and lipotoxic environment characteristic of diabetes. After 24 h of exposure, these conditions significantly reduced cell proliferation, reflecting the detrimental impact of glucolipotoxicity on cellular health.

ATP levels, a key indicator of mitochondrial function, were significantly diminished under high glucose and palmitate (HG+Pal) exposure. However, treatment with compound **7.6** (**$p < 0.01$) and the methanolic extract (*$p < 0.05$) restored ATP levels, demonstrating their potential to alleviate mitochondrial dysfunction. In contrast, other compounds showed negligible effect on ATP restoration, suggesting that compound **7.6** and the crude extract may mitigate the bioenergetic deficits induced by HG+Pal conditions.

The observed effects align with findings from previous studies. For example, Aodah et al. (2024) and Ferreira (2024) demonstrated that kaempferol-3-O-rhamnoside (**7.6**) enhances mitochondrial function by activating the AMPK pathway, which plays a critical role in regulating energy homeostasis, metabolic enzyme activity, and mitochondrial biogenesis.

These mechanisms likely strengthen the ability of compound **7.6** and the crude extract to restore ATP production under glucolipotoxic stress, enabling cells to maintain energy balance despite adverse conditions.

Additionally, compound **7.6** is also known to act as a NOS and NADPH oxidase inhibitor, in addition to its anti-inflammatory, anti-apoptotic, and anti-tumour properties, further explaining its ability to inhibit apoptotic pathways and thereby offering cardioprotection in the DCM model.

7.5 Conclusion

The isolation of 11 compounds, including a novel metabolite, highlights the richness of phenolic compounds in *P. venus* with potent free radical scavenging properties. The observed non-cytotoxic effects at 100 µg/mL and the increased ATP production under high-glucose and

palmitate stress in H9c2 cells further emphasise the cardioprotective potential of both *P. venus* extract and compound **7.6**.

Although restoring ATP levels is a key indicator of improved mitochondrial function, further research is required to determine whether these effects translate into functional benefits, such as improved cardiomyocyte contractility, reduced fibrosis, or decreased apoptosis. Exploring pathways such as AMPK activation and ROS modulation could provide valuable insights into the underlying mechanisms of their protective effects.

References

Aodah, A. H., Alkholifi, F. K., Alharthy, K. M., Devi, S., Foudah, A. I., Yusufoglu, H. S., & Alam, A. (2024). Effects of kaempherol-3-rhamnoside on metabolic enzymes and AMPK in the liver tissue of STZ-induced diabetes in mice. *Scientific Reports*, 14: 1-14.

Benzie, I. F. F. & Strain, J. J. (1996). Ferric reducing ability of plasma as measure of antioxidant power: The FRAP assay. *Analytical Biochemistry,* 238: 70-76.

Challice, J. S., Williams, A. H., & Ashton, L. (1968). compounds of the genus pyrus: the occurrence of flavones and phenolic acid derivatives of 3,4-dihydroxybenzyl alcohol 4-glucoside in *Pyrus calleryana*. *Phytochemistry*, 7: 119-130.

Diantini, A., Subarnas, A., Lestari, K., Halimah, E., Susilawati, Y., Supriyatna, Julaeha, E., Achmad, T. H., Suradji, E. W., Yamazaki, C., Kobayashi, K., Koyama, H. & Abdulah, R. (2012). Kaempferol-3-*O*-rhamnoside isolated from the leaves of *Schima wallichii* Korth. inhibits MCF-7 breast cancer cell proliferation through activation of the caspase cascade pathway. *Oncol Lett*., 3(5): 1069-1072.

Duncan, G., Brown, N. & Nurrish, L. (2013). *Grow proteas*. Kirstenbosch Gardening Series. South African National Biodiversity Institute: Cape Town.

Duncan, J. G. (2011). Mitochondrial dysfunction in diabetic cardiomyopathy. *Biochimica et Biophysica Acta,* 1813(2011): 1351-1359.

Ferreira, J. (2024). Kaempferol-3-rhamnoside can help treat diabetes in mice. *Lab Anim*, 53: 223.

Gollmer, J., Zirlik, A., & Bugger, H. (2020). Mitochondrial mechanisms in diabetic cardiomyopathy. *Diabetes and Metabolism Journal*, 44: 33-53.

Gopi, K., Anbarasu, K., Renu, K., Jayanthi, S., Vishwanath, B.S. & Jayaraman, G. (2016). Quercetin-3-*O*-rhamnoside from Euphorbia hirta protects against snake Venom induced toxicity. *Biochim Biophys Acta*, 1860(7): 1528-40.

Leonhardt, K. W. & Criley, R. A. (1999). Proteaceae floral crops: cultivar development and underexploited uses. In: Janick J (ed.). *Perspectives on new crops and new uses*. Alexandria, Virginia. ASHS Press: 410-430.

Pellegrini, N., Re, R., Yang, M. & Rice-Evans, C.A. (1999). Screening of dietary carotenoid rich fruit extracts for antioxidant activities applying ABTS radical cation decolorisation assay. *Methods in Enzymology*, 229: 379-389.

Perold, G. W., Beylis, P., & Howard, A. S. (1973). Metabolites of Proteaceae. Part Vl1.l Lacticolorin, a Phenolic Glucoside Ester, and Other Metabolites of Protea lacticolor Salisb. *Journal of the Chemical Society*, 638-643.

Rebelo, T. 1995. *Sasol proteas: a field guide to the proteas of Southern Africa*. Fernwood Press (Pty) Ltd. Pretoria, South Africa.

Vogts, M. M., Paterson-Jones, C. & Slingsby, P. (1982). *South Africa's' Proteaceae': know them and grow them*. Struik Publishers. Cape Town, South Africa

Werner, H. F. (1951). South African Proteaceae and their cultivation. *Journal of the Botanical Society of South Africa*, 36: 1-7.

Yalo, M., Makhaba, M., Hussein, A. A., Sharma, R., Koki, M., Nako, N. & Mabusela, W. T. (2022). Characterization of Four New Compounds from Protea cynaroides Leaves and Their Tyrosinase Inhibitory Potential. *Plants*, 1-12.

Zarfos, S. D., Deans, B. J., Ho, C. C., Jordan, G. J., Smith, J. A. & Bissember, A. C. (2023). Distinctive Arbutin-Containing Markers: Chemotaxonomic Significance and Insights into the Evolution of Proteaceae Phytochemistry. *Chemistry and Biodiversity*, *20*(11):1-10.

CHAPTER EIGHT: Phytochemical Profiling and Therapeutic Potential of *Leucadendron xanthoconus*

Kadidiatou O. Ndjoubi [1], Rabia Johnson [2, 3], Fanie Rautenbach [4], Jeanine Marnewick [4] and Ahmed A. Hussein [1*]

[1] Chemistry Department, Cape Peninsula University of Technology, Symphony Rd. Bellville, Cape Town 7535, South Africa
[2] Biomedical Research and Innovation Platform (BRIP), South African Medical Research Council (SAMRC), Tygerberg, 7505, South Africa
[3] Division of Medical Physiology, Faculty of Health Sciences, Stellenbosch University, Tygerberg, South Africa
[4] Department of Biomedical Sciences and, Oxidative Stress Research Centre, Cape Peninsula University of Technology, South Africa
*Correspondence: mohammedam@cput.ac.za

Abstract

The phytochemical analysis of the methanolic leaf extract of *Leucadendron xanthoconus* led to the isolation of seven compounds (**6.5**, **8.1**-**8.6**). Compounds **8.1** and **8.2** were identified as novel, marking new discoveries within this species. The remaining compounds are known, with compounds **6.5**, **8.5**, and **8.6** reported for the first time in any *Leucadendron* species. Compound **8.6** exhibited moderate antioxidant activity and weak cytotoxicity against H9c2 cells, with an IC_{50} value of 85.79±1.56 µM. However, none of the isolated compounds, including the extract, showed any cardioprotective effects. Similarly, compounds **6.5** and **8.3**, as well as the crude extract with a phenolic content of 183.21±3.28 mg GAE/g, demonstrated minimal antioxidant and cytotoxic effects.

This study represents the first phytochemical investigation of *L. xanthoconus*, providing new insights into its secondary metabolites while highlighting its limited bioactivity.

Keywords: *Leucadendron xanthoconus*, phytochemical, antioxidant, cytotoxicity

8.1 Introduction

Leucadendron xanthoconus, commonly known as the sickle-leaf conebush or blinkblaartolbos in Afrikaans, is a dense, single-stemmed, perennial shrub endemic to the Western Cape region of South Africa (SANBI, 2007). This ornamental species belongs to the genus *Leucadendron* within the Proteaceae family, a diverse group of plants that has received limited attention in both phytochemical and pharmacological research. Species of the Proteaceae family are known to biosynthesise an array of secondary metabolites, including arbutin derivatives, flavonoids, and other phenolic compounds. These metabolites have been reported to exhibit a range of bioactivities, such as antioxidant, antimicrobial, cytotoxic, and antitumor effects, contributing

to growing scientific interest in the family and its genera (Gadea et al., 2021; Ncube et al., 2021; Govender et al., 2016).

Despite the increasing attention toward the Proteaceae family, the genus *Leucadendron* remains one of its least-studied genera. Phytochemical investigations of *Leucadendron* species have been sporadic, with most conducted between 1938 and 1980 (Gadea et al., 2021; Zhang et al., 2023). These studies primarily reported the isolation of cyanogenic glycosides and bislactonic spiro compounds. However, these compounds have never been subjected to biological evaluation. Consequently, significant knowledge gaps persist regarding *Leucadendron* species' phytochemistry and potential therapeutic applications.

This study addresses this gap by isolating and characterising secondary metabolites from *L. xanthoconus* and evaluating their antioxidant, cytotoxicity and cardioprotective properties.

8.2 Methodology

8.2.1 Extraction

Fresh leaves of *L. xanthoconus* were cut into small pieces, ground, and macerated in methanol for 24 h at room temperature, then filtered. The extraction process was repeated twice. The combined filtrates were concentrated to dryness, yielding 18 g of a brownish extract.

8.2.2 Isolation

The fractionation of the methanolic crude extract (18 g) yielded 10 fractions (Ic-Xc). Through TLC analysis, fractions exhibiting similar characteristics were combined and weighed. Only fractions IIIc, Vc, VIc, and VIIIc underwent further purification.

8.2.2.1 Processing of fractions IIIc, and Vc, and isolation of compounds 8.1 and 8.3

Fraction IIIc (0.2709 mg) was subjected to sequential isocratic column chromatography using Hexane (85%) and ethyl acetate (15%), followed by semi-preparative HPLC. This resulted in the isolation of compound **8.1** (3.2 mg).

Fraction Vc (3.8147 g) produced a crystalline solid precipitate, which was separated from its surfactant. The crystalline precipitate was identified as compound **8.3 (**2.4368 g**)**.

8.2.2.1 Processing of fractions VIc and VIIIc and isolation of compounds 6.5, 8.2, and 8.4-8.6

Fraction VIc (1.9314 g) was subjected to sequential column chromatography using hexane: ethyl acetate to generate compound **8.5** (937 g)

Faction VIIIc (0.6954 g) was subjected to sequential sephadex LH-20, followed by semipreparative HPLC to yield compounds **8.2** (2.9 mg, R_t 36.63 min), **8.4** (3.4 mg, R_t 20.56 min), **6.5** (4.1 mg, R_t 23.76 min) and **8.6** (3.1 mg, R_t 40.20 min).

8.2.3 Bioassays

The antioxidant, cytotoxic and cardioprotective protocol is written in section 5.5

8.3 Results

8.3.1 Purification of *L. xanthoconus* isolated compounds

The phytochemical analysis of the methanolic leaf extracts of *L. xanthoconus* led to the isolation of 7 compounds (**6.5**, **8.1-8.6**), as shown in Figure 8.1.

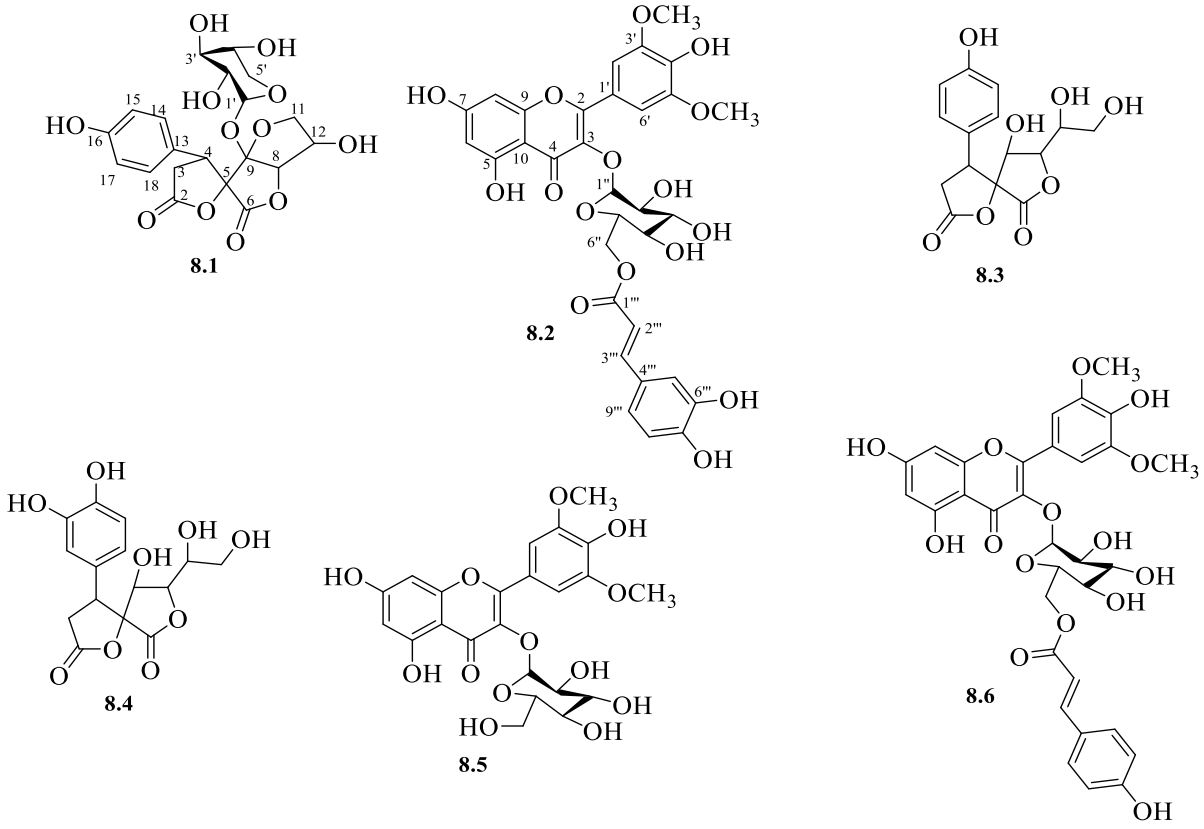

Figure 8.1: *L. xanthoconus* isolated compounds (**8.1-8.6**)

The ^{1}H and ^{13}C NMR data of compounds **8.1**-**8.6** is tabulated in Table 8.1

Table 8.1: ^{1}H and ^{13}C NMR of compounds **8.1**-**8.6**

	8.1		**8.2**		**8.3**		**8.4**		**8.5**		**8.6**	
Nº	**^{13}C**	**^{1}H, *muti.* (*J*= Hz)**	**^{13}C**	**^{1}H, *muti.* (*J*= Hz)**	**^{13}C**	**^{1}H, *muti.* (*J*= Hz)**	**^{13}C**	**^{1}H, *muti.* (*J*= Hz)**	**^{13}C**	**^{1}H, *muti.* (*J*= Hz)**	**^{13}C**	**^{1}H, *muti.* (*J*= Hz)**
2	174.4		159.9		175.1		175.2		156.8		156.9	
3	33.2	2.90, dd (8.8; 17.1) 3.09, d (5.0)	133.7		33.6	2.94, dd (9.1; 17.7) 3.15*	33.6	2.80, dd (8.7; 17.1) 3.15, dd (12.7; 17.1)	133.8		133.7	
4	43.3	4.59, d (2.7)	177.6		41.4	4.28, q (9.1)	41.8	4.30, dd (8.8; 12.9)	177.8		177.6	
5	89.5		161.6		90.4		90.3		161.7		161.5	
6	170.9		99.6	6.14, d (1.5)	172.4		172.3		99.2	6.21, d (1.8)	99.6	6.07, d (2.1)
7			165.8						164.6		166.7	
8	88.2	4.01, s	94.6	6.40, d (1.5)	80.2	3.71, dd (1.3; 8.7)	80.2	3.78, dd (2.2; 8.8)	94.3	6.50, d (1.8)	94.5	6.33, d (2.1)
9	107.7		156.4		69.6	4.66, d (4.7)	69.8	4.75, d (8.8)	156.7		156.4	
10			103.9		68.4	3.51, q (7.5)	68.9	3.66, dt (2.4; 7.0)	104.5		103.9	
11	75.8	3.93, dd (3.7; 9.8) 4.33, d (3.7)			61.7	3.15* 3.34, quintet (5.5)	61.6	3.42, dd (7.0; 11.4) 3.50, dd (6.6; 10.9)				
12	73.7	4.23, q (4.6)			123.8		124.4					
13	123.4				130.4	7.15, d (8.5)	115.2	6.71, d (8.2)				
14	130.4	7.17, d (8.7)			115.9	6.70, d (8.3)	145.3					
15	115.9	6.76, d (8.7)			157.6		145.2					
16	158.1				115.9	6.70, d (8.3)	115.5	6.87, d (2.2)				
17	115.9	6.76, d (8.7)			130.4	7.15, d (8.5)	120.3	6.77, dd (2.2; 8.2)				
18	130.4	7.17, d (8.7)										
1´	97.0	4.62, d (7.4)	120.3						120.3		120.2	
2´	70.8	3.54, m	107.2	7.50, s					107.3	7.53, s	107.3	7.43, s
3´	73.1	3.43, d (2.7)	147.9						147.9		147.9	
4´	68.4	3.52, m	139.0						139.1		139.1	
5´	67.2	3.44, d (10.0) 3.68, d (2.7)	147.9						147.9		147.9	
6´			107.2	7.50, s					107.3	7.53, s	107.3	7.43, s

1′′			101.8	5.52, d (7.7)					102.0	5.55, d (8.1)	102.0	5.48, d (8.3)
2′′			71.5	3.59, t (9.2)					71.7	3.58, m	71.6	3.53, t (8.0)
3′′			73.3	3.72, t (6.2)					73.5	3.40, m	73.3	3.67, q (5.1)
4′′			68.6	3.69, d (2.9)					68.4	3.70, m	68.6	3.62, d (3.2)
5′′			73.3	3.45, dd (6.2; 9.2)					76.4	3.37, m	73.4	3 39, d (3.2)
6′′			63.5	4.13, d (6.2)					60.8	4.38, d (8.0) 3.48, m	63.6	4.08, dd (8.0; 12.5)
1′′′			166.7								166.7	
2′′′			113.7	5.99, d (16.0)							114.1	6.09, d (16)
3′′′			145.7	7.30, d (16.0)							145.2	7.26, d (16)
4′′′			125.7								125.4	
5′′′			114.9	6.92, s							116.2	6.69, d (8.3)
6′′′			146.2								130.6	7.25, d (8.3)
7′′′			149.1								160.3	
8′′′			116.0	6.75, d (3.5)							130.6	7.25, d (8.3)
9′′′			121.8	6.72, d (3.5)							116.2	6.69, d (8.3)
3′ and 5′-OCH_3			56.7	3.83, s					56.8	3.84, s	56.7	3.77, s

* Partially or fully overlapped signals.

8.3.2 Antioxidant activity of *L. xanthoconus crude* extract *and* isolated compounds

The antioxidant activities of the crude extract and isolated compounds (**6.5**, **8.3** and **8.5**) were assessed using two assays: Ferric Ion Reducing Antioxidant Power (FRAP) and Trolox Equivalent Absorbance Capacity (TEAC), as presented in Table 8.2. These assays provide insight into the antioxidant potential of each compound, which was selected based on their quantities (more than 3.5 mg).

Table 8.2: Antioxidant activities of the crude extract and isolated compounds

	FRAP (umol AAE/g)	**TEAC (umol TE/g)**	**TEAC (IC_{50} - mg/mL)**
Extract	369.65±0.13	912.81±0.67	0.532±2.07
6.5	132.55±3.09	909.51±3.63	0.647±3.54
8.3	242.34±0.15	1238.53±0.13	0.510±3.13
8.5	2228.86±0.21	2295.02±0.34	0.071±0.82
Controls	5743.56±0.27 (vitamin C)	4010.17±0.21 (vitamin E)	0.152±0.67 (vitamin E)

8.3.3 Cytotoxicity assessment of *L. xanthoconus* crude extract and isolated compounds in H9c2 cell lines

The crude extract and compounds **8.3** and **8.5** were investigated for their cytotoxicity potential against H9c2 cells. Compounds **6.5**, **8.1**, **8.2, 8.4**, and **8.6** were not assessed due to their small quantities. The percentage of cell viability after treatment is illustrated in Figure 8.2. The Data were normalised to the vehicle control (0.53% DMSO) labelled 'control'.

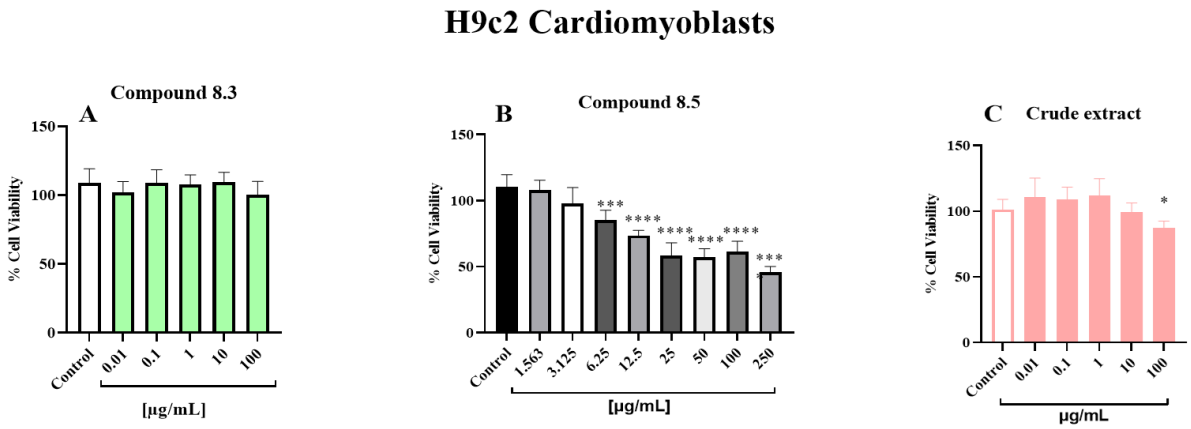

Figure 8.2: Cell viability assessment using the MTT assay. H9c2 cells were treated for 24 h with *L. xanthoconus* isolated compounds and crude extract. Data presented as mean±SD, n= 3. Control= 0.53% DMSO. Significance is indicated as *p < 0.05, ***p < 0.001, ****p < 0.0001 compared to control.

8.4 Discussion

8.4.1 Structure elucidation

8.4.1.1 Dichotomain C (8.1)

Compound **8.1** molecular formula was confirmed as $C_{20}H_{21}O_{12}$ by HRESIMS with an ion peak of 453.3812 *m/z*. The ^{1}H NMR showed signals of two methylene groups at δ_H 2.90 (*dd*, *J*= 8.8; 17.1 Hz, H-3α), 3.09 (*d*, *J*= 5.0 Hz, H-3β), 3.93 (*dd*, *J*= 3.7; 9.8 Hz, H-11α), and 4.33 (*d*, *J*= 3.7 Hz, H-11β). Signals of four aromatic protons at δ_H 7.17 (*d*, *J*= 8.7 Hz, H-14 and H-18) and 6.76 (*d*, *J*= 8.7 Hz, H-15 and H-17) were detected, suggesting the presence of za *p*-substituted benzene ring. Three additional methine units belonging to the aglycone were observed at δ_H 4.59 (*d*, *J*= 2.7 Hz, H-4), 4.01 (*s*, H-8) and 4.23 (*q*, *J*= 4.6 Hz, H-12).

The ^{13}C NMR spectrum showed 20 signals (see Table 8.1) consisting of three methylenes (C-3, C-11 and C-5´), eleven methines (C-4, C-8, C-12, C-14, C-15, C-17, C-18, C-1´, C-2´, C-3´, and C-4´), two lactone carbonyl groups (C-2 and C-6), two mono-oxygenated quaternary carbons (C-5 and C-16), one dioxygenated quaternary carbons (C9), and one quaternary carbon (C-13).

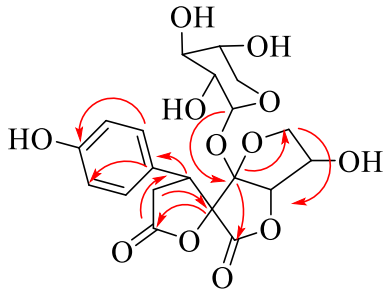

HMBC correlations of compound **8.1** (H→C)

The HMBC correlation from H-3α/H-3β to C-2, C-5, C-13, C-4 as well as the correlation from C-5 to C-2, C-3, C-6, C-9,C-13, C-14, C-5´,C-3´ indicate that C-5 is the spiro carbon of a 1,7-dioxaspiro[4.4]nonane-2,6-dione skeleton. Furthermore, C-9 is linked to H-1´, C-8, C-11, and C-12 implying the sugar group is attached to its aglycon at C-9 and carbons 8, 9, 11 and 12 form the tetrahydrofuran-3-ol moiety, which is similar with dichotomain B (Figure 8.3) data as reported by Li et al. (2006).

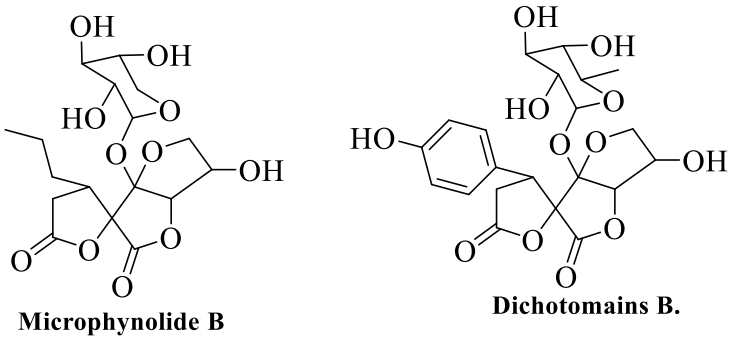

Figure 8.3: Chemical structure of microphynolide B and dichotomain B

However, The ^{1}H NMR also showed signals of an anomeric proton at δ_H 4.62 (*d*, *J*= 7.4 Hz, H-1′) as well as a cluster of protons resonances at δ_H 3.54 (*m*, H-2′), 3.43 (*d*, *J*= 2.7 Hz, H-3′), 3.52 (*m*, H-4′), and 3.44 (*d*, *J*= 10.0 Hz, H-5′α), 3.68 (*d*, *J*= 2.7 Hz, H-5′β). These data, coupled with HMBC and HSQC spectra, showed that H-1′ correlates with C-5′, C-3′ and C-2′, thereby indicating the presence of the pentose *β*-arabinose like in microphynolide B (Ghanema et al., 2014) instead of the hexose *D*-fucose like in dichotomain B. Based on these results, compound **8.1** was characterised as dichotomain C.

8.4.1.2 Syringetin-3-*O*-(6′′-caffeoyl)-*β*-*D*-glucopyranoside (8.2)

The ^{1}H NMR signals showed the presence of two methoxy groups at δ_H 3.83 (*s*, OCH_3); seven aromatic protons at δ_H 6.14 (*d*, *J*= 1.5 Hz, H-6), 6.40 (*d*, *J*= 1.5 Hz, H-8), 7.50 (*s*, H-2′ and H-6′), 6.92 (*s*, H-5′′′), 6.75 (*d*, *J*= 3.5 Hz, H-8′′′) and 6.72 (*d*, *J*= 3.5 Hz, H-9′′′). The signal of two olefinic protons at δ_H 5.99 (*d*, *J*= 16 Hz, H-2′′′) and 7.30 (*d*, *J*= 16 Hz, H-3′′′) was also observed. Additionally, the presence of an anomeric proton at δ_H 5.52 (*d*, *J*= 7.7 Hz, H-1′′), as well as a cluster of oxygenated methine at δ_H 3.59 (*t*, *J*= 9.2 Hz, H-2′′), 3.72 (*t*, *J*= 6.2 Hz, H-3′′), 3.69 (*d*, *J*= 2.9 Hz, H-4′′), 3.45 (*dd*, *J*= 6.2; 9.2 Hz, H-5′′), and a methylene unit at δ_H 4.13 (*d*, *J*= 6.2 Hz, H-6′′) characteristic of *β*-*D*-glucopyranosyl moiety, were observed.

The ^{13}C NMR spectrum displayed 32 peaks, 17 of which were attributed to the aglycon syringetin, 6 to the sugar glucose, and 9 to the caffeoyl moiety. The 32 peaks are classified with the help of DEPT-135 into two methoxy groups at δ_C 56.7 (3′-OCH_3 and C-5′-OCH_3); a methylene 63.5 (C-6′′); fourteen methines at δ_C 99.6 (C-6), 94.6 (C-8), 107.2 (C-2′ and C-6′), 101.8 (C-1′′), 71.5 (C-2′′), 73.3 (C-3′′ and C-5′′), 68.6 (C-4′′), 113.7 (C-2′′′), 145.7 (C-3′′′), 114.9 (C-5′′′), 116.0 (C-8′′′) and 121.8 (C-9′′′) as well as twelve quaternary carbons at δ_C 156.9 (C-2), 133,7 (C-3), 177.6 (C-4), 161.5 (C-5), 165.8 (C-7), 156.4 (C-9), 103.9 (C-10),

120.3 (C-1´), 147.9 (C-3´ and C-5´), 139.0 (C-4´), 166.7 (1´´´), 125.7 (C-4´´´), 146.2 (C-6´´´) and 149.1 (C-7´´´).

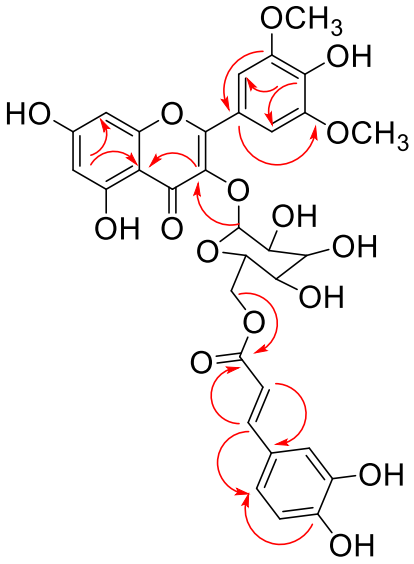

HMBC correlations of compound **8.2** (H→C)

According to the COSY and HMBC, the aromatic protons H-6 and H-7 are attached to the ortho benzene ring (ring A), while protons H-2´ and H-6´ are attached to the trisubstituted benzene ring (ring C). These four aromatic protons and the two methoxy resonances attached to the quaternary carbon C-3´ and C-5´ of ring C were attributed to the aglycon syringetin. It was also observed that the anomeric proton H-1´ correlated with C-2, C-3, and C-4, implying that the *β-D*-glucopyranosyl group is attached to the aglycon at position 3. Additionally, the double bonds peaks at δ_C 113.7 (C-2´´´) and 145.7 (C-3´´´) correlated with the carbonyl group C-1´´´ and the quaternary carbon C-4´´´ showing the presence of a caffeoyl moiety. The caffeoyl unit was observed to be attached to the methylene group of the *β-D*-glucopyranosyl moiety linked to C-3, meaning that the side chain at C-3 is a 1-*O*-(6´´-caffeoyl)-*β-D*-glucopyranosyl group.

From the NMR data, compound **8.2** molecular formula was deduced as $C_{32}H_{29}O_{16}$ by HRESIMS with an ion peak of 669.5596 *m/z* and characterised as syringetin-3-*O*-(6´´-caffeoyl)-*β-D*-glucopyranoside.

8.4.1.3 Leucodrin (8.3)

The ^{1}H NMR showed signals of two methylene groups at δ_H 2.94 (*dd*, *J*= 9.1; 17.7 Hz, H-3α), 3.15 (*m*, H-3β), 3.15 (*m*, H-11α), and 3.34 (*quintet*, *J*= 5,5 Hz, H-11β). Signals of eight methine groups at δ_H 4.28 (*q*, *J*= 9.1 Hz, H-4), 3.71 (*dd*, *J*= 1.3; 8.7 Hz, H-8), 4.66 (*d*, *J*= 4.7 Hz, H-9),

3.51 (*q*, *J*= 7.5 Hz, H-10), 7.15 (*d*, *J*= 8.5 Hz, H-13 and H-17), and 6.70 (*d*, *J*= 8.3 Hz, H-14 and H-16) were detected.

The ^{13}C NMR spectrum showed 15 signals (see Table) consisting of two methylenes at δ_C 33.6 (C-3), and 61.7 (C-11); eight methines at δ_C 41,4 (C-4), 80.2 (C-8), 69.6 (C-9), 68.4 (C-10), 130.4 (C-13 and C-17), and 115.9 (C-14 and C-16), two lactone carbonyl groups at δ_C 175.1 (C-2) and 172.4 (C-6) as well as three quaternary carbons at δ_C 90.4 (C-5), 123.8 (C-12), and 157.6 (C-15).

These NMR data are similar to leucodrin, a compound previously isolated from *Leucadendron*. Spp. by Billing, 1991.

8.4.1.4 Leudrin (8.4)

The ^{1}H NMR showed signals of two methylene groups at δ_H 2.8 (*dd*, *J*= 8.7; 17.4 Hz, H-3α), 3.15 (*dd*, *J*= 12.7; 17.1 Hz, H-3β), 3.42 (*dd*, *J*= 7.0; 11.4 Hz, H-11α), and 3.50 (d*d*, *J*= 6.6; 10.9 Hz, H-11β). Signals of eight methine groups at δ_H 4.30 (*dd*, *J*= 8.8; 12.9 Hz, H-4), 3.78 (*dd*, *J*= 2.2; 8.8 Hz, H-8), 4.75 (*d*, *J*= 8.8 Hz, H-9), 3.66 (*dt*, *J*= 2.4; 7.0 Hz, H-10), 6.71 (*d*, *J*= 8.2 Hz, H-13), 6.87 (*d*, *J*= 2.2 Hz, H-16) and 6.77 (*dd*, *J*= 2.2; 8.2 Hz, H-17) were detected.

The ^{13}C NMR spectrum showed 15 signals (see Table) consisting of two methylenes at δ_C 33.6 (C-3), and 61.6 (C-11); eight methines at δ_C 41,8 (C-4), 80.2 (C-8), 69.8 (C-9), 68.9 (C-10), 115.2 (C-13), 115.5 (C-16) and 120.34 (C-17); two lactone carbonyl groups at δ_C 175.2 (C-2) and 172.3 (C-6) as well as four quaternary carbons at δ_C 90.3 (C-5), 124.4 (C-12), 145.3 (C-14), and 145.2 (C-15).

These NMR data are similar to leudrin, a compound previously isolated from *Leucadendron* spp. by Perold 1988.

8.4.1.5 Syringetin-3-*O*-*β*-*D*-glucopyranoside (8.5)

From the 1D and 2D NMR spectra, compound **8.5** differs from compound **8.2** by the absence of a caffeoyl group at position C-6´´. The absence of the caffeoyl group at C-6´´ does change the side chain at C-3 from a 1-O-(6´´-caffeoyl)-β-D-glucopyranosyl group to *β-D*-glucopyranosyl group. Based on the NMR data compound **8.5** was characterised as syringetin-3-O-*β-D*-glucopyranoside, previously isolated from *Heliciopsis lobata* (Li et al., 2008).

8.4.1.6 syringetin-3-*O*-(6''*p*-coumaroyl)-*β*-*D*-glucopyranoside (8.6)

From the 1D and 2D NMR spectra, compound **8.6** differs from compound **8.2** by the absence of a hydroxyl group at position C-6´´´. The absence of the hydroxyl group at C-6´´´ does change the side chain at C-3 from a 1-*O*-(6´´-caffeoyl)-*β*-*D*-glucopyranosyl group to a 1-*O*-(6´´-*p*-coumaroyl)-*β*-*D*-glucopyranosyl group.

The NMR data deduced compound **8.6** molecular formula as $C_{32}H_{29}O_{16}$ and characterised as syringetin-3-*O*-(6"-*p*-coumaroyl)-*β*-*D*-glucopyranoside.

8.4.2 Spectroscopy data

- **Dichotomain C** ($C_{20}H_{21}O_{12}$): colourless crystal; IR: 3325 cm-^{1} (OH), 2952 cm-^{1} (CH), 1663 cm-^{1} (C=O), 1450 cm-^{1} (C=C), 1117 cm-^{1} (C-O); HRESIMS: 453.3812 $[M^{+}H]^{+}$ (calculated for $C_{20}H_{21}O_{12}$, 453.3760); ^{1}H NMR (DMSO-D_6) and ^{13}C NMR (DMSO-D_6): see Table 8.1

- **Syringetin-3-*O*-(6´´-caffeoyl)-*β*-*D*-glucopyranoside** ($C_{32}H_{29}O_{16}$): yellowish solid; IR: 3341 cm-^{1} (OH), 2949 cm-^{1} (CH), 1660 cm-^{1} (C=O), 1450 cm-^{1} (C=C), 1116 cm-^{1} (C-O); HRESIMS: 669.5596 $[M^{+}H]^{+}$ (calculated for $C_{32}H_{29}O_{16}$, 669.5680); ^{1}H NMR (DMSO-d_6) and ^{13}C NMR (DMSO-D_6): see Table 8.1

8.4.3 Total phenolic content, antioxidant, cytotoxic and cardioprotective potential of *L. xanthoconus* crude extract and isolated compounds

The total phenolic content of the crude extract was measured as 183.21±3.28 mg GAE/g, indicating a moderate level of phenolic compounds. However, antioxidant assays showed weak antioxidant potential for the crude extract and compounds **6.5**, **8.3**, and **8.5**, with IC_{50} values of 0.532±2.07, 0.647±3.54, 0.510±3.13, and 0.071±0.82 µg/mL, respectively. Among these, compound **8.5** is the only one showing antioxidant potential.

Regarding cytotoxicity, compound **8.5** exhibited weak activity with an IC_{50} of 85.79±1.56 µM. The crude extract, at a concentration of 100 µg/mL, significantly reduced cell proliferation (87.28±5.11 vs. control 102.34±8.29 µg/mL, *$p < 0.05$). However, based on the cytotoxicity thresholds defined by López-García et al. (2014), the crude extract is classified as non-cytotoxic.

Interestingly, Figure 8.2 shows that compound **8.5** exhibited toxicity at a concentration as low as 6.25 µg/mL, which likely explains its inability to protect H9c2 cells from HG+Pal induced stress. Furthermore, neither compound **8.3**

nor the crude extract demonstrated any cardioprotective effects.

8.5 Conclusion

L. xanthoconus is distinguished by its abundance of bislactonic spiro compounds (**8.1**, **8.3**, and **8.4**) and flavonoid glycosides (**8.2**, **8.5**, and **8.6**). Notably, this study is the first to report Sutherlandioside D (**6.5**) isolation from a species other than *L. frutescens*. While these findings underscore the unique secondary metabolite profile of *L. xanthoconus* and its potential for further phytochemical exploration, the crude extracts and isolated compounds did not exhibit significant therapeutic effects under the conditions tested.

References

Billing, D.G., Boeyens, J. C. A., Carlton, L., Combrink, D. & Michael, J. P. (1991). Comparison of the NMR coupling paths in leucodrin and conocarpin by low-temperature X-ray structure analysis. *Journal of the Chemical Society*, 2: 695-700.

Gadea, A., Khazem, M. & Gaslonde, T. (2022). Current knowledge on chemistry of Proteaceae family, and biological activities of their bis-5-alkylresorcinol derivatives. *Phytochemistry Reviews*, 21(6): 1969-2005

Ghanem, H., Haba, H., Marcourt, L., Benkhaled, M. & Wolfender, J. L. (2014). Microphynolides A and B, new spiro-γ-lactone glycosides from *Thymelaea microphylla*. *Natural Product Research*, 28(20): 1732-1738.

Li, D., Liu, M. S., Li, Z. L., Kang, S. L. & Hua, H. M. (2008). Studies on chemical constituents of *Heliciopsis lobata* II. *Zhongguo Zhongyao Zazhi (China Journal of Chinese Materia Medica)*, 33: 409-411.

Li, X. L., Cheng, X., Yang, L. M., Wang, R. R., Zheng, Y. T., Xiao, W. L., Zhao, Y., Xu, G., Lu, Y., Chang, Y., Zheng, Q. T., Zhao, Q. S. & Sun, H. D. (2006). Dichotomains A and B: Two new highly oxygenated phenolic derivatives from *Dicranopteris dichotoma*. *Organic Letters*, *8*(9): 1937-1940.

Perold, G. W., Carlton, L., Howard, A. S. & Michael, J. P. (1988). The structure of leucodrin, and the nucleophilic substitution of its primary hydroxy group by bromine. *Journal of the Chemical Society, Perkin Transactions 1*, 881-884.

SANBI. (2007). *Leucadendron xanthoconus*. PlantZAfrica. Available at: https://pza.sanbi.org/leucadendron-xanthoconus (Accessed: 20 November 2023).

Zhang, J., Netzel, M. E., Pengelly, A., Sivakumar, D. & Sultanbawa, Y. (2023). A Review of Phytochemicals and Bioactive Properties in the Proteaceae Family: A Promising Source of Functional Food. *Antioxidants*, 12: 1-32.

CHAPTER NINE: Computational approaches in drug discovery: *in silico* analysis of drug-likeness, pharmacokinetics, and molecular docking of natural compounds from *L. frutescens*, *P. venus*, and *L. xanthoconus*

9.1 Introduction

Computational (*in silico*) approaches have been created and extensively utilised for hypothesis generation and testing in pharmacology. These methods include databases, quantitative structure-activity relationships (QSAR), similarity searches, pharmacophores, homology modelling, and other molecular modelling techniques. They also encompass machine learning, data mining, network analysis, and data analysis tools that rely on computer systems. These techniques are frequently applied in discovering and optimising new molecules with target affinity, understanding absorption, distribution, metabolism, excretion, and toxicity (ADMET) properties, and characterising physicochemical attributes (Ekins et al., 2007).

A key area of interest for medicinal chemists and pharmacologists has been evaluating the drug-likeness of bioactive compounds, often through Lipinski's Rule of Five (Ro5). This rule assesses whether a compound possesses the necessary physical and chemical characteristics for oral administration based on a study of over 2000 successful drugs. According to these guidelines, poor absorption is often observed when a compound has more than (i) 5 hydrogen-bond donors (HBD), (ii) 10 hydrogen-bond acceptors (HBA), (iii) a molecular weight (MW) above 500 Da (optimal range: 250-350 g/mol), or (iv) a calculated Log P (cLogP) exceeding 5 (Lipinski et al., 1997; Pillai et al., 2001).

Over the past three decades, molecular docking has become a powerful tool in structural biology and structure-based drug discovery. Fuelled by significant advancements in computational power and the increasing accessibility of molecular and protein databases, it has become an essential part of drug discovery. Molecular docking has several key applications in drug discovery, including studying structure-activity relationships, optimising lead compounds, virtual screening for potential drug leads, supporting mutagenesis predictions, aiding x-ray crystallography, and designing combinatorial libraries (Morris & Lim-Wilby, 2008).

This chapter examines the predicted toxicological profile, physiological and pharmacokinetic properties, drug-likeness, and lead-likeness of compounds isolated from *L. frutescens*, *P. venus* and *L. xanthoconus*. From the 28 isolated compounds, 17 (**6.3**-**6.11**, **7.3**-**7.6**, **7.9**, **8.3** and **8.5**)

with sufficient yields were selected for molecular docking studies. Protein targets for docking were identified using SuperPred predictions.

Compounds **6.3**-**6.11** were evaluated against PD-related targets, DJ-1 (Protein Deglycase PARK7) and Monoamine Oxidase B (MAO-B). These proteins mitigate oxidative damage through distinct mechanisms: MAO-B reduces oxidative stress by inhibiting dopamine breakdown (George et al., 2009), while DJ-1 scavenges ROS (Canet-Aviles et al., 2004).

Similarly, compounds **7.1**-**7.6**, **7.9**, **8.3** and **8.5** were assessed against DCM-related targets such as Kelch-like ECH-associated protein 1-Nuclear factor erythroid 2 related factor 2 (KEAP1-NRF2), glutathione peroxidase 4 (GPX4) and beta-1 adrenergic receptor (β_1-AR). KEAP1-NRF2 enhances antioxidant defences (Murakami et al., 2023), GPX4 prevents ferroptosis and preserves cardiomyocyte integrity (Ingold et al., 2018), and β_1-AR modulates adrenergic signalling involved in cardiac remodelling and apoptosis (Lohse et al., 2003).

Docking studies evaluated ligand-protein interactions based on docking scores, hydrophobic interactions, hydrogen bonding, and binding strength, aligning the results with hypothesised therapeutic mechanisms.

9.2 Methodology

9.2.1 Toxicology profiling

ProTox (ProTox 3.0; AG Preissner; Charite Berlin) was used to predict acute toxicity (LD_{50}), organ toxicity (hepatotoxicity, neurotoxicity, and cardiotoxicity) and toxicological endpoints (mutagenicity, cytotoxicity, and carcinogenicity). The toxicological profiling of the compounds is done by employing molecular similarity, pharmacophores, fragment propensities, and machine-learning models. ProTox webserver also incorporates data from *in vitro* assays (such as Tox21 assays and Ames tests) and *in vivo* studies (Banerjee et al., 2024).

9.2.2 Drug-likeness and ADME properties

The SwissADME online server was utilised to predict various physicochemical parameters, including molecular formula, molecular weight (MW), number of heavy atoms (HA), number of rotatable bonds (RB), number of hydrogen bond acceptors (HBA), and hydrogen bond donors (HBD). It also estimated lipophilicity (iLogP), water solubility (logS), pharmacokinetic properties (GI absorption, BBB permeation, and P-glycoprotein substrate(P-gp), drug-likeness (Lipinski's rule and bioavailability), as well as lead-likeness of the compounds. The canonical

SMILES of the tested compounds were generated using ChemOffice Pro 2015 (version 15.00). The generated SMILES were submitted to the SwissADME server to predict the compounds' absorption, distribution, metabolism and excretion (ADME) properties (Daina et al., 2017).

9.2.3 Boiled egg method

The SwissADME also provides the Boiled Egg plot, a visual tool for predicting a compound's potential for GI absorption and BBB penetration based on its physicochemical properties (Daina et al., 2017).

9.2.4 Biological Target Predictions

To assess the biological relevance of the potential drug leads, the SuperPred target prediction server was used thoroughly to identify potential biological targets for all the phytochemical compounds that exhibited favourable ADMET properties and were available in sufficient quantities for biological evaluation. The prediction is based on a combination of 2D and 3D similarity, utilising a chemical library. The previously generated canonical SMILES were imported into the SuperPred Target Prediction system for processing (Gallo et al., 2022).

9.2.5 Molecular Docking

9.2.4.1 Phytochemical Compounds Acquisition and Geometry Optimisation

The 3D structures of the tested compounds were obtained on the PubChem database and geometrically optimised using Avogadro (version 1.1.0) through energy minimisation. Avogadro is integrated with the Ghemical and UFF forcefield to optimise the molecular geometries of the natural compounds and the steepest descent algorithm for structural minimisation (Hanwell et al., 2012). All the compounds were generated as .mol2 files, an input file recognised as a ligand in UCSF Chimera software.

9.2.4.2 Protein Acquisition and Preparation

The protein crystal structures for MAO-B (PDB ID: 1GOS), DJ-1 (PDB ID: 1P5F), KEAP1-NRF2 (PDB ID: 2FLU), β_1-AR (PDB ID: 4GPO) and GPX4 (PDB ID: 2OBI) were obtained from RSCB PDB as .pdb files, an input file recognised as a receptor in UCFS Chimera (Berman, 2000). Before docking, the proteins underwent a thorough preparation process, including removing repeated monomers and any other non-essential substrates, including water. The

protein structure was further prepared for molecular docking using the dock prep module on UCSF Chimera (version 1.11.2) to add hydrogens and partial residue replacement using the Dunbrack rotamer library, conversion of bromo-UMP to UMP, conversion of selenomethionine to methionine, and conversion of methylsulfonyl-dCMP to CMP. The AMBER.ff14SB force field was employed to distribute the Gasteiger charges on the protein molecule. The augmented proteins were then used for docking, ensuring the reliability of the results.

9.2.4.3 Molecular Docking

The molecular docking process, conducted with the Autodock Vina Plugin (version 1.2.0) available on Chimera with default docking parameters, is a precise method for predicting the binding affinity of the compounds when they are complex with their respective biological targets. Before docking, Gasteiger charges were added to the compounds, and the non-polar hydrogen atoms merged into carbon atoms. The phytochemical compounds were then docked into the binding pocket of MAO-B and DJ-1 (*L. frutescens*), KEAP1-NRF2, β_1-AR and GPX4 (*P. venus* and *L. xanthoconus*), providing valuable information on the compounds' binding mode and geometric fit for comparison with known drugs.

Table 9.1 presents the active site residues of MAO-B, DJ-1, KEAP1-NRF2, β_1-AR and GPX4. Using the AutoDock Vina tool in UCSF Chimera, a grid box encompassing all active site residues was created.

Table 9.1: Active sites and Gridbox coordinates of the molecular docking simulations

	Active sites	**Gridbox coordinates**	**References**
MAO-B	Phe343, Tyr398, Cys172, Leu171, Tyr326, Ile199, Phe166, Ile198, Gln206, Tyr435, Tyr60	Centre: x= 55.9272, y= 139.396, z= 22.5688	Binda et al., 2002
		Size: X= 16.3698, Y= 19.3539, Z= 16.0801	
DJ-1	His126, Val166, Cys106, Glu18, Leu166	Centre: x= 24.986, y= 26.1791, z= 33.5016	Wilson et al., 2003
		Size: X= 26.7396, Y= 28.2147, Z= 21.4311	
KEAP1-NRF2	E82, E83, E78, E79, F83, Arg483, Arg415, Arg380, Asn382, Gln530, His436, Ser 555, Ser363, Ser508, Ser602, Tyr525, and Tyr334	Centre: x= 6.02888, y= 13.6967, z= 2.32762	Lo et al., 2006
		Size: X= 22.5578, Y= 21.743, Z= 23.9207	
β_1-AR	Asp121, Arg139, Asn310, Asn329, Glu285, Phe201, Phe299, Thr203, Trp303	Centre: x= -33.7488, y= -29.6449, z= 22.4074	Huang et al., 2013
		Size: X= 36.1587, Y=23.255, Z= 35.2899.	
GPX4	Cys46, Gln81, Trp136	Centre: x= 27.8613, y= -16.229, z= -11.4257	Scheerer et al., 2007

		Size: X= 28.1109, Y= 16.3618, Z= 27.1943	

9.3 Results and Discussion

The phytochemical analysis of *L. frutescens*, *P. venus*, and *L. xanthoconus* resulted in the isolation of 28 compounds (see Chapters Six, Seven and Eight for techniques and methods used for their isolation and characterisation).

9.3.1 Toxicological profile of the compounds

Pharmaceutical companies increasingly employ computational tools to improve drug safety and reduce toxicity-related development-stage failures. For example, the ProTox 3.0 web server predicts acute, organ-specific, and endpoint toxicology of analysed compounds, which aids drug design and risk assessment by anticipating potential adverse effects early in drug discovery. These tools and customised retrospective assays provide a "safety net" to address specific toxicity concerns that may arise in later-stage *in vitro* and *in vivo* studies (Pognan et al., 2023).

In this study, the toxicological profiles of 28 compounds, comprising an amino acid (**6.10**), two sugars (**6.11** and **7.11**), six cycloartane glycosides (**6.1**-**6.6**), eight flavonoids (**6.7**-**6.9**, **7.6**-**7.8**, **8.2**, **8.5** and **8.6**) and 11 phenolic compounds (**7.1**-**7.5**, **7.9**, **7.10**, **8.1**, **8.3** and **8.4**) isolated from *L. frutescens* (**6.1**-**6.11**), *P. venus* (**7.1**-**7.10**) and *L. xanthoconus* (**6.5** and **8.1**-**8.6**) are summarised in Table 9.2. Additionally, the median lethal dose (LD_{50}), representing the dose at which 50% of test subjects are predicted to die, was evaluated.

The compounds were categorised into toxicity classes (Banerjee et al., 2024) as follows:

- Class III: Toxic if ingested ($50 < LD_{50} < 300$ mg/Kg)
- Class IV: Harmful when swallowed ($300 < LD_{50} < 2000$ mg/Kg)
- Class V: Possibly harmful when swallowed ($2000 < LD_{50} < 5000$ mg/Kg)
- Class VI: Non-toxic ($LD_{50} > 5000$ mg/Kg)

Given their elevated predicted LD_{50} values, these findings suggest that *P. venus* and *L. xanthoconus* compounds are unlikely to induce significant toxic effects at doses below 1000 mg/Kg. On the other hand, *L. frutescens* compounds, particularly compound **6.4**, show a higher potential for toxicity. However, it is worth noting that compound **6.6** from *L. frutescens* is classified as non-toxic.

Among the 11 compounds isolated from *L. frutescens*, compound **6.9** is the only one without cardiotoxic activity. Compounds **6.1** and **6.3** are predicted to be cytotoxic if consumed above their respective LD_{50} values. None of the *L. frutescens* compounds showed activity for neurotoxicity, hepatotoxicity, mutagenicity, or carcinogenicity, supporting the claimed safety of *L. frutescens* preparations, such as decoctions and tablets.

Compounds from *P. venus* showed no predicted mutagenicity, cytotoxicity, or neurotoxicity (except for compounds **7.5** and **7.8**). Compounds **7.5** and **7.8** displayed activities for neurotoxicity and hepatotoxicity. Some compounds like **7.5**, **7.7**, and **7.9**, were flagged for their potential carcinogenicity. Additionally, compounds **7.1**, **7.3**, **7.4**, **7.6**, and **7.7**, along with *L. xanthoconus* flavonoids (**8.2**, **8.5**, and **8.6**), exhibited predicted cardiotoxicity.

Our predictive toxicology results align with our empirical data, instilling confidence in the safety of compounds **6.3-6.11**. These compounds were non-cytotoxic to SHSY5Y cells at 2.5-10 µg/mL (Chapter Six). However, the low concentrations at which these compounds were tested warrant caution, as some, including compounds **6.4** (55 mg/Kg), **6.7** (900 mg/Kg), **6.8** (500 mg/Kg), and **6.11** (804 mg/Kg), have LD_{50} values ranging between 55–900 mg/Kg. Similarly, compounds (**7.3-7.6** and **7.9)** confirmed a lack of cytotoxicity at concentrations below 100 µg/mL against C3A, H9c2 and MCF-7 cells (Chapters Seven), reinforcing the reliability of predictive toxicology for these compounds, which aligns with findings from the literature.

Compound **8.5**, however, presented a significant discrepancy. Predictive models indicated cardiotoxicity only at doses ≥ 5000 mg/Kg, yet experimental data revealed cardiotoxic effects at much lower concentrations, with an IC_{50} of 85.79±1.56 µM in H9c2 cells (Chapter Eight). This divergence highlights the limitations of predictive models, which may not fully account for compounds with limited prior assessment, unknown mechanisms of action, or poorly understood interactions with biological targets. Furthermore, these models may fail to accurately predict how such compounds are metabolised in the body, leading to discrepancies between *in silico* predictions and empirical observations. This highlights the critical need for empirical validation to complement predictive analyses and ensure accurate safety assessments.

Table 9.2: Toxicological profile of the *L. frutescens*, *P. venus* and *L. xanthoconus* isolated compounds

Compounds	Predicted LD_{50} (mg/Kg)	Predicted toxicity class	Hepatoxicity	Neurotoxicity	Carcinogenicity	Cardiotoxicity	Mutagenicity	Cytotoxicity
6.1	1750	IV	Inactive	Inactive	Inactive	Active	Inactive	Active
6.2	1750	IV	Inactive	Inactive	Inactive	Active	Inactive	Inactive
6.3	5000	V	Inactive	Inactive	Inactive	Active	Inactive	Active
6.4	55	III	Inactive	Inactive	Inactive	Active	Inactive	Inactive
6.5	4500	IV	Inactive	Inactive	Inactive	Active	Inactive	Inactive
6.6	10000	VI	Inactive	Inactive	Inactive	Active	Inactive	Inactive
6.7	900	IV	Inactive	Inactive	Inactive	Active	Inactive	Inactive
6.8	500	IV	Inactive	Inactive	Inactive	Active	Inactive	Inactive
6.9	5000	V	Inactive	Inactive	Inactive	Inactive	Inactive	Inactive
6.10	1000	IV	Inactive	Inactive	Inactive	Active	Inactive	Inactive
6.11	804	IV	Inactive	Inactive	Inactive	Active	Inactive	Inactive
7.1	5000	V	Inactive	Inactive	Inactive	Active	Inactive	Inactive
7.2	3750	V	Inactive	Inactive	Inactive	Inactive	Inactive	Inactive
7.3	5000	V	Inactive	Inactive	Inactive	Active	Inactive	Inactive
7.4	5000	V	Inactive	Inactive	Inactive	Active	Inactive	Inactive
7.5	1190	IV	Active	Active	Inactive	Inactive	Inactive	Inactive
7.6	5000	V	Inactive	Inactive	Active	Active	Inactive	Inactive
7.7	5000	V	Inactive	Inactive	Active	Active	Inactive	Inactive
7.8	1190	IV	Active	Active	Inactive	Inactive	Inactive	Inactive
7.9	2000	IV	Inactive	Inactive	Active	Inactive	Inactive	Inactive
7.10	2200	V	Inactive	Inactive	Inactive	Inactive	Inactive	Inactive
8.1	5000	V	Inactive	Inactive	Inactive	Inactive	Inactive	Inactive
8.2	5000	V	Inactive	Inactive	Inactive	Active	Inactive	Inactive
8.3	1175	IV	Inactive	Inactive	Inactive	Inactive	Inactive	Inactive
8.4	2000	IV	Inactive	Inactive	Inactive	Inactive	Inactive	Inactive
8.5	5000	V	Inactive	Inactive	Inactive	Active	Inactive	Active
8.6	3750	V	Inactive	Inactive	Inactive	Active	Inactive	Inactive

9.3.2 Physiological, pharmacokinetic, drug-likeness and lead-likeness properties of the isolated compounds

In drug discovery and development, natural, synthetic, and semi-synthetic compounds are evaluated based on physiological parameters, pharmacokinetics properties, lipophilicity, water solubility, bioavailability score, drug-likeness and lead likeness potential. These parameters are essential for assessing a compound's ADME properties, which helps reduce failures during clinical trials. Tools like SwissADME predict these physiochemical properties of compounds based on their molecular structure. This software incorporates Lipinski's Ro5, a well-established guideline that identifies compounds with favourable properties for oral absorption. Additionally, SwissADME used the boiled egg model to predict the likelihood of a compound being well-absorbed in the GI tract and its potential to cross the BBB. The server also features algorithms that are particularly useful in medicinal chemistry, assisting in identifying promising lead compounds.

The Boiled Egg plots (Figure 9.1) reveal that compounds **6.1**, **6.2**, **6.4**, **6.5**, **6.6** and **6.11** lie outside the white and yellow regions of the egg, indicating that these compounds are unlikely to be absorbed in the GI tract or penetrate the BBB. This can be attributed to various factors, such as compound **6.11**'s low solubility and hydrophilicity or the high lipophilicity and solubility of compounds **6.1**, **6.2**, **6.4**, **6.5** and **6.6**. Compounds **6.3** and **6.9** fall outside the plot's range due to their high Topological Polar Surface Area (TPSA), making them too polar to cross the lipid-rich BBB or the intestinal epithelium. As a result, compounds **6.1**-**6.6**, **6.9** and **6.11** are considered unsuitable for oral administration or targeting the central nervous system (CNS), especially compounds **6.3** and **6.9**. In contrast, compound **6.10** falls within the white region of the egg, indicating high GI absorption and no BBB permeability, reducing its potential for CNS penetration. Compounds **6.7** and **6.8**, on the other hand, are within the egg yolk, indicating high GI absorption, optimal lipophilicity, and the ability to cross the BBB. However, their potential as CNS-targeted compounds could be compromised due to their status as P-gp substrates. The efflux action of P-gp could limit the compounds' ability to reach therapeutic concentrations in the brain, possibly necessitating higher doses to achieve the desired therapeutic effects.

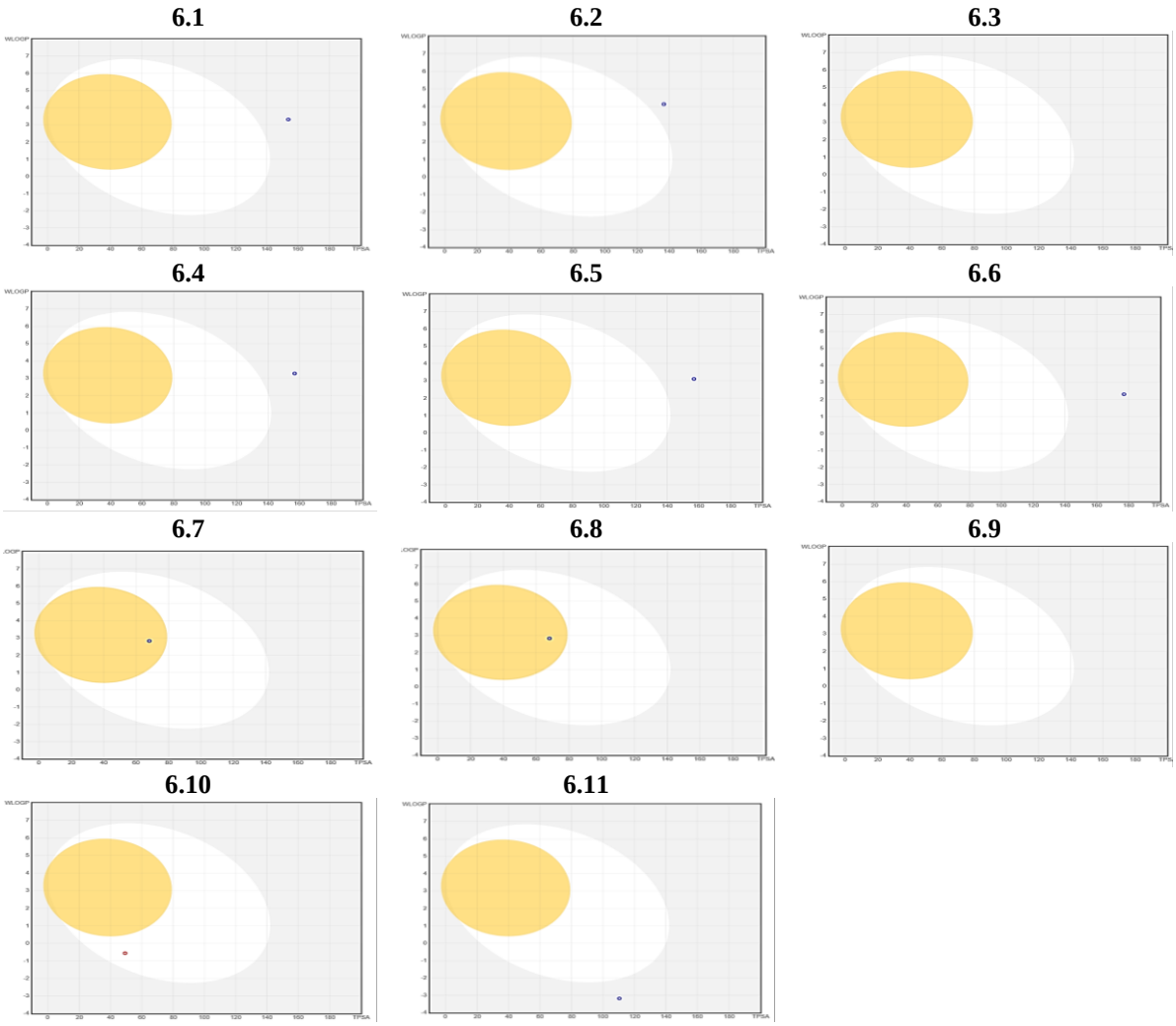

Figure 9.1: Boiled Egg model of compounds **6.1**-**6.11.** Compounds within the yellow region are predicted to cross the BBB. Compounds within the white region are predicted to passively been absorbed by the GI tract. The blue dots represent compounds predicted to effluated from the CNS by P-gp, while the red dots represent compounds predicted not to be effluated from the CNS by P-gp.

The ADME properties of the isolated compounds are presented in Table 9.3, and their physicochemical properties are illustrated in Figure 9.2. Table 9.3 and Figure 9.2 show that compounds **6.7**, **6.8**, **8.3**, and **8.4** are the only compounds that meet Lipinski's Ro5 and lead-likeness criteria, with a bioavailability score of 0.55. However, while compounds **8.3** and **8.4** are moderately lipophilic and not P-gp substrates, their high TPSA limit their ability to diffuse across the lipophilic cell membranes of the GI epithelium, explaining their low GI absorption. Despite these challenges, these compounds show potential for drug optimisation. Their low oral bioavailability and high solubility suggest that strategies such as prodrug design (to mask polar groups and temporarily enhance permeability), encapsulation in nanoparticles (to bypass

permeability barriers), or parenteral administration (e.g., intravenous or subcutaneous injection) may offer more effective routes of administration.

Compound **7.2** also displays good drug-likeness and lead-likeness, although it violates one of Lipinski's rules due to exceeding five HBD.

Several other compounds lack lead-likeness due to factors such as (a) a molecular weight outside the optimal range (250–350 g/mol), (b) more than 7 rotatable bonds, or (c) an XLOGP3 exceeding 3.5. The cycloartane glycosides from *L. frutescens* violate two or more lead-likeness criteria (compounds **6.3**, **6.6**, and **6.9** violate criteria a and b, while compounds **6.1**, **6.2**, **6.4**, and **6.5** violate all three). The bioavailability score of these cycloartane glycosides (**6.3**-**6.6**) and flavonoids **7.8**, **8.2** and **8.5** ranges from 0.11 to 0.17, except for compounds **6.1** and **6.2**, which show a bioavailability score of 0.55. Other compounds with a bioavailability score of 0.55 include compounds **6.7**, **6.8**, **6.10**, **6.11**, **7.6**, and **8.6**. Additionally, none of the flavonoids or cycloartane glycosides meet the criteria for drug-likeness due to two or three violations of Lipinski's rules, except for compounds **6.1**, **6.2**, and **7.6**, which have only one violation.

In addition to compounds **6.7** and **6.8**, compounds **6.10**, **7.9**, and **7.10** also show high GI absorption. Compound **7.10** not only exhibited good GI absorption but also demonstrated BBB permeability along with a high bioavailability score of 0.86. Moreover, compounds **7.9** and **7.10** are moderately soluble, with logS values of -1.86 and -2.07, respectively, and neither compound exhibits P-gp efflux activity. Both compounds are also moderately lipophilic. These characteristics indicate that compounds **7.9** and **7.10** have the potential to reach adequate drug concentrations for absorption, positioning them as promising candidates for oral formulations if optimised to meet pharmaceutical standards. Compounds **6.1**-**6.9**, **6.11**, **7.2**, **7.8**, **8.1**, and **8.5** are also P-gp substrates, which may affect their therapeutic potential.

6.1

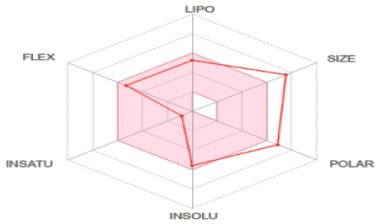

6.2

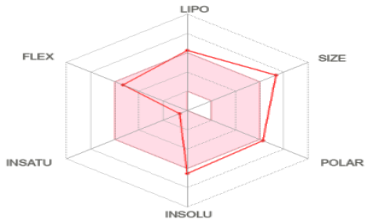

6.3

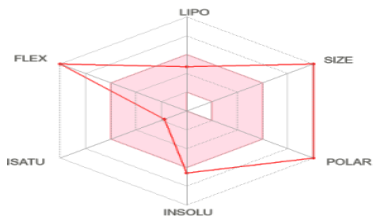

6.4

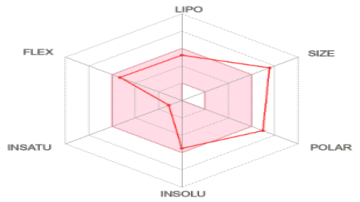

6.5

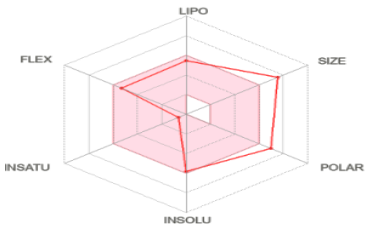

6.6

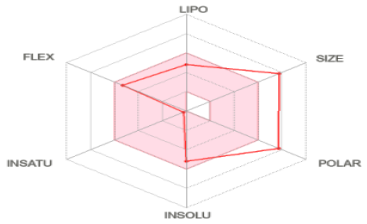

6.7

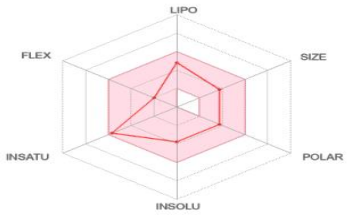

6.8

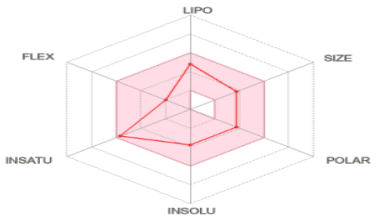

6.9

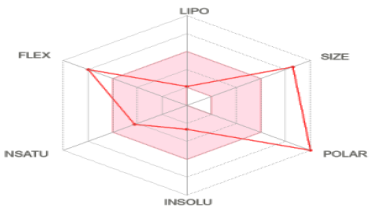

6.10

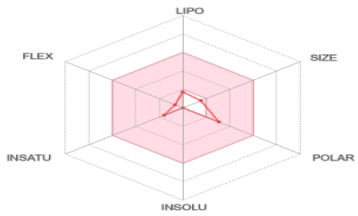

6.11

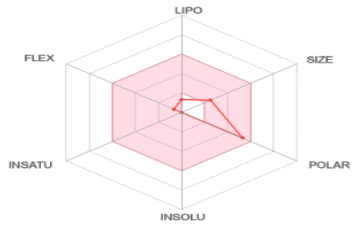

7.1

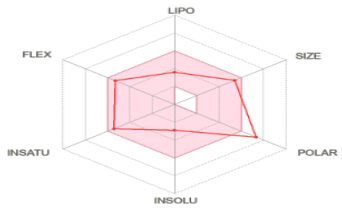

7.2

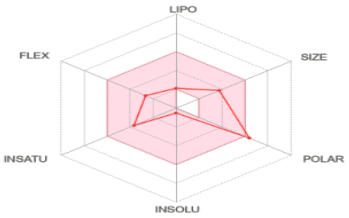

7.3

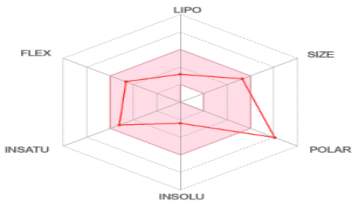

7.4

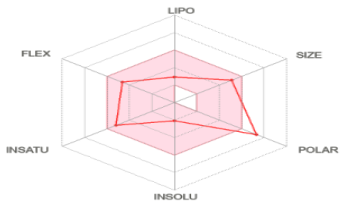

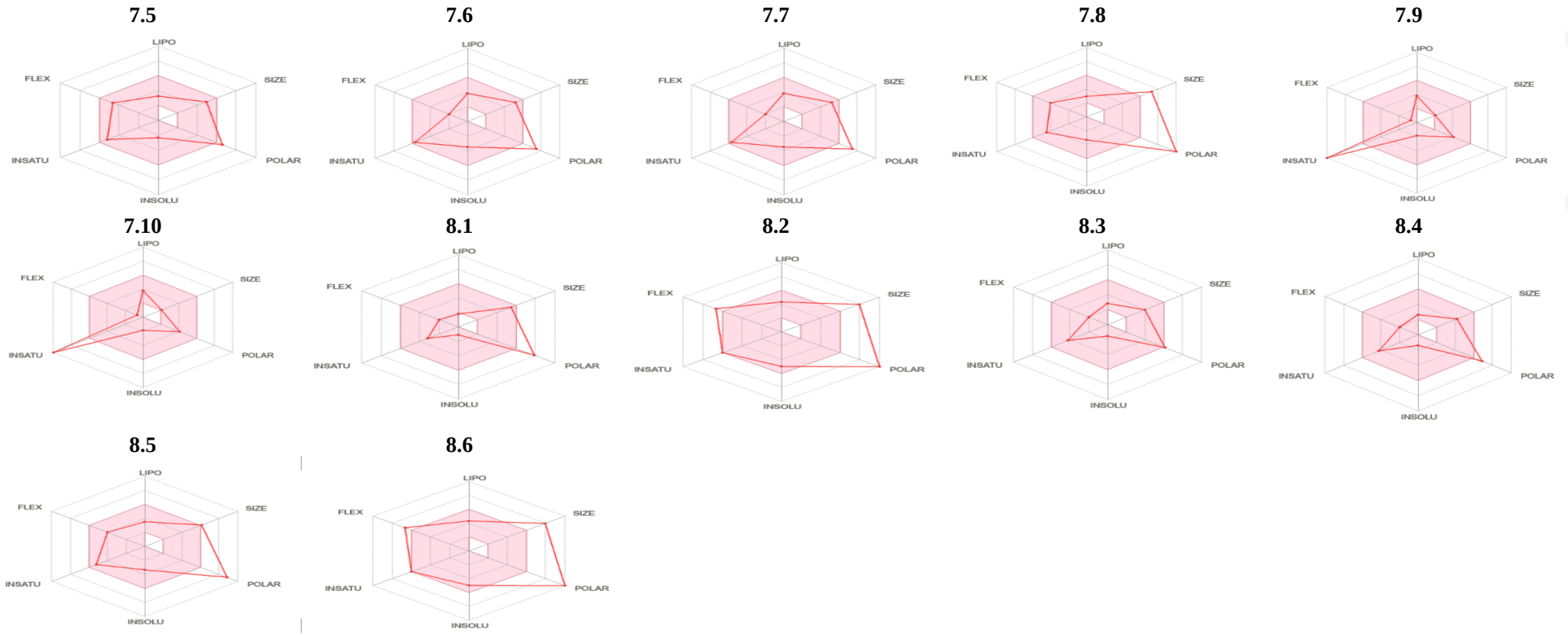

Figure 9.2: Physicochemical properties of compounds **6.1-6.11**, **7.1-7.10,** and **8.1-8.6**

Table 9.3: Physiological, pharmacokinetic, drug-likeness and lead-likeness properties of *L. frutescens*, *P. venus* and *L. xanthoconus* isolated compounds

	Physiochemical Parameters						Lipophilicity	Water Solubility	Pharmacokinetic Properties			Drug Likeliness/ Medicinal Chemistry		
Compounds	**Formula**	**MW (g/mol)**	**HA**	**RB**	**HBA**	**HBD**	**iLOGP**	**Log S (ESOL)**	**Gi Absorption**	**BBB Permeation**	**P-gp substrate**	**Lipinski rule**	**Bioavailability score**	**Lead likeness**
6.1	$C_{36}H_{56}O_9$	632.82	45	8	9	5	3.46	-5.59	Low	No	Yes	Yes; 1 violation	0.55	No; 3 violations
6.2	$C_{36}H_{58}O_8$	618.84	44	8	8	5	4.36	-6.54	Low	No	Yes	Yes; 1 violation	0.55	No; 3 violations
6.3	$C_{51}H_{74}O_{17}$	959.12	68	15	17	9	3.69	-6.58	Low	No	Yes	No; 3 violations	0.17	No; 2 violations
6.4	$C_{36}H_{58}O_9$	634.84	45	8	9	6	4.79	-5.53	Low	No	Yes	No; 2 violations	0.17	No; 3 violations
6.5	$C_{36}H_{58}O_9$	634.84	45	8	9	6	3.84	-5.80	Low	No	Yes	No; 2 violations	0.17	No; 3 violations
6.6	$C_{36}H_{60}O_{10}$	652.86	46	8	10	7	4.28	-5.18	Low	No	Yes	No; 2 violations	0.17	No; 2 violations
6.7	$C_{17}H_{18}O_5$	302.32	22	3	5	2	2.69	-3.75	High	Yes	Yes	Yes; 0 violations	0.55	Yes; 0 violation
6.8	$C_{17}H_{18}O_5$	302.32	22	3	5	2	2.69	-3.75	High	Yes	Yes	Yes; 0 violations	0.55	Yes; 0 violation
6.9	$C_{32}H_{36}O_{19}$	724.62	51	12	19	10	1.07	-2.65	Low	No	Yes	No; 3 violations	0.11	No; 2 violations
6.10	$C_5H_9O_2$	115.13	8	1	3	2	0.83	1.09	High	No	No	Yes; 0 violations	0.55	No; 1 violation
6.11	$C_7H_{14}O_6$	194.18	13	1	6	5	-0.24	1.02	Low	No	Yes	Yes; 0 violations	0.55	No; 1 violation
7.1	$C_{22}H_{24}O_{10}$	448.42	32	8	10	6	2.12	-2.89	Low	No	Yes	Yes; 1 violation	0.55	No; 2 violations
7.2	$C_{13}H_{22}O_9$	302.28	21	4	8	6	1.56	-2.33	Low	No	No	Yes; 1 violation	0.55	Yes; 0 violation
7.3	$C_{20}H_{22}O_{11}$	438.38	31	7	11	7	1.59	-2.41	Low	No	No	No; 2 violations	0.55	No; 1 violation
7.4	$C_{20}H_{22}O_{10}$	422.38	30	7	10	6	2.09	-2.07	Low	No	No	Yes; 1 violation	0.55	No; 1 violation

7.5	$C_{20}H_{22}O_9$	406.38	29	7	9	5	1.82	-2.33	Low	No	No	Yes; 0 violation	0.55	No; 1 violation
7.6	$C_{21}H_{20}O_{10}$	432.38	31	3	10	6	1.40	-3.47	Low	No	No	Yes; 1 violation	0.55	No; 1 violation
7.7	$C_{27}H_{30}O_{16}$	610.52	43	6	16	10	1.56	-3.30	Low	No	yes	No; 3 violations	0.17	No; 1 violation
7.8	$C_{21}H_{20}O_{11}$	448.38	32	3	11	7	1.43	-3.33	Low	No	No	No; 2 violations	0.17	No; 1 violation
7.9	$C_7H_7O_4$	154.12	11	1	4	3	0.66	-1.86	High	No	No	Yes; 0 violation	0.56	No; 1 violation
7.10	$C_7H_6O_3$	138.12	10	1	3	2	0.85	-2.07	High	Yes	No	Yes; 0 violation	0.85	No; 1 violation
8.1	$C_{20}H_{22}O_{12}$	454.38	32	3	12	5	1.07	-1.09	Low	No	Yes	Yes; 1 violation	0.55	No; 1 violation
8.2	$C_{32}H_{30}O_{16}$	670.57	22	10	16	8	3.19	-3.33	Low	No	No	No; 3 violations	0.17	No; 2 violations
8.3	$C_{15}H_{16}O_8$	324.28	23	3	8	4	0.82	-1.51	Low	No	No	Yes; 0 violation	0.55	Yes; 0 violation
8.4	$C_{15}H_{16}O_9$	340.28	24	3	9	5	0.98	-1.38	Low	No	No	Yes; 0 violation	0.55	Yes; 0 violation
8.5	$C_{23}H_{24}O_{13}$	508.43	36	6	13	7	2.55	-3.34	Low	No	yes	No; 3 violations	0.17	No; 1 violation
8.6	$C_{32}H_{30}O_{15}$	654.57	22	10	15	7	2.84	-5.10	Low	No	No	No; 3 violations	0.55	No; 2 violations

9.3.3 Molecular docking

Docking methods are used to position a ligand in a protein's active site and generate a scoring energy that helps estimate the compound's biological activity by analysing its interactions with the target. Known inhibitors and activators of the protein are also docked to calculate their scoring energies, which aids in determining whether the test compounds behave as activators or inhibitors. This approach also helps predict which molecules are more likely to exhibit effects against the target *in vitro* or *in vivo* assays. The docking score of the compounds with enough quantity for bioassay was assessed, and their binding affinity with the target proteins will be detailed in the following section.

9.3.3.1 Molecular docking of *L. frutescens* compounds

Neurodegeneration in PD involves the degradation of dopaminergic neuronal cells through the misfolding and aggregation of α-synuclein (SNCA), oxidative stress, mitochondrial dysfunction, excitotoxicity, ferroptosis, dysfunctional protein clearance, and neuroinflammation (Schapira, 2010; Devos et al., 2020). One of the critical therapeutic strategies employed in the management of PD is centred around levodopa. However, the prolonged utilisation of levodopa causes dyskinesia, drowsiness, low blood pressure, nausea, vomiting, and psychosis. This requires a diligent exploration of alternative treatment modalities like dopamine agonists, MAO-B inhibitors, COMT inhibitors, anticholinergics, N-methyl-D-aspartate receptor antagonists and medicinal plants having PD inhibitory effects to address the complexities of PD and optimise patient care (Kouli et al., 2018).

In this study, only biologically studied compounds (compounds **6.3-6.11)** were selected for molecular docking studies with the proteins DJ-1 and MAO-B, two biomarkers crucial in regulating neurodegenerative diseases, particularly PD (Ariga et al., 2013). By docking these compounds to DJ-1 and MAO-B, we aim to evaluate their binding affinities and potential therapeutic effects in PD using levodopa, curcumin, and resveratrol as controls. The tested compounds' binding affinities were determined through their docking score (Figures 9.3 and 9.4). To further validate the docking results, ligand interaction plots were generated using LigPlot (Tables 9.4 and 9.5), highlighting the intermolecular interactions stabilising these compounds within the active sites of MAO-B and DJ-1.

9.3.3.1.1 Monoamine Oxidase B (MAO-B)

The high level of MAO-B in the brain, coupled with its catalytic role in accelerating dopamine breakdown, leads to decreased dopamine in the PD brain (George et al., 2009). Inhibiting the MAO-B enzyme effectively maintains dopamine levels in the PD brain (Krishna et al., 2014). MAO-B inhibitors commonly used are rasagiline and selegiline (Riederer et al., 2004; Bianchi et al., 2018). Like dopamine agonists, they can serve as an initial therapy to delay the need for levodopa and alleviate levodopa-related motor symptoms (National Collaborating Centre for Chronic Conditions, 2006). While effective in the early stage of the disease, most patients eventually transition to levodopa-based treatment (Zahoor et al., 2018). When taken with L-DOPA, these inhibitors can withstand the response of L-DOPA for a year or more (Riederer et al., 2004).

In this MAO-B docking analysis, it was observed that compounds **6.3**-**6.6** and **6.9** do not bind to the protein, maybe due to structural instability of the molecule or geometric challenges (flexible docking, using Autodock Vina, only allows conformational variation in the ligand). However, compounds **6.7**, **6.8**, **6.10** and **6.11** do, with compounds **6.7** and **6.8** binding to the active site similar to that of selegiline, while compounds **6.10** and **6.11** bind like resveratrol (Figure 9.1), an inhibitor of MAO-B (Li et al., 2020; Carradori et al., 2022). Moreover, compounds **6.7** and **6.8** have the most optimal docking scores, highlighting their strong binding affinity to the binding site.

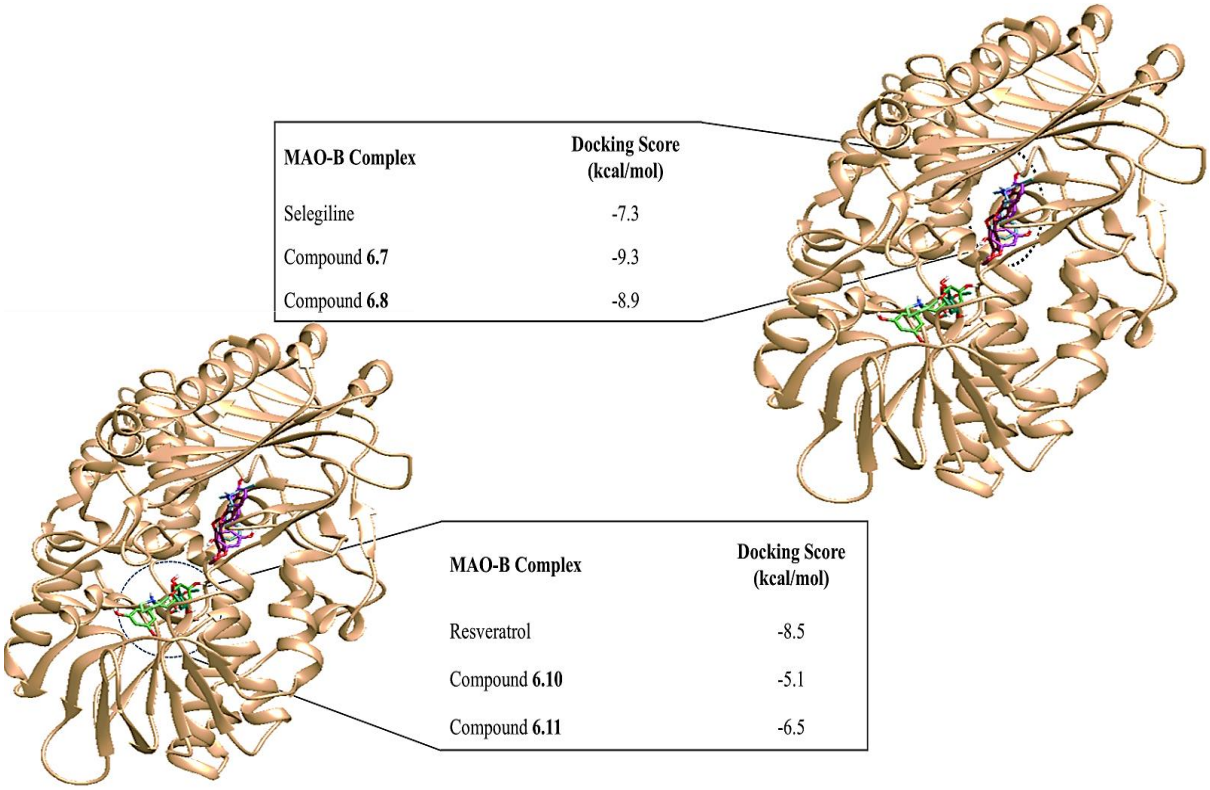

Figure 9.3: *In silico* binding affinity scores and superimposed docked complexes of *L. frutescens* tested compounds bound to MAO-B

Like Selegiline, compound **6.10** does not form hydrogen bonds (Table 9.4). Selegiline interacts with Gln206, Gly434, Leu171, Phe343, Tyr60, Tyr326, Tyr398, and Tyr435. Compound **6.7** interact with Cys172, Gln206, Gly434, Ile198, Leu171, Met436, Phe343, Tyr326, Tyr398 and forms a hydrogen bond with Tyr60 (3.60 Å). On the other hand, compound **6.8** interacts with Gly434, Gln206, Met436, Phe343, Tyr60, Tyr398, and Tyr435, and forms a hydrogen bond with Arg42 (2.85 Å). The inclusion of Leu171 and Tyr435 in compounds **6.7** and **6.8** hydrophobic interactions, respectively, strengthens their similarity to selegiline. However, the fact that compound **6.8** does not form a hydrogen bond with Tyr60 like selegiline but forms a hydrogen bond with Arg42 like resveratrol might make it a better MAO-B inhibitor than compound **6.7**.

Resveratrol binds with Ala35, Ala263, Glu34, Gly13, Gly41, Ile264, Lys271, Ser394, and Tyr393, forming hydrogen bonds with Arg42 (3.05 Å), Val10 (2.75 Å), and Leu33 (3.14 Å). Compound **6.10** displays more similar hydrophobic interactions with resveratrol than compound **6.11**. The fact that some of the hydrophobic interactions' residues in resveratrol form hydrogen bonds in compound **6.11** might affect the compound's potency.

Selegiline is a better MAO-B inhibitor, and compounds **6.7** and **6.8** have BBB permeability, good antioxidant properties, high GI, and a P-gp substrate, reinforcing their promising potential as neuroprotective drugs. Compounds **6.10** and **6.11**, although not displaying BBB permeability, can be administered intravenously or intranasally.

Table 9.4: Molecular docking score and ligand interaction plot analysis of *L. frutescens* compounds bound to MAO-B

Compounds	Docking score (kcal/mol)	Hydrophobic interactions	Hydrogen bonds (length-Å)
Selegiline	-7.3	Gln 206, Gly434, Leu171, Phe343, Tyr60, Tyr326, Tyr398, Tyr435	
Resveratrol	-8.5	Ala35, Ala263, Glu34, Gly13, Gly41, Ile264, Lys271, ser394, Tyr393	Arg42 (3.05), Val10 (2.75), Leu33 (3.14)
6.7	-9.3	Cys172, Gln206, Gly434, Ile198, Leu171, Met436, Phe343, Tyr326, Tyr398	Tyr60 (3.60)
6.8	-8.9	Cys397, Gly57, Gly58, Gly434, Gln206, Met436, Phe343, Tyr60, Tyr398, Tyr435	Arg42 (2.85)
6.10	-5.1	Ala35, Glu34, Ile264, Leu268, Tyr393	
6.11	-6.5	Ala263, Gly11, Gly41, Gly13, Gly12, Ile264, Pro265, Tyr393	Arg36 (2.71), Arg42 (2.94/2.76), Glu34 (3.14), Ser394 (2.88/3.05)

9.3.3.1.2 Parkinson Protein 7 (DJ-1)

DJ-1 is a protein related to the early onset of PD that exhibits neuroprotective effects, including the regulation of the PI3K/Akt pathway, antioxidant activity, transcriptional control, as well as chaperone and protease activities (Canet-Aviles et al., 2004). This protein serves as a protective function for dopamine neurons against damage induced by SNCA mutation, rotenone, 6-hydroxydopamine (6-OHDA), and hydrogen peroxide, mainly through its antioxidant property (Zimprich et al., 2004). The disease-causing mutants, such as L166P, E64D, M26I, and D149A, tend to heterodimerise with the wild-type DJ-1. Additionally, these mutated proteins frequently show misfolding, instability, and rapid degradation by the proteasome, thus compromising their neuroprotective and antioxidant activity (Klein & Westenberger, 2012). Deficiency in DJ-1 displays impaired locomotion, reduced activity in D2-type dopamine receptors, and heightened sensitivity to MPTP in mice (Ibanez & Andressoo, 2017). DJ-1 has been observed to co-localize with p-tau and SNCA, suggesting its potential significance in tauopathies and synucleinopathies (Blaszczyk, 2016). It also interacts with various chaperones, aiding in the degradation of

misfolded SNCA and influencing the expression of the tyrosine hydroxylase (TH) gene (Ariga et al., 2013).

In this docking study, the selected compounds exhibited varied binding affinities and interaction patterns, like either curcumin or levodopa. Molecular docking analysis (Figure 9.4) shows that compounds **6.3**, **6.5**, **6.6**, and **6.9** share the same binding pocket as curcumin, while compounds **6.7**, **6.8**, **6.10** and **6.11** bind in the same pocket as levodopa. Compound **6.5** demonstrated the highest binding score, followed by compounds **6.3**, **6.7**, **6.6**, **6.8**, **6.9**, **6.11**, and **6.10**.

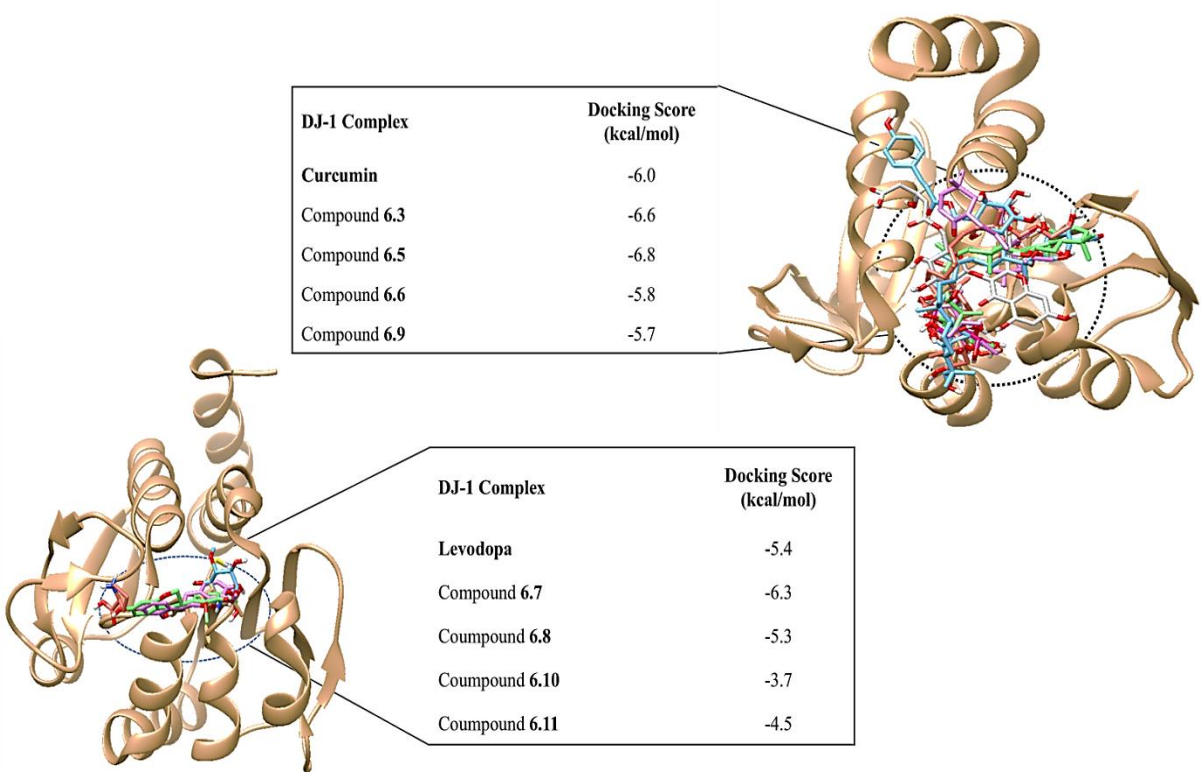

Figure 9.4: *In silico* binding affinity scores and superimposed docked complexes of *L. frutescens* tested compounds bound to DJ-1

While plotting the docking results, it was found that compound **6.4** broke into three fragments. As explained above, this could also be due to structural instability or geometric challenges. Curcumin has hydrophobic interactions with residues Arg156, Cys106, Glu15, Gly75, Gly159, His126, Pro158, and Thr160, and it forms multiple hydrogen bonds with Arg145 (2.88/2.93/3.11) and Asn76 (2.91/3.17). Cys106, particularly in its oxidised sulfinate form, is critical for DJ-1's cytoprotective functions, including ROS modulation, mitochondrial protection, inhibition of α-synuclein fibrillation, and DJ-1 translocation (Dash et al., 2020). Hydrophobic interactions between Cys106 and compounds **6.7**, **6.8**, and **6.11** suggest these

compounds may support DJ-1's cytoprotective effects. Compound **6.6** is the only compound forming multiple hydrogen bonds with Arg145, while compound **6.11** is the only one forming multiple hydrogen bonds with Asn76, like curcumin. These similarities suggest that compounds **6.6** and **6.11** might activate DJ-1's neuroprotective effects through antioxidant or anti-inflammatory mechanisms, like curcumin. However, forming extra hydrogen bonds with amino acids besides Arg145 and Asn76, as well as having slightly different hydrophobic interactions than curcumin's interaction profile, may influence the compounds' potency, either by enhancing or reducing it.

Compounds **6.8** and **6.10** do not display hydrogen bonds. However, they interact with all residues, forming hydrogen bonds or hydrophobic interactions with Levodopa, which suggests they might enhance DJ-1's neuroprotective effects comparable to levodopa.

Table 9.5: Molecular docking score and ligand interaction plot analysis of *L. frutescens* compounds bound to DJ-1

Compounds	**Docking scores (Kcal/mol)**	**Hydrophobic interactions**	**Hydrogen bonds (length-Å)**
Levodopa	-5.4	Asn76, Gly13, Gly75	Arg48 (3.35), Cys46 (3.07), Leu77 (2.87), Gln45 (2.51), Lys12 (3.00), Ser47 (3.22)
Curcumin	-6.0	Arg156, Cys106, Glu15, Gly75, Gly159, His126, Pro158, Thr160	Arg145 (2.88/2.93/3.11), Asn76 (2.91/3.17)
6.3	-6.6	Gly159, His126, Leu187, Leu128, Phe162, Pro158, Pro127, Thr160	Arg48 (3.06), Arg145 (3.11/2.87/2.97/ 2.97/3.11), Arg156 (2.97), Asn76 (2.80)
6.5	-6.8	Arg145, Arg156, Cys106, Glu15, Gly75, Gly159, His126, Pro158, Pro127, Thr160	Arg48 (2.91), Asn76 (2.95/3.03)
6.6	-5.8	Arg48, Arg156, Asn76, Gly157, His126, Pro158, Pro127	Arg145 (3.02/3.16), Gly159 (3.27), Glu (2.90)
6.7	-5.4	Arg48, Asn76, Cys46, Cys106, Gly75, His126, Leu128, Ser47	Gly13 (2.70), Leu77 (2.80)
6.8	-6.3	Arg48, Asn76, Cys46, Cys106, Gly13, Gly75, His126, Leu77, Ser47	
6.9	-5.7	Gly159, His126, Met17, Pro127	Arg48 (2.89/3.01), Arg145 (2.93/3.21), Pro158 (3.00)
6.10	-3.7	Asp49, Cys46, Gln45, Gly13, Lys12, Leu77, Ser47	
6.11	-4.5	Cys106, Glu15, Gly75, His126, Leu128, Pro158	Arg48 (3.01/3.23), Asn76 (3.01/324)

The fact that compounds **6.7** and **6.8** bind at the same binding pocket with levodopa and selegiline indicates their potential as promising drugs for neurodegenerative diseases like PD.

Compound **6.10** has high GI absorption and a lack of interaction with P-gp substrate, implying it will remain in the body longer when administered, potentially enhancing its efficacy. This could explain its significance ($p < 0.01$) in the ATP assay in Chapter Six, where it outperformed compound **6.11**, which may be more quickly eliminated due to being a P-gp substrate with low GI absorption.

While computational tools provide valuable insights into drug discovery, limitations remain in predictive models, particularly post-COVID adjustments in software such as ProtoxII and SwissADME. Given these predictive constraints, *in vivo* studies of compounds **6.7** and **6.8** are recommended to verify and expand upon the computational and *in vitro* findings.

9.3.3.2 Molecular docking of *P. venus* and *L. xanthoconus* compounds

DCM is characterised by oxidative stress, inflammation, myocardial fibrosis, autophagy, mitochondrial dysfunction, and lipid peroxidation, all exacerbated by hyperglycemia. Accumulated ROS activate the NRF2 signalling pathway, triggering antioxidant defences and modulating glucose metabolism. Lipid peroxides and ferroptosis further contribute to cardiomyocyte apoptosis and cardiac dysfunction, while glutathione peroxidase 4 (GPX4) activity mitigates lipid peroxidation and ferroptosis, offering a protective role (Xie et al., 2024). In this study the cardioprotective potential of compounds **7.3**-**7.6**, **8.3**, and **8.5** were investigated through molecular docking with key DCM biomarkers: KEAP1-NRF2, GPX4, and β1-AR (Brennan et al., 2017; Chen et al., 2021). Molecular docking was employed to assess their binding affinities and potential therapeutic effects. Antioxidants like ascorbic acid, curcumin, and vitamin E were included as controls for KEAP1-NRF2 and GPX4, each combating oxidative stress through distinct mechanisms. Curcumin directly modifies KEAP1 cysteine residues to prevent NRF2 degradation, promoting cytoprotective gene activation (Shin et al., 2020). Ascorbic acid scavenges ROS (Akram et al., 2017), while vitamin E neutralises lipid peroxides (Niki, 2021), complementing NRF2's antioxidant pathways.

For β1-AR, the β-blocker metoprolol and the agonist dobutamine known for preventing receptor overstimulation, reducing cardiomyocyte damage, and improving left ventricular function, were used as controls (Wang et al., 2018). Ligand interaction plots generated with LigPlot (Tables 9.6-9.8) further validated the docking results by highlighting the intermolecular interactions stabilising these compounds within the active sites of KEAP1-NRF2, GPX4, and β_1-AR.

9.3.3.2.1 Kelch-like ECH-associated protein 1-Nuclear factor erythroid-2-related factor 2 (KEAP1-NRF2)

The KEAP1-NRF2 system is a crucial defence mechanism against oxidative stress, regulating cytoprotective gene expression, mitochondrial function, and cellular energy metabolism (Murakami et al., 2023). Suppression of KEAP1 activates NRF2, enhancing mitochondrial membrane potential, boosting ATP production, and facilitating fatty acid uptake and oxidation. These effects preserve mitochondrial integrity, ensuring a stable energy supply and protecting against metabolic dysfunction and oxidative damage (Luchkova et al., 2024).

The KEAP1-NRF2 docking analysis revealed that the compounds successfully bound to the protein's active site, as shown in Figure 9.5. When comparing the binding affinities, curcumin, a known NRF2 activator with a protective effect against DCM had a docking score of -7.5 kcal/mol (Guan et al., 2019; Yu et al., 2016). The antioxidants ascorbic acid and vitamin E have docking scores of -6.1 kcal/mol and -5.7 kcal/mol. The selected compounds exhibited varying binding affinities, as reflected in their binding scores. Compound **7.5** demonstrated the strongest binding, showing a higher affinity than curcumin. In contrast, compound **8.5** had the weakest binding score, indicating a lower affinity compared to curcumin.

Keap1-Nrf2 Complex	Docking Score (kcal/mol)
Curcumin	-7.5
Ascorbic acid	-6.1
Vitamin E	-5.7
Compound **7.3**	-7.4
Compound **7.4**	-7.0
Compound **7.5**	-7.8
Compound **7.6**	-7.6
Compound **8.3**	-7.2
Compound **8.5**	-6.5

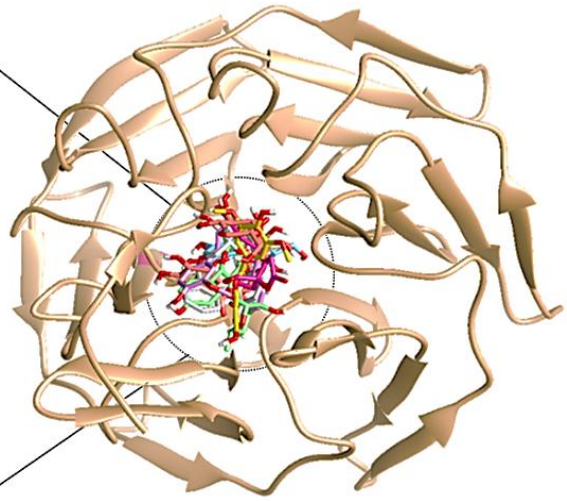

Figure 9.5: *In silico* binding affinity scores and superimposed docked complexes of *P. venus* and *L. xanthoconus* tested compounds bound to KEAP1-NRF2

In the KEAP1-NRF2 interaction plot, curcumin stabilises within the binding pocket primarily through hydrophobic interactions with crucial residues Gln75, Glu79, Asp77, Ile461, Arg415,

Arg380, Gly433, His436, Ser431, and Phe478. It also forms four hydrogen bonds with Arg483 (2.94 Å), Asn414 (3.05/2.77 Å), Glu78 (3.01 Å), and Leu84 (3.01 Å), strengthening its stability. Similarly, compound **7.6** forms hydrogen bonds with these four residues and additional bonds with Arg415 (3.08 Å), Arg380 (2.76 Å), Asp389 (3.30 Å), and Gly433 (2.70 Å). While compound **7.6** exhibits similar hydrophobic interactions to curcumin, three residues (Arg415, Arg380, and Gly433) involved in hydrophobic interactions in curcumin form hydrogen bonds in compound **7.6**. This suggests that compound **7.6** may mimic curcumin's activator role. However, its extra hydrogen bonds and reduced hydrophobic interactions could affect its hydrophobic stability and, consequently, protective efficacy.

Compound **7.5** forms hydrophobic interactions with Arg380, Leu84, His436, Ile461, and Phe478. Additionally, it engages in hydrogen bonds with Arg483 (3.08 Å), Glu78 (2.91/3.23 Å), Arg415 (3.26 Å), Asp77 (2.96 Å), Leu76 (3.20 Å), Glu79 (3.21 Å), and Gly433 (3.11 Å). Although it has fewer hydrophobic interactions compared to some other compounds, its higher number of hydrogen bonds, particularly with key residues such as Glu78, Arg380, and Asp77, significantly enhances its binding affinity, as reflected in its high docking score. Despite this, compound **7.5** did not significantly impact the experimental assay, reinforcing that computational predictions do not always align with empirical results.

Compounds **7.3**, **7.4**, and **8.5** exhibit hydrophobic interactions similar to those of vitamin E, highlighting their potential for scavenging lipid peroxyl radicals. However, their lack of significant cardioprotective effects suggests they may lack the chemical reactivity required to effectively neutralise these radicals or fail to target other critical mechanisms of DCM, such as mitochondrial dysfunction or inflammation.

Table 9.6: Molecular docking scores and ligand interaction plot analysis of *P. venus* and *L. xanthoconus* compounds bound to KEAP1-NRF2

Compounds	**Docking score (Kcal/mol)**	**Hydrophobic interaction**	**Hydrogen bonds (length-Å)**
Curcumin	-7.5	Gln75, Glu79, Asp77, Ile461, Arg415, Arg380, Gly433, His436, Ser431, Phe478	Arg483 (2.94), Asn414 (3.05/2.77), Glu78 (3.01) Leu84 (3.01)
Ascorbic acid	-6.1	Ala366, Ala556, Gly462, Gly509, Gly603, Leu557	Arg415 (3.13/3.23), Ala510 (3.08), Ile416 (2.79/2.88), Leu365 (2.87), Val463 (3.00)
Vitamin E	-5.7	Asp77, Arg483, Asn414, Cys434, Glu78, Gly433, Gly480, His436, Ile461, Leu84, Leu76, Phe478	Arg380 (2.95)

7.3	-7.4	Glu79, Asp77, Ile461, Leu84 His436, Phe83, Phe478	Arg483 (3.18), Arg415 (3.15), Arg380 (3.04), Leu76 (2.71), Glu78 (3.21), Glu82 (2.87), Gln75 (2.86)
7.4	-7.0	Arg380, Arg483, Arg415, Asp77, Gln75, Glu79, His436, Ile461, Leu84	Glu78 (3.16), Leu76 (2.67)
7.5	-7.8	Arg 380, Leu84, His436, Ile461, Phe478	Arg483 (3.08), Arg415 (3.26), Asp77 (2.96), Leu76 (3.20), Glu79 (3.21), Glu78 (2.91/3.23), Gly433 (3.11)
7.6	-7.6	Gln75, Glu79, Asp77, Ile461, His436, Ser431, Phe478	Arg483 (2.81), Arg415 (3.08), Arg380 (2.76), Asp389 (3.30), Leu84 (3.05), Glu78 (3.26), Gly433 (2.70), Asn414 (3.17)
8.3	-7.2	Ile461, Arg483, Phe478	Arg380 (3.21/3.16), Asp77 (3.12), Leu84 (3.05), Glu78 (3.09), Glu79 (3.19), His436 (3.12), Ser431 (2.97), Asn414 (2.94)
8.5	-6.5	Glu78, Asp77, Ile461, Arg380, Gly433, Gly480, Leu84, Leu76, Phe478	Arg483 (3.02), Arg415 (3.29), Ser431 (3.06), Asn414 (2.83)

9.3.3.2.2 Glutathione peroxidase 4

GPX4 is a key selenoprotein antioxidant enzyme crucial for detoxifying oxidative damage to membrane lipids and regulating ferroptosis, a non-apoptotic cell death triggered by oxidative stress and lipid peroxidation (Ran et al., 2007; Weaver & Skouta, 2022). Using glutathione (GSH) as a cofactor, GPX4 uniquely reduces lipid hydroperoxides, including those from cholesterol and phospholipids, into their respective alcohols, protecting cell membranes and maintaining mitochondrial integrity (Oh et al., 2022). Among its three isoforms: cytosolic (c-GPX4), mitochondrial (m-GPX4), and nuclear (n-GPX4), the mitochondrial form plays a crucial role in protecting cells from oxidative stress. It plays an indispensable role in maintaining mitochondrial integrity and function by preventing lipid peroxidation within the mitochondrial membrane, a process essential for energy production and cellular homeostasis (Cole-Ezea et al., 2012).

In the GPX4 complex (Figure 9.6), ascorbic acid, curcumin, and vitamin E have binding scores of -4.6, -5.2, and -5.9 kcal/mol. Compounds **7.3**-**7.6**, **8.3**, and **8.5** have binding scores ranging from -5.3 to -6.4 kcal/mol, with compound **7.5** showing the highest binding score (Table 9.7, Figure 9.6).

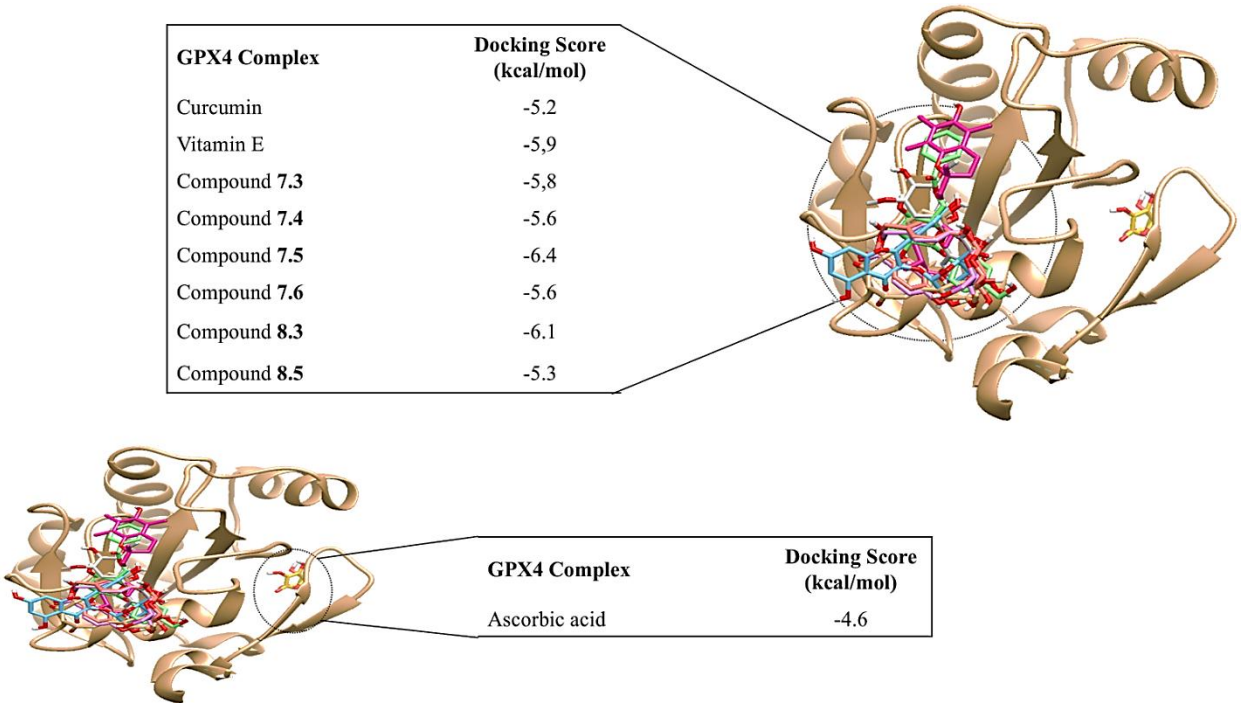

Figure 9.6: *In silico* binding affinity scores and superimposed docked complexes of *P. venus* and *L. xanthoconus* tested compounds bound to GPX4

The GPX4 protein binding profiles revealed unique and shared residues among the controls and tested compounds. Curcumin and vitamin E shared common hydrophobic interaction residues such as Ala133, Asn109, Ile122 and Trp8. Curcumin also interacts with Arg9 and Gly131, while vitamin E forms additional interactions with Lys121, Lys135, and Phe78. Ascorbic acid primarily interacted with residues such as Asp21, Val27, and Phe103. There is no overlap in the hydrogen bonds formed with residues in terms of controls. Additionally, ascorbic acid does not bind at the same site as curcumin and vitamin E on GPX4, as shown in Figure 9.6.

Compound **7.6** aligned closely with curcumin among the tested compounds, sharing hydrophobic interactions with residues such as Ala133, Gly131, Asn109 and Trp8. It also formed hydrogen bonds with Asn312, Arg9, Lys121and Gly110. However, Arg9 is a residue that has a hydrophobic interaction with curcumin, and the residue Lys 121 is distinct to vitamin E. Unlike curcumin, compound **7.6** lacked interactions with Ile122, a curcumin-specific residue.

Compound **7.3** showed a similar structural profile to curcumin but with additional hydrophobic interactions involving Asn232 and Lys118, which are some of the residues forming hydrogen bonds with curcumin. Like compound **7.6**, it formed hydrogen bonds with Arg9 and Lys121.

Compound **8.3** formed hydrogen bonds with Asn132, Gly110, and Lys118, resembling curcumin's interaction profile but differed in its unique hydrophobic interactions by binding with Asp111 instead of Ala133 and Gly131. This alteration in binding could account for the absence of antioxidant and cardioprotective activity of compound **8.3**.

Table 9.7: Molecular docking score and ligand interaction plot analysis of *P. venus* and *L. xanthoconus* compounds bound to GPX4

Compounds	Docking score (kcal/mol)	**Hydrophobic interaction**	**Hydrogen bonds (length-Å)**
Ascorbic acid	-4.6	Asp21, Val27, Phe103	Asp101 (2.85/2.86), Lys31 (2.98/3.10/3.19), Met102 (2.77)
curcumin	-5.2	Ala133, Arg9, Asn109, Gly131, Ile122, Trp8	Asn132 (2.88/3.19), Gly110 (2.97/3.14), Lys118 (3.16)
Vitamin E	-5.9	Ala133, Asn109, Asn132, Gly110, Ile122, Lys118, Lys121, Lys135, Phe78, Trp8	Gln77 (2.75)
7.3	-5.8	Ala133, Asn109, Asn132 Gly131, Ile122, Lys118, Trp8	Arg9 (2.96), Gly110 (2.92/3.11), Lys121 (2.99/3.26)
7.4	-5.6	Asn109, Asn132, Gly131, Ile122, Lys118, Trp8	Ala133 (3.21), Asp111 (3.11), Gly110 (2.91/3.11), Lys121 (3.00/3.25)
7.5	-6.4	Asn109, Gly131, Lys118, Trp8	Ala133 (3.10), Asn132 (3.03), Gly110 (2.95/3.00), Lys121 (2.96/3.08)
7.6	-5.6	Ala133, Asn109, Gly131, Lys118, Trp8	Arg9 (3.05), Asn132 (2.98), Gly110 (2.99), Lys121 (3.24)
8.3	-6.1	Arg9, Asp111, Asn109, Ile122, Trp8	Asn132 (2.87), Gly110 (3.06/3.09/3.24), Lys118(2.89)
8.5	-5.3	Ala133, Asn109, Gly110, Ile122, Lys121, Trp8	Lys118 (2.75)

9.3.3.2.3 Beta-1 adrenergic receptor (β_1-AR)

The β_1-AR plays a central role in the pathophysiology of heart disease and is a key therapeutic target. The β_1-AR is the primary subtype on cardiomyocytes. When activated, it increases cardiac contractility by triggering protein kinase A (PKA)-mediated phosphorylation of key proteins. These proteins regulate intracellular Ca^{2+} levels and myofilament sensitivity, including L-type Ca^{2+} channels, ryanodine receptors, phospholamban, and troponin I (Salazar et al., 2007; Devic, 2001). Dysregulation of β_1-AR signalling, as seen in heart failure, leads to cardiomyocyte hypertrophy and progressive dysfunction (Baker, 2005). β-blockers, including carvedilol, bisoprolol, and metoprolol, mitigate this by preventing receptor overstimulation, normalizing signaling, and improving left ventricular function (Wang et al., 2018).

In the β_1-AR complex (Figure 9.7), the isolated compounds **7.3** (-6.0 kcal/mol), **7.6** (-6.0 kcal/mol), and **8.3** (-5.6 kcal/mol) did not bind at the active site, indicating that they likely do

not exert a protective effect through the β_1-AR pathway (Figure 9.4). On the other hand, compound **8.5** showed a binding score of -8.1 kcal/mol, identical to that of dobutamine, a known β_1-AR activator. Similarly, compound **7.5** had a binding score of -6.9 kcal/mol, the same as metoprolol, a β_1-AR inhibitor. Compounds **7.4** exhibited binding scores of -8.5 kcal/mol which is higher than dobutamine binding score.

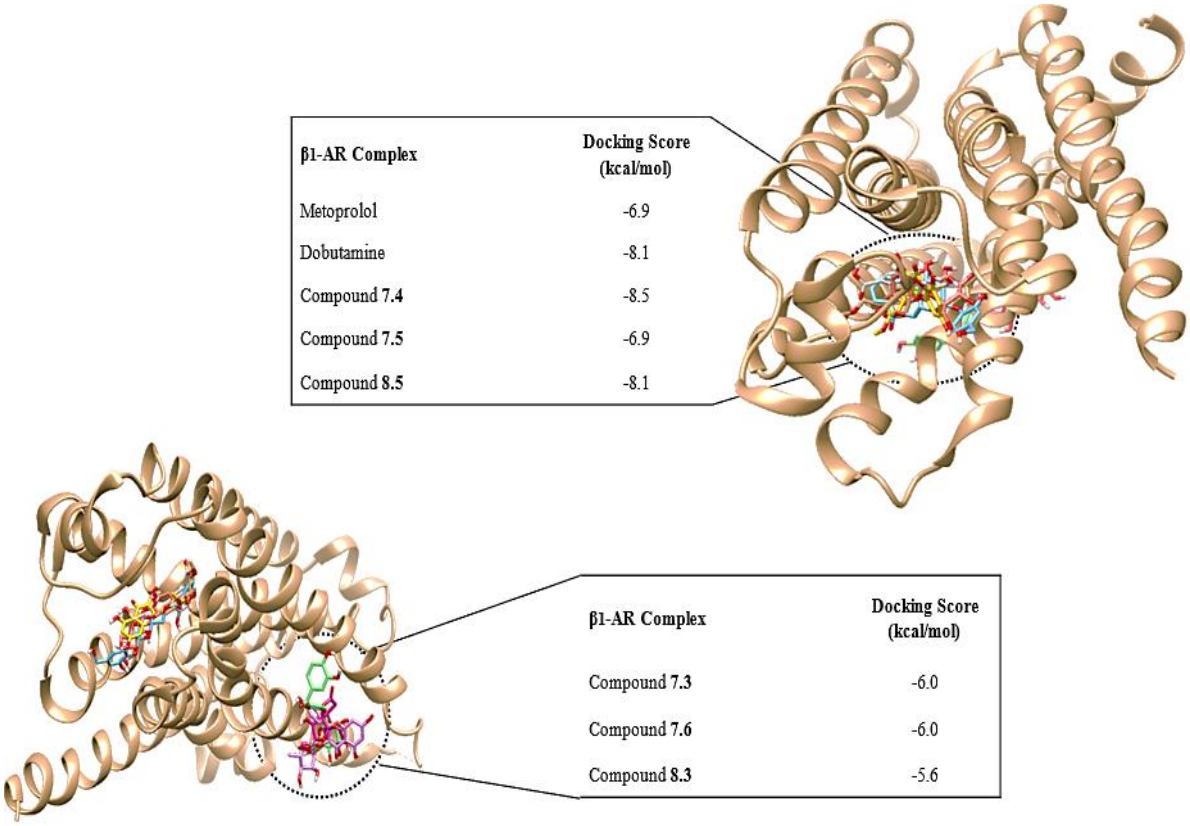

Figure 9.7: *In silico* binding affinity scores and superimposed docked complexes of *P. Venus* and *L. xanthoconus* tested compounds bound to β_1-AR

In the β-1 AR interaction plot, metoprolol exhibits strong binding affinity due to its two hydrogen bonds with Cys199 (2.78 Å) and Asn310 (2.87 Å), which confer high binding stability and likely explain its effective β-1 AR inhibition. Dobutamine, on the other hand, forms hydrogen bonds with Tyr333 (3.15 Å), Ser211 (3.03/2.79 Å), and Gly98 (3.0 Å). Though these bonds are slightly longer, they stabilise the binding pocket. It also shares several hydrophobic interactions with metoprolol (Asn329, Asp200, Trp330, and Phe306), contributing to its binding affinity.

Compound **7.4** demonstrates a higher binding score than dobutamine and exhibits a similar hydrophobic interaction profile. Additionally, compound **7.4** forms hydrogen bonds with

Asp121 (2.98 Å), Asn310 (3.11 Å), and Ser211 (3.12 Å), indicating it may share binding characteristics with dobutamine. Compound **7.5** shows hydrophobic interactions similar to metoprolol and dobutamine, potentially indicating a similar receptor-binding profile. It also forms hydrogen bonds with Asp121 (2.71 Å) and Asp200 (3.05 Å), which are also involved in metoprolol binding, as well as additional interactions with residues such as Asn310, Asn329, Trp117, Val122, Val326, Leu101, Phe201, Phe306, and Phe325.

Some tested compounds, such as **7.3**, **7.6**, and **8.3**, exhibit hydrophobic interactions and hydrogen bonds that imply binding at a different pocket than metoprolol or dobutamine. These compounds each form only one hydrogen bond, suggesting moderate interaction and potentially weaker stability relative to metoprolol and dobutamine.

Compound **8.5** demonstrates promising binding affinity to β_1-AR by forming hydrogen bonds with Asp200 (3.08 Å), Asn310 (2.79/3.01 Å), and Asn329 (2.92 Å), in addition to multiple hydrophobic interactions with Cys199, Asp121, Trp117, Thr118, Val122, Val326, Phe201, Phe306, Phe307, and Phe325. While both compound **8.5** and metoprolol share several hydrophobic interactions, there are notable differences. Metoprolol forms a hydrogen bond with Cys199 (2.78 Å), whereas compound **8.5** engages Cys199 in hydrophobic interactions. Furthermore, while metoprolol relies on hydrophobic interactions with Asp200 and Asn329, these residues form hydrogen bonds with compound **8.5**. These differences in their interaction profiles could explain their distinct pharmacological effects.

Table 9.7: Molecular docking scores and ligand interaction plot analysis of *P. venus* and *L. xanthoconus* compounds bound to β_1-AR

Compounds	**Docking score (kcal/mol)**	**Hydrophobic interaction**	**Hydrogen bonds (length-Å)**
Metoprolol	-6.9	Asn329, Asp200, Ala208, Asp121, Trp117, Tyr333, Trp330, Val326, Phe201, Phe306, Ser211, Thr203, Tyr207	Cys199 (2.78), Asn310 (2.87)
Dobutamine	-8.1	Asn329, Asp200, Trp117, Trp330, Val122, Leu101, Phe201, Phe306, Phe325, Phe 307	Tyr333 (3.15), Ser211 (3.03/2.79), Gly98 (3.0)
7.3	-6.0	Tyr231, Gly297, Ile224, Thr300, Met296, Leu220, Leu220, Ile224, Thr300, Met296	Lys 290 (3.09)
7.4	-8.5	Asn329, Leu101, Phe201, Phe325, Phe306, Phe307, Trp117, Trp303, Val102, Val326	Asp121 (2.98), Asn310 (3.11), Ser211 (3.12)
7.5	-6.9	Asn310, Asn329, Trp117, Val122, Val326, Leu101, Phe201, Phe306, Phe325, Phe 307	Asp121 (2.71), Asp200 (3.05)
7.6	-6.0	Tyr231, Gly297, Ile224, Thr300, Met296, Leu228, Gly293, Ile294	Lys 290 (2.73)
8.3	-5.6	Gly297, Ala227, Leu228, Ile224, Tyr231	Gly 293 (2.74)

8.5	-8.1	Cys199, Asp121, Trp117, Thr118, Val122, Val326, Phe201, Phe306, Phe307, Phe325	Asp200 (3.08), Asn310 (2.79/3.01), Asn329 (2.92)

The findings emphasize curcumin's strong interaction network within KEAP1-NRF and GPX4, reinforcing its role as a potent NRF2 activator and modulator of oxidative stress. Ascorbic acid and vitamin E, while functioning primarily as complementary antioxidants, exhibited interaction profiles that support their roles in maintaining redox homeostasis. However, based on the binding interactions and scoring energy, the tested compounds are likelier to exhibit activity through the KEAP1-NRF2 pathway rather than the β_1-AR mechanism of action. Among the tested compounds, compound **7.6** emerges as the most promising candidate to showcase the cardioprotective effect through the KEAP1-NRF2 pathway. Nevertheless, compound **7.6** was the only tested compound (see Chapter Seven) to show some cardioprotective effect. While compound **7.6** has moderate protective effects, its low GI absorption suggests oral administration might not be ideal. Instead, alternative routes like intravenous could be more effective, allowing the drug to reach target sites without GI limitations.

Conclusion

The computational analysis of selected phytochemicals from *L. frutescens*, *P. venus*, and *L. xanthoconus* has identified promising candidates for addressing PD and DCM.

Compounds **6.7** and **6.8** demonstrated strong binding affinities to PD-related targets, DJ-1 and MAO-B, suggesting their potential as neuroprotective agents. These compounds exhibited favourable docking profiles, optimal pharmacokinetic properties, and positive *in vitro* results.

For DCM-related targets, compounds **7.6**, **7.3** and **8.5** showed significant binding interactions with KEAP1-NRF2, GPX4 and β_1-AR, respectively. Furthermore, it was observed that *P. venus* and *L. xanthoconus* compounds are more likely to exert their cytoprotective effect through the KEAP1-NRF2 pathway. While *in vitro* studies demonstrated that only compound **7.6** displayed a moderate cardioprotective effect. It is crucial to understand that although docking studies provide valuable insights into geometric fit, they are limited in predicting real-world biological activity. Thus, further *in vitro* and *in vivo* investigations and molecular dynamics simulations are crucial to better understand the compounds' binding affinities and their therapeutic potential.

Nevertheless, this study paves the way for future research on compounds **6.7** and **6.8**, which show the most promise for advancing into the drug development pipeline as potential therapeutic agents for PD.

References

Akram, N. A., Shafiq, F. & Ashraf, M. (2017). Ascorbic acid-a potential oxidant scavenger and its role in plant development and abiotic stress tolerance. *Frontiers in Plant Science*, 8(613): 1-17.

Ariga, H., Takahashi-Niki, K., Kato, I., Maita, H., Niki, T. & Iguchi-Ariga, S. M. M. (2013). Neuroprotective function of DJ-1 in Parkinson's disease. *Oxidative Medicine and Cellular Longevity*, 2013: 1-9.

Banerjee, P., Kemmler, E., Dunkel, M. & Preissner, R. (2024). ProTox 3.0: A webserver for the prediction of toxicity of chemicals. *Nucleic Acids Research*, 52(1): 513-520.

Berman, H. M., Westbrook, J., Feng, Z., Gilliland, G., Bhat, T. N., Weissig, H., Shindyalov, I. N. & Bourne, P. E. (2000). The Protein Data Bank. *Nucleic Acids Research*, 28(1): 235-242.

Bianchi, P., Cerri, S., Dani, M., Nuzzi, A., Spadoni, G. & Blandini, F. (2018). The evolving role of MAO-B inhibitors in Parkinson's disease treatment. *Parkinsonism & Related Disorders*, 60: 32-38.

Binda, C., Newton-Vinson, P., Hubálek, F., Edmondson, D. E. & Mattevi, A. (2002). Structure of human monoamine oxidase B, a drug target for the treatment of neurological disorders. *Nature Structural Biology*, 9(1): 22-26.

Blaszczyk, J. W. (2016). Parkinson's disease and neurodegeneration: Gaining insight into disease mechanisms. *Frontiers in Aging Neuroscience*, 8: 31.

Brennan, J. P., Bardswell, S. C., Burgoyne, J. R., Fuller, W., Schröder, E., Wait, R. & Eaton, P. (2017). NRF2 is a key regulator of diabetic cardiomyopathy development. *Free Radical Biology and Medicine*, 112: 64-74.

Canet-Avilés, R. M., Wilson, M. A., Miller, D. W., Ahmad, R., McLendon, C., Bandyopadhyay, S. & Cookson, M. R. (2004). The Parkinson's disease protein DJ-1 is neuroprotective due to cysteine-sulfinic acid-driven mitochondrial localization. *Proceedings of the National Academy of Sciences*, 101(24): 9103-9108.

Carradori, S., Secci, D., Bolasco, A. & Chalupova, Z. (2022). Monoamine oxidase B inhibitors and their potential in Parkinson's disease. *European Journal of Medicinal Chemistry*, 232: 114167.

Chen, Y., Wei, Y., Zhao, X., Tao, L. & Zhang, L. (2021). β-adrenergic receptor signaling and its differential effects on cardiac function in diabetic cardiomyopathy. *Biochimica et Biophysica Acta (BBA) - Molecular Basis of Disease*, 1867(6): 166042.

Cole-Ezea, P., Swan, D., Shanley, D. & Hesketh, J. (2012). Glutathione peroxidase 4 has a major role in protecting mitochondria from oxidative damage and maintaining oxidative phosphorylation complexes in gut epithelial cells. *Free Radical Biology and Medicine*, 53(3): 488-497.

Daina, O., Michielin, V. & Zoete, A. (2017). SwissADME: a free web tool to evaluate pharmacokinetics, drug-likeness and medicinal chemistry friendliness of small molecules. *Scientific Reports*, 7: 42717.

Devos, D., Hirsch, E. & Wyse, R. (2021). Seven solutions for neuroprotection in Parkinson's disease. *Journal of Movement Disorders*, 36: 306-316.

Ekins, S., Mestres, J. & Testa, B. (2007). In silico pharmacology for drug discovery: Applications to targets and beyond. *British Journal of Pharmacology*, 152 (1): 21-37.

George, D. S., Varghese, T. S., Manjari, S. & Pillai, R. K. (2009). Monoamine oxidase B and its inhibitors in neurodegenerative disease. *Journal of Neurochemistry*, 109(6): 1360-1372.

Gallo, K., Goede, A., Preissner, R. & Gohlke, B. (2022). SuperPred 3.0: drug classification and target prediction—a machine learning approach. *Nucleic Acids Research*, 50(1): 726-731.

Guan, G., Lei, L., Lu, Q., Gong, Y. & Yang, L. (2019). Curcumin attenuates palmitic acid-induced cell apoptosis by inhibiting endoplasmic reticulum stress in H9c2 cardiomyocytes. *Human and Experimental Toxicology*, 38(6): 655-664.

Hendlich, M. (1998). Databases for protein-ligand complexes. *Acta Crystallographica Section D Biological Crystallography*, 54: 1178-1182.

Huang, J., Chen, S., Zhang, J. J. & Huang, X. Y. (2013). Crystal structure of oligomeric β 1-adrenergic G protein-coupled receptors in ligand-free basal state. *Nature Structural and Molecular Biology*, 20(4): 419-425.

Ibáñez, P. & Andressoo, J. O. (2017). Mouse models of Parkinson's disease with deficits in the DJ-1 gene: Effects on dopamine receptor activity and responses to MPTP. *Journal of Neurochemistry*, 142(2): 267-280.

Ingold, I., Berndt, C., Schmitt, S., Doll, S., Poschmann, G., Buday, K., Roveri, A., Peng, X., Porto Freitas, F., Seibt, T., Mehrabadi, J. F., Aichler, M., Walch, A., Lamp, D., Jastroch, M., Miyamoto, S., Wurst, W., Ursini, F., Arnér, E.S.J., Fradejas-Villar, N., Schweizer, U., Zischka, H., Angeli, J. P. F. & Conrad, M. (2018). Selenium utilization by GPx4 is required to prevent hydroperoxide-induced ferroptosis. *Cell*, 172(3): 409-422.

Klein, C. & Westenberger, A. (2012). Genetics of Parkinson's disease. *Cold Spring Harbor Perspectives in Medicine*, 2(1): a008888.

Kouli, A., Torsney, K. M., & Kuan, W. L. (2018). Parkinson's disease: Etiology, neuropathology, and pathogenesis. *Parkinson's Disease: Pathogenesis and Clinical Aspects*. Stoker, T. B., Greenland, J. C., Eds. Codon Publications: Brisbane, Australia, 1-45.

Krishna, R., Johnson, M. E., Zaleska, M. & Samanta, S. (2014). Targeting MAO-B in neurodegenerative disorders: A promising therapeutic strategy. *European Journal of Pharmacology*, 765: 173-181.

Li, X., Feng, Y., Deng, Z., & Zhao, D. (2020). Resveratrol as a multifunctional agent: A promising therapeutic strategy in neurodegenerative diseases. *Antioxidants*, 9(7): 616.

Lipinski, C. A., Lombardo, F., Dominy, B. W. & Feeney, P. J. (1997). Experimental and computational approaches to estimate solubility and permeability in drug discovery and development settings. *Advanced Drug Delivery Reviews*, 23(1): 3-25.

Lo, S. C., Li, X., Henzl, M. T., Beamer, L. J. & Hannink, M. (2006). Structure of the KEAP1 interface provides mechanistic insight into NRF2 signaling. *EMBO Journal*, 25(15): 3605-3617.

Lohse, M. J., Engelhardt, S. & Eschenhagen, T. (2003). What Is the Role of β-Adrenergic Signaling in Heart Failure?. *Circulation Research*, 93(10): 896-906.

Lu, W., Zhu, M., Lin, Q., Liu, C. & Wang, J. (2019). Modulation of the KEAP1-NRF2 signaling pathway for diabetic cardiomyopathy treatment. *Frontiers in Physiology*, 10: 741.

Luchkova, A., Mata, A. & Cadenas, S. (2024). Nrf2 as a regulator of energy metabolism and mitochondrial function. *FEBS Letters*, 598: 2092-2105

Maita, C., Maita, H., Iguchi-Ariga, S. M., & Ariga, H. (2009). Monomer DJ-1 and its N-terminal sequence are necessary for mitochondrial localization of DJ-1 mutants. *PLoS One*, 4(12): e8316.

Miyamae, Y., Shibata, H. & Kondo, T. (2014). Molecular docking analysis of neuroprotective effects of DJ-1 ligands. *Biological and Pharmaceutical Bulletin*, 37(2): 301-305.

Morris, G. M. & Lim-Wilby, M. (2008). Molecular Docking. In: Kukol, A. (eds) *Molecular Modeling of Proteins. Methods Molecular Biology*. Humana Press.

Murakami, S., Kusano, Y., Okazaki, K., Akaike, T. & Motohashi, H. (2023). NRF2 signalling in cytoprotection and metabolism. *British Journal of Pharmacology*, 1-14.

National Collaborating Centre for Chronic Conditions. (2006). *Parkinson's Disease: National Clinical Guideline for Diagnosis and Management in Primary and Secondary Care*. London: Royal College of Physicians.

Niki, E. (2021). Lipid oxidation that is, and is not, inhibited by vitamin E: Consideration about physiological functions of vitamin E. *Free Radical Biology and Medicine*, 176: 1-15.

Oh, S. J., Ikeda, M., Ide, T., Hur, K. Y. & Lee, M. S. (2022). Mitochondrial event as an ultimate step in ferroptosis. *Cell Death Discovery*, 8(1): 1-13.

Pillai, O., Dhanikula, A. B. & Panchagnula, R. (2001). Drug delivery: an odyssey of 100 years. *Current Opinion in Chemical Biology*, 5: 439-446.

Pognan, F., Beilmann, M., Boonen, H. C. M., Czich, A., Dear, G., Hewitt, P., Mow, T., Oinonen, T., Roth, A., Steger-Hartmann, T., Valentin, J. P., Van Goethem, F., Weaver, R. J. & Newham, P. (2023). The evolving role of investigative toxicology in the pharmaceutical industry. *Nature Reviews Drug Discovery*, 22(4): 317-335.

Ran, Q., Liang, H., Ikeno, Y., Qi, W., Prolla, T. A., Jackson Roberts, L. I., Wolf, N., VanRemmen, H., Richardson, A. & Antonio, S. (2007). Reduction in Glutathione Peroxidase 4 Increases Life Span Through Increased Sensitivity to Apoptosis. *Journal of Gerontology: BIOLOGICAL SCIENCES*, 62A(9): 932-942.

Riederer, P., Laux, G. & Nagatsu, T. (2004). Parkinson's disease and neurotransmission. *Journal of Neural Transmission*, 111(11-12): 1365-1378.

Schapira, A. H. V. (2010). Neuroprotection in Parkinson's Disease. *Blue Books Neurol*, 34: 301-320.

Scheerer, P., Borchert, A., Krauss, N., Wessner, H., Gerth, C., Höhne, W. & Kuhn, H. (2007). Structural basis for catalytic activity and enzyme polymerization of phospholipid hydroperoxide glutathione peroxidase-4 (GPx4). *Biochemistry*, 46(31): 9041–9049.

Shin, J. W., Chun, K. S., Kim, D. H., Kim, S. J., Kim, S. H., Cho, N. C., Na, H. K. & Surh, Y. J. (2020). Curcumin induces stabilization of Nrf2 protein through Keap1 cysteine modification. *Biochemical Pharmacology*, 173, 1-12.

Wang, Y. D., Zhang, Y., Sun, B., Leng, X. W., Li, Y. J. & Ren, L. Q. (2018). Cardioprotective effects of rutin in rats exposed to pirarubicin toxicity. *Journal of Asian Natural Products Research*, 20(4): 361-373.

Weaver, K. & Skouta, R. (2022). The Selenoprotein Glutathione Peroxidase 4: From Molecular Mechanisms to Novel Therapeutic Opportunities. *Biomedicines*, 10: 1-20.

Xie, L., Yu, Z. Q., Zhang, R., Zhang, Z. P., Zhang, Y., Jin, M. Y., Ju, Y., Zhao, X. H. & Guo, J. P. (2024). Phloridzin prevents diabetic cardiomyopathy by reducing inflammation and oxidative stress. *European Journal of Pharmacology*, 984, 1-12.

Yu, W., Zha, W., Ke, Z., Min, Q., Li, C., Sun, H. & Liu, C. (2016). Curcumin Protects Neonatal Rat Cardiomyocytes against High Glucose-Induced Apoptosis via PI3K/Akt Signalling Pathway. *Journal of Diabetes Research*, 2016: 1-11.

Zahoor, I., Shafi, A. & Haque, R. (2018). Parkinson's disease: Recent advances in the development of therapeutics. *International Journal of Health Sciences*, 12(6): 21-29.
Zimprich, A., Biskup, S., Leitner, P., Lichtner, P., Farrer, M., Lincoln, S. & Gasser, T. (2004). Mutations in LRRK2 cause autosomal-dominant parkinsonism with pleomorphic pathology. *Neuron*, 44(4): 601-607.

CHAPTER TEN: Conclusion and Recommendations

10.1 Conclusion

For centuries, plants have been vital in treating ailments. However, the rise of synthetic drug development in the late 19th century shifted focus away from natural products due to lengthy isolation processes and limited yields. Recently, interest in medicinal plants has resurged, driven by concerns over synthetic drug side effects and the recognition of plants as untapped reservoirs of therapeutic secondary metabolites. Despite this resurgence, many plants remain understudied, including *L. frutescens*, *P. venus*, and *L. xanthoconus*. While *L. frutescens* is well-researched for its ethnobotanical uses, *P. venus* and *L. xanthoconus*, though primarily ornamental, belong to a family rich in bioactive phenolic compounds with therapeutic potential. This study conducted a comprehensive phytochemical analysis of these plants, resulting in the isolation of 28 compounds: 6 cycloartane glycosides (**6.1**-**6.6**), 8 flavonoids (**6.7**-**6.9**, **7.6**-**7.8**, **8.2**, **8.5**, and **8.6**), 11 phenolic compounds (**7.1**-**7.5**, **7.9**, **7.10**, **8.1**, **8.3**, and **8.4**), 2 sugars (**6.11** and **7.11**), and 1 amino acid (**6.10**). Among these, five novel compounds namely lessertiosides A (**6.1**) and B (**6.2**), *p*-coumaroylcalleryanin (**7.1**), dichotomain C (**8.1**), and syringetin-3-*O*-(6′′-caffeoyl)-*β*-*D*-glucopyranoside (**8.2**), were discovered, underscoring the rich phytochemical diversity of these plants.

From *L. frutescens*, compounds **6.3**-**6.11** demonstrated neuroprotective potential by enhancing cell viability, maintaining ATP production, and reducing apoptotic activity in SH-SY5Y-induced MPP^+ toxicity, with compound **6.8** being the most potent. Compounds **6.7** and **6.8** emerged as promising candidates for PD therapy, exhibiting favourable pharmacokinetic profiles and docking affinities with MAO-B and DJ-1 comparable to standard treatments such as levodopa and selegiline. However, their classification as P-gp substrates suggests that dose optimisation or alternative delivery methods may be necessary to achieve therapeutic concentrations in the brain. These findings align with the plant's use in managing stress-related and neurodegenerative conditions, further validating its therapeutic potential.

The study also marks the first phytochemical investigation of *P. venus*. Compounds **7.3** and **7.9** exhibited excellent antioxidant activity, likely via the SET mechanism. In contrast, compound **7.6** showed moderate cardioprotective effects by enhancing ATP levels, with computational studies suggesting its activity operates through the KEAP1-NRF2 pathway. However, low gastrointestinal absorption for compound **7.6** indicates that intravenous administration may be more effective than oral delivery. Minimal cytotoxicity against H9c2, C3A, and MCF-7 cells

further supports the safety profile of *P. venus* extracts and compounds, highlighting their potential for therapeutic applications.

Similarly, the phytochemical exploration of *L. xanthoconus* represents a groundbreaking contribution, as this species had not been studied previously. Compound **8.5** exhibited good antioxidant activity and weak cytotoxicity against H9c2 cells, while the crude extract and compound **6.5** displayed weak antioxidant activity. No cardioprotective effects were observed among *L. xanthoconus* compounds and crude extract. Computational studies on leucodrin (**8.3**) and leudrin (**8.4**) revealed that, despite their low gastrointestinal absorption, these compounds possess drug optimisation potential through approaches such as prodrug design, nanoparticle encapsulation, or parenteral administration.

Overall, this research highlights the therapeutic potentials of *L. frutescens, P. venus*, and *L. xanthoconus*. These plants underscore the importance of biodiversity-driven drug discovery by addressing global health challenges such as neurodegenerative and cardiovascular diseases, which remain significant burdens worldwide. The findings contribute to understanding South Africa's fynbos flora as a rich reservoir of bioactive compounds with potential applications in neuroprotection, antioxidant therapy, and cardioprotection.

10.2 Recommendations

The following recommendations are proposed:

❖ Pharmacological and mechanistic studies

Future research should focus on the *in vivo* validation of compounds **6.7**, **6.8**, **7.3**, **7.9**, and **7.6** to confirm their therapeutic effects, specifically for neurodegeneration, antioxidant activity, and cardioprotection. The mechanisms of action of these compounds should be further investigated to gain deeper insights into their pharmacodynamic properties.

❖ Drug delivery optimisation

Drug delivery optimisation is essential for improving the bioavailability and pharmacokinetics of these compounds. To enhance their therapeutic efficacy, compounds with low bioavailability should be explored using nanoparticle-based systems, prodrug design, and parenteral administration.

❖ **Molecular simulations**

Molecular dynamics simulations should be employed to study the compounds' stability, binding affinity, and interaction patterns with their targets under physiological conditions. This will guide the refinement of structure-activity relationships (SAR) and help optimise compounds for enhanced efficacy.

❖ **Sustainable harvesting and conservation strategies**

Sustainable harvesting practices and conservation strategies must be implemented to ensure the long-term availability of key species such as *L. frutescens*, *P. venus*, and *L. xanthoconus*. These strategies consist of controlled cultivation, habitat preservation, and regulated harvesting to protect these valuable species and ensure they remain accessible for future pharmacological research and drug discovery.

Appendix A: NMR spectra of compound 6.1 (CD_3OD)

Appendix A1: ^1H NMR spectrum of compound 6.1

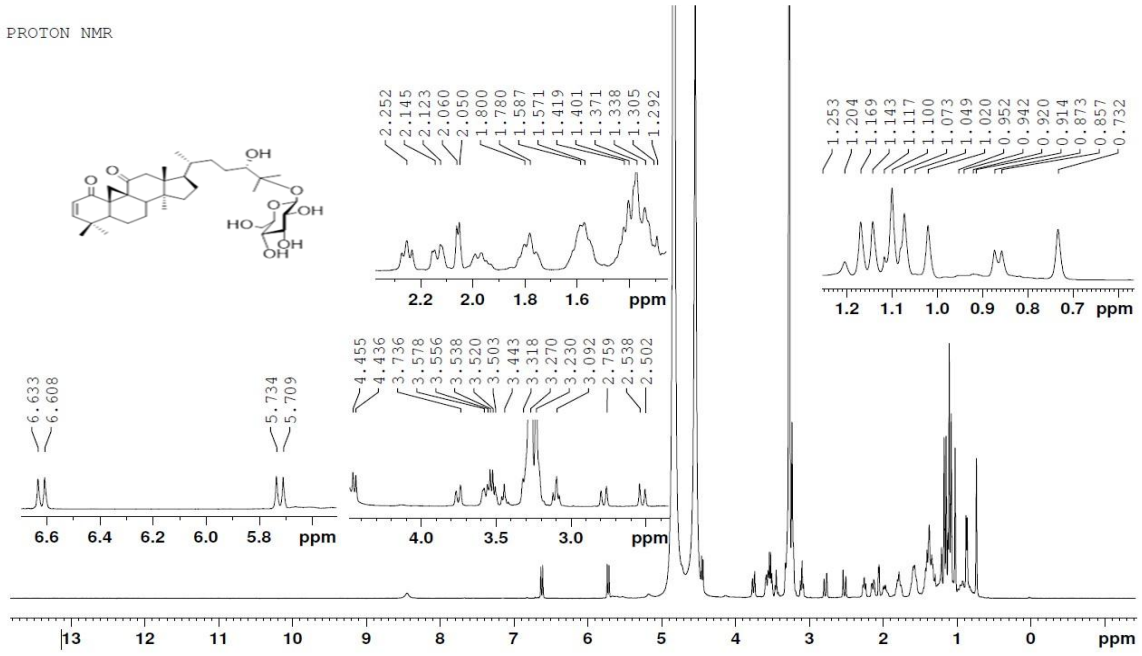

Appendix A2: ^{13}C NMR spectrum of compound 6.1

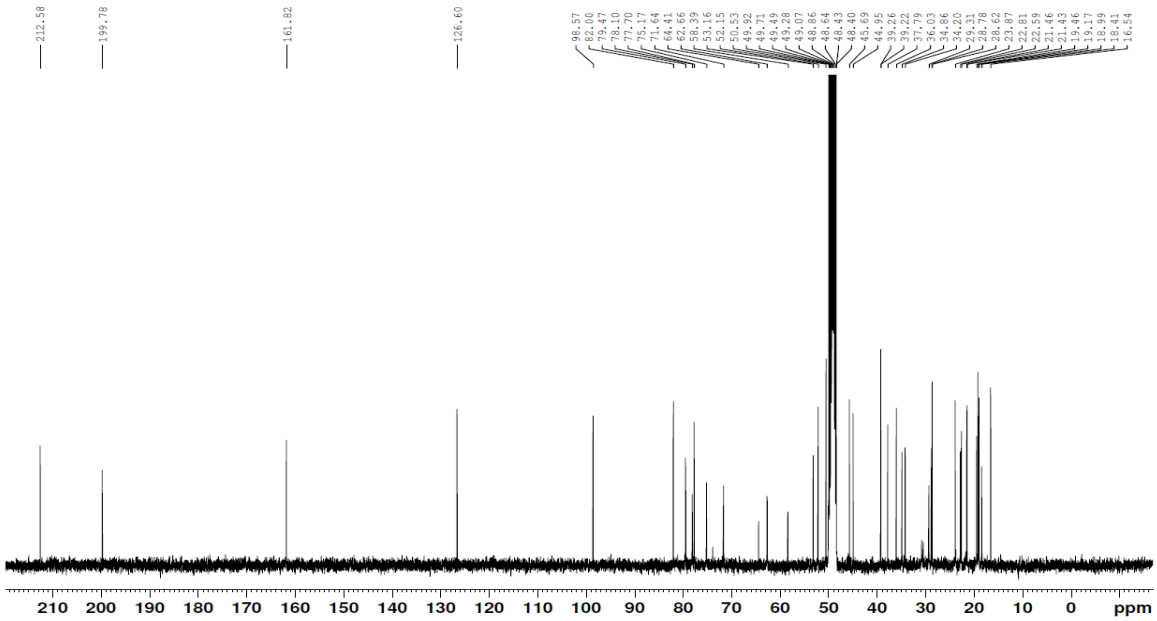

Appendix A3: DEPT-135 NMR spectrum of compound 6.1

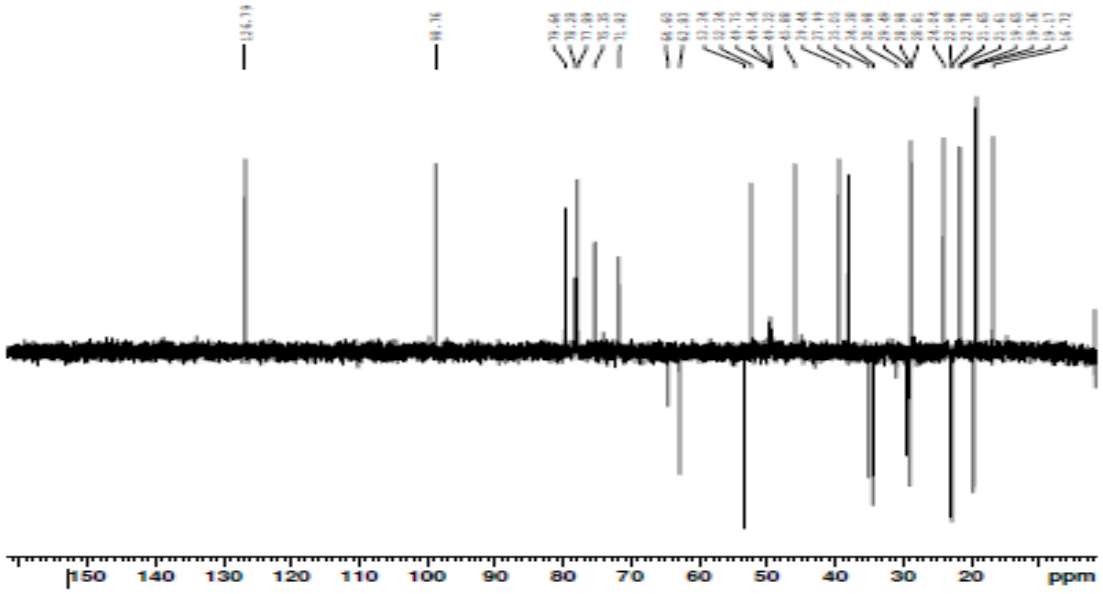

Appendix A4: COSY spectrum of compound 6.1

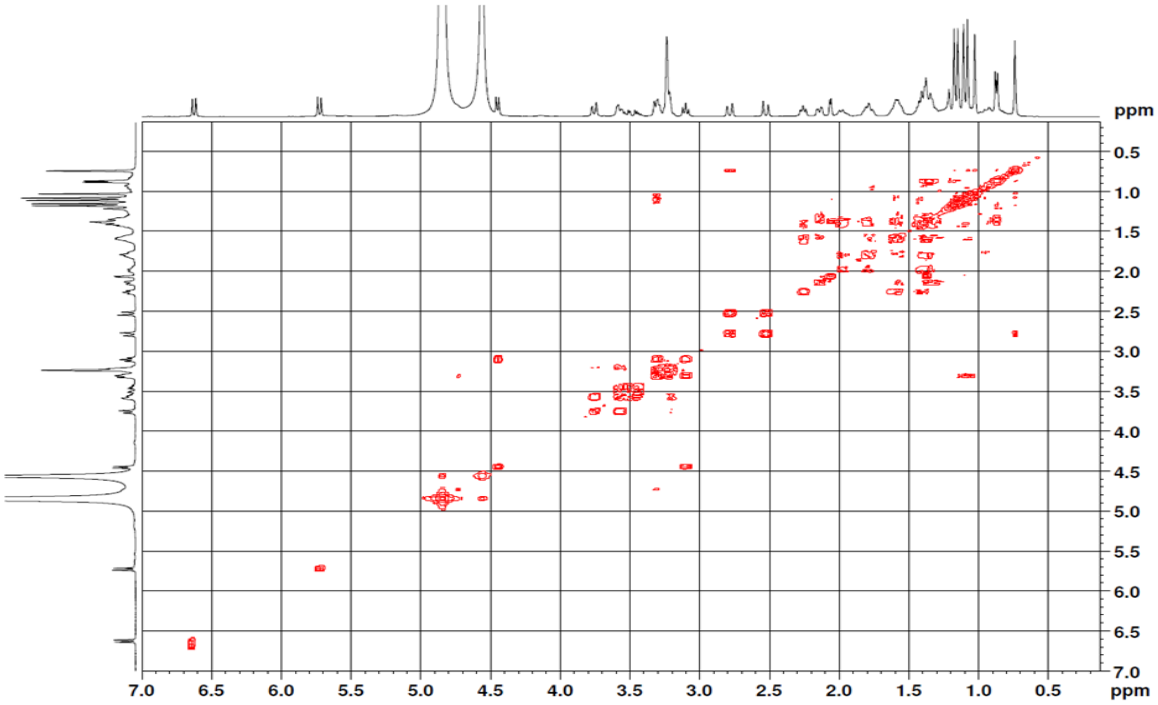

Appendix A5: HMBC spectrum of compound 6.1

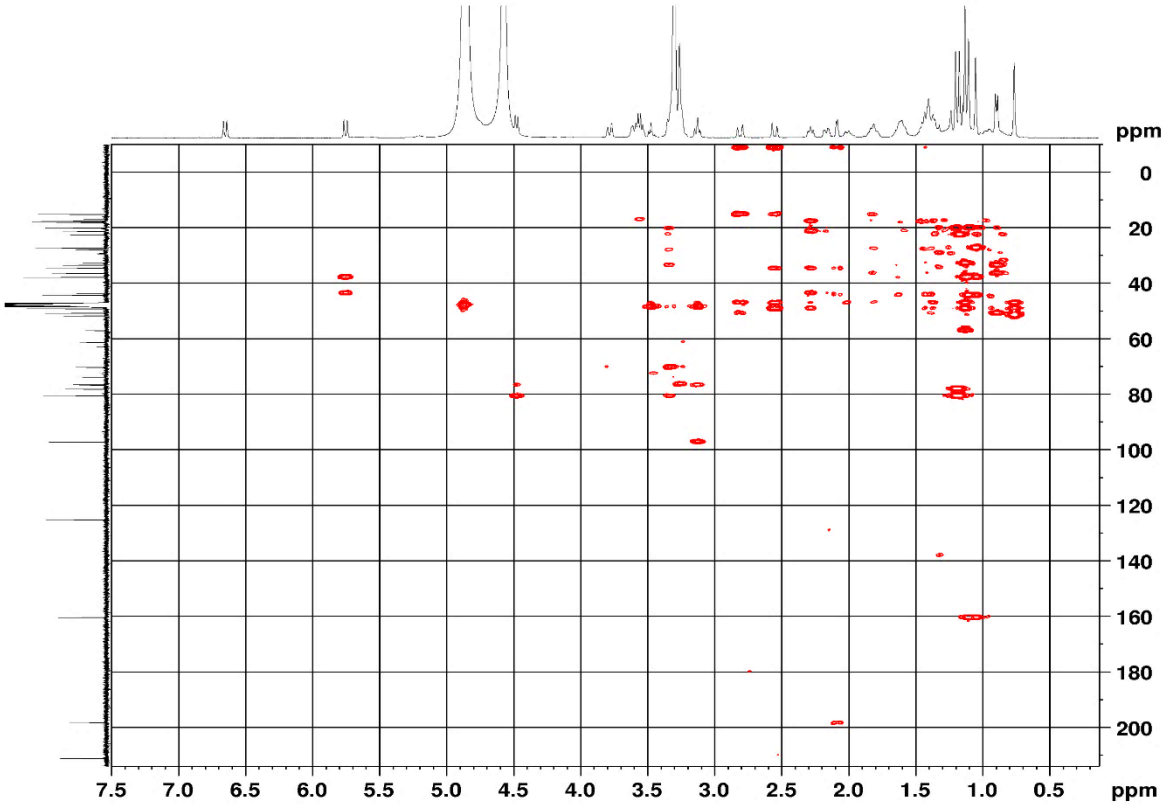

Appendix A6: HSQC spectrum of compound 6.1

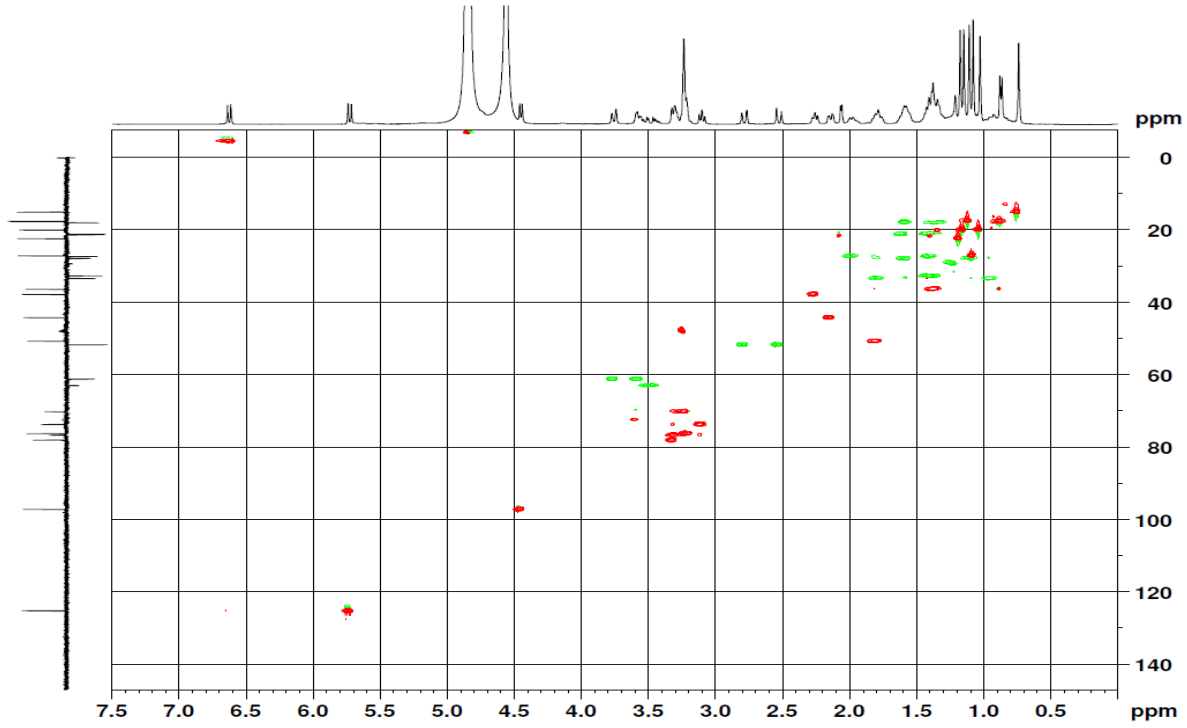

Appendix B: NMR spectra of compound 6.2 (CD_3OD)

Appendix B1: ^{1}H NMR spectrum of compound 6.2

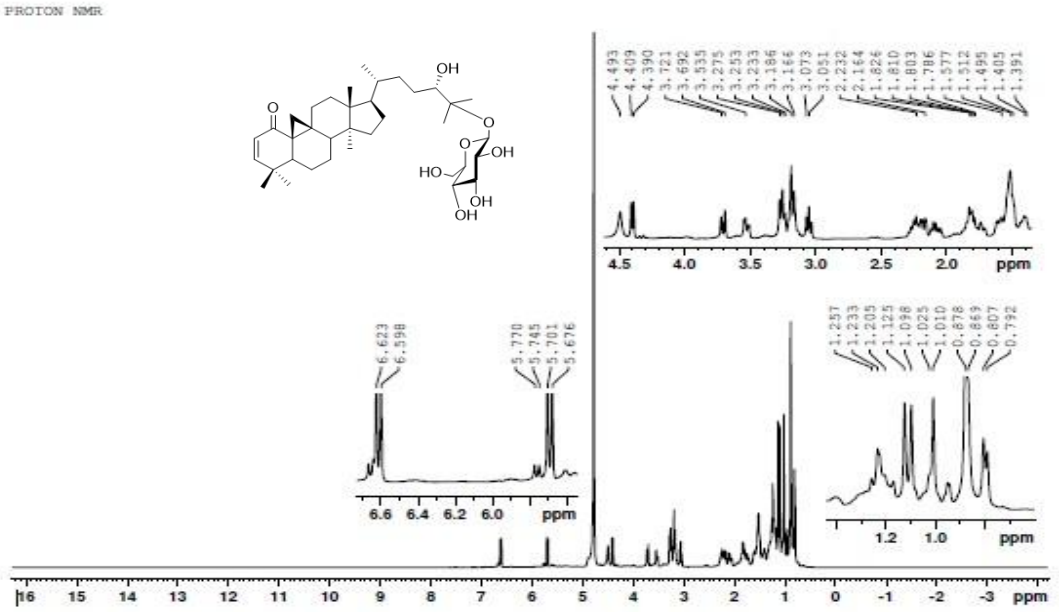

Appendix B2: ^{13}C NMR spectrum of compound 6.2

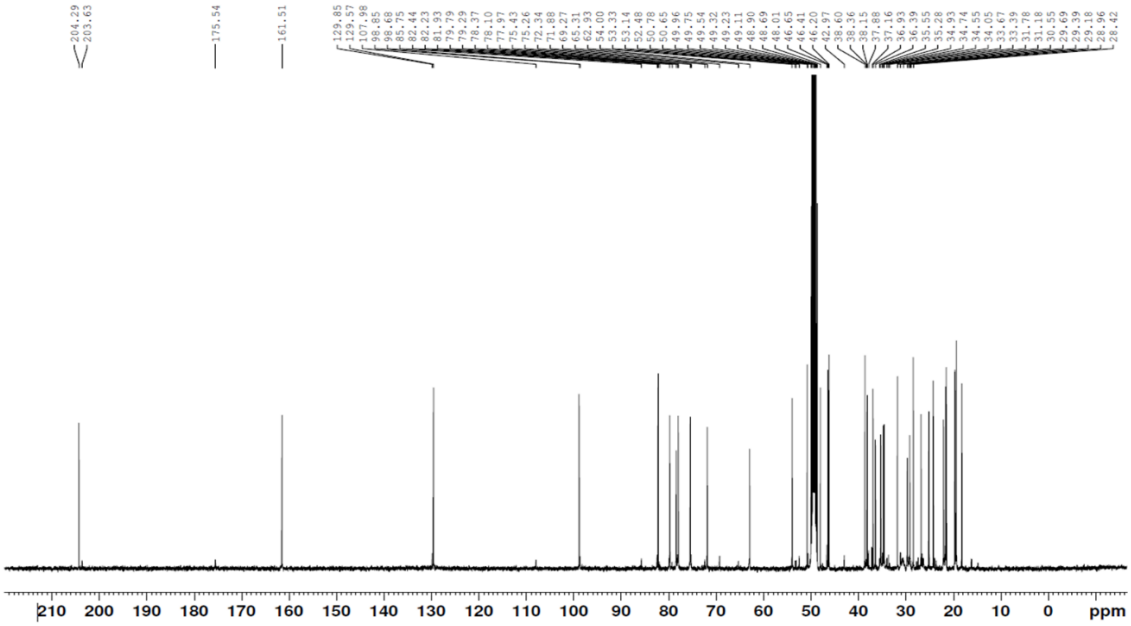

Appendix B3: DEPT-135 NMR spectrum of compound 6.2

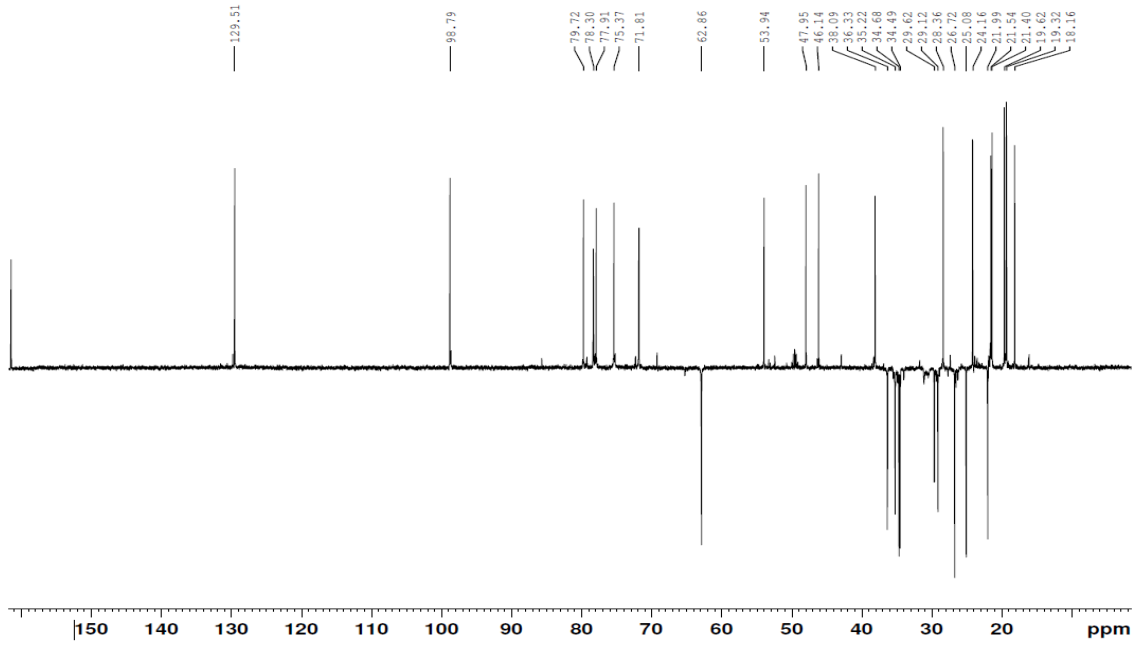

Appendix B4: COSY spectrum of compound 6.2

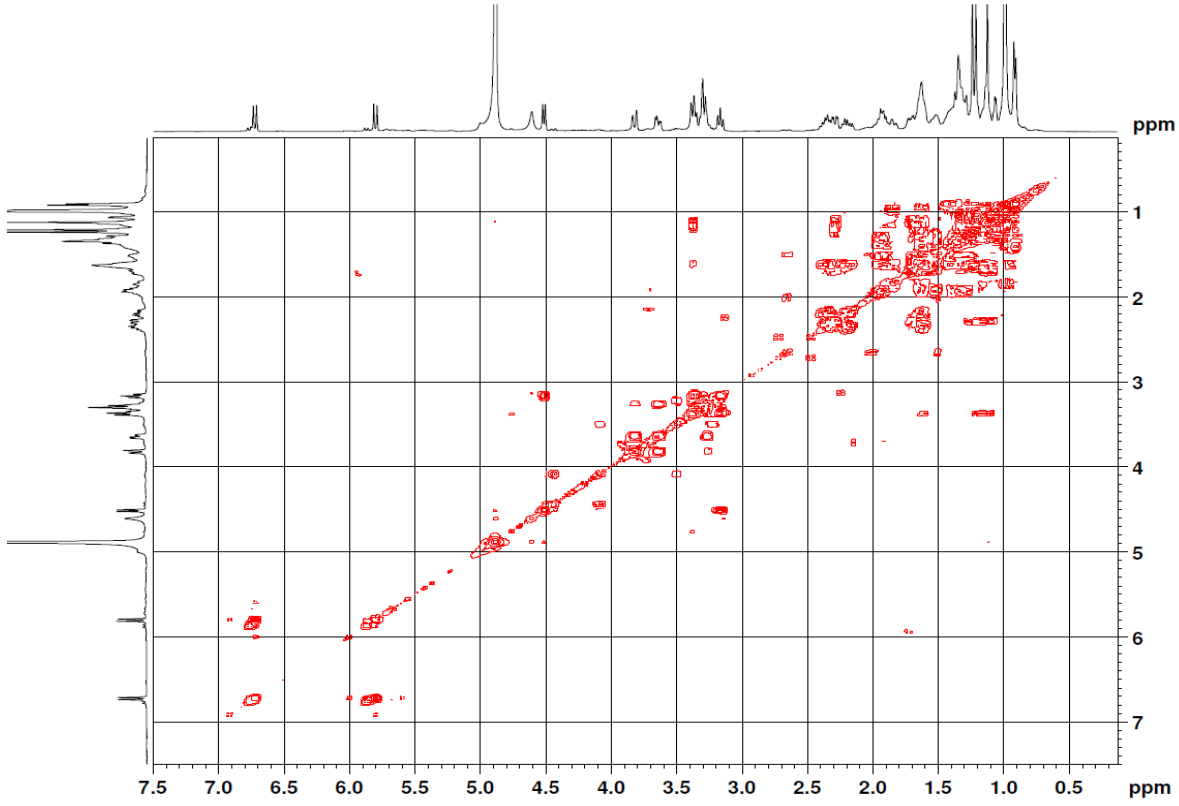

Appendix B5: HMBC spectrum of compound 6.2

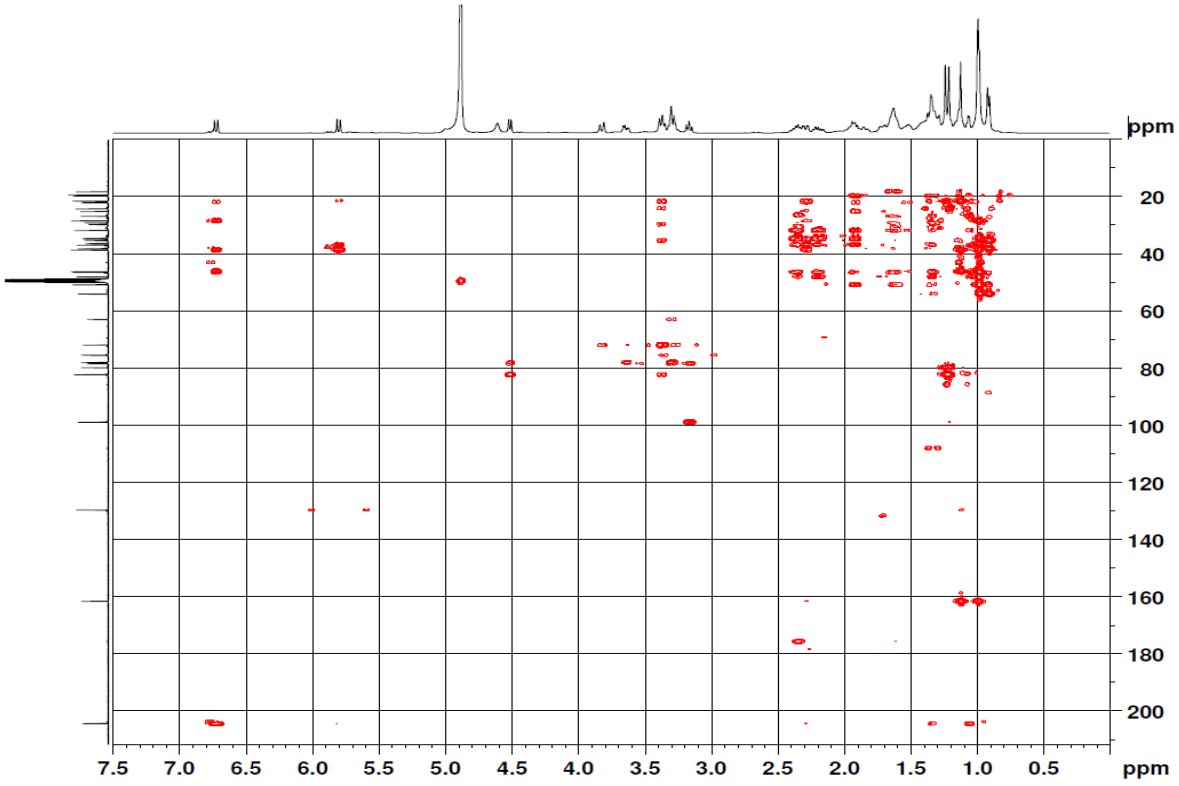

Appendix B6: HSQC spectrum of compound 6.2

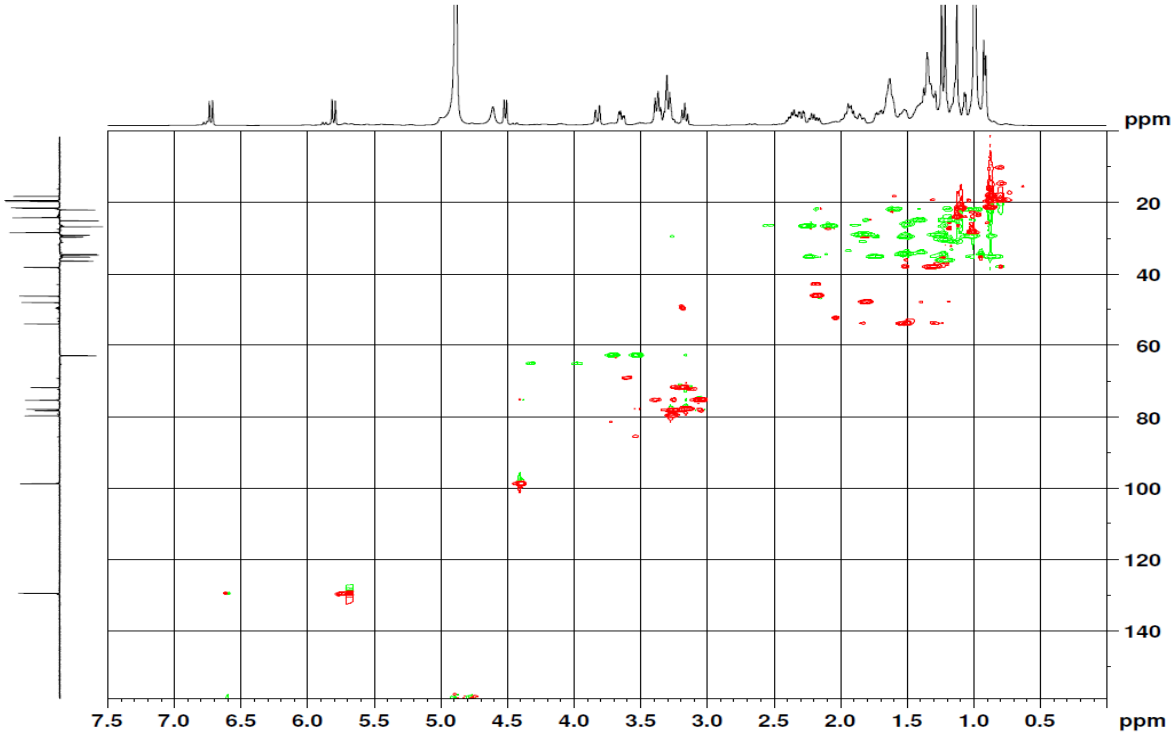

Appendix C: ^{1}H and ^{13}C NMR data of compounds **6.3-6.6**

	6.3		**6.4**		**6.5**		**6.6**	
Nº	**^{13}C**	**^{1}H (*J*= Hz)**	**^{13}C**	**^{1}H (*J*= Hz)**	**^{13}C**	**^{1}H (*J*= Hz)**	**^{13}C**	**^{1}H (*J*= Hz)**
1	206.2		202.8		201.0		211.6	
2	45.8	3.08, dd (9.7, 2.9) 2.24, dd (10.2, 2.9)	127.0	5.80, d (10.5)	128.1	5.87, d (10)	47.3	2.30, dd (9.5, 4.4) 2.90, dd (9.5, 5.1)
3	79.9	3.83, (9.7)	162.1	6.77, d (10.5)	159.8	6.77, d (10)	77.4	3.64
4	39.7		38.1		36.2		38.7	
5	43.1	2.12, d (2.9)	45.6	1.57*	41.2	2.29, dd (13.5; 2.8)	37.2	2.36*, dd (11.3, 2.9)
6	33.0	2.01*, t (7.5) 1.23*	36.1	1.57* 1.67*	33.7	1.89* 1.14*	27.6	1.58, m 1.85, m
7	25.6	0.98* 1.23*	72.6	3.87, d (4.5)	67.6	3.70, m	67.9	3.65, d (4.4)
8	39.2	2.01*, t (7.5)	56.3	2.17, s	55.1	2.14, d (3.8)	49.8	2.02, d (2.9)
9	36.3*	1.23*	136.6		32.0		29.1	
10	33.1		48.5	2.36, dq (15.3, 8.9)	35.5		39.03	
11	212.1		128.4	5.48, s	24.9	2.04* 2.69, dt (15.9; 4.5)	29.4	1.79* 2.39*, dd (11.3, 2.9)
12	51.4	2.60, d (16.1) 2.35, d (17.0)	39.1	1.98, d (5.5) 2.03*	33.2	1.63, d (5.5) 1.35, d (10.5)	32.4	1.58* 1.80*
13	48.4		46.7		44.9		45.0	
14	48.4		49.8		48.9		49.1	
15	27.3	1.86, d (3.4) 1.29*	29.6	1.62* 1.34*	32.3	1.49, d (4.9) 1.99*	32.9	1.58* 1.41*
16	22.7	1.29* 1.08*	29.5	1.34* 1.62*	27.3	1.92* 1.37*	27.3	1.38* 1.86*
17	51.0	1.67, t (8.9)	52.2	1.57*	51.6	1.59, d (3.5)	51.2	1.56*
18	15.7	0.70, s	15.8	0.74, s	14.4	0.98, s	14.2	0.91, s
19	17.7	0.78, s	33.8	2.48, dd (7.8, 4.9) 2.82, d (14.4)	27.9	1.14* 1.63*	23.2	0.68, d (4.8) 1.38*
20	36.3	1.23*	38.1	1.39*	36.6	1.42	36.6	1.56*
21	17.5	1.00, d (6.6)	19.4	0.92, d (6.4)	17.7	0.94, d (4.9)	17.9	0.87, d (4.4)
22	33.2	1.61, d (3.4) 1.08*	39.7	1.76* 2.03*	27.6	1.14* 1.59, d (3.5)	33.7	1.80* 0.93*
23	27.6	1.08* 1.63, d (3.4)	35.3	0.96* 1.84*	29.5	1.28* 1.93*	27.9	1.08* 1.58*
24	86.6	3.50, d (8.8)	79.8	3.35, t (8.8)	78.1	3.35, t (8.8)	76.7	3.67, d (4.4)
25	82.1		82.4		80.5		80.5	
26	18.4	1.29, s	21.5	1. 20, s	20.0	1.20, s	20.3	0.86, s
27	23.4	1.24, s	24.2	1.23, s	22.5	1.23, s	23.4	0.94, s
28	24.1	0.98, s	28.2	1. 14, s	26.7	1.13, s	22.5	1.19, s
29	20.1	1.20, s	19.9	1.06, s	19.9	0.96, s	19.9	1.16, s
30	17.7	0.90, s	19.3	0.87, s	17.9	0.91, s	17.5	0.91, s
1’	96.8	4.52, d (7.3)	98.8	4.50, d (8.2)	97.2	4.51, d (7.7)	97.2	4.46, d (7.3)
2’	73.9	3.21*	75.4	3, 2 t (8.2)	73.7	3.15, t (8.7)	73.8	3.11, t (7.3)
3’	76.4	3.37*	78.4	3.30*	76.7	3.38*	78.1	3.32*
4’	70.5	3.35*	71.9	3.27*	70.2	3.29*	70.2	3.26*
5’	74.3	3.19*	77.9	3.36*	76.3	3.27*	76.3	3.23*
6’	61.2	3.67, dd (11.2, 4.9) 3.81, d (9.4)	62.9	3.63, dd (11.2, 5.3) 3.82, d (9.4)	61.2	3.64, dd (12.5; 6.8) 3.81, d (11.2)	61.2	3.57, dd (8.0, 4.3) 3.77 d (10.2)
1’’	103.6	4.79, d (8.3)						
2’’	73.5	3.21*						
3’’	77.2	3.37*						
4’’	70.5	3.35*						
5’’	76.3	3.37*						
6’’	63.9	4.36, d (2.9)						
1’’’	167.8							
2’’’	113.8	6.38, d (16.1)						
3’’’	145.6	7.69, d (16.4)						
4’’’	125.8							
5’’’	130.0	7.48, d (7.8)						
6’’’	115.6	6.81, d (7.8)						
7’’’	160.1							
8’’’	115.6	6.81, d (7.8)						
9’’’	130.0	7.48, d (7.8)						

Appendix D: ^{1}H and ^{13}C NMR data of compounds **6.7-6.11**

	6.7		**6.8**		**6.9**		**6.10**		**6.11**	
No	**^{13}C**	**^{1}H (*J*= Hz)**	**^{13}C**	**^{1}H (*J*= Hz)**	**^{13}C**	**^{1}H (*J*= Hz)**	**^{13}C**	**^{1}H (J= Hz)**	**^{13}C**	**^{1}H (*J*= Hz)**
1							166.8		73,2	4.73, brd
2	69.8	4.26, dq (10.6) 3,96, t (10.0)	70.5	4.23, dq (10.5) 3.94, d (2.5)	160.5		60.9	3.68, t (7.0)	72.4	4.53, dd (13.8, 4.5
3	32.1	3.45, m	31.7	3.50, m	156.0		29.5	2.004, m 1.90, m	84.3	3.00, t (9.5)
4	30.1	2.79, d (5.0) 2.83, dd (10.8, 14.1)	31.4	2.78, d (5.1) 2.82, d (6.5)	177.8		24.4	1.76, m 1.68, m	71.3	3,62brs
5	121.9	6.70, d (8.2)	130.4	6.87, d (8.5)	164.5		45.5	3.18, m 3.04, m	72.9	4.36, d (5.7)
6	135.4		107.9	6.32, dd (5.8, 2.7)	99.1	6.2 s			70.5	4.64, brd
7	103.5	6.36, d (8.5)	155.1		170.5					
8	151.2		103.2	6.29, d (2.3)	94.1	6.4 s				
9	147.5		154.9		156.7					
10	113.8		114.7		105.0					
11										
1’	120.5		127.4		121.2					
2’	154, 9		145.3		131.3	8.06, d (9.8)				
3’	103.0	6.27, d (2.5)	138.7		115.7	6.90, d (8.3)				
4’	155.7		146.7		161,7					
5’	108.2	6.33, dd (6.4, 2.0)	106.5	6,56, q (9.0)	115.7	6.90, d (8.3)				
6’	130.3	6.84, d (7.8)	117.0	6,56, q (9.0)	133.1	8.06, d (9.8)				
1’’					98.3	5.6, d (7.2)				
2’’					81.9	3.46, d (8.3)				
3’’					76.6	3.14*				
4’’					70.2	3.33*				
5’’					74.6	3.14*				
6”					63.3	4.15, d (12.0) 3.89, q (5.2)				
1’’’					104.3	4.61, d (7.3)				
2’’’					74.2	3.08*				
3’’’					76.9	3.68				
4’’’					69.9	3.31				
5’’’					66.2	3.08* 3.74, dd (6.3, 4.8)				
1’’’’					172.9					
2’’’’					45,5	2.29*, q (14.1)				
3’’’’					69.1					
4’’’’					45.5	2.29*, q (14.1)				
5’’’’					170.5					
6’’’’					27.6	1.04, s				
6-OCH_3									60.1	3.44, s
2’-OCH_3			61.1	3.88, d (5.1)						
4’-OCH_3	55.7	3.76, s	56.2	3.87, d (5.0)						
8-OCH_3	60.9	3.81, s								

Appendix E: NMR spectra of compound 7.1 (DMSO-D6)

Appendix E1: ^{1}H NMR spectrum of compound 7.1

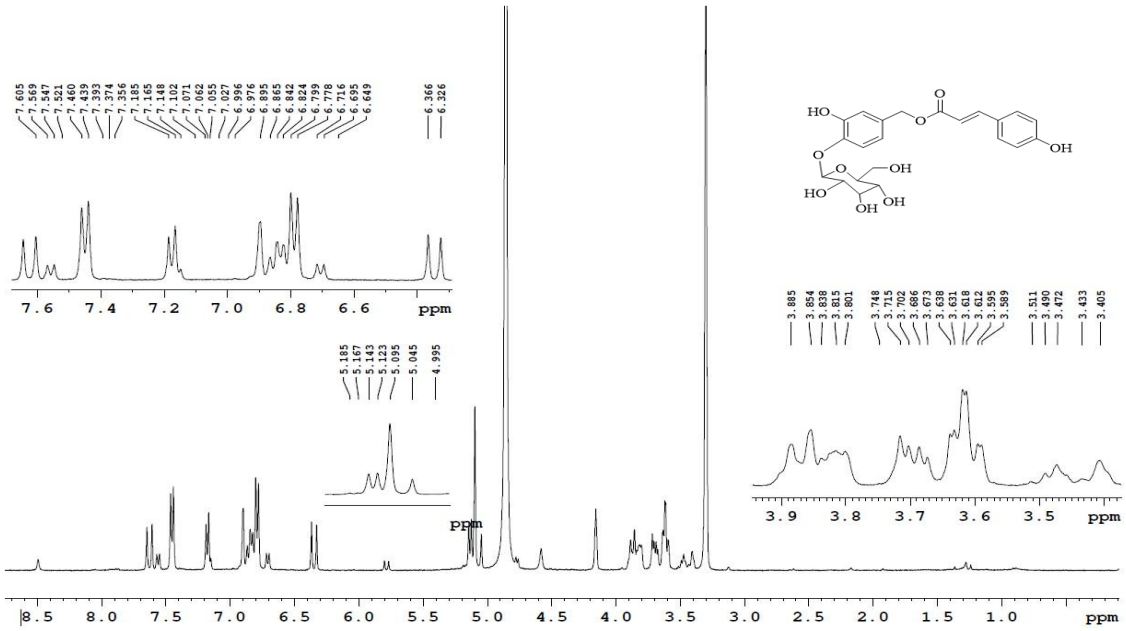

Appendix E2: ^{13}C NMR spectrum of compound 7.1

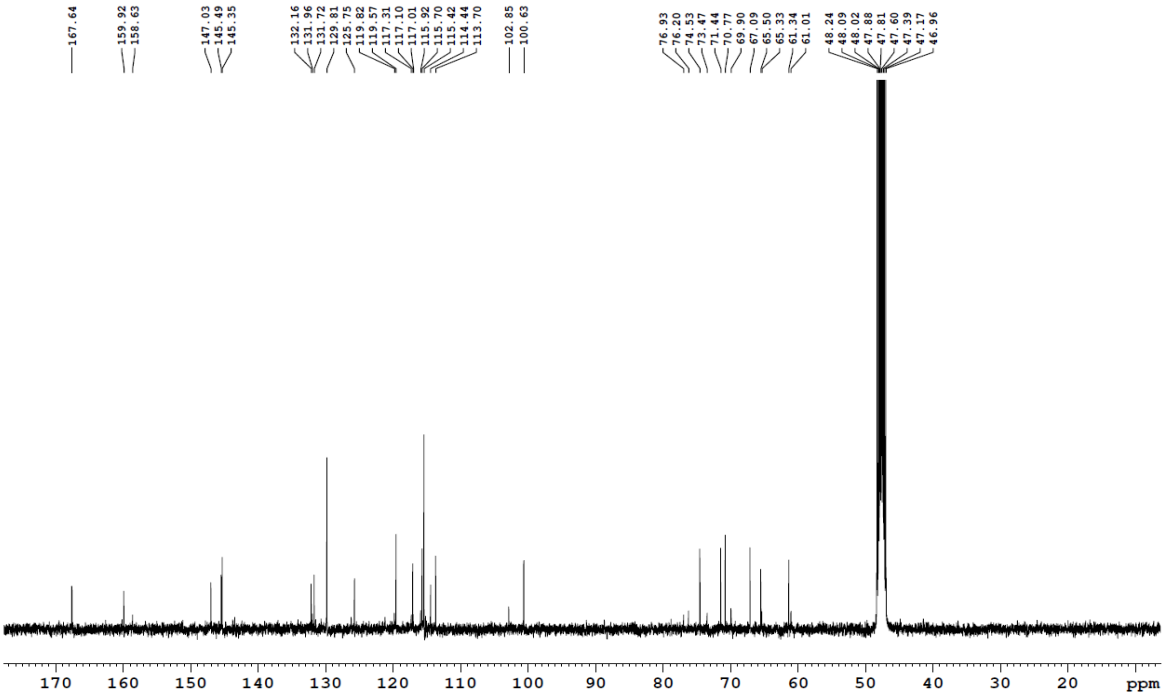

Appendix E3: DEPT-135 NMR spectrum of compound 7.1

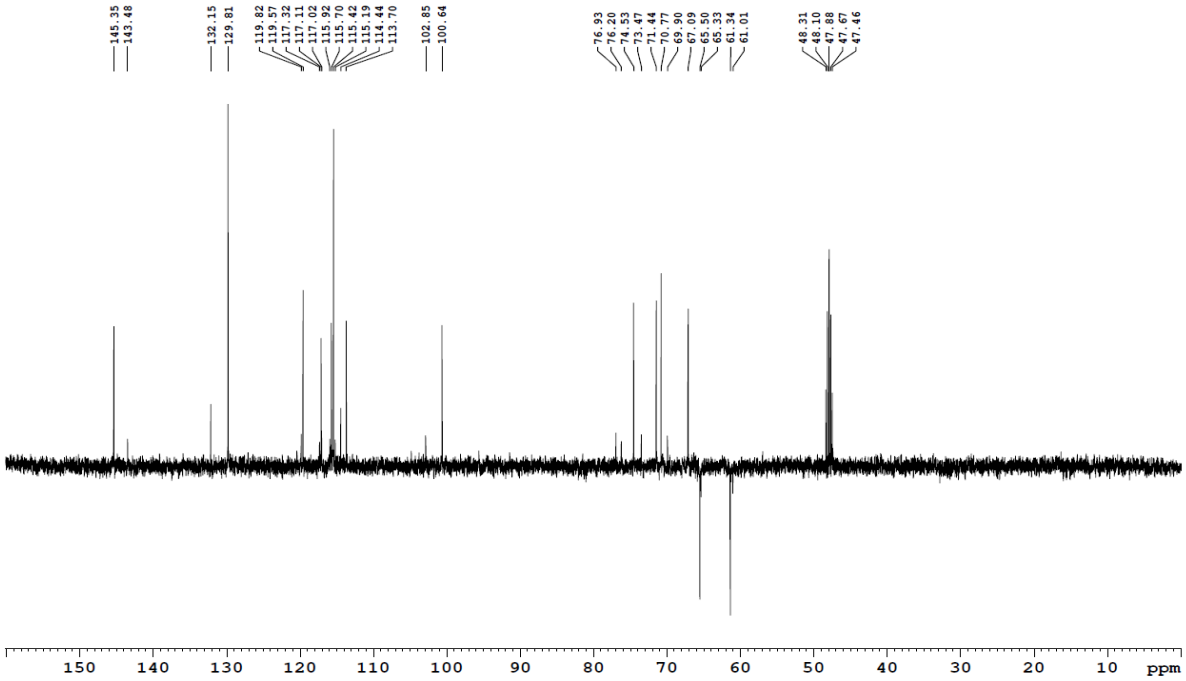

Appendix E4: COSY spectrum of compound 7.1

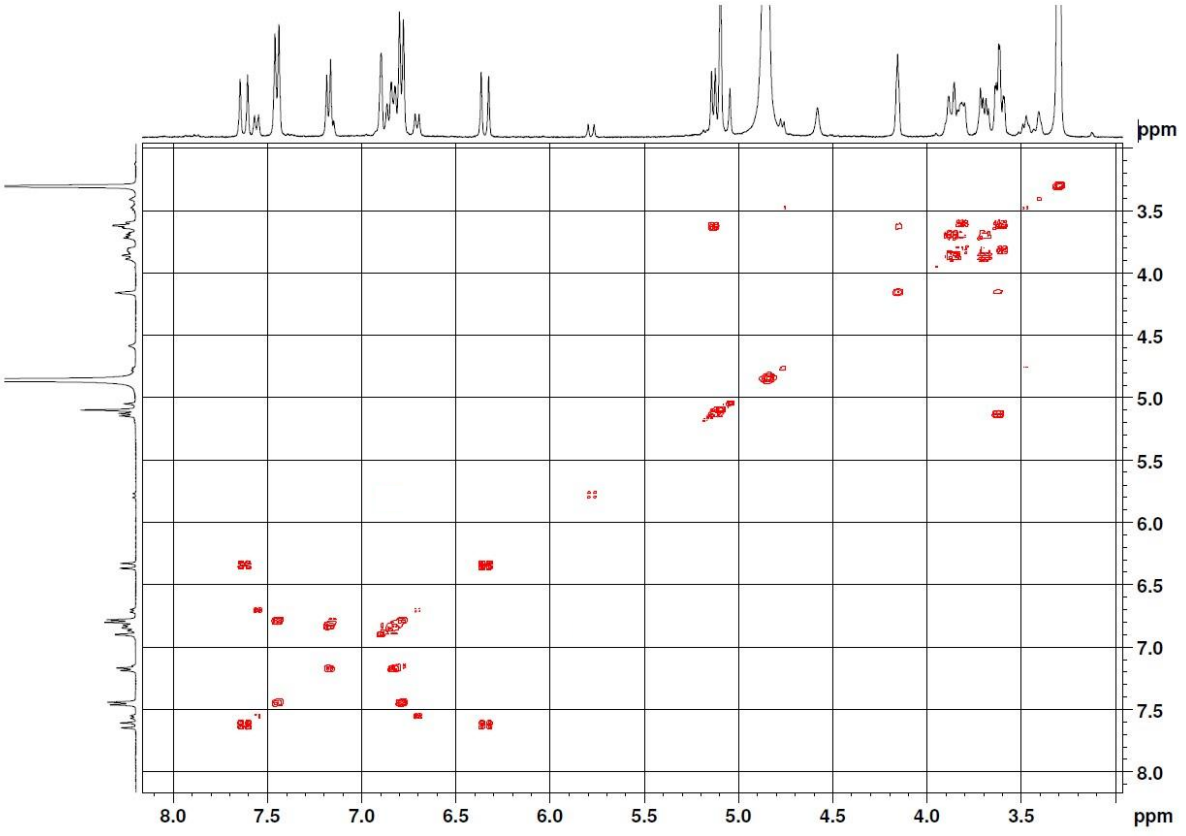

Appendix E5: HMBC spectrum of compound 7.1

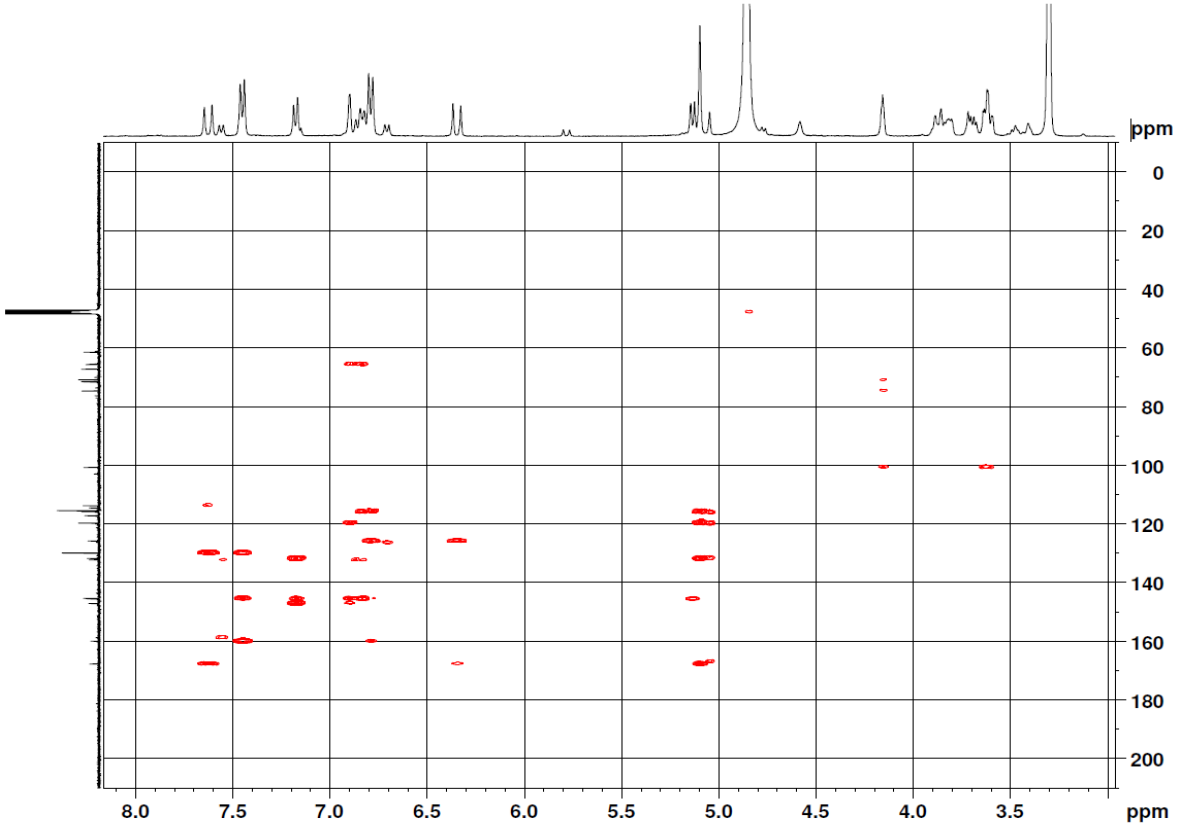

Appendix E6: HSQC spectrum of compound 7.1

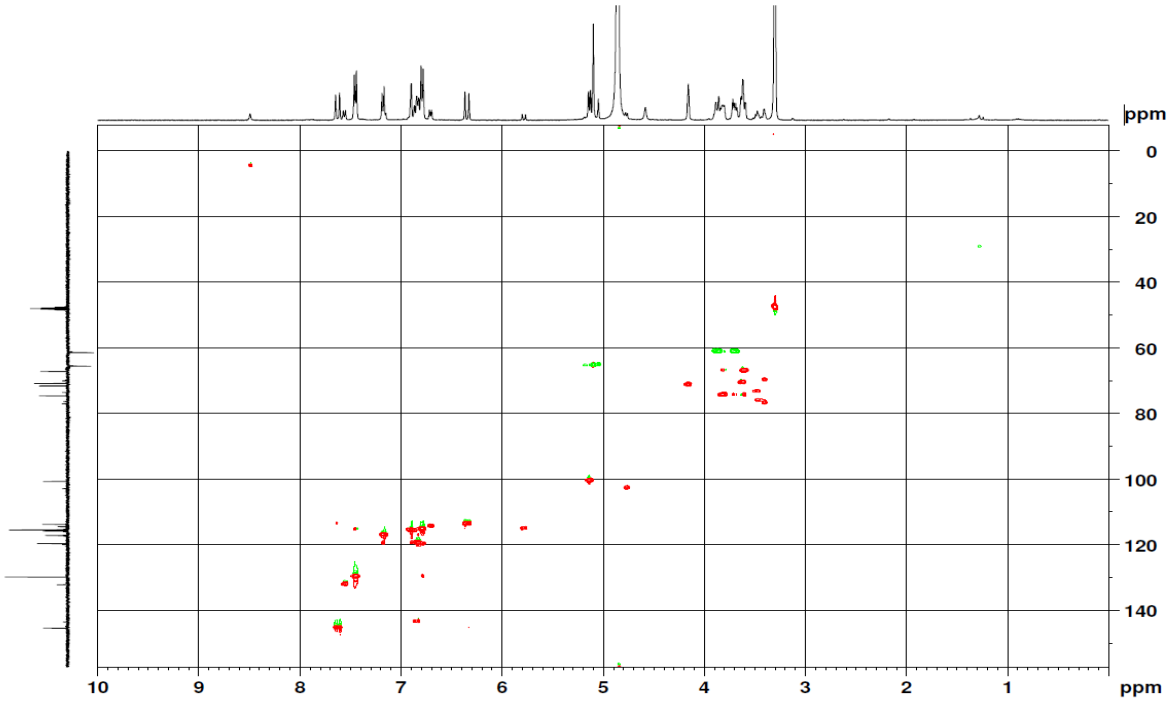

Appendix F: NMR spectra of compound 8.1 (DMSO-D6)

Appendix F1: ^{1}H NMR spectrum of compound 8.1

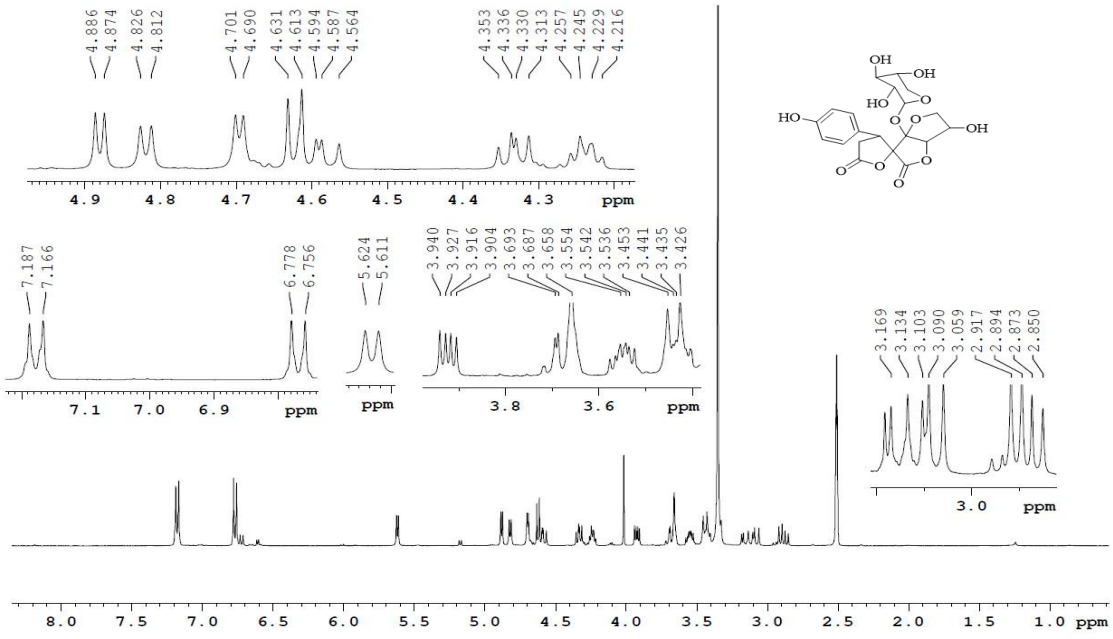

Appendix F2: ^{13}C NMR spectrum of compound 8.1

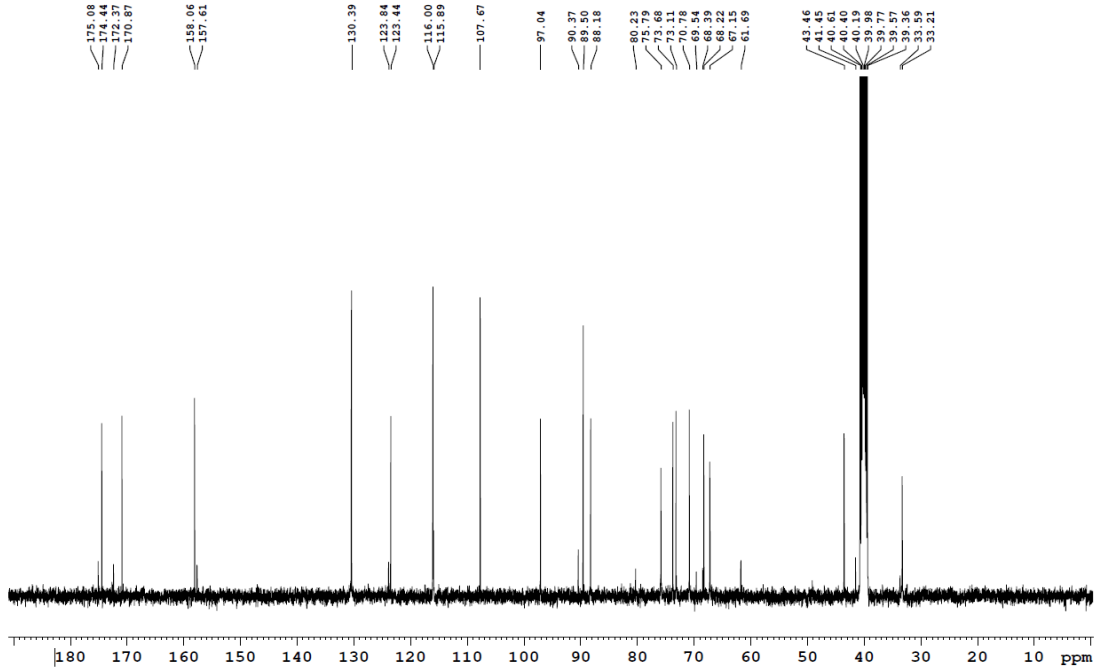

Appendix F3: DEPT-135 NMR spectrum of compound 8.1

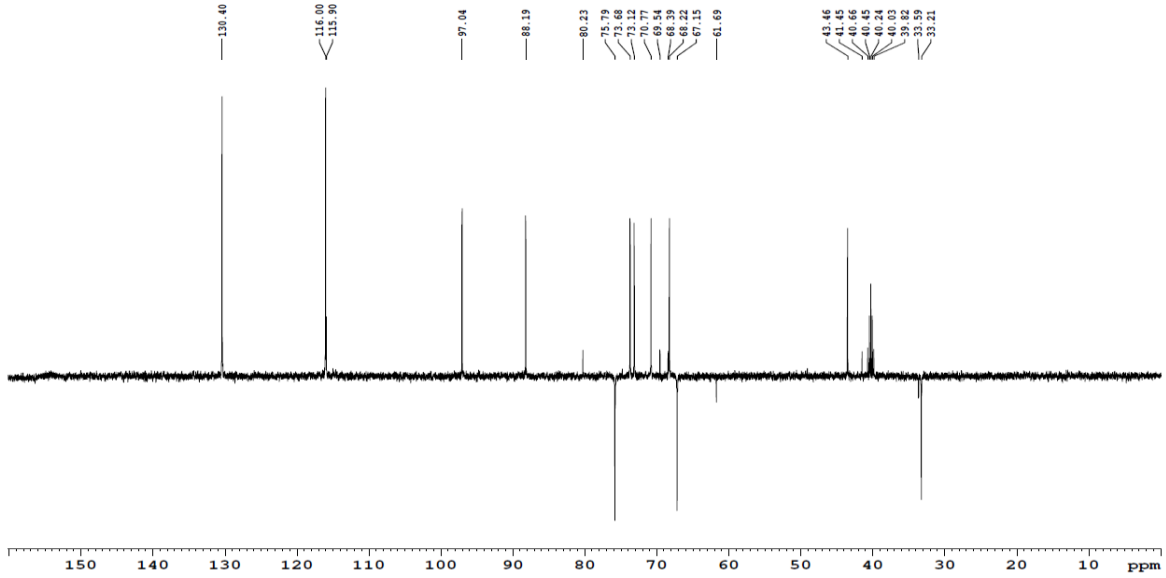

Appendix F4: COSY spectrum of compound 8.1

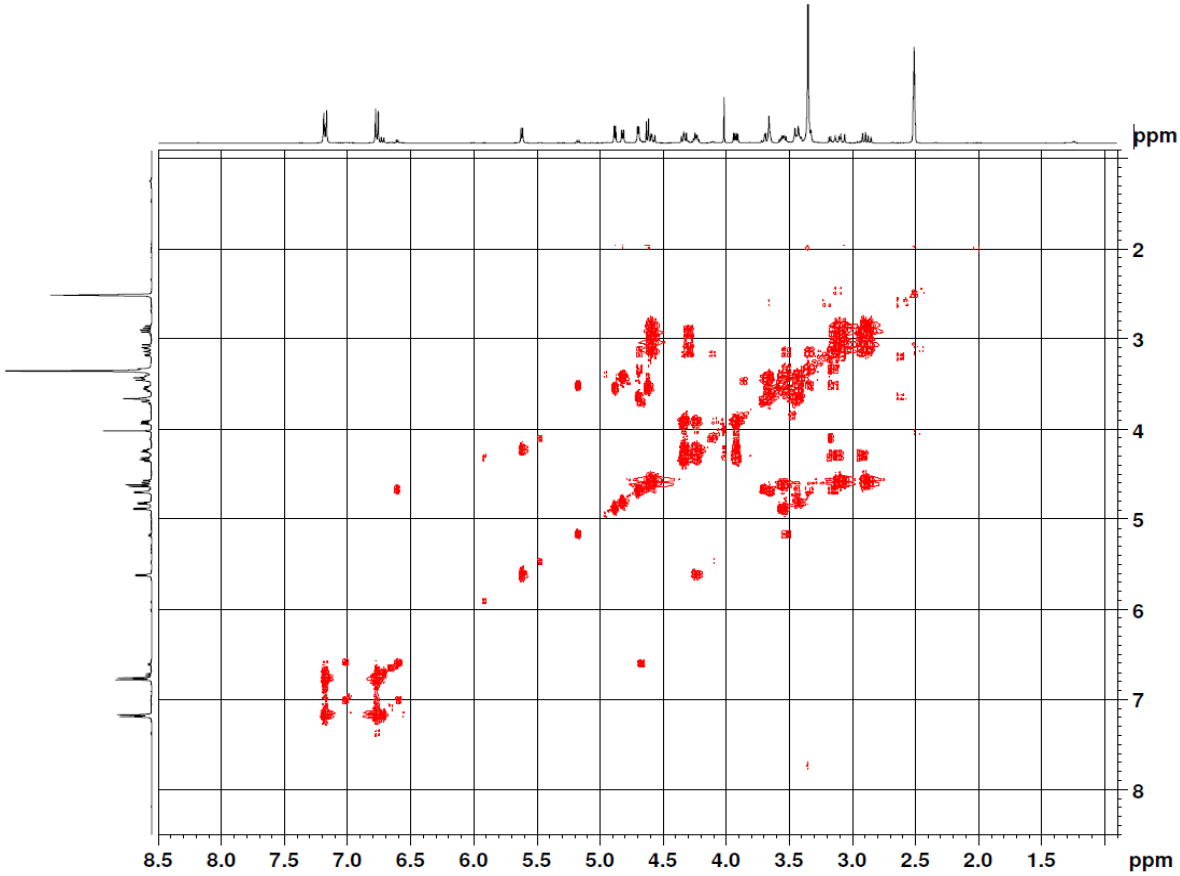

Appendix F5: HMBC spectrum of compound 8.1

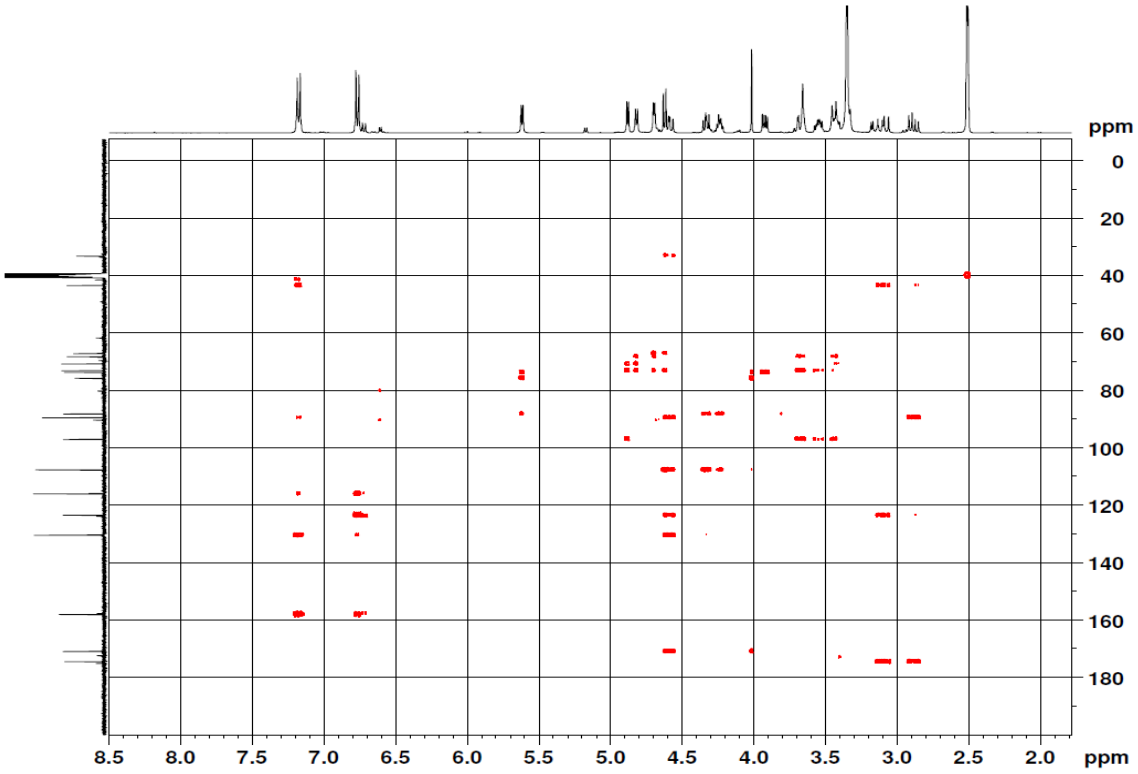

Appendix F6: HSQC spectrum of compound 8.1

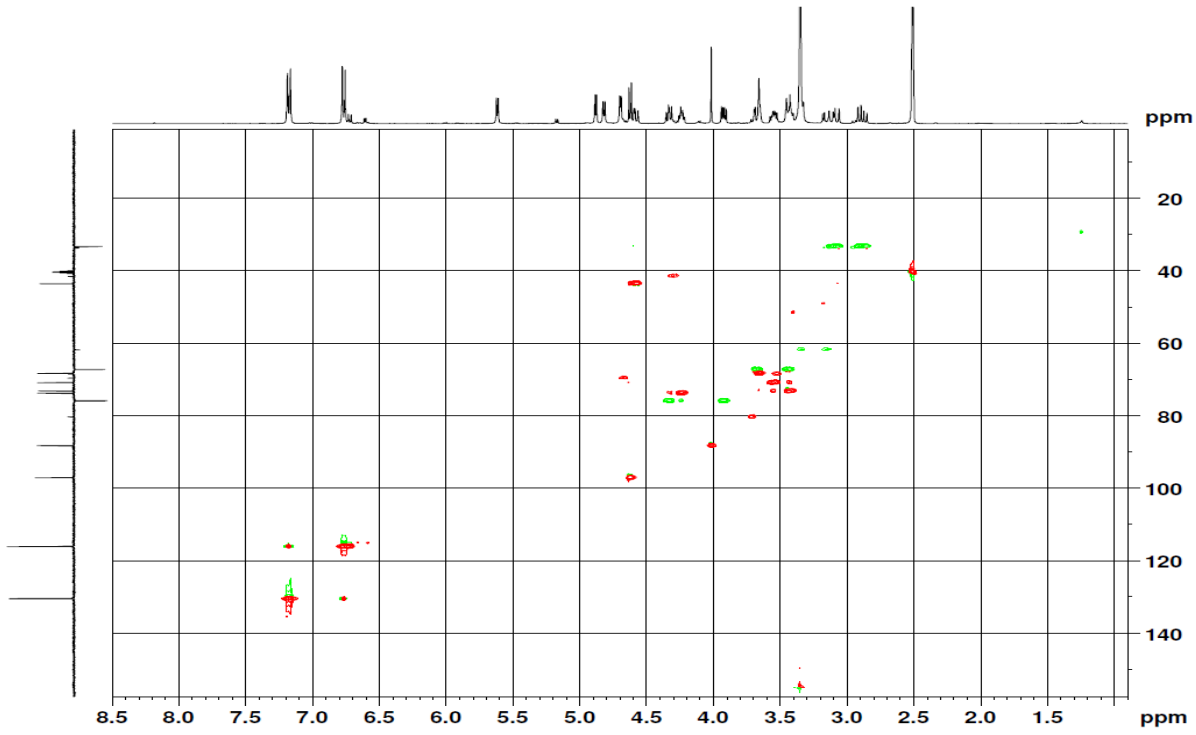

Appendix G: NMR spectra of compound 8.2 (DMSO-D6)

Appendix G1: ^{1}H NMR spectrum of compound 8.2

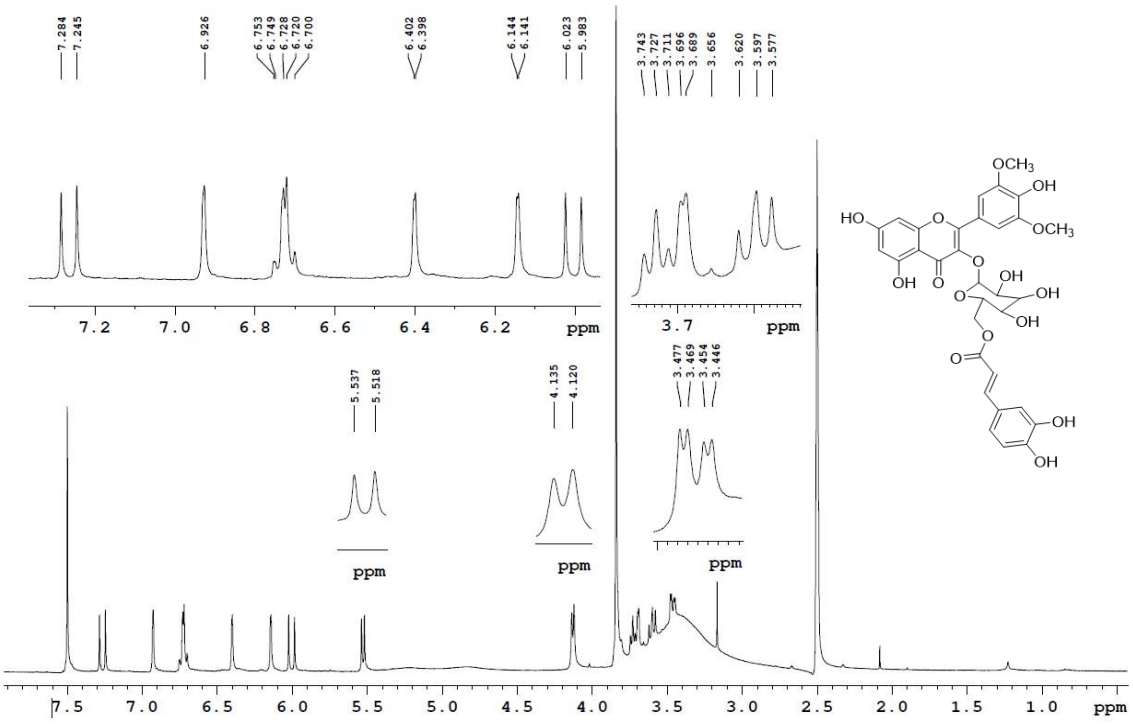

Appendix G2: ^{13}C NMR spectrum of compound 8.2

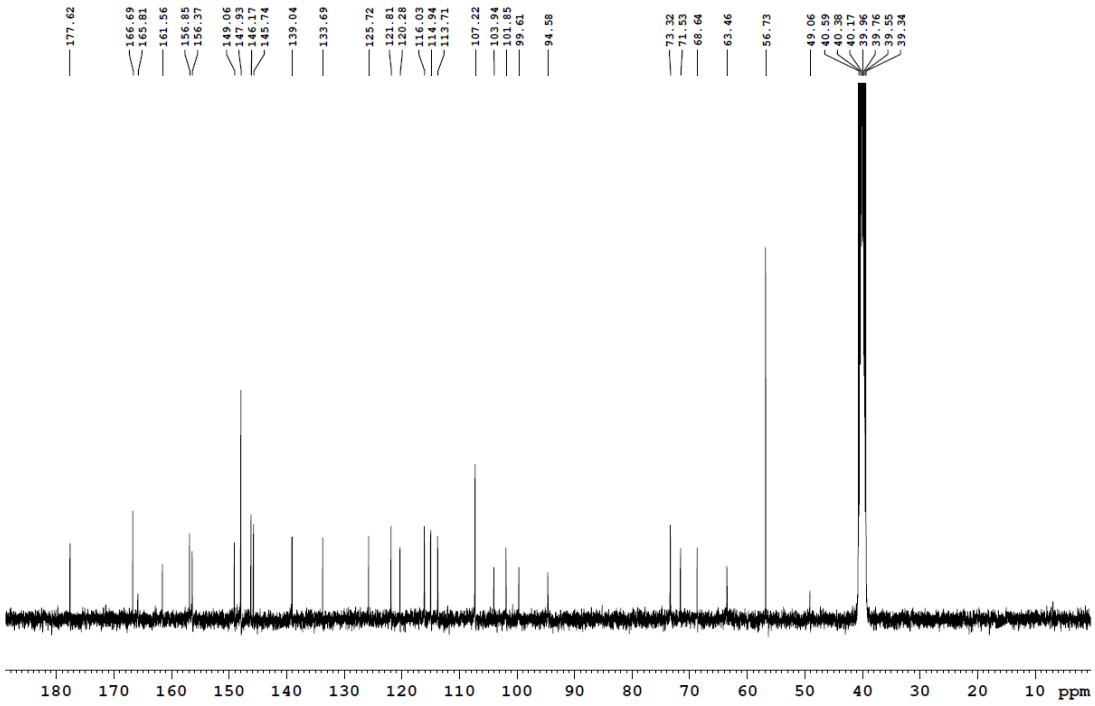

Appendix G3: DEPT-135 NMR spectrum of compound 8.2

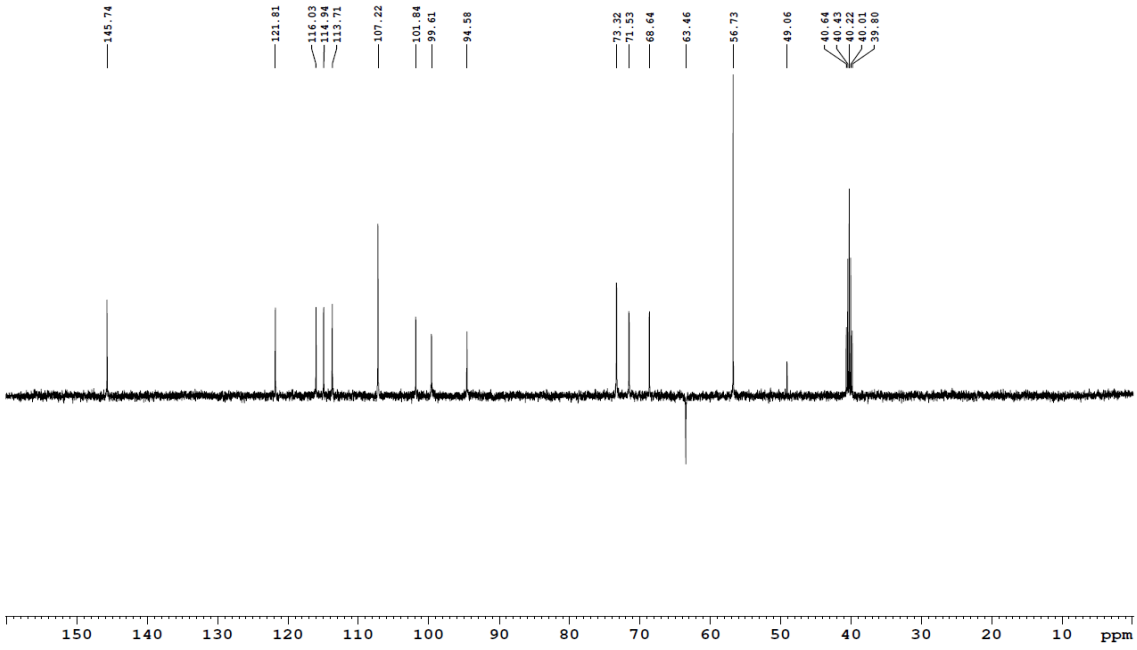

Appendix G4: COSY spectrum of compound 8.2

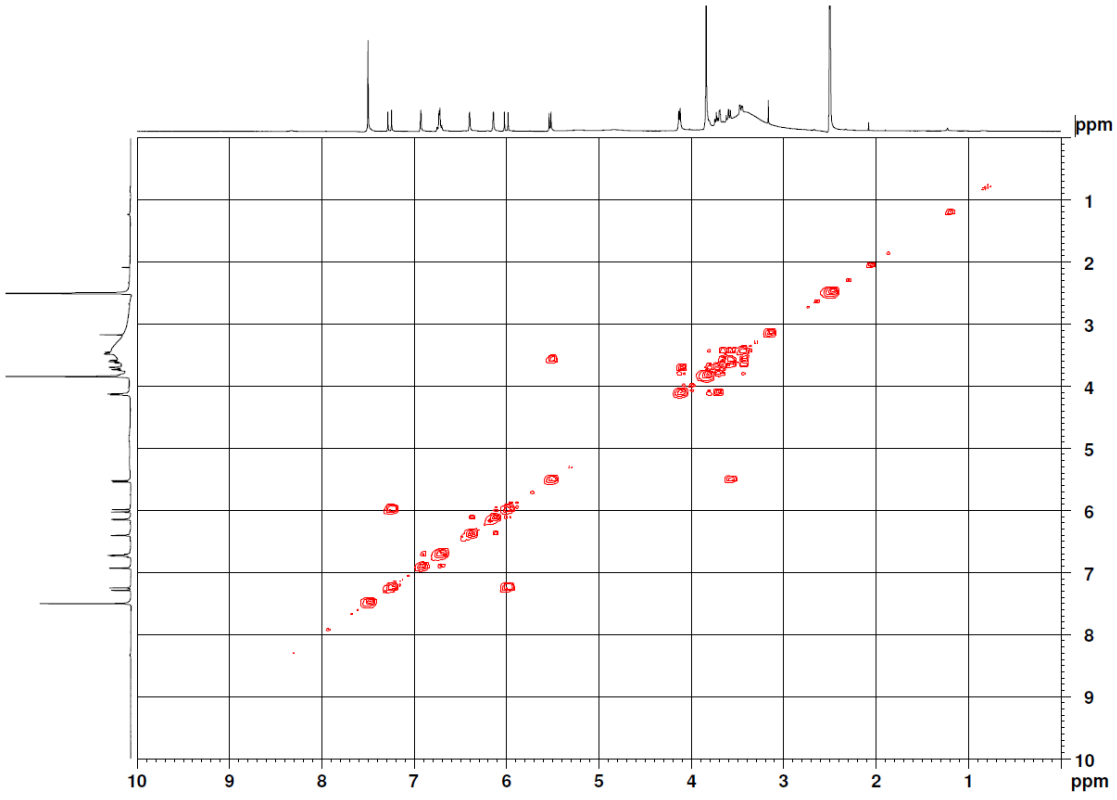

Appendix G5: HMBC spectrum of compound 8.2

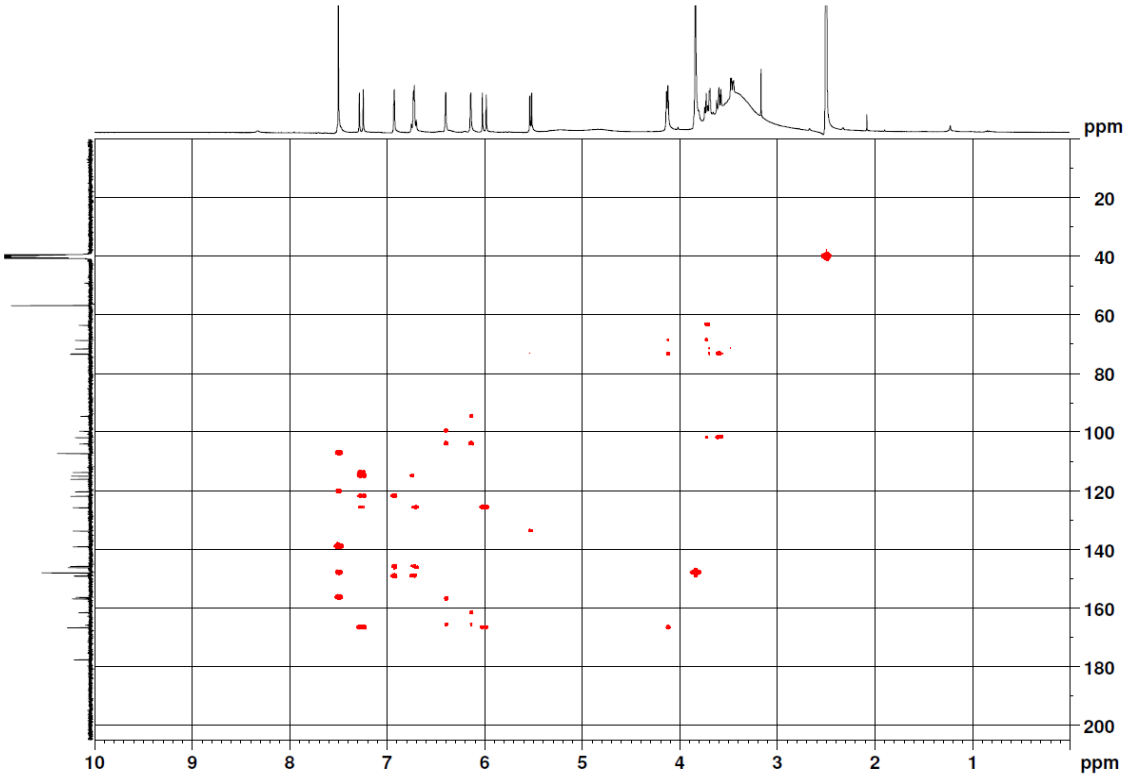

Appendix G6: HSQC spectrum of compound 8.2

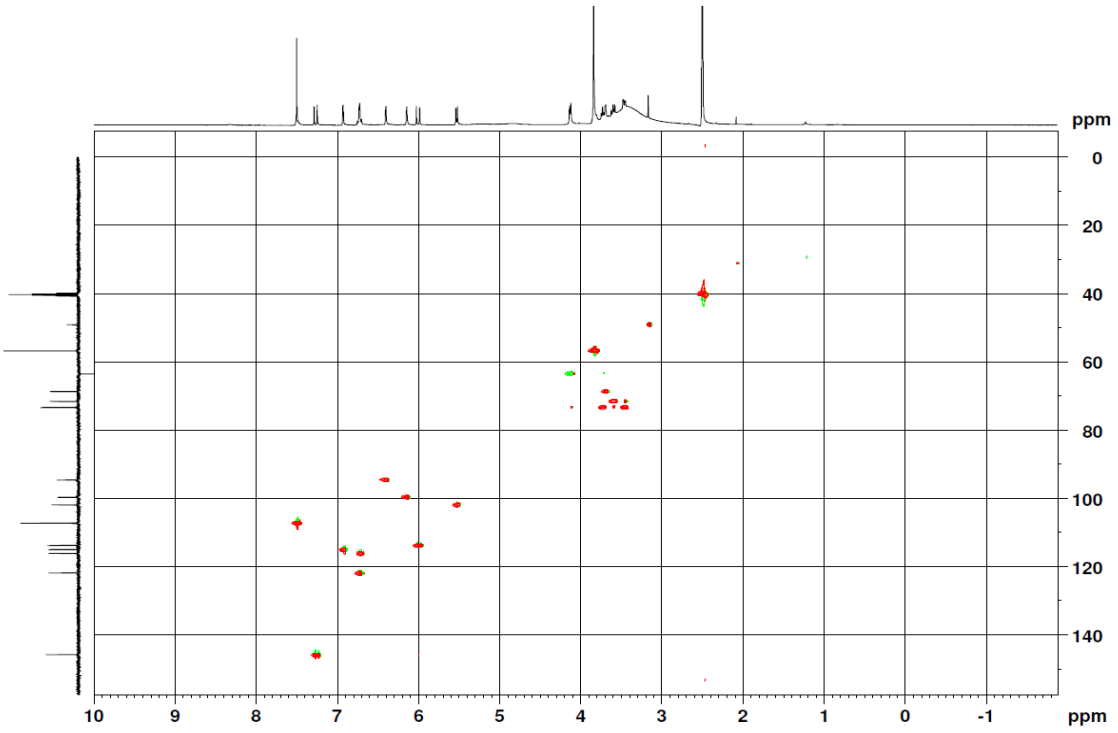

Appendix H: LigPlot diagrams showing binding interactions of compounds 6.7-6.11, selegiline and resveratrol with MAO-B

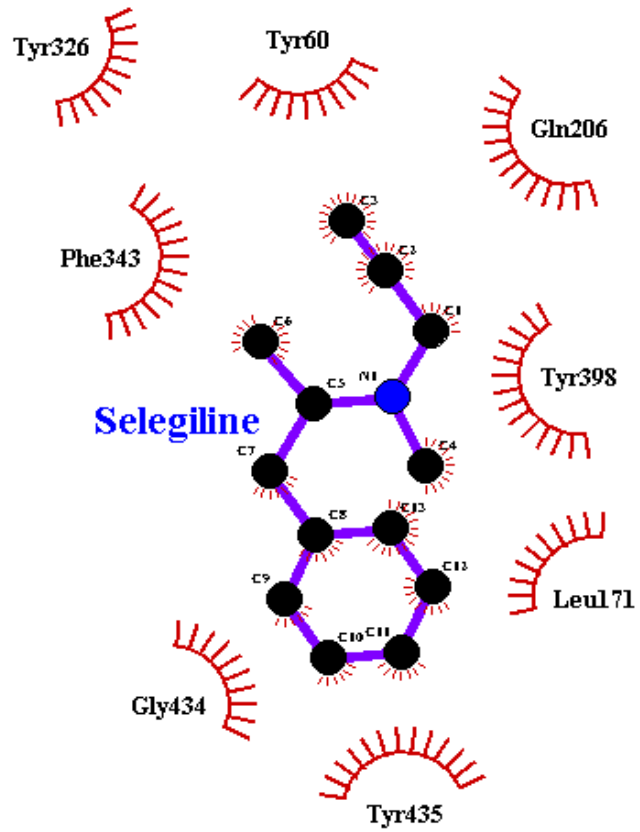

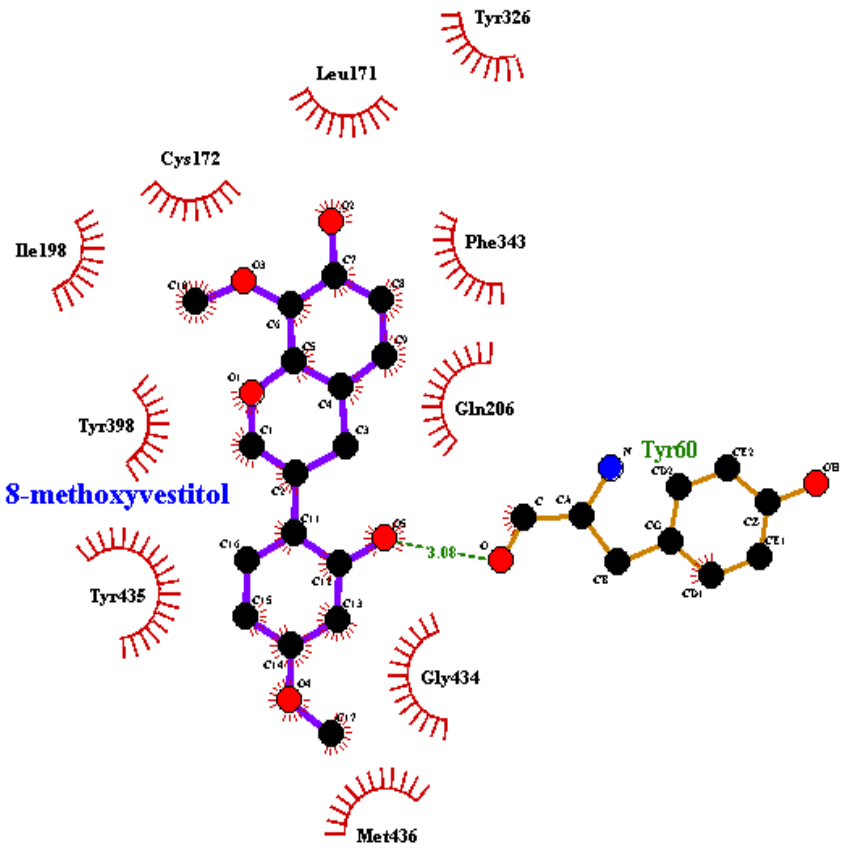

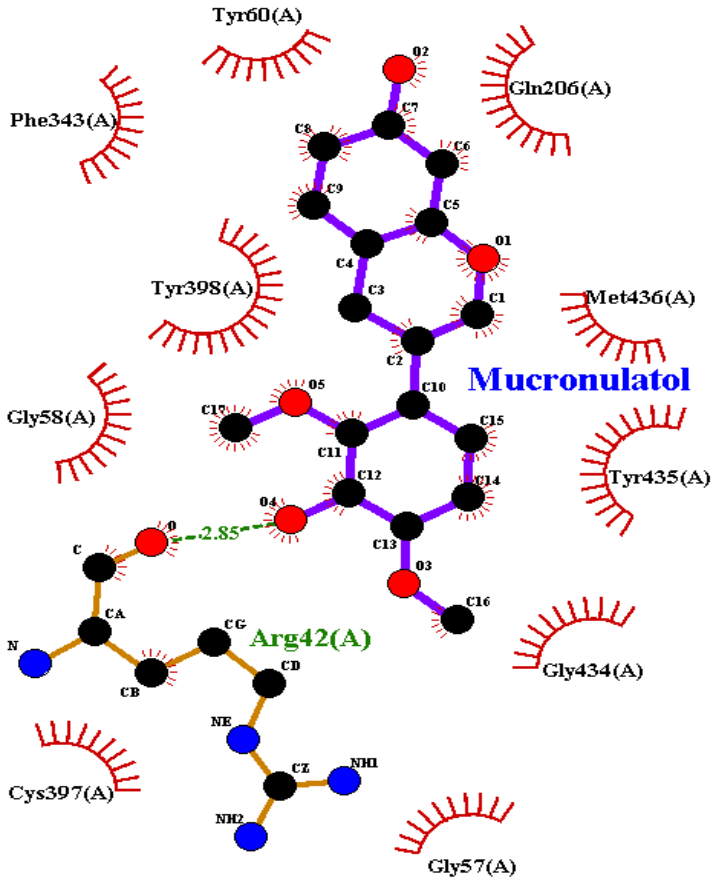
Tyr60(A)
Gln206(A)
Phe343(A)
Tyr398(A)
Met436(A)
Mucronulatol
Gly58(A)
Tyr435(A)
2.85
Arg42(A)
Gly434(A)
Cys397(A)
Gly57(A)

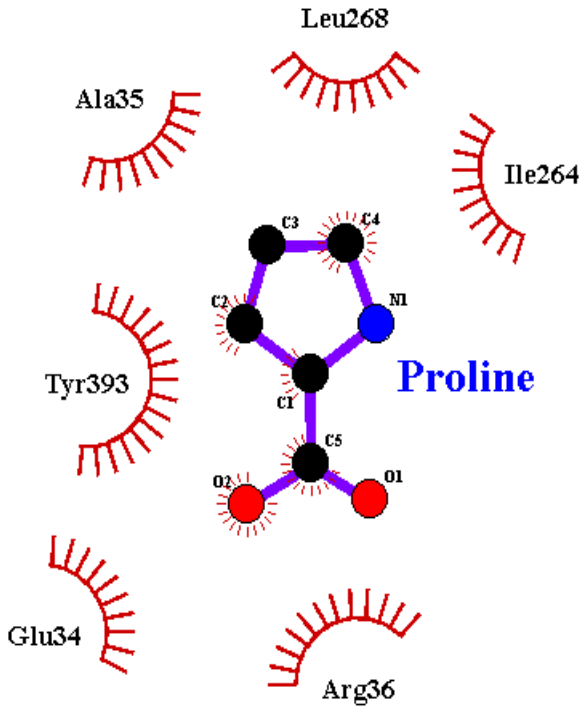
Leu268
Ala35
Ile264
Proline
Tyr393
Glu34
Arg36

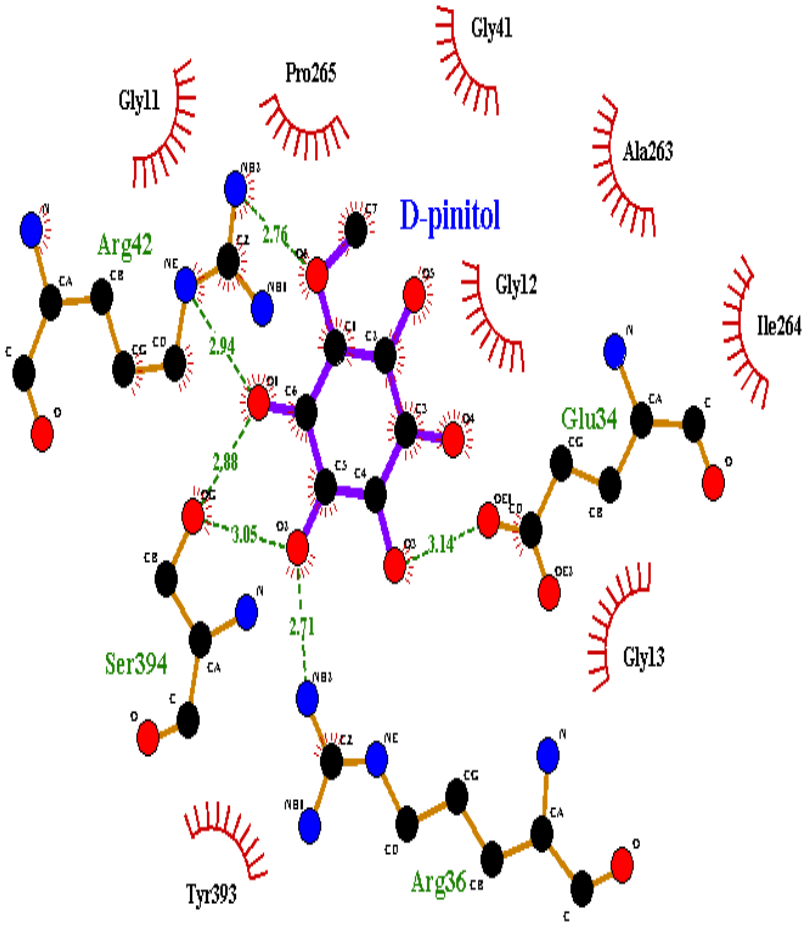
Gly41
Pro265
Gly11
Ala263
D-pinitol
Arg42
Gly12
Ile264
Glu34
Ser394
Gly13
Tyr393
Arg36

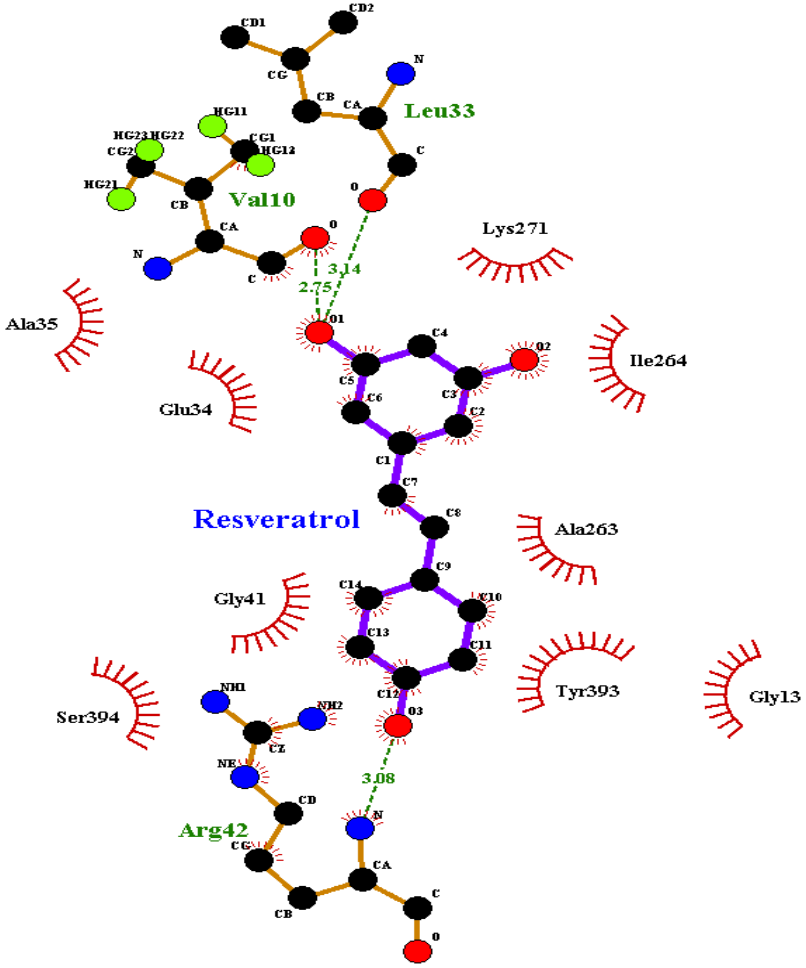
Leu33
Val10
Lys271
Ala35
Ile264
Glu34
Resveratrol
Ala263
Gly41
Tyr393
Gly13
Ser394
Arg42

Appendix I: LigPlot diagrams showing binding interactions of compounds 6.3-6.11, levodopa, and curcumin with DJ-1

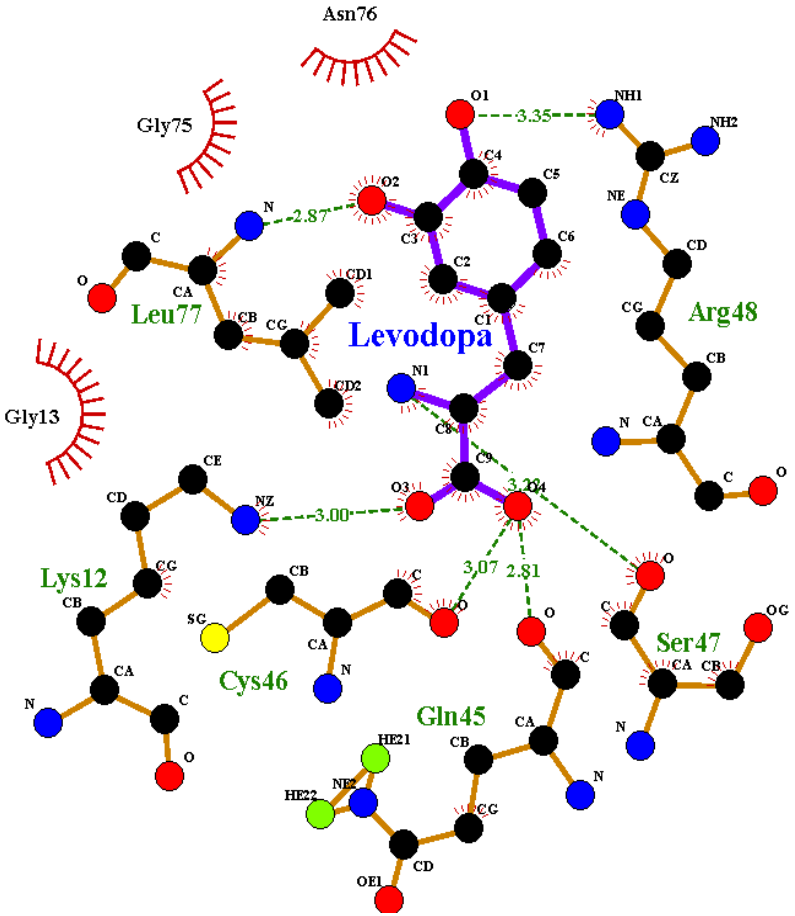

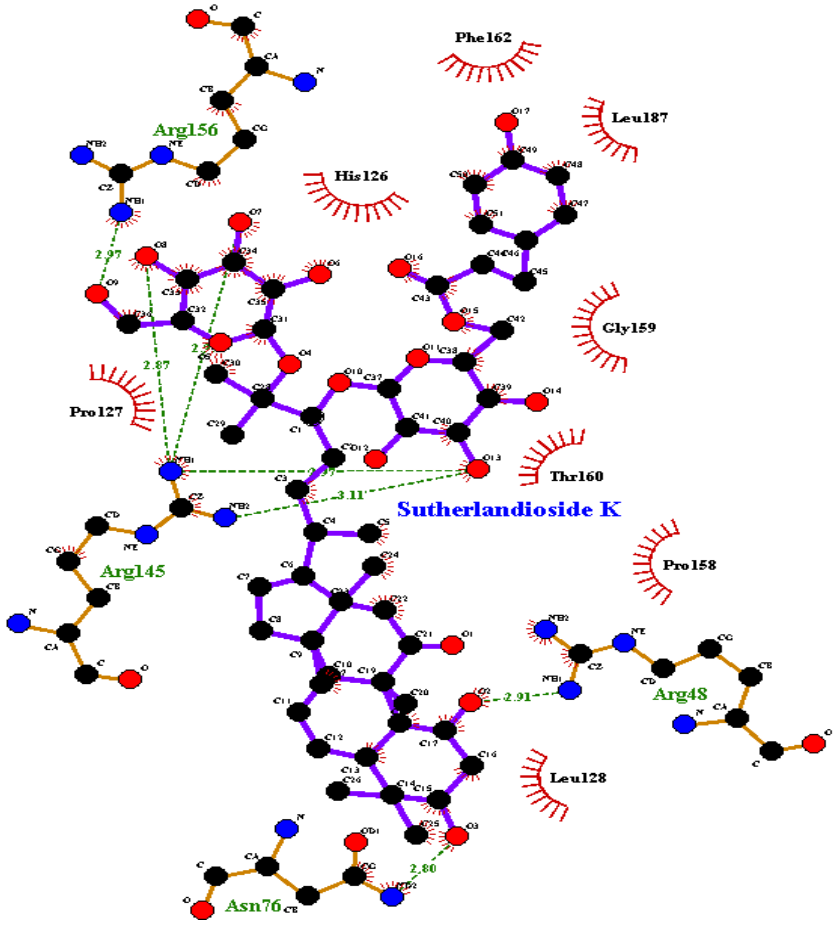

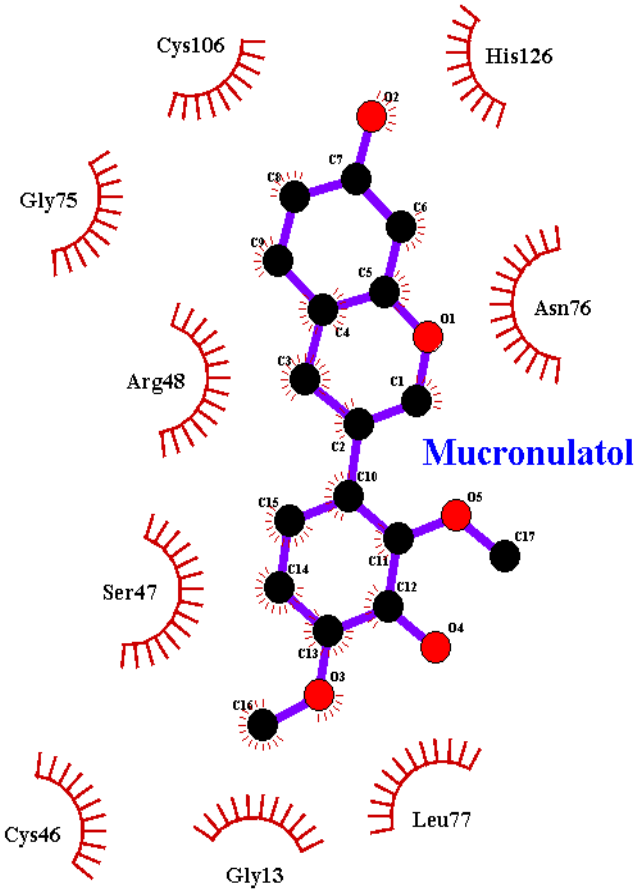
Cys106
His126
Gly75
Asn76
Arg48
Mucronulatol
Ser47
Cys46
Gly13
Leu77

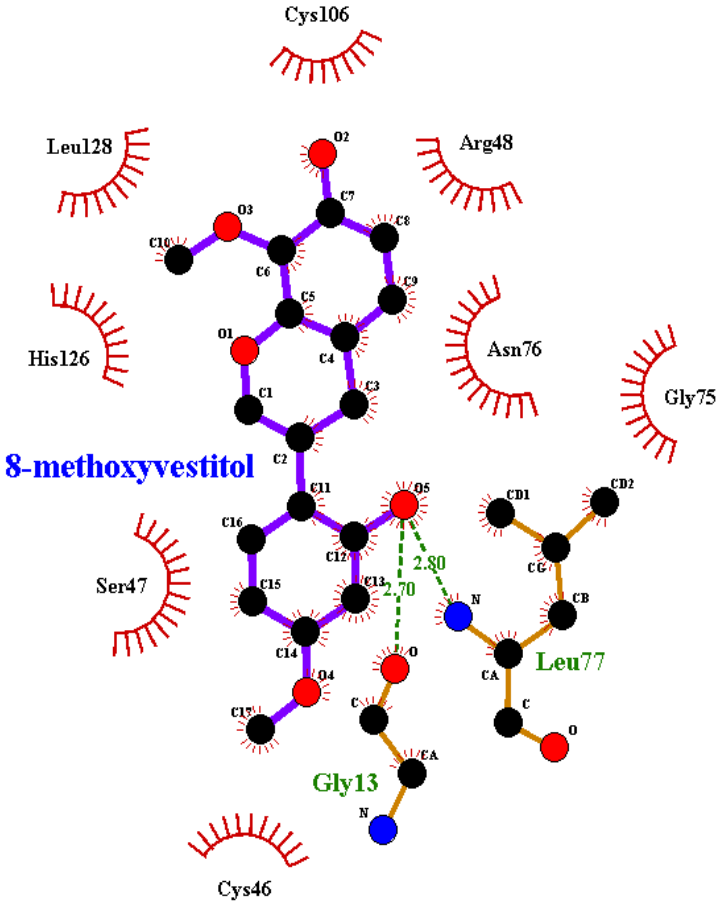
Cys106
Leu128
Arg48
His126
Asn76
Gly75
8-methoxyvestitol
Ser47
2.80
2.70
Leu77
Gly13
Cys46

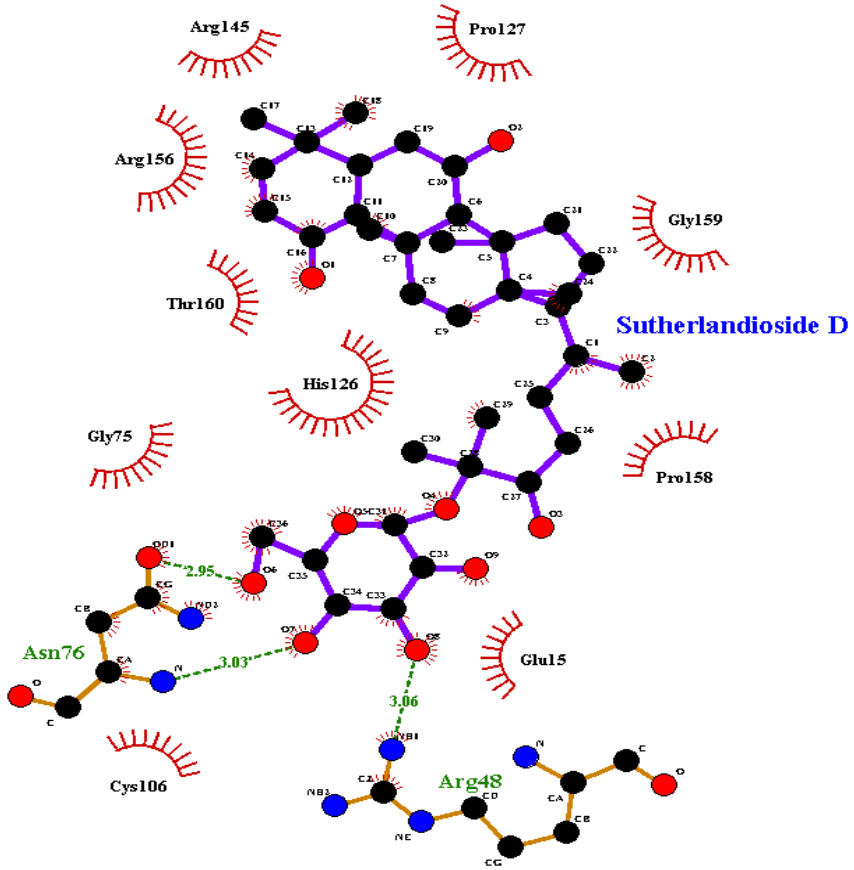
Arg145
Pro127
Arg156
Gly159
Thr160
Sutherlandioside D
His126
Gly75
Pro158
2.95
Asn76
3.03
Glu15
3.06
Cys106
Arg48

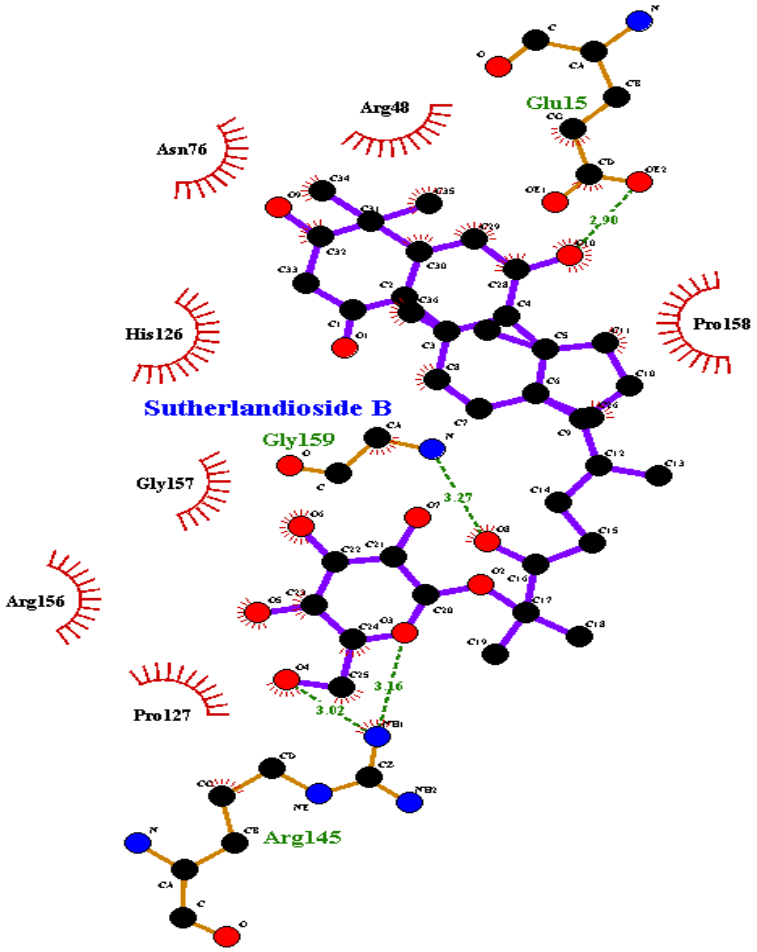
Arg48
Glu15
Asn76
2.90
His126
Pro158
Sutherlandioside B
Gly159
Gly157
3.27
Arg156
3.16
3.02
Pro127
Arg145

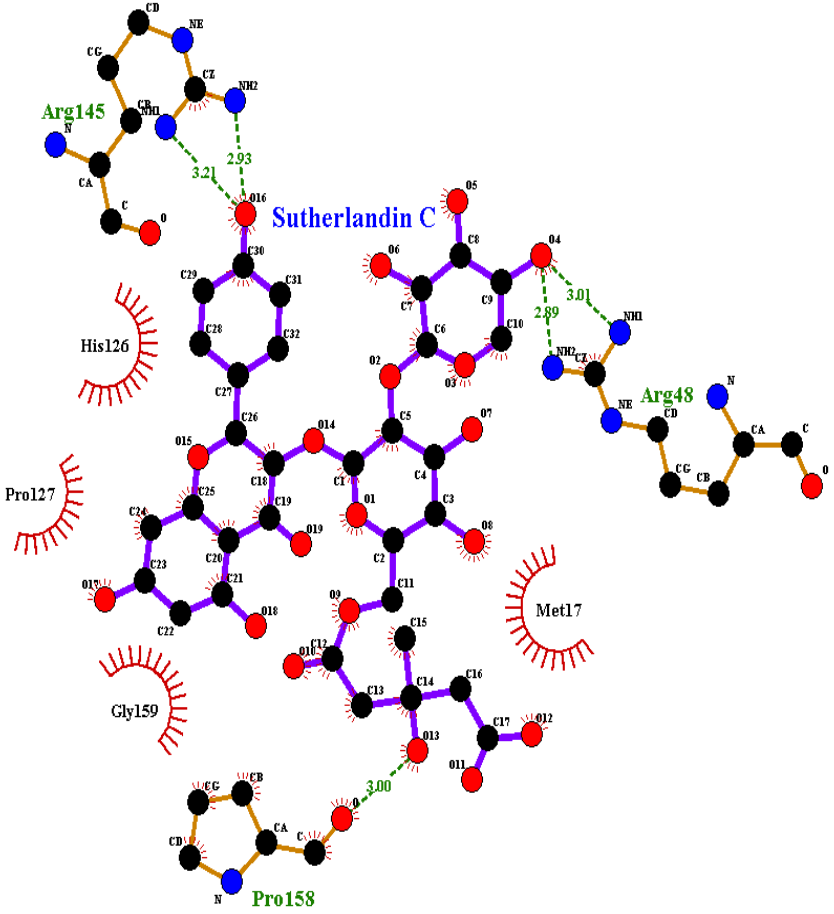
Arg145
Sutherlandin C
His126
Arg48
Pro127
Met17
Gly159
Pro158
2.93
3.21
3.01
2.89
3.00

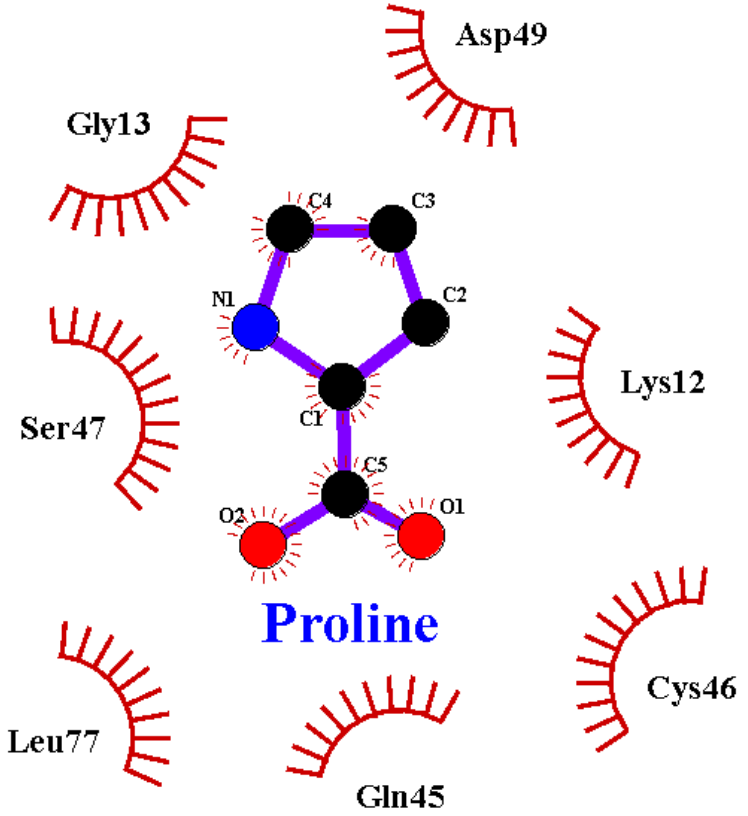
Asp49
Gly13
Lys12
Ser47
Proline
Cys46
Leu77
Gln45

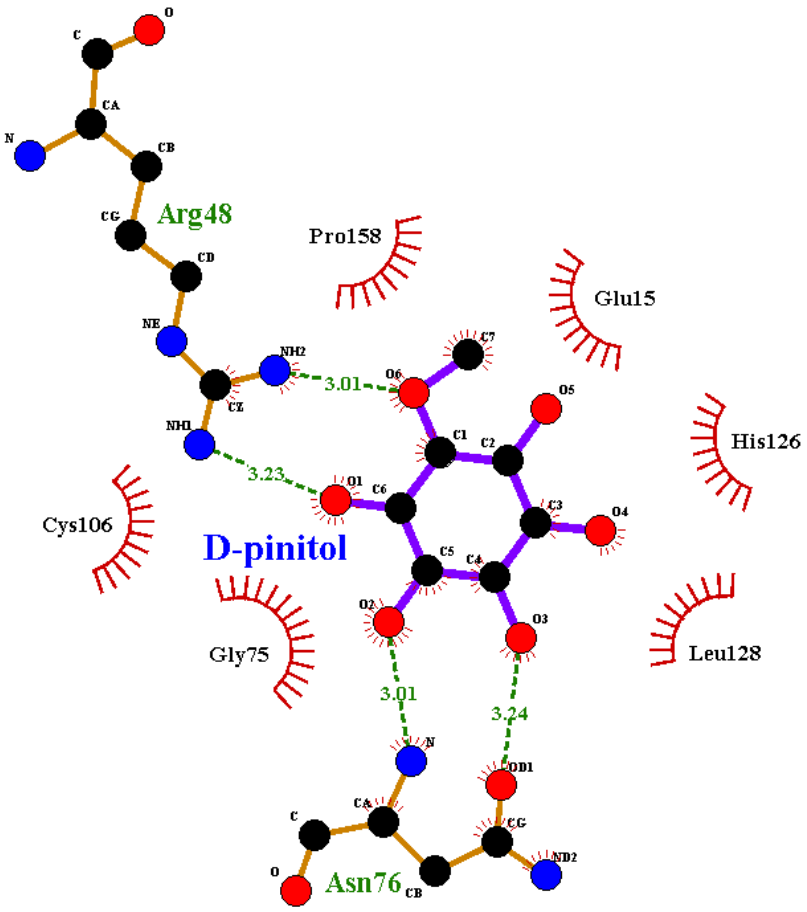
Arg48
Pro158
Glu15
His126
Cys106
D-pinitol
Gly75
Leu128
Asn76
3.01
3.23
3.01
3.24

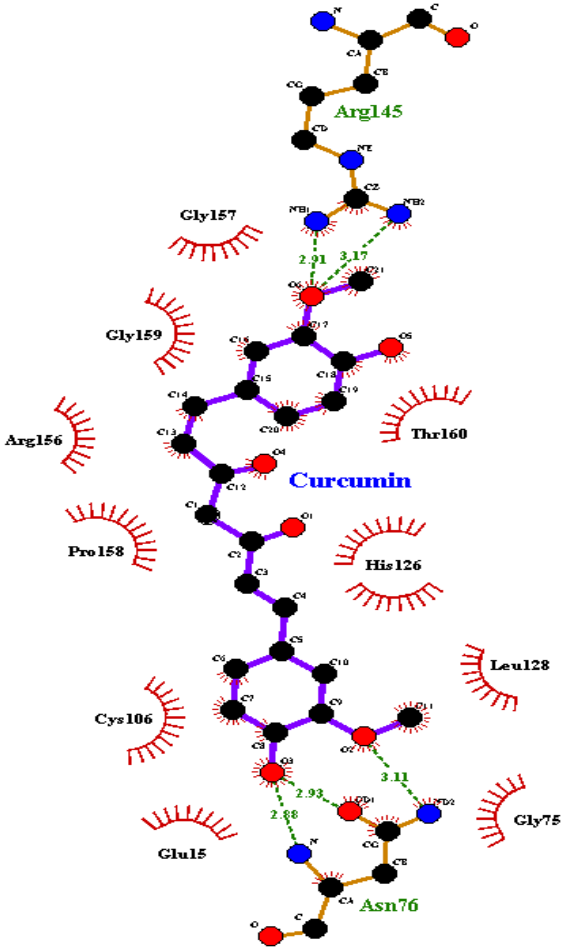
Arg145
Gly157
Gly159
Thr160
Arg156
Curcumin
Pro158
His126
Leu128
Cys106
Glu15
Gly75
Asn76
2.91
3.17
3.11
2.93
2.88

Appendix J: LigPlot diagrams showing binding interactions of compounds 7.3-7.6, 7.9, 8.3, 8.5, curcumin, ascorbic acid, and vitamin E with Keap-Nrf2

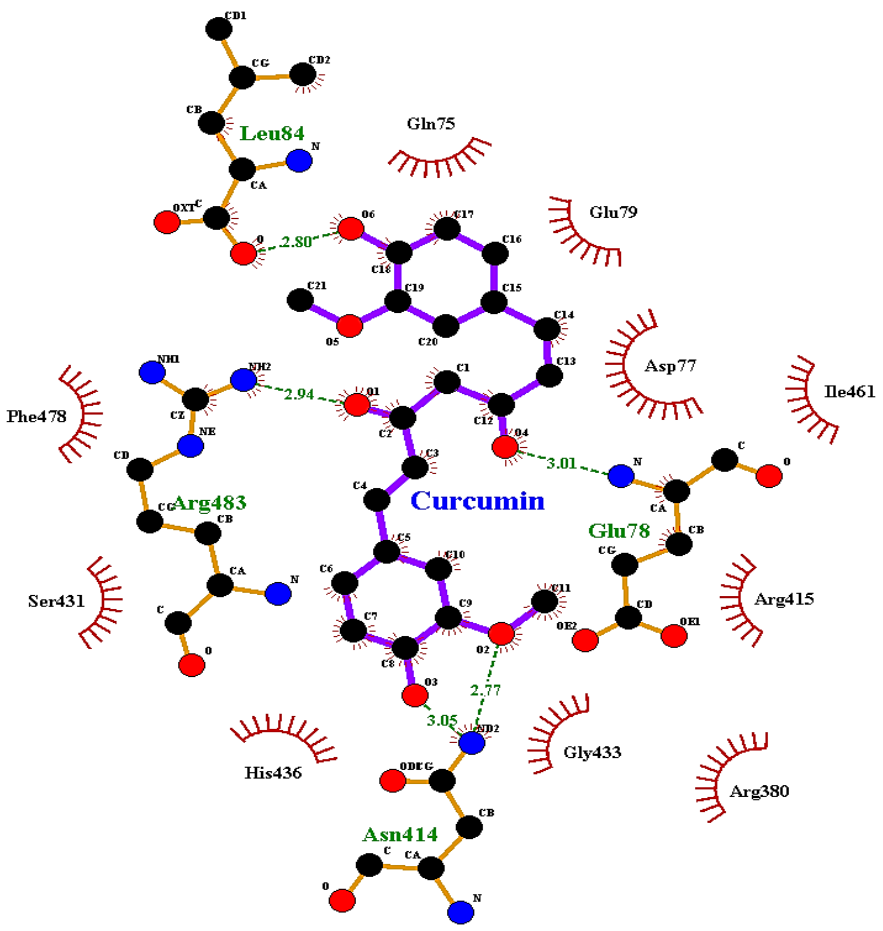

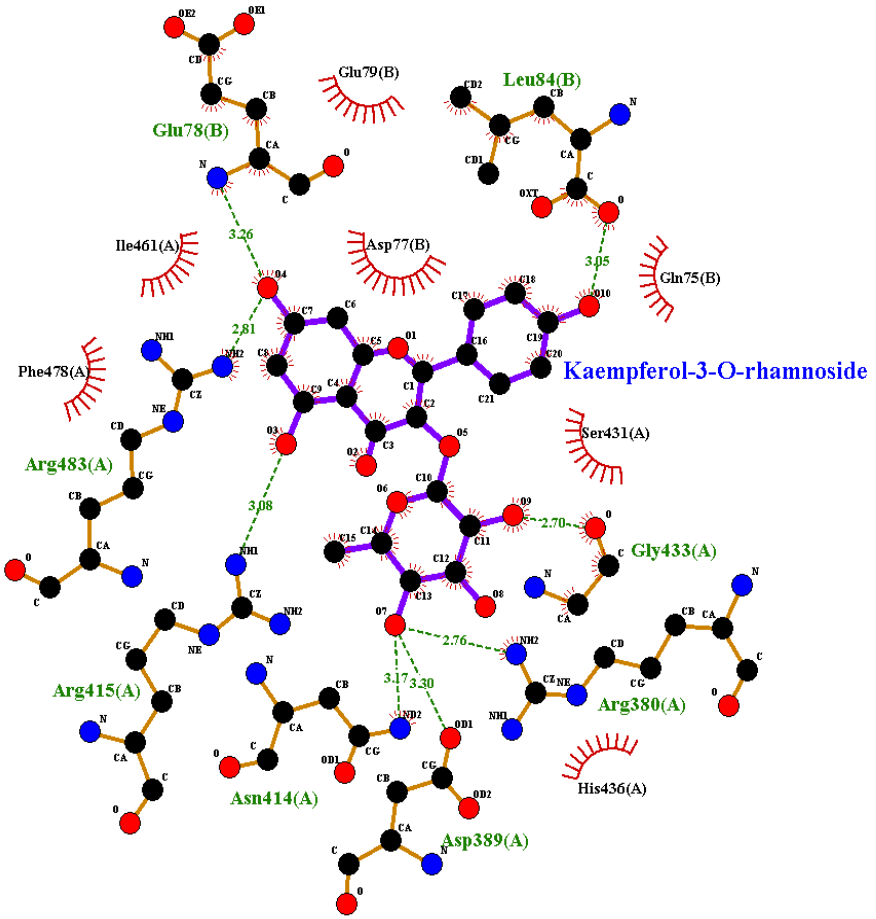

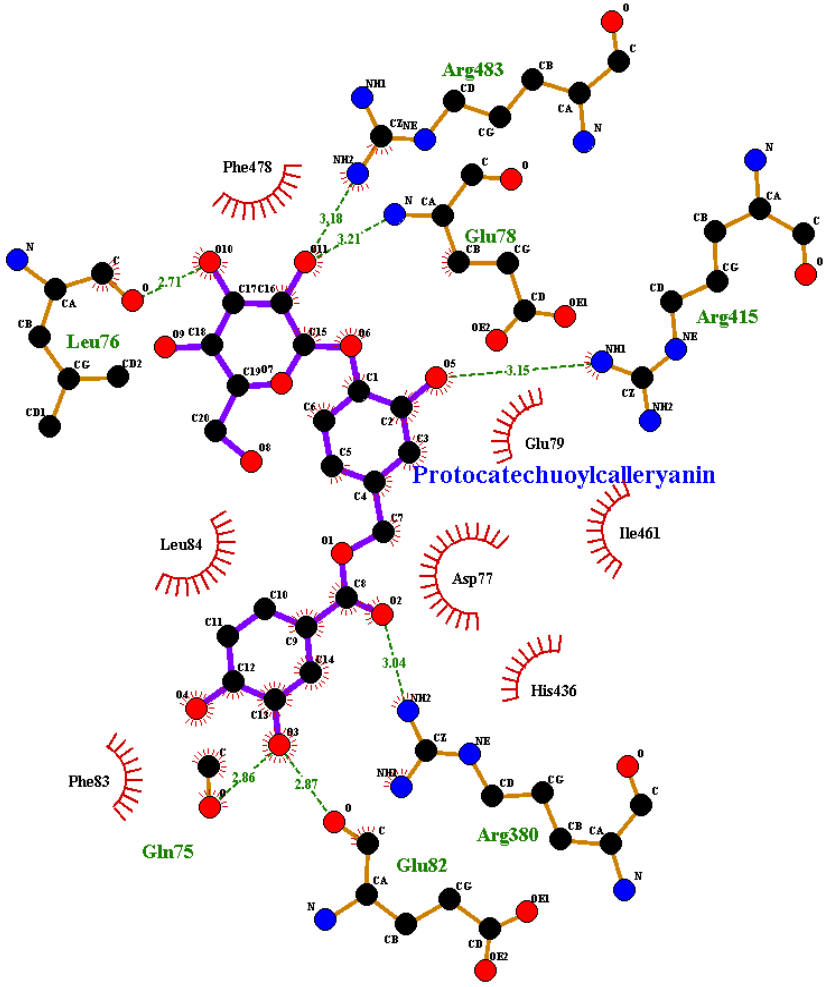
Arg483
Phe478
Glu78
Leu76
Arg415
Glu79
Protocatechuoylcalleryanin
Ile461
Leu84
Asp77
His436
Phe83
Gln75
Arg380
Glu82

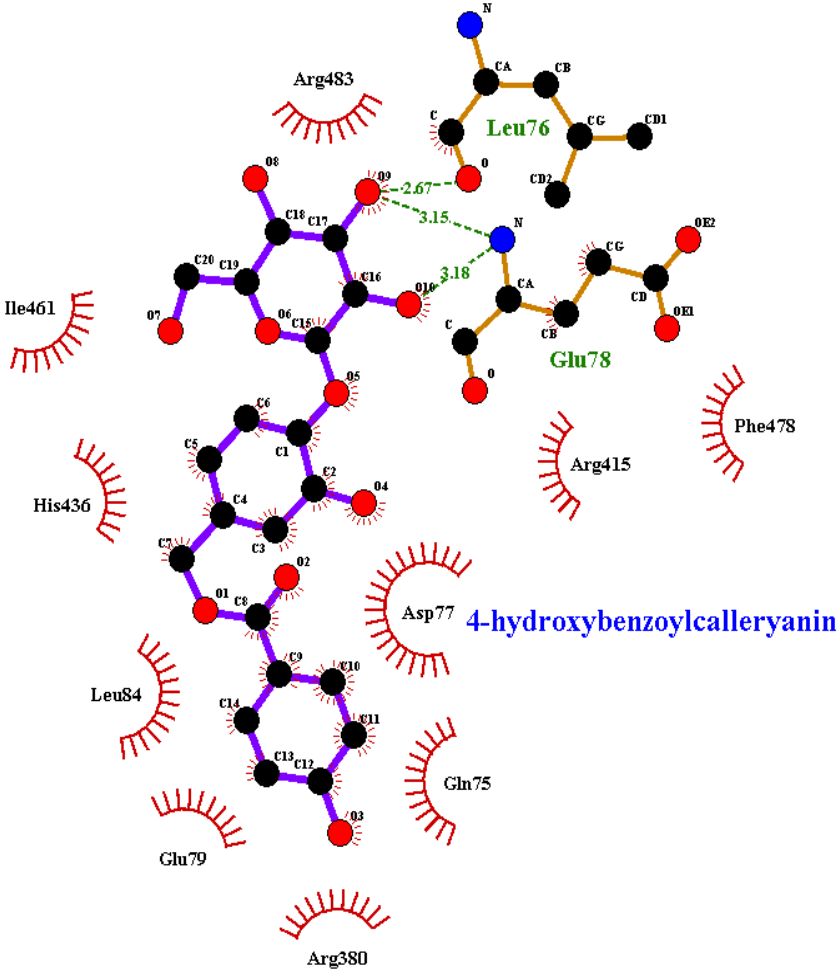
Arg483
Leu76
Ile461
Glu78
Phe478
Arg415
His436
Asp77
4-hydroxybenzoylcalleryanin
Leu84
Gln75
Glu79
Arg380

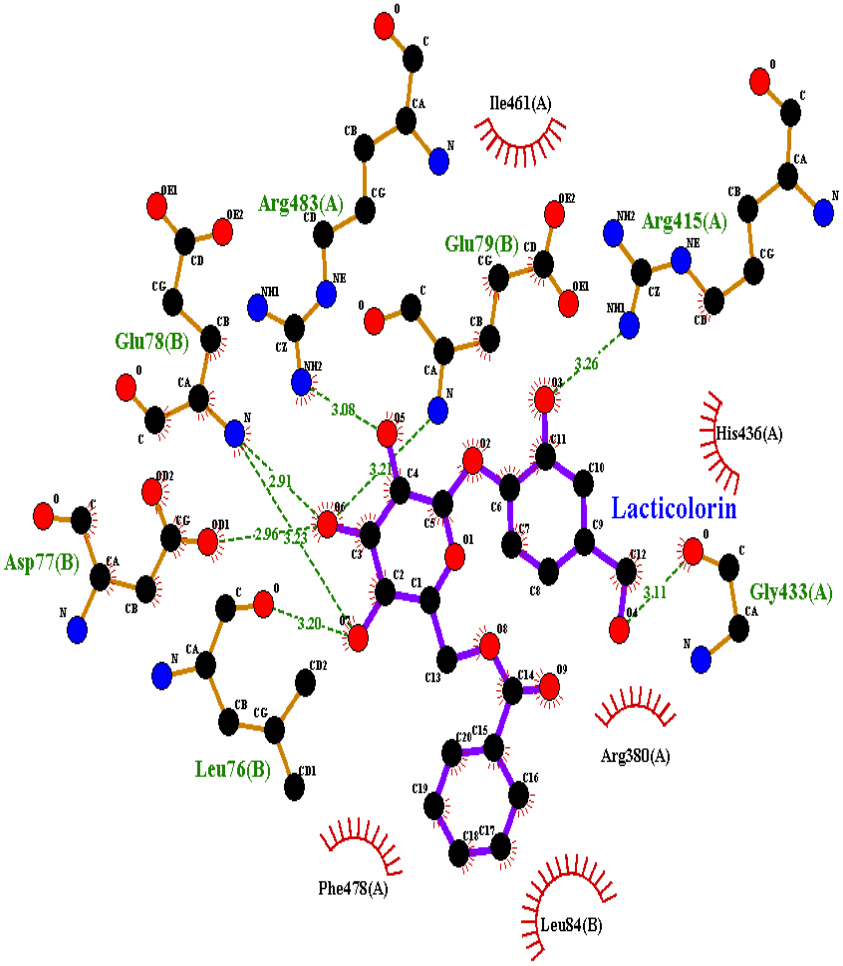
Ile461(A)
Arg483(A)
Glu79(B)
Arg415(A)
Glu78(B)
His436(A)
Lacticolorin
Asp77(B)
Gly433(A)
Leu76(B)
Arg380(A)
Phe478(A)
Leu84(B)

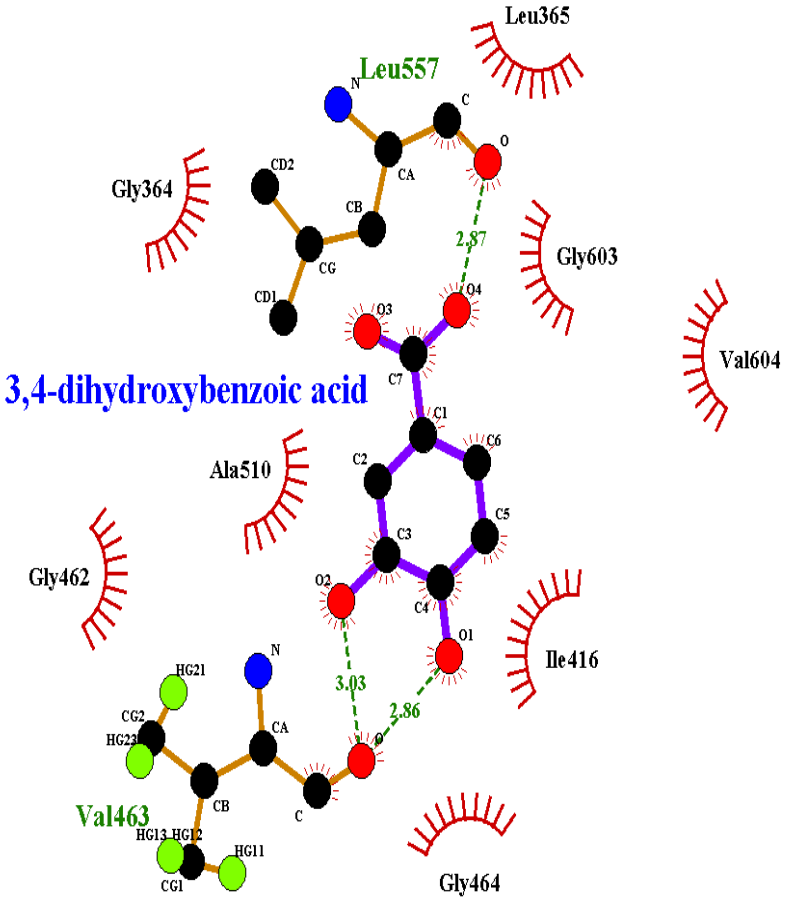
Leu365
Leu557
Gly364
Gly603
Val604
3,4-dihydroxybenzoic acid
Ala510
Gly462
Ile416
Val463
Gly464

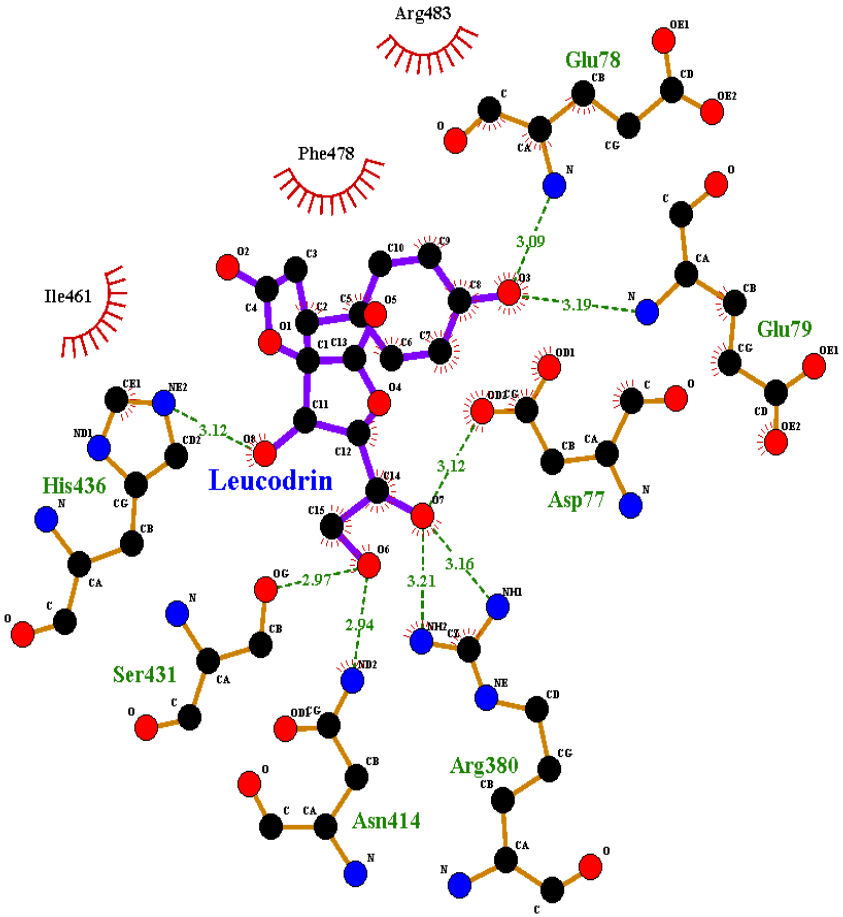
Arg483
Glu78
Phe478
Ile461
Glu79
His436
Leucodrin
Asp77
Ser431
Arg380
Asn414
3.09
3.19
3.12
3.12
2.97
2.94
3.21
3.16

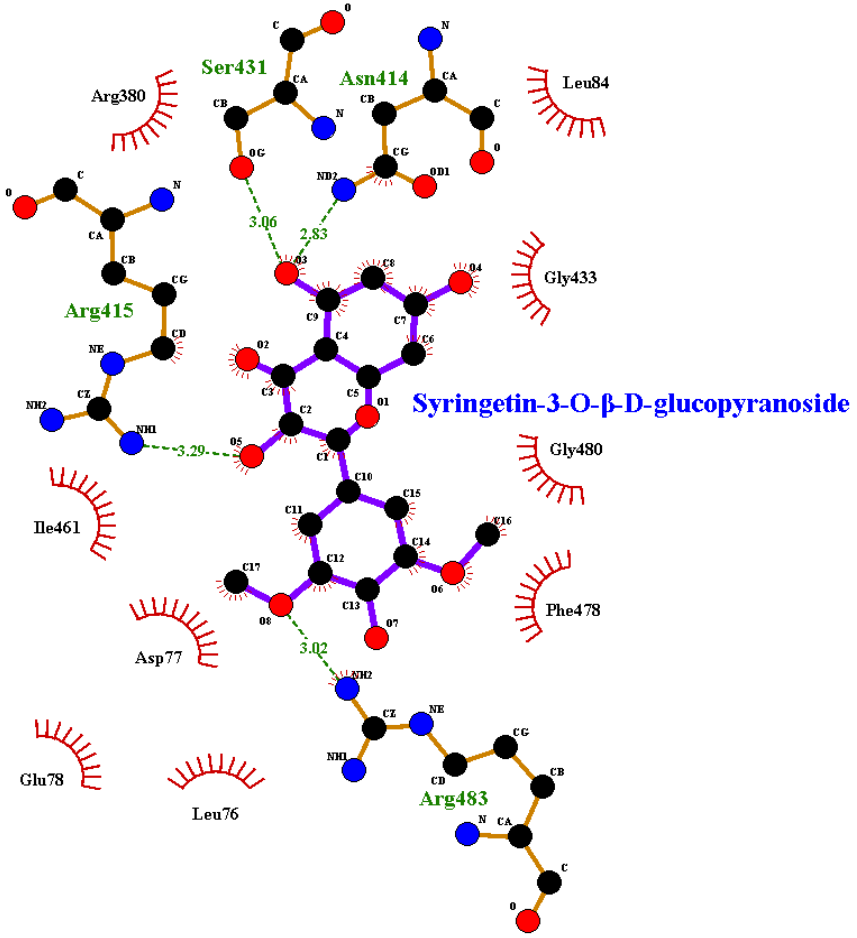
Ser431
Asn414
Arg380
Leu84
Gly433
Arg415
Syringetin-3-O-β-D-glucopyranoside
Gly480
Ile461
Phe478
Asp77
Glu78
Leu76
Arg483
3.06
2.83
3.29
3.02

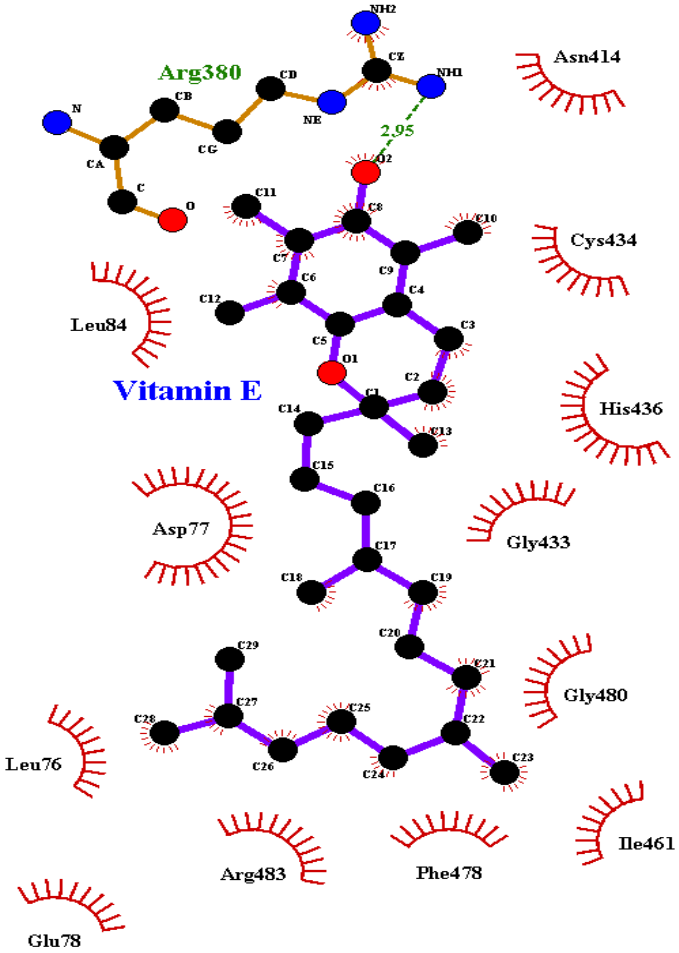
Arg380
Asn414
Cys434
Leu84
Vitamin E
His436
Asp77
Gly433
Gly480
Leu76
Arg483
Phe478
Ile461
Glu78
2.95

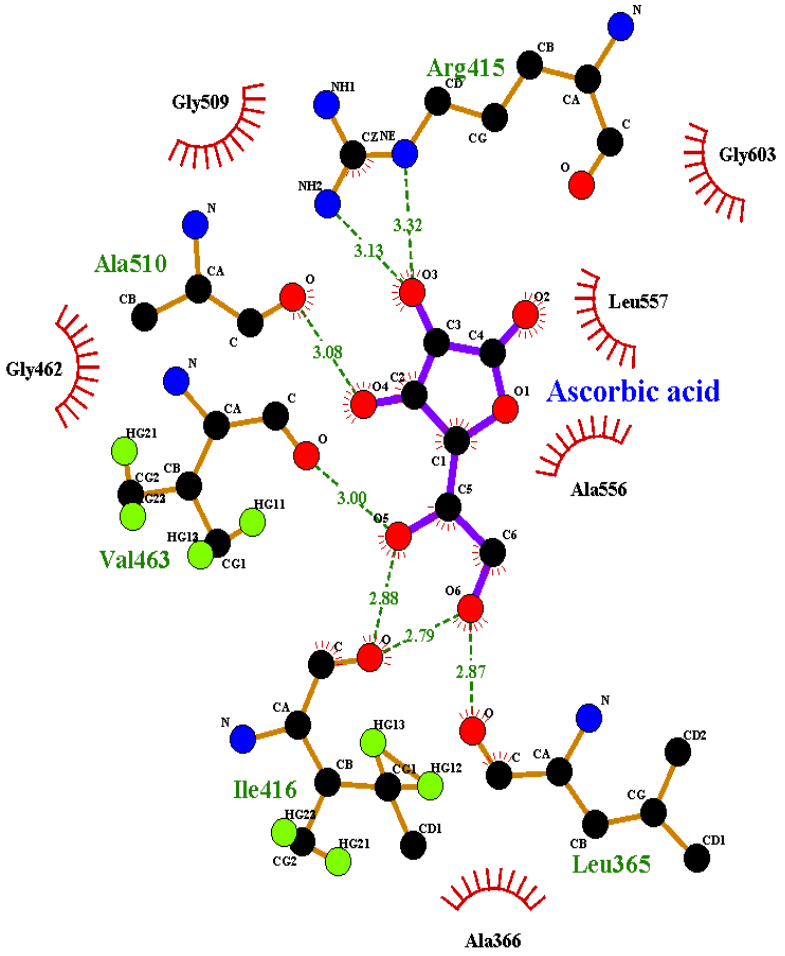
Arg415
Gly509
Gly603
Ala510
Leu557
Gly462
Ascorbic acid
Ala556
Val463
Ile416
Leu365
Ala366
3.32
3.13
3.08
3.00
2.88
2.79
2.87

Appendix K: LigPlot diagrams showing binding interactions of compounds 7.3-7.6, 7.9, 8.3, 8.5, curcumin, ascorbic acid, and vitamin E with GPX4

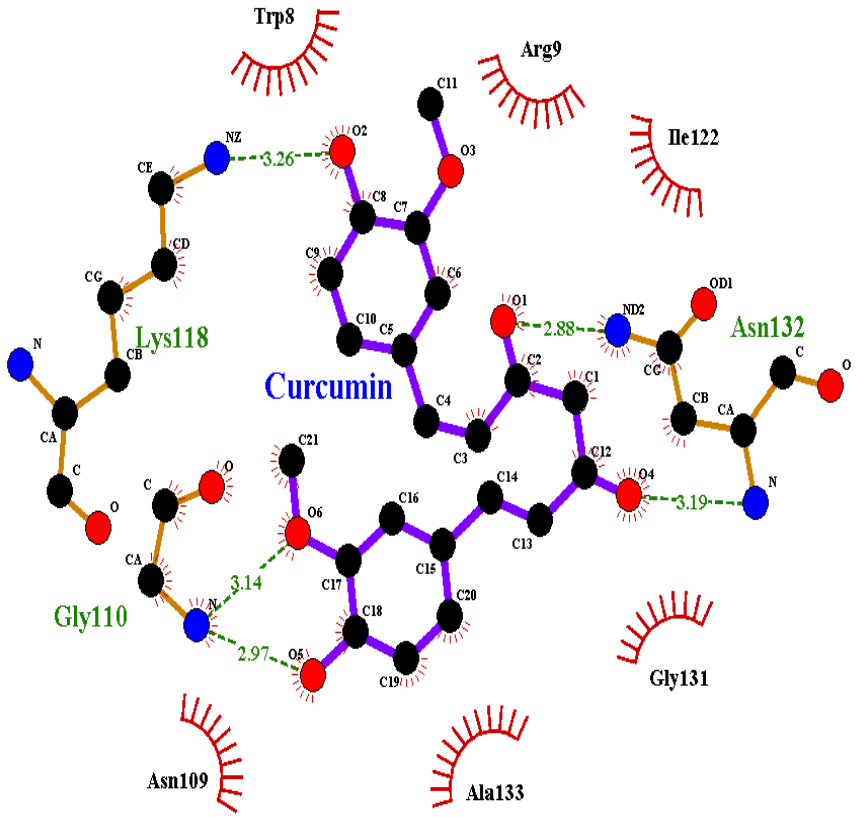

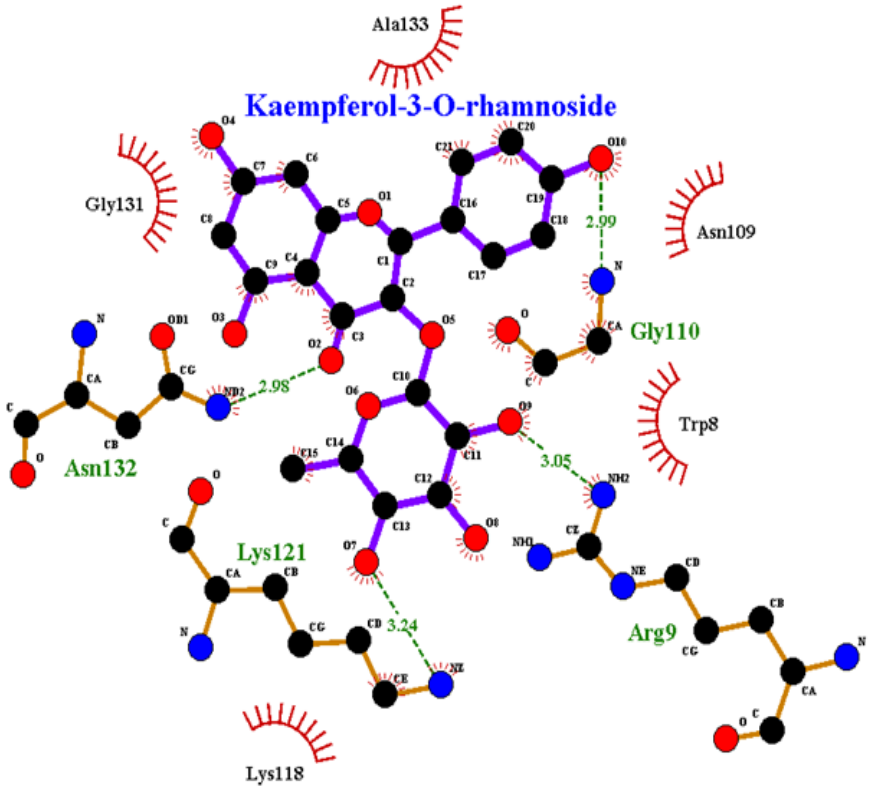

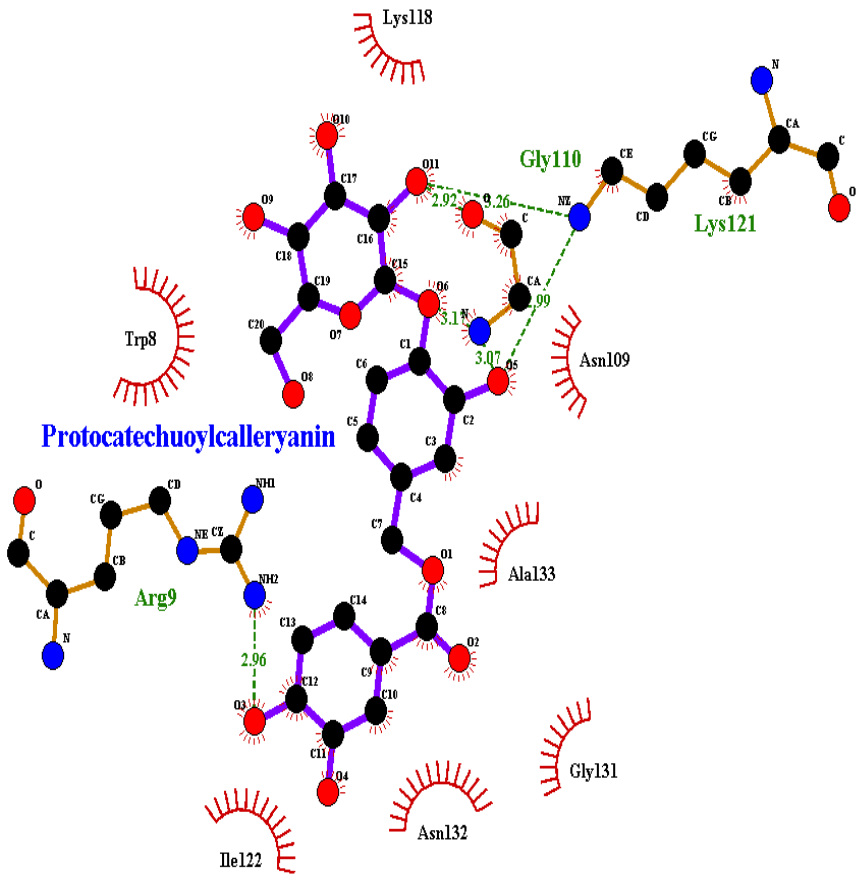
Lys118
Gly110
Lys121
Trp8
Asn109
Protocatechuoylcalleryanin
Arg9
Ala133
Gly131
Asn132
Ile122

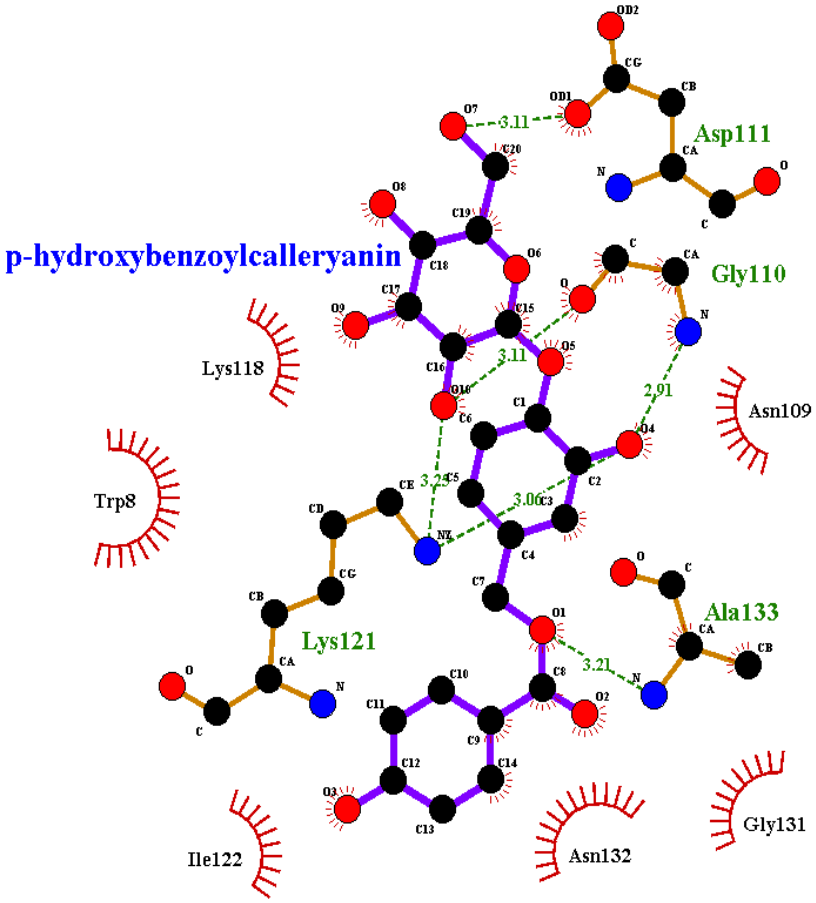
p-hydroxybenzoylcalleryanin
Asp111
Gly110
Lys118
Asn109
Trp8
Lys121
Ala133
Gly131
Asn132
Ile122

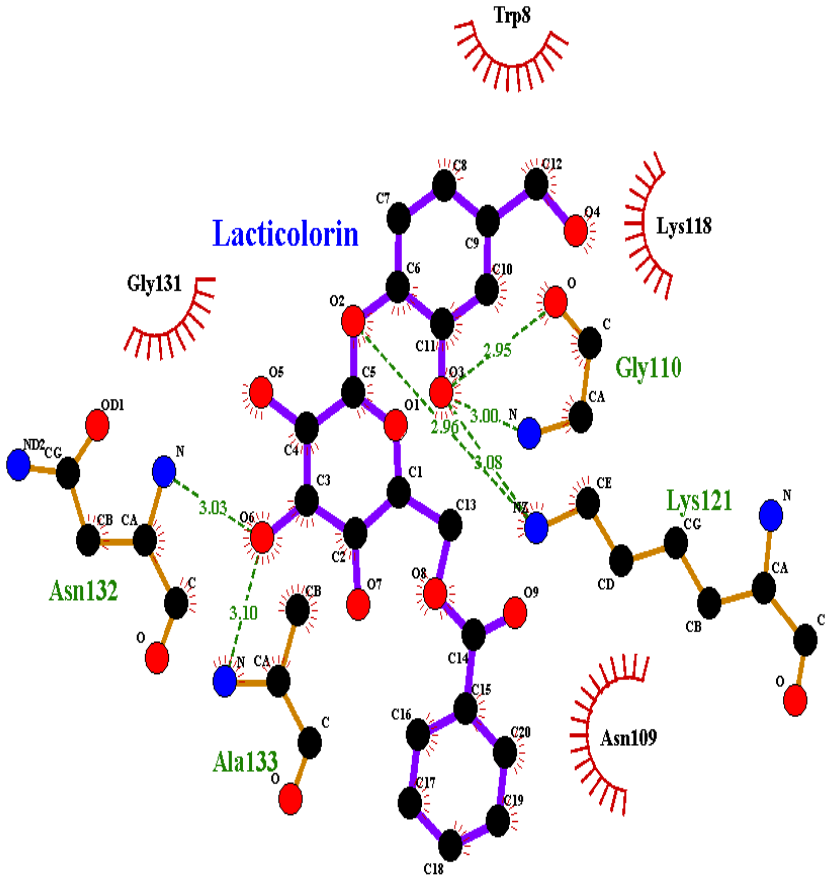
Trp8
Lacticolorin
Lys118
Gly131
Gly110
Asn132
Lys121
Asn109
Ala133

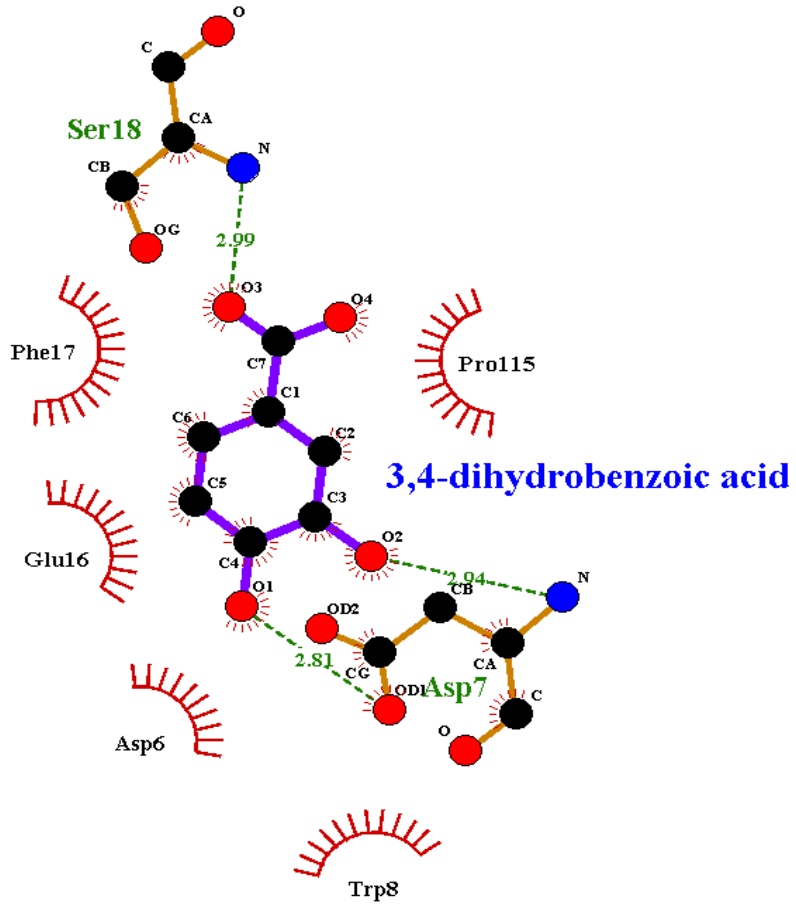
Ser18
Phe17
Pro115
3,4-dihydrobenzoic acid
Glu16
Asp7
Asp6
Trp8

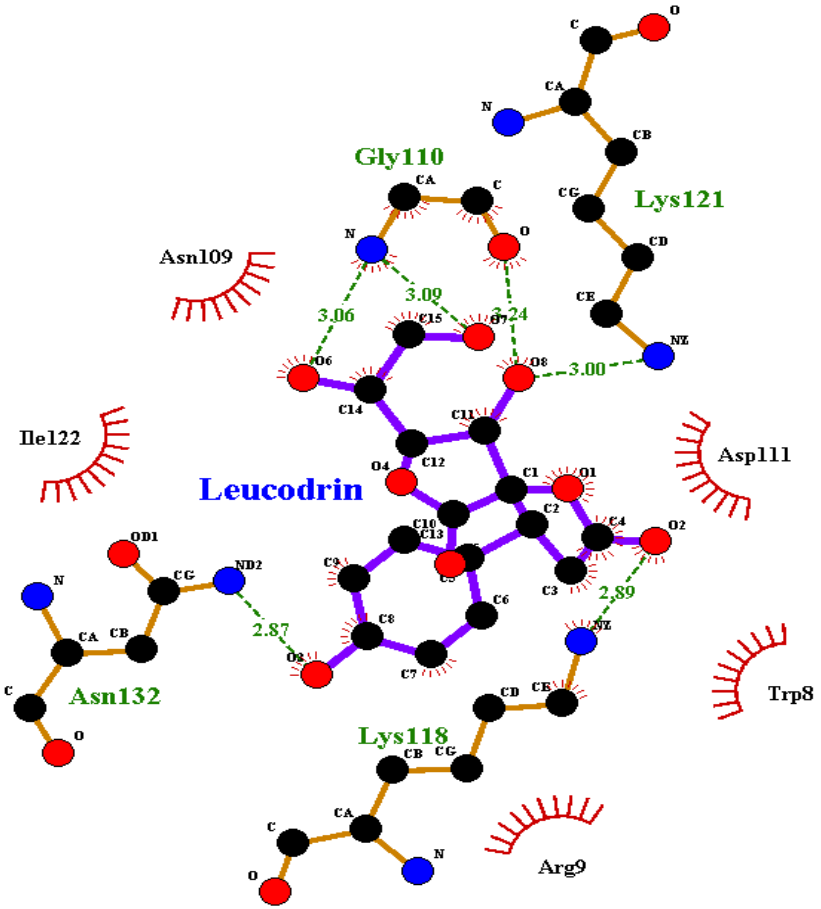

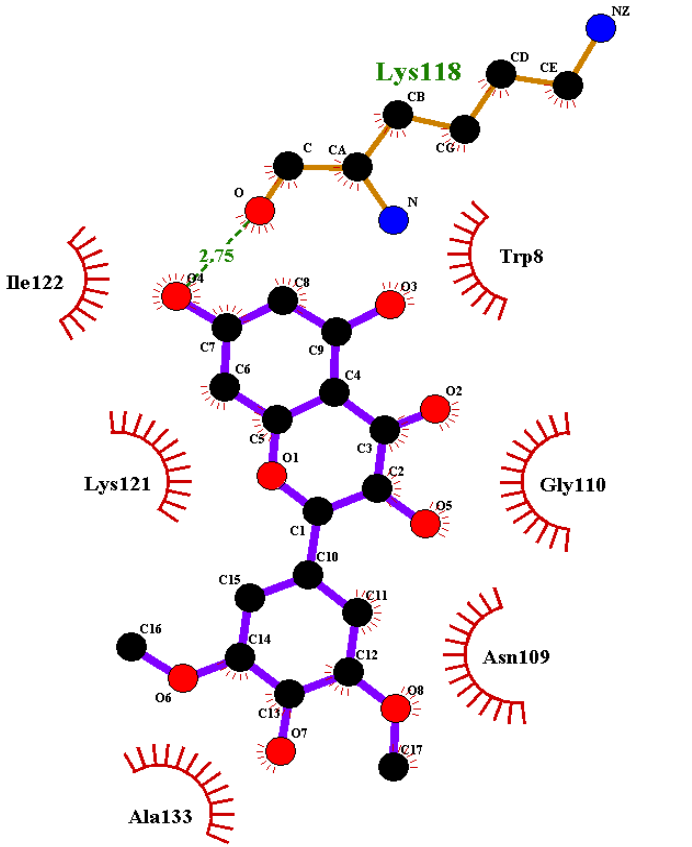

Syringetin-3-O-β-D-glucopyranoside

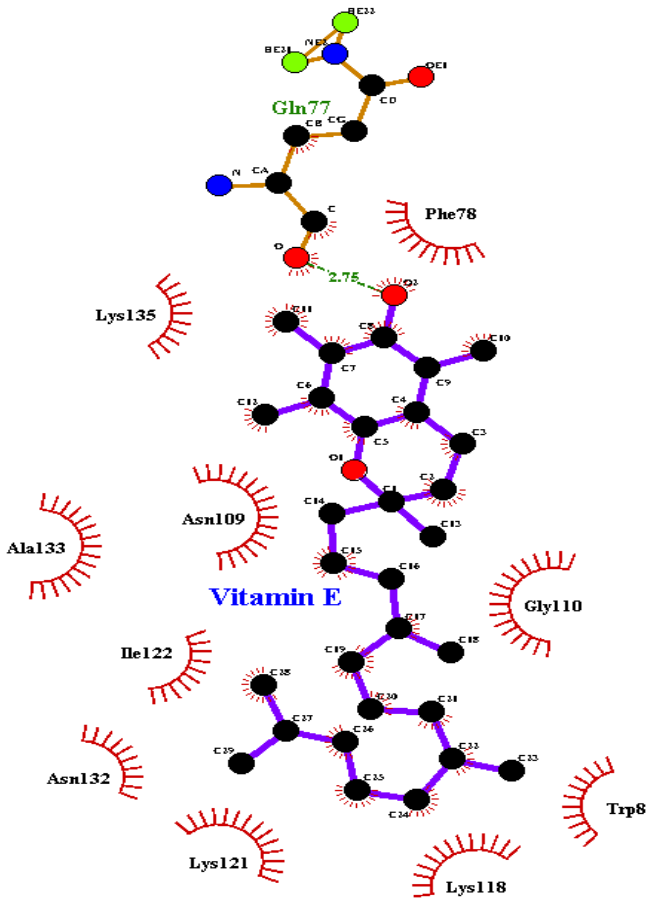
Gln77
Phe78
2.75
Lys135
Asn109
Ala133
Vitamin E
Gly110
Ile122
Asn132
Trp8
Lys121
Lys118

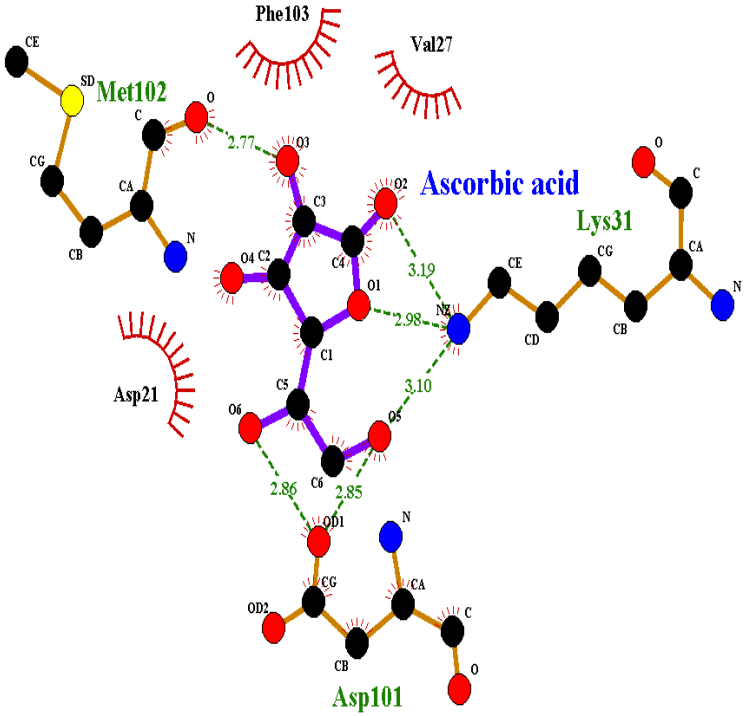
Phe103
Val27
Met102
2.77
Ascorbic acid
Lys31
3.19
2.98
3.10
Asp21
2.86
2.85
Asp101

Appendix L: LigPlot diagrams showing binding interactions of compounds 7.3-7.6, 7.9, 8.3, 8.5, metoprolol, and dobutamine with β_1-AR

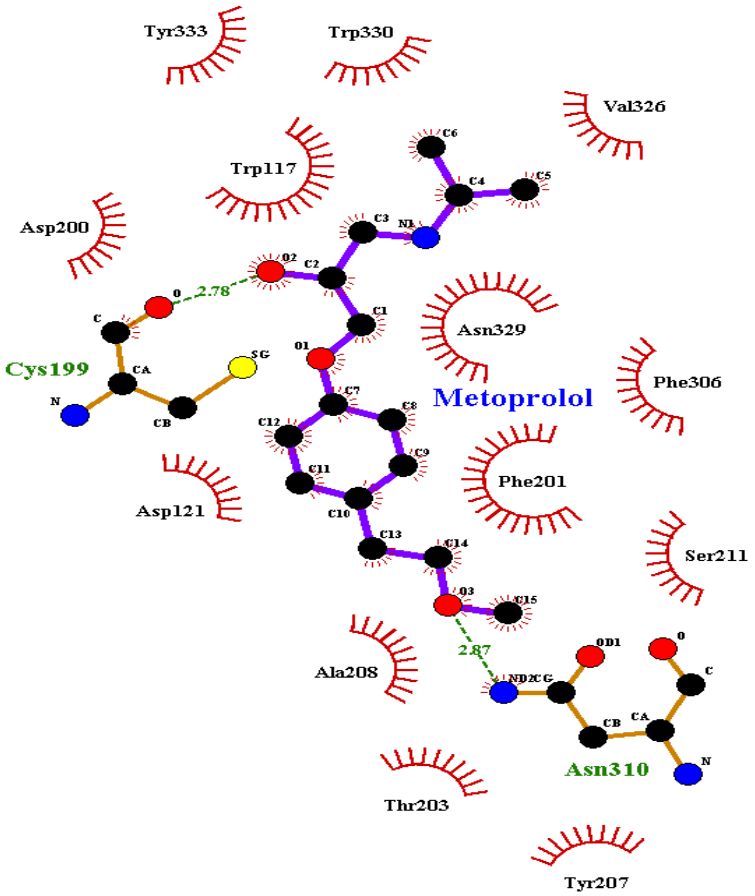

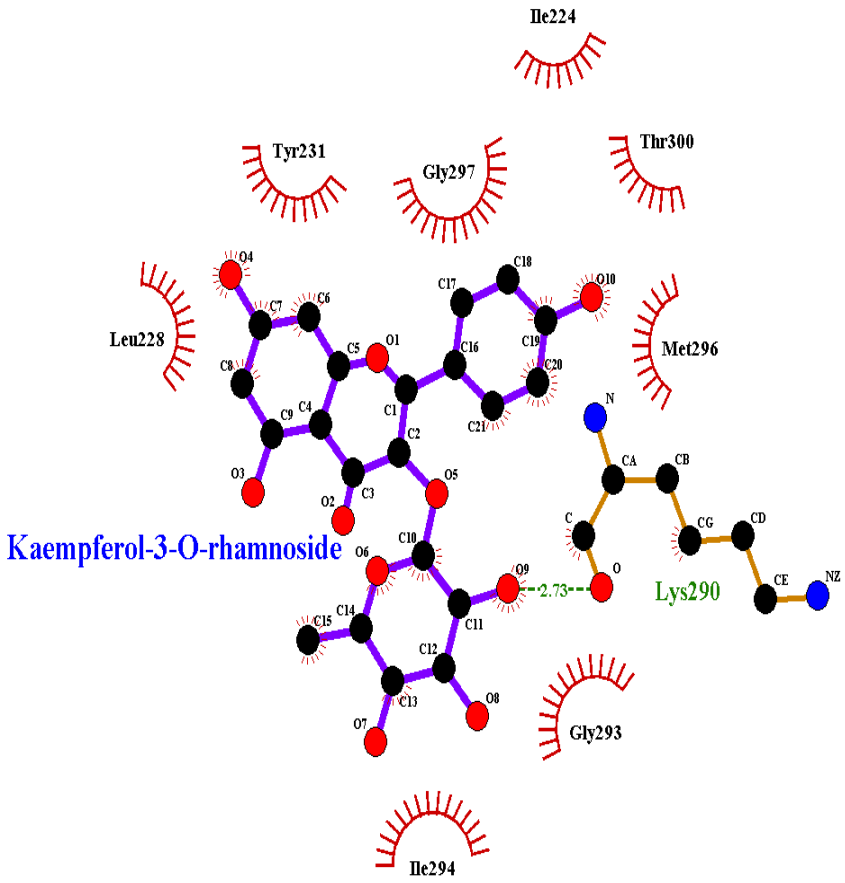

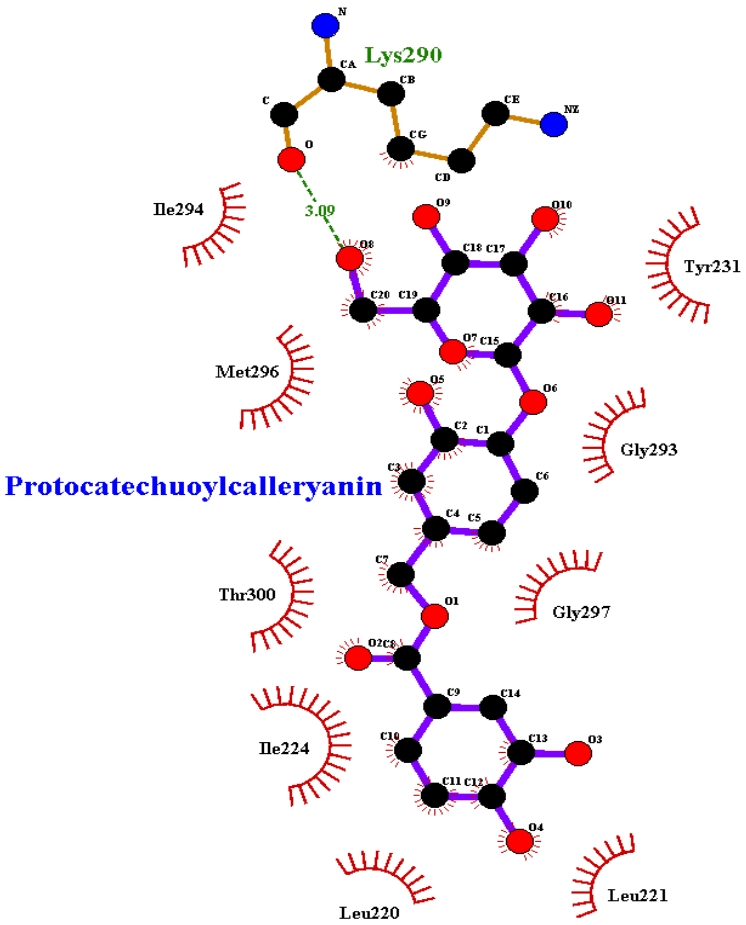
Lys290
Ile294
3.09
Tyr231
Met296
Gly293
Protocatechuoylcalleryanin
Thr300
Gly297
Ile224
Leu220
Leu221

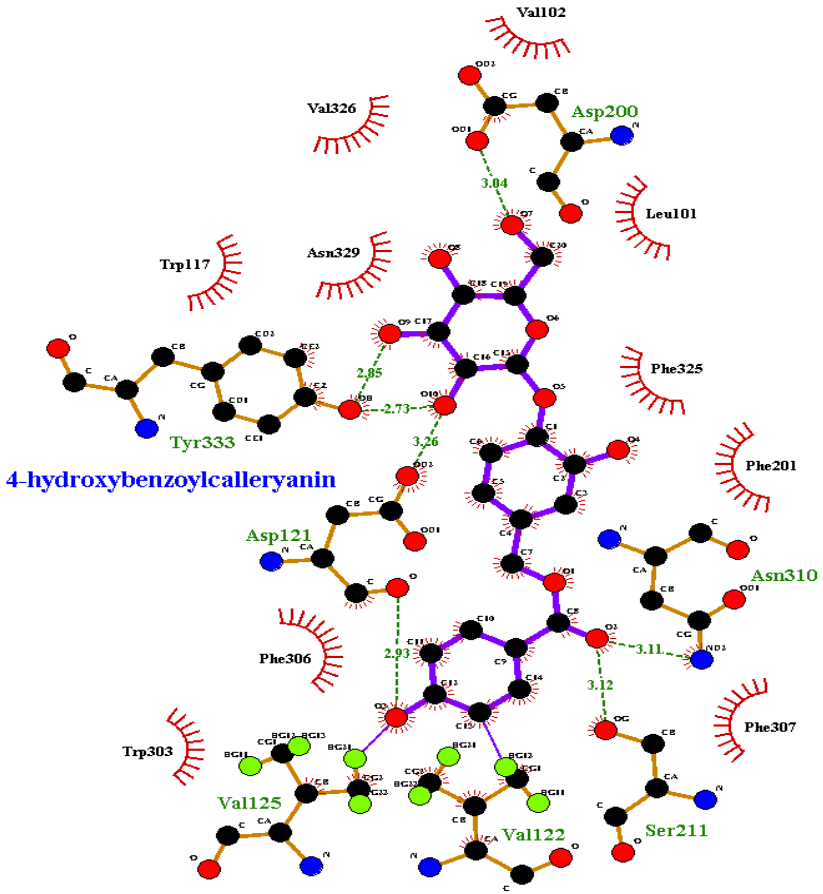
Val102
Val326
Asp200
3.04
Leu101
Trp117
Asn329
Phe325
2.85
2.73
Tyr333
3.26
4-hydroxybenzoylcalleryanin
Phe201
Asp121
Asn310
Phe306
2.93
3.11
3.12
Phe307
Trp303
Val125
Val122
Ser211

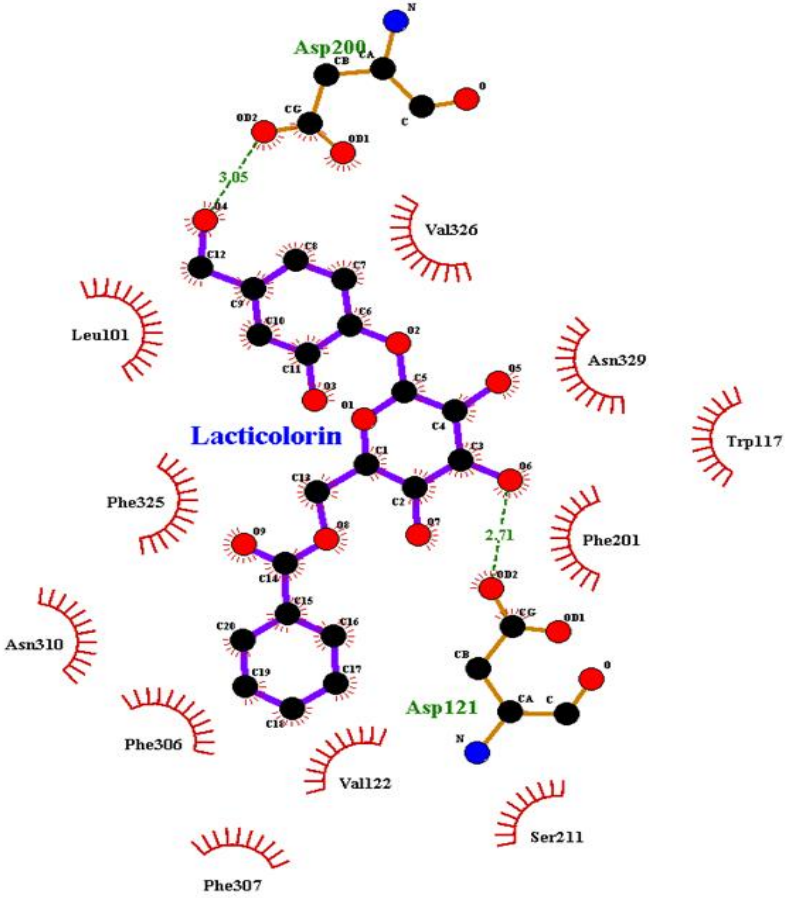
Asp200
3.05
Val326
Leu101
Asn329
Trp117
Lacticolorin
Phe325
Phe201
2.71
Asn310
Asp121
Phe306
Val122
Ser211
Phe307

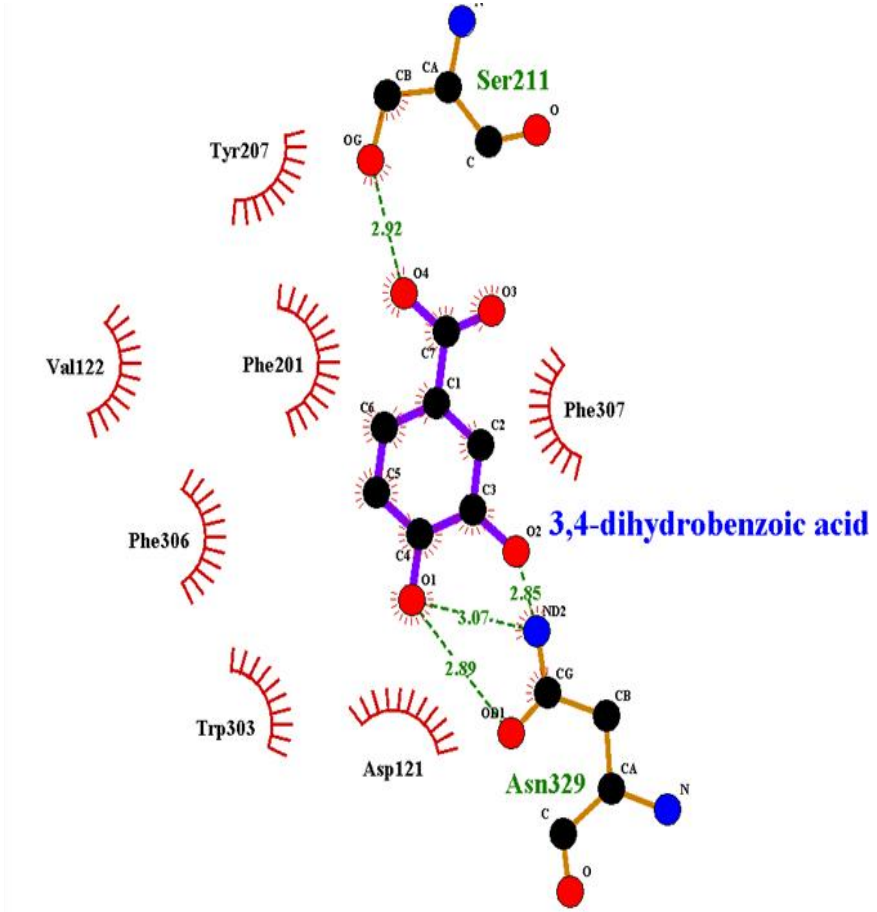
Ser211
Tyr207
2.92
Val122
Phe201
Phe307
3,4-dihydrobenzoic acid
Phe306
2.85
3.07
2.89
Trp303
Asp121
Asn329

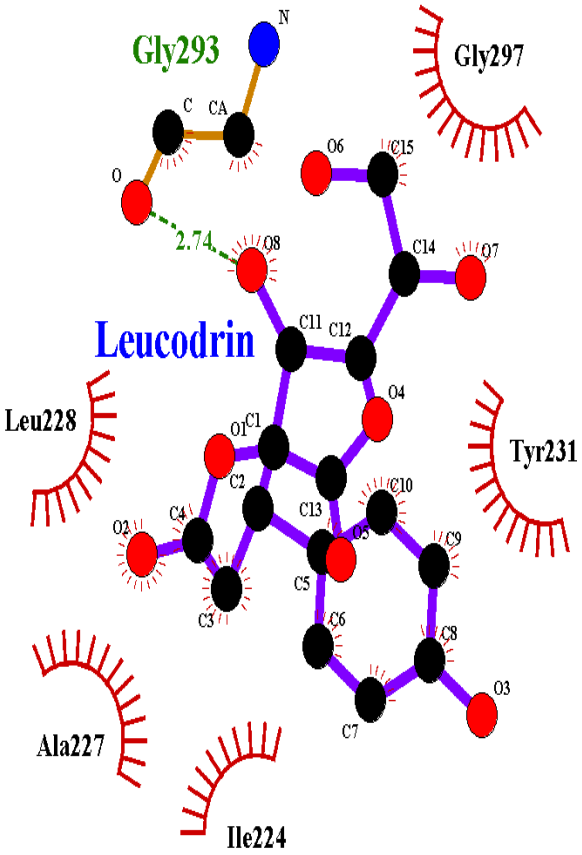

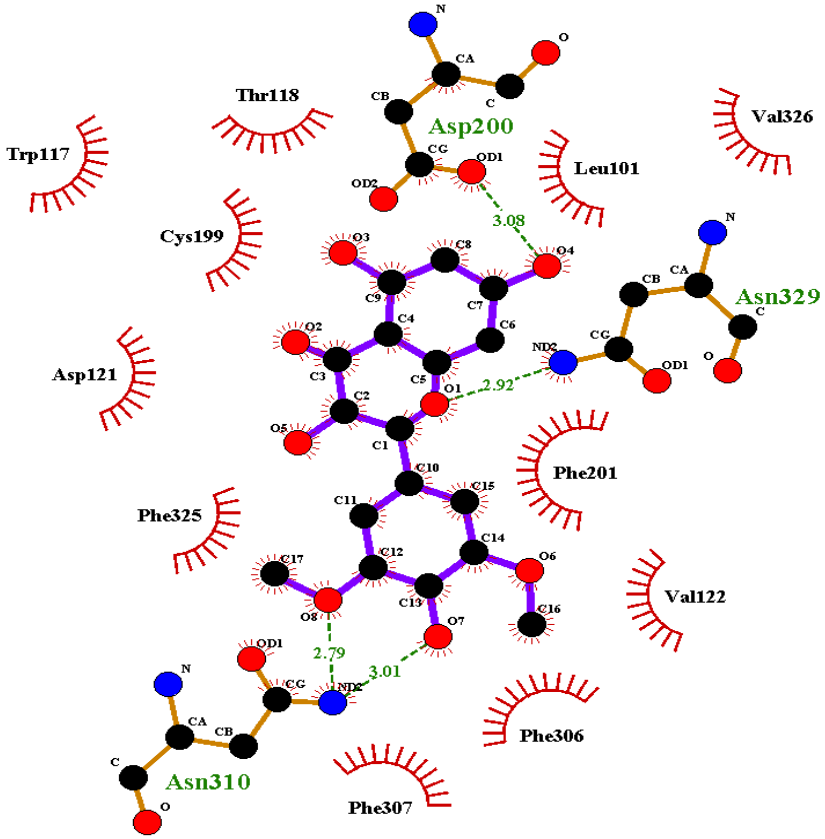

Syringetin-3-O-β-D-glucopyranoside

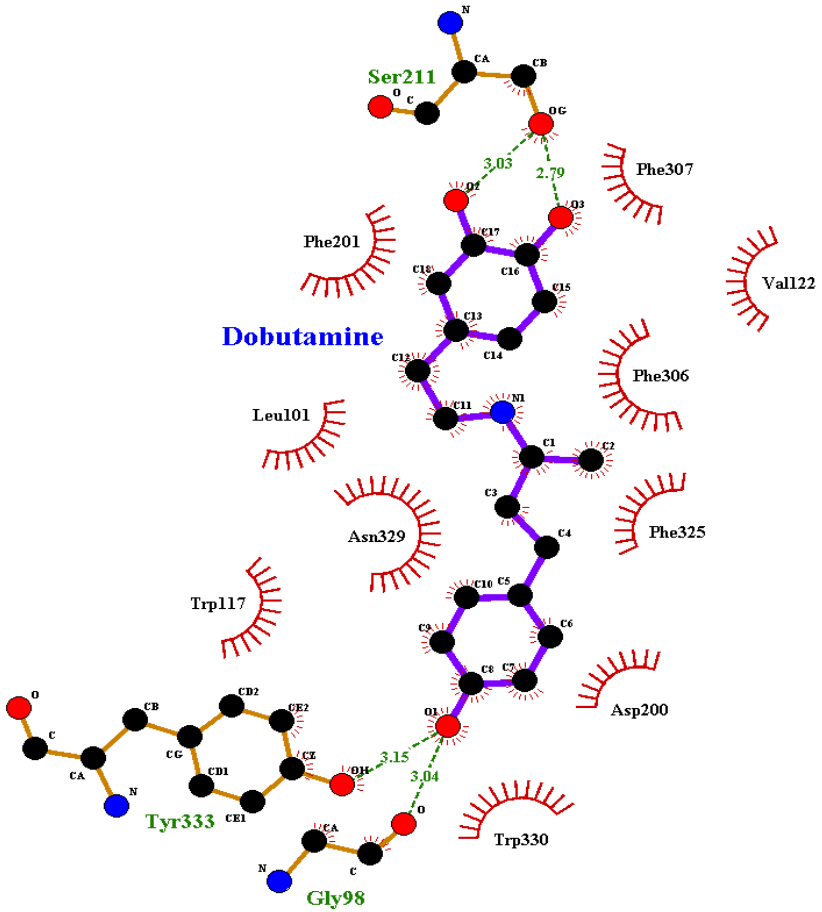
Ser211
Phe307
Phe201
Val122
Dobutamine
Phe306
Leu101
Asn329
Phe325
Trp117
Asp200
Tyr333
Trp330
Gly98
3.03
2.79
3.15
3.04